ADVANCES IN EARTHQUAKE PREDICTION

Research and Risk Mitigation

Ragnar Stefánsson

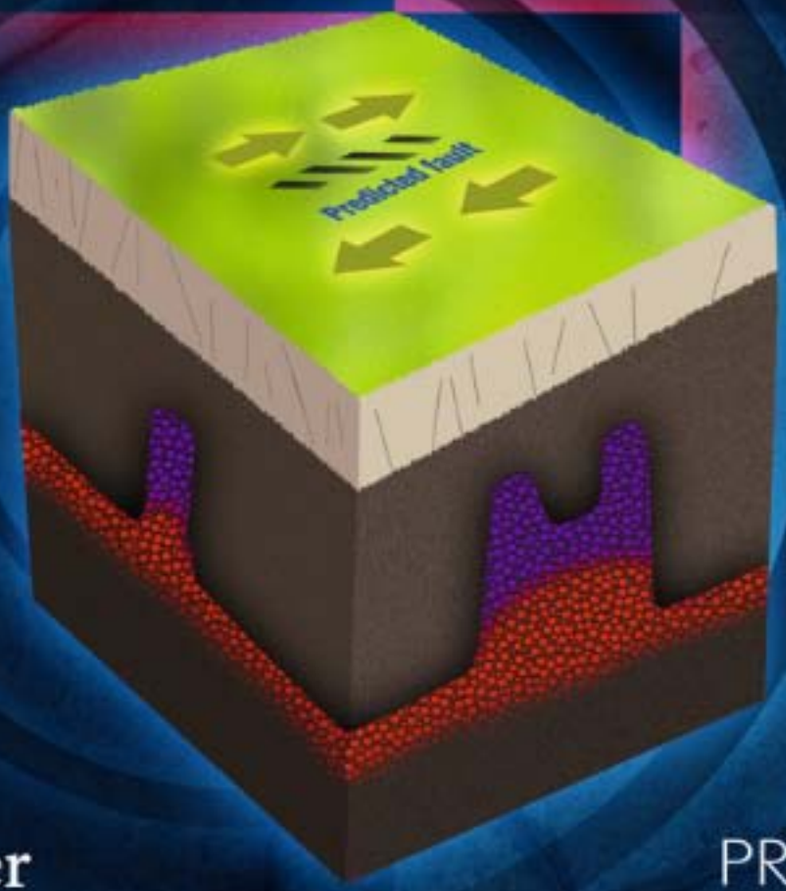

Springer

PRAXIS

Advances in Earthquake Prediction

Research and Risk Mitigation

IRANCE
Geological Academy of IRAN

Ragnar Stefánsson

Advances in Earthquake Prediction

Research and Risk Mitigation

Springer

Published in association with
Praxis Publishing
Chichester, UK

PRAXIS

IRANOE
Geological Academy of IRAN

Professor Ragnar Stefánsson
University of Akureyri
Akureyri
Iceland

SPRINGER–PRAXIS BOOKS IN GEOPHYSICAL SCIENCES
SUBJECT *ADVISORY EDITOR*: Philippe Blondel, C.Geol., F.G.S., Ph.D., M.Sc., F.I.O.A., Senior Scientist, Department of Physics, University of Bath, Bath, UK

ISBN 978-3-540-47569-9 e-ISBN 978-3-540-47571-2
DOI 10.1007/978-3-540-47571-2
Springer Heidelberg Dordrecht London New York

Library of Congress Control Number: 2011930134

Cover design: Jim Wilkie
Project management: OPS Ltd, Gt Yarmouth, Norfolk, UK

Printed on acid-free paper

Springer is part of Springer Science + Business Media (www.springer.com)

Contents

Preface

IS IT REALLY POSSIBLE TO PREDICT EARTHQUAKES?

When I mention to people that I am writing a book on advances in earthquake prediction, the response I often encounter is one of incredulity: "Is it really possible to predict earthquakes?" My short answer has for quite a long time been: "Yes, gradually and by intensive studies, we will be able to predict more and more aspects of an impending earthquake ..." Furthermore, we will also be able to provide useful information about the time of a future earthquake. My long answer—and my full explanation for those who have doubts—is in this book.

The opinion that earthquake prediction is and always will be impossible is very popular in both Western academies and leading scientific academies worldwide. This view is both negative and mistaken and has led to distrust and disregard of research whose main objective is to warn people of the imminence of an earthquake so that they can take measures to protect themselves and their families. Four to five centuries ago it was believed that the Earth was at the center of the Universe. The official science at that time maintained that "epicycles" could explain all the observable tracks of the stars and that the Earth stood in the center. When new observations did not fit the established system, astronomers simply added a new circle with its center on some of the older circle tracks. It took tremendous courage to change this religion-based scientific position to the new understanding that the Sun was at the center of our solar system and that the Earth and the other planets rotated around it. Not so many decades ago, cancer was considered incurable and some felt that it always would be. However, the determination of researchers to find a cure coupled with the firm belief that it was possible had the effect of pushing research forward, gradually leading to the cure of more and more kinds of cancer. At times when I found opposition to earthquake prediction research particularly difficult to handle, the director of the Icelandic Meteorological Office, Magnús Jónsson, would remind me that only half a century ago many academics believed weather

prediction would never be possible. OK, I thought, maybe weather prediction is not exactly a good example, but his words of encouragement always served to inspire me to do even better.

The academic discussion on earthquake prediction is often polarized and unconstructive. Academics on both sides of the debate regularly resort to polemics, where the main objective is to disprove the other side's theories instead of striving to get a constructive fusion of ideas and methods. You might argue that such is the way of reaching the truth in a free debate. But, is the debate really free? Money, political power, and academic power strongly interfere with constructive debate. For instance, the position that claims it is impossible to predict earthquakes can be very helpful to some politicians because it gives them an excuse for their lack of preparedness. They might furthermore rationalize that the money of taxpayers could be better spent on something more immediately useful, not on scientific games that will never play out in reality. This state of not knowing, not understanding, is also preferred by many landowners who do not want attention drawn to anything that might devalue their property.

Much of the discussion about earthquake prediction revolves around the definition proposed at an early stage by some scientists that the site, time, and magnitude of an earthquake, together with an estimation of error limits, had to be given as part of the prediction. This was probably thought to be necessary in light of so-called scientists whose motivation for predicting earthquakes was to seek popularity and admiration. When their predicitions failed, they would simply claim that they were in fact accurate, because seismic activity perhaps occurred closeby or maybe even around the same time. But should we let these so-called scientists hinder research into the most important challenge facing seismology: accurate earthquake prediction?

From the time that seismological measurements began, efforts to predict large earthquakes have mostly been based on discovering traces at the same site of smaller preceding earthquakes or on finding, on either a long-term or short-term basis, the characteristic patterns in seismicity that precede them. However, in our short history of seismology, large earthquakes seldom repeat at the same place. So, to find characteristic pre-earthquake patterns, scientists have to rely on statistics of seismic patterns preceding earthquakes at many places around the world in their search for common universal precursors that would help predictions at particular sites.

The basic model of earthquake occurrence frequently applied in seismic research is the simple mechanical model proposed by Reid (1910), which explains how tectonic forces bend the crust until the stress across a fault in the bent region exceeds its frictional strength. Despite more Earth-realistic models being developed, studies aimed at assessing hazards that are time-independent and those that are time-dependent (sometimes called "predictions") continue to be based on this simple model of Reid, on seismic history, and on good statistics. However, experience has shown us that no two earthquakes are the same. Moreover, the very faint signals preceding large earthquakes are never the same, not even at the same site. However, as I will argue, the basic physics of the process may be the same.

ADVANCES GAINED BY USING THE PHYSICAL APPROACH

In this book I describe some significant results of earthquake prediction research in the South Iceland Seismic Zone (SISZ). For almost 20 years this earthquake-prone area has been a test site where scientists from a number of European countries have participated in various projects. These research projects adopted a multidisciplinary approach that explored the physics of processes leading up to large earthquakes.

Among the main findings of this approach are the following:

- Earthquakes occur at sites where they have previously occurred. Earthquakes that occurred hundreds or thousands of years ago leave scars in the crust (i.e., volumes of heterogeneity that demonstrate the size of their faults). These volumes display a significantly different rheology compared with their surroundings. Rheology and heterogeneity within these volumes are significantly variable in time and space.
- Fluids migrating upward into the Earth's cold and brittle crust (where earthquakes occur) play a significant role in modifying crustal conditions in ways that favor rupture. This helps to determine where the next earthquake will occur and the size of the fault plane of an impending earthquake.
- Crustal processes taking place near faults of earthquakes that occurred hundreds of years ago can be observed decades before the sudden onset of a new large earthquake.
- No two earthquakes nor their preparatory processes are the same. We learn a lot about an impending earthquake by observing preparatory processes at the fault, finding the constitutive relationship that governs the processes, and then extrapolating that relationship into the future. Therefore, our approach to predicting an earthquake has a number of stages: finding the fault, monitoring the preparatory processes of the fault as precisely as possible, using our new understanding gained from the fault processes, and extrapolating this understanding to the close environment, to gradually ascertain the site, size, and time of the next large earthquake. Such real-time research (investigating every individual fault that is deemed suspicious) must be multidisciplinary and constrained by using all available observations when modeling the ongoing process.
- Useful warnings can be issued along the way, from the time we discover a fault showing signs of preparatory processes, which predicts the site of occurrence, right up to the time of rupture. Such warnings could be issued to the local Civil Protection group that finds itself closest to the fault by government agencies in cooperation with scientists and include information about how the group should prepare for the earthquake and directives on enhanced observations.
- The real-time monitoring and real-time research necessary to establish earthquake warnings is not only expensive, it is labor-intensive as well. However, humanity is the beneficiary of such investment. We are duty-bound to learn all we can about the forces of the Earth and their underlying processes in an effort to make it a safer place.

What we have said here about predicting earthquakes is just as applicable to predicting volcanic eruptions. Volcanic eruptions are generally believed to be easier to predict. We only need to listen to rumblings inside the volcano and measure the strains created when eruptive materials start to migrate upward through the crust. It is probably easier to detect the very moment an eruption starts as well. Nevertheless, the processes are comparable and both involve fluid–rock interactions occurring long before crustal rupture. For both volcanic eruptions and earthquakes, warnings can be issued at various stages of development (i.e., from the time the nucleating process is discovered up until the eruption).

OTHER GAINS BY USING THE PHYSICAL APPROACH

The study of forces and processes inside and below the Earth's crust can contribute significantly to the quality of our lives in a variety of ways. The driving force behind using micro-earthquakes for earthquake prediction research in Iceland was the ability to predict earthquakes and their effects. Yet the technology developed with this purpose in mind proved to be very useful for finding veins of hot water at depth in the crust and is now widely used to extract thermal energy. The discovery of water-conducting veins deep down in the crust may have significant benefits for life on Earth itself. All water on the Earth's surface comes from the Earth's mantle and is still coming from there—the speed of upward migration is particularly fast in rift zones. Along with the water comes an array of materials that both sustain and threaten life on Earth. Despite knowing quite a lot already about the atmosphere, the hydrosphere, and the biosphere, we still have much to learn about what is happening below us. Interactive studies of deep dynamic crustal processes, vital for earthquake prediction, and studies of hydrochemical processes in and below the crust may offer us knowledge and benefits far beyond anything we can currently imagine.

Ragnar Stefánsson

Roadmap and acknowledgments

This book is written for readers interested in earthquake prediction, maybe because they are living in earthquake-prone areas or simply want to know more about recent progress in earthquake prediction research. The book is meant to be understandable for a broad group of readers: geologists, university students, members of civil protection groups and rescue teams, community leaders and politicians in earthquake-prone countries, and non-specialist journalists. All these groups may find in this book answers to pressing questions regarding the possibility of providing warnings ahead of earthquakes.

The level of understanding will vary by both reader and chapter. The Preface, Chapter 1, and Chapter 8 are particularly relevant to those involved in the debate about the feasibility of earthquake prediction. Chapter 2 is of especial interest for those who work with science policy or are interested in understanding how innovative scientific work may be initiated and developed at both national and international levels. Chapter 3 concerns the tectonics and observational facilities in the test region, the South Iceland Seismic Zone, and should not only be of interest to geologists but also everyone attracted by geology and especially that of Iceland. Chapter 4 concerns observations of pre-earthquake signals and Chapter 5 is about modeling—these two chapters should be of interest to scientists and students who are studying the basic methods and approaches that have been applied during the last 20 years to understand physical processes preceding large earthquakes. In addition to the summary of observations given in Section 4.13, the main results of these two chapters are summarized in Chapter 6, along with general sketches of what happens before and during earthquakes. Finally, emergency service and rescue workers should find Chapter 7, which deals with earthquake warnings, especially interesting. The book overall should be of use to politicians, community leaders, and scientific advisors who live in earthquake-prone areas, as it provides the full picture of current earthquake prediction research, how it is applied in Iceland, and how it might be adapted to specific circumstances in other parts of the world.

Whether or not this is a textbook is a moot point, but for all those who adhere to creative learning—in high schools, colleges, or universities—they should consider it as such. Although it does not provide ready-made formulas or methods, it references articles, journals, and reports which delve deeper into the subject. This book is based on the first-hand experience of earth-watchers who are actively trying to understand the signals that come from the weak processes that precede large earthquakes. The writing of the book benefited from knowledge garnered from specialists in the basic sciences—seismology, physics, geophysics, chemistry. In writing this book, I have also applied the experience gained in cooperation with the emergency services, community leaders, and political leaders in attempts to mitigate risks, not only by providing early warning of earthquakes but also by constantly providing updates of hazards that are especially long lasting.

This book relates the story of the South Iceland Seismic Zone and its study. Although this is a nostalgic story—after two decades of work and a great deal of success—it is also a story of scientific development, how new results emerge, how people from different fields of science and different services can cooperate. It is a good example of how dedicated efforts can build toward significant results. This underlying lesson is significant for those aiming to build up the infrastructure for effective geohazard warning anywhere in the world.

Although this book is written by a single author, it is the result of dedicated work by many collaborators during two decades of multinational earthquake prediction research in the South Iceland Seismic Zone. While these researchers are mostly scientists and technical engineers—some of whom are mentioned in Appendix 2.B—many others have been involved, such as emergency service personnel, community leaders, politicians, and farmers, the latter are among our most reliable earth-watchers. They are too many to list individually, but they all contributed—in different ways and to different degrees—to the success of earthquake prediction research as presented in this book.

The center where the work was undertaken and the results achieved—making this book possible—was the Icelandic Meteorological Office (IMO). Its Geophysics Group, in collaboration with scientists from many countries, played the major role. The work behind this book enjoyed financial support from various EU framework programs for research and technological development, from the Nordic Minister Council, from science foundations in various Nordic countries, from science funds and institutions in many other European countries, and from the Icelandic Emergency Organization. The operation of significant geophysical monitoring systems in Iceland has been an invaluable source of data. The same is true of continued support from the Carnegie Institution of Washington to the strong borehole strainmeter network in southern Iceland.

As a professor at the University of Akureyri, Iceland, I want to thank the university for the support provided. I also want to thank my former institution, the Icelandic Meteorological Office and, of course, its Geophysics Group.

Many figures in this book were prepared and given to me by researchers who I have been closely cooperating with for two decades. Partly, this book is a tribute to their contribution to the earthquake prediction research which I try to describe here.

Appendix 2.B is dedicated to these people and describes their contribution. Many thanks to them for allowing me to use their figures in the book. In cases where the figures have been earlier published in journals, I have made full reference to them in the figure captions as well as to the journals in which they appeared. I have tried to obtain formal permission from copyright holders when that was needed and only received very positive responses. I thank them for this and also those journals and copyright holders who claim that such an application is not necessary when reusing the images in scientific publications. Every effort has been made to source and obtain copyright permission but with takeovers and mergers in the publishing industry it has not always been possible to trace the original copyright source. Apologies to any that have been overlooked for such reasons.

Special thanks to scientists Gunnar B. Guðmundsson, Sigurlaug Hjaltadóttir, Mathew J. Roberts, and Corinne Dempsey for their valuable help.

Ragnar Stefánsson

Figures

Abbreviations and acronyms

BSSA	*Bulletin of the Seismological Society of America* (a journal)
CFS	Coulomb Failure Stress
CMT	Centroid Moment Tensor
CFT	Coulomb Failure Threshold
DC level	Low-frequency level of amplitude spectra
EUROCODE 8	Regulations for designing earthquake resistant structures
EWIS	Early Warning Information System (a warning system for geological hazards)
EVZ	Eastern Volcanic Zone
FVT	Fast Visualizing Tool
FOA	(later FOI) The Swedish Defence Research Institute
FORESIGHT	Frequent, Observation-driven, Realistic Evaluation and Simulation of Interacting Geophysical Hazard Triggers
GMT	Greenwich Mean Time
GPS	Global Positioning System
GSM	Global System for Mobile Communication
HC	Horizontal Compressions
H-L	Hydrostatic–Lithostatic pressure conditions
ICPA	Iceland Civil Protection Agency
IMO	Icelandic Meteorological Office
InSAR	Interferometric Synthetic Apperture Radar
M	Magnitude of earthquake* (see footnote at the end of this list)
NCPA	National Civil Protection Agency
NEIC	National Earthquake Information Center
OACC	Oceanic Area Control Center
PGA	Peak Ground Acceleration
PGV	Peak Ground Velocity

PRENLAB I and II	Prediction REsearch in a Natural LABoratory (EC projects)
PREPARED	Earthquake prediction research to develop technology for improving PREPAREDness and mitigating risk (an EC project)
RETINA	Realistic Evaluation of Temporal Interactions of Natural Hazards
RP	Reykjanes Peninsula
SAU	Station name—SIL seismic station
SAFER	Seismic early warning system for Europe (an EC project)
SWS	Shear Wave Splitting
SIL	South Iceland Lowland
SIL Project	Earthquake Prediction Research in the South Iceland Lowlands (Nordic project)
SISZ	South Iceland Seismic Zone
SRAM	Seismicity Ratios with Assumed Mechanisms
TFZ	Tjörnes Fracture Zone
TRANSFER	Tsunami Risk ANd Strategies For the European Region (an EC project)
USGS	U.S. Geological Survey
VAN	Methodology suggested by Varotsos, Alexopoulos, and Nomikos
VAAC	Volcanic Ash Advisory Center
WVZ	Western Volcanic Zone

* M is based on the Richter magnitude scale of 1935. All magnitude scales are, in some way or another, made comparable with this scale. What we hear in the news media when reporting earthquakes is a single number for the magnitude, even if different methods, applied at different places, give different numbers for it. When magnitudes are used in scientific papers they refer to different attributes of the scale explaining how they are calculated. Some usual examples of magnitude scales include:

(1) m_b is based on the maximum amplitudes of body waves (P and S). This is frequently used for earthquakes at short or medium-range distances.
(2) M_s is based on the maximum amplitudes of long-period surface waves. This is often used for earthquakes occurring at long distances.
(3) M_L is based on the maximum amplitudes of small local earthquakes.
(4) M_w (moment magnitude) is based on calculating moment energy from earthquake records or other observations—the result is correlated to M on the Richter scale. Recently, it has often been used for very large earthquakes.

The Wikipedia page *p://en.wikipedia.org/wiki/Richter_magnitude_scale* contains a good overview on Richter magnitudes, has links to other magnitudes, and has many references to journals and reports about the subject.

About the author

Ragnar Stefánsson was born in Iceland in 1938. He studied in Sweden, mainly at the University of Uppsala, from which he graduated in 1966 with a Fil. Lic. (comparable with a Ph.D.). The focus of his thesis work was the study of focal mechanisms. After graduation, he became Head of the Geophysical Section of the Icelandic Meteorological Office (IMO), and held that position for 40 years. In 2006, he was appointed Professor of Geohazards at the University at Akureyri (Iceland), where he is now Professor Emeritus.

During his long time at IMO, he became known by many to be the main earthquake watcher in Iceland. As a result of his studies, he has been able to issue significant hazard information and successful warnings regarding earthquakes and volcanic eruptions. He was responsible for building up geophysical monitoring systems like the South Iceland Lowland (SIL) system (for automatic monitoring of seismic processes in Iceland) and the continuous GPS array and borehole strainmeter system (for monitoring crustal deformation).

He coordinated four large multinational research projects in the field of earthquake prediction between 1986 and 2006. In addition to this mainly European collaborative work, he has closely cooperated with scientists in the U.S.A., Japan, and India on projects in earthquake prediction research. He is an active lecturer and organizer of international conferences in geophysics and was Vice-President of the (ESC) European Seismological Commission between 1996 and 1998. The author may be contacted by email: *raha@simnet.is*

To my wife Ingibjörg Hjartardóttir

1

Introduction: Background to the work

1.1 THE DREAM TO BE REALIZED

Since the beginning of seismology 100 years ago it has been the hope of seismologists to be able to predict earthquakes in order to help populations across the globe avoid destruction and casualties. Nonetheless, earthquakes continue to occur without warning.

Throughout the decades, many have claimed to have noticed something unusual before earthquakes occurred, something akin to precursors to them. These included light phenomena, sounds, the anomalous activity of small precursor earthquakes, strange animal behavior, a change in ground water level, and even dreams. There is no reason to reject all such claims as the rantings of people who recently suffered a major earthquake. In some cases, people had already pointed out such phenomena before the earthquake struck. However, such experiences did not help in making predictions. Hence there predominated a pessimistic view about earthquakes, one that viewed them as among the many inevitably unpredictable forces of nature.

1.2 OPTIMISM AND PESSIMISM

1.2.1 The Chinese success in 1975

It was great news in the world of science and for people living in earthquake-prone areas when the Chinese succeeded in warning the local population about a large earthquake in Haicheng (a city in northern China) in 1975. The magnitude of the earthquake on the Richter Scale was 7.3. As a consequence of the warning, people were moved (at short notice) from several areas within the city to the outskirts. The city's inhabitants numbered 500,000. It was estimated that 90% of the buildings in the city collapsed in the earthquake, resulting in 2,000 people losing their lives. It has

R. Stefánsson, *Advances in Earthquake Prediction: Seismic Research and Risk Mitigation*,
Springer Praxis Books, DOI 10.1007/978-3-540-47571-2_1, © Springer-Verlag Berlin Heidelberg 2011

been estimated that the warning saved the lives of thousands of people, perhaps as many as 100,000 (Celin Wang *et al.*, 2006). The notion that earthquake prediction was possible was gaining impetus.

The Chinese prediction was based on a number of observations. To name a significant few, they observed small earthquakes, changes in the levels and chemical content of groundwater, changes in surface elevation, as well as changes in the magnetic field and electrical signals. Closer to the event, people noticed strange behavior in animals—in livestock as well as in wild animals. Animals that typically live underground appeared on the surface, apparently escaping some threat, possibly groundwater changes or other changes in their environment.

In short, the leadup to the Haicheng prediction was as follows. In 1970 a long-term warning was issued stating that a large earthquake was to be expected in this region of China. The region is a 1,000 km elongated area running northeast to southwest in northern China, where relatively high seismic activity had been noticed (Figure 1.1). This long-term warning was mainly based on measurements of earthquake activity, but some other observations supported this long-term prediction. It led to enhanced surveillance of the region. Many scientists were summoned to participate in this work and as a result more measurements were

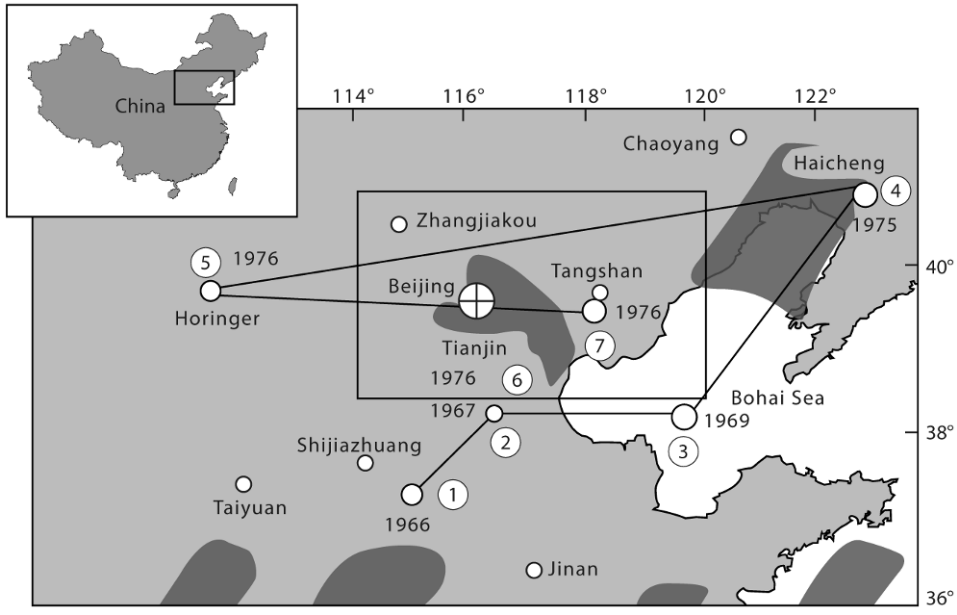

Figure 1.1. The northern region of China that suffered high seismic activity in the 1970s. Numbers in circles (1–7) show migration of large earthquakes through the region with time (between 1966 and 1976). The shading marks areas of expected high- to medium-range earthquake hazard (i.e., magnitudes between 5 and 6), as predicted at a national meeting of seismologists in 1974 (modified from Chen Yong *et al.*, 1988).

taken. Phenomena that are potentially associated with an impending earthquake increased gradually, especially during the final days before the event. Just before the earthquake, a short-term warning was distributed throughout the whole area on the morning of February 4, 1975. The warning announced that a large earthquake was going to occur that very day. Instructions about precautionary actions were distributed among the inhabitants. People moved to tents and temporary shelters that had been built previously. At half past seven in the evening the earthquake struck (Ma Zongjin *et al.*, 1990; Celin Wang *et al.*, 2006).

This successful prediction was, in addition to the general scientific understanding at this time, partly based on 1,000-year-old documentation of earlier earthquakes in this area and of even earlier observed phenomena and partly on the involvement of the many people carrying out measurements and observations of all sorts of phenomena that were precursors of an impending earthquake. This public involvement helped to make the public response to warnings so effective, even when they were issued on the day of the earthquake.

1.2.2 Optimism and a setback

The optimism that was gaining momentum about the possibility of earthquake prediction was significantly shaken the very next year (1976) when a still larger earthquake (magnitude 7.8 on the Richter Scale) occurred without a useful warning in the densely populated industrial area of Tangshan (Figure 1.1), 400 km to the southwest of Haicheng. It became known as one of the most destructive earthquakes in history. Its epicenter was directly under the large industrial city of Tangshan, which had a million inhabitants. It is estimated that 240,000 people lost their lives.

Located, as already stated, only 400 km from Haicheng, the Tangshan earthquake occurred in one of the earthquake zones that had been given the status in 1970 as long-term prediction zones (Figure 1.1).

There was much speculation advanced by Western media and academia, and by specialists all over the world, as to why a prediction had not been possible in Tangshan when it had been in Haicheng. Some blamed Tangshan's lack of predictability on political or administrative problems, while some scientists claimed that Haicheng's successful prediction was just a fluke.

1.2.3 Chinese seismologists were alert to the possibility of a Tangshan earthquake early in 1976

A number of Chinese seismologists, led by the State Seismological Bureau of China, held a conference early in 1976 (before the Tangshan earthquake) to discuss the general earthquake probability after the Haicheng earthquake of 1975. The conclusion of the conference was that seismicity in northeast China was still high and the ongoing intensive work in monitoring the region should continue for one or two more years in an effort to establish warnings for the next large earthquake. In June and July of 1976, just before the Tangshan earthquake, signals identified as possible

precursors to a new earthquake caught the attention of seismologists (Chen Yong *et al.*, 1988). According to studies conducted after the earthquake, scientists seem to have been baffled by the fact that these possible precursors were spread over a very large area, much larger than the area of the Haicheng earthquake. It is easy to conclude in hindsight that the scientists were looking too specifically for the same kind of precursor activity as was observed before the Haicheng earthquake, and that they should have understood, at an early stage, that widespread seismic activity was a sign of a much larger earthquake. Microseismic activity, comparable with what was so significant in predicting the Haicheng earthquake, seemed to be absent in Tangshan.

Post-seismic investigation indicated that many phenomena—like groundwater changes, strange animal behavior, electromagnetic anomalies, light phenomena, and earthquake sound—did appear in abundance one to two days before the Tangshan earthquake, but that these phenomena had appeared too late for the seismologists to evaluate the situation (Chen Yong *et al.*, 1988).

Chinese seismologists considered the lack of warning before the Tangshan earthquake to be a major blunder and a major setback to the enormous efforts and hopes that the Haicheng success had inspired. As a result, Chinese seismology suffered for many years to come.

It is nonetheless significant that Chinese seismologists succeeded in observing many changes in natural phenomena before the Tangshan earthquake, even if they did not have the knowledge or time needed to prepare a short-term warning (Chen Yong *et al.*, 1988). These observations are extremely significant for future earthquake prediction.

Many claim that the examples of Haicheng and Tangshan demonstrate the need for further field studies to ascertain the meaning of the observations we have made on the Earth's surface. We have to find out what causes the observed phenomena. We cannot limit our attempts at earthquake prediction by searching for statistical patterns among symptomatic phenomena. We have to approach the goal of earthquake prediction by better understanding the physics of the changes that precede large earthquakes. What do these symptoms reflect? Immediately apparent pre-earthquake changes are manifold and often differ between locations and even between earthquakes that occur at the same place. No two earthquakes are the same but the physics behind them suggests that, at a deeper level, they have much in common.

1.2.4 Predictions that fail to occur

Mistaken predictions add significantly to public disillusion regarding the possibility of earthquake prediction. The most widely noted and discussed "mistake" was prediction of the Parkfield earthquake in the U.S.A. Perceptions of the sophistication of American seismology had the effects of aggravating this mistake and contributed to serious disillusion about scientists' ability to predict earthquakes. Parkfield is located within the huge San Andreas Fault system in California (Figure 1.2).

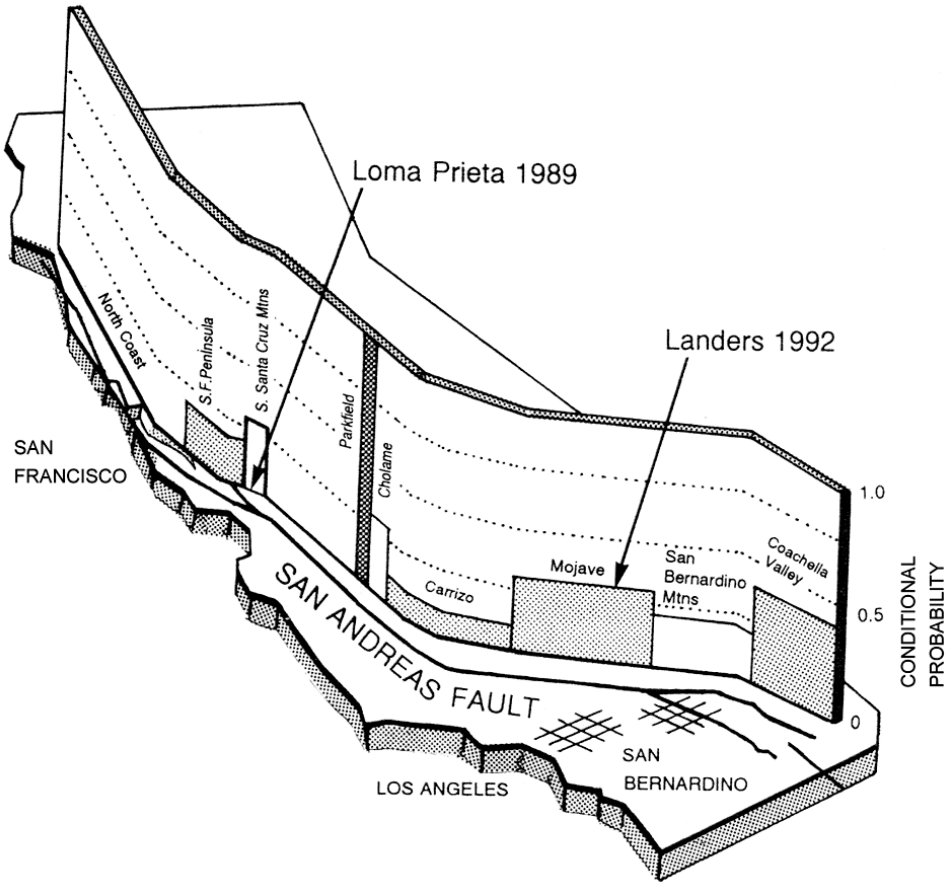

Figure 1.2. A map of California showing forecast probabilities of earthquakes to occur between 1988 and 2018 in the San Andreas Fault Zone. The map was published by the Working Group on Californian Earthquake Prediction and by the U.S. National Earthquake Prediction Evaluation Council. The figure shows the Parkfield fault segment's very high probability of suffering a large earthquake within the next 30 years (reproduced from Filson, 1988).

As seen in Figure 1.2, the Parkfield area is a small part of this huge fault system. In Parkfield six earthquakes with magnitudes around 6 occurred in 1857, 1881, 1901, 1922, 1934, and 1966. So, on average, there were 22 years between earthquakes. Armed with (1) this regularity, (2) knowledge of how earthquakes were expected to be released in this huge fault system, and (3) an explanation underlying the 1934 earthquake pattern (Figure 1.3), two scientists in California concluded that "the next characteristic Parkfield earthquake should occur in the 1983–1993 interval" (Bakun and McEvilly, 1984, p. 3057). As a result, the U.S. Geological Survey warned that an earthquake of magnitude about 6 was likely to occur, with 95% probability, in the Parkfield area by 1988 $\pm$ 5 years (Figure 1.2).

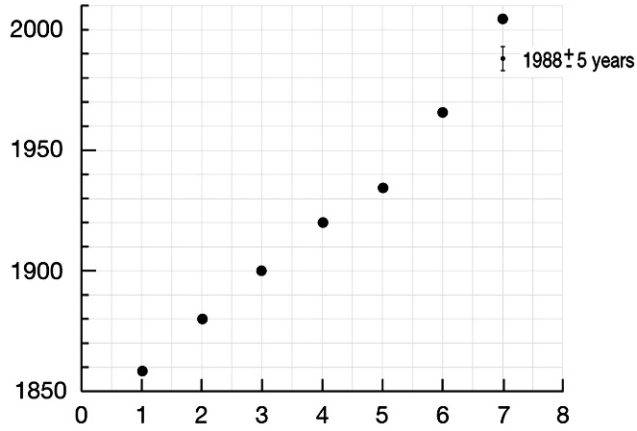

Figure 1.3. Points show the sequence of large earthquakes (magnitude around 6) in the Parkfield area, California, since 1850, the actual number in the sequence, and the year of occurrence. The vertical line shows the ±5-year margin-of-error bar of the predicted time of the seventh earthquake (i.e., 1988) (modified from Bakun and McEvilly, 1984). The time of the actual occurrence of the seventh earthquake (September 28, 2004) is shown by a point above it (modified from Bakun and McEvilly, 1984).

However, an earthquake close to this magnitude did not occur until September 28, 2004 (Figure 1.3). The pattern outlined above was studied using well-established statistical methods (see Bakun and McEvilly, 1984) and the prediction was based on these methods. I have no doubt about their validity. However, the model on which the prediction was based regarding crustal conditions governing the sequence of the Parkfield earthquakes was too simple—it was not Earth-realistic (i.e., did not take into account all known and relevant rheological parameters of the crust). Implicitly made assumptions that these conditions would be unchanged during the long time-span of the sequence were wrong. It is easy to speculate with hindsight that the Loma Prieta earthquake of 1989 (near Santa Cruz, magnitude 7.1) and the Landers earthquake of 1992 (Mojave, magnitude 7.6) (Figure 1.1) might have disturbed conditions governing the observed regularity of the Parkfield earthquakes. Moreover, the fault process that caused these two large earthquakes might also have directly influenced crustal conditions at Parkfield. Some have speculated that the initial earthquake in 1857 (Figure 1.3) may have transferred an elastic load to the Parkfield area and that the effects of this loading may well have faded out with time, resulting in longer time periods between earthquakes.

The physical grounds for this prediction were based on the elastic rebound theory developed by Reid (1910). It indicates that fault slip occurs when strain accumulation or shearing exceeds the strength of contacts between fault surfaces. So, if strain accumulates at a constant rate (which is a fair assumption for general and large-scale plate motion) and if the strength of the fault does not change over time, it follows that the time intervals between released earthquakes will be constant. The oversimplification here is to assume that the strength of the fault is unchanged

with time. If the pressure normal to the fault changes at a particular location, its strength will change. It is also an oversimplification to assume that strain accumulates at a constant rate in this particular part of the fault system. Strain releases at any place within the large fault system can cause significant disturbances in local strain accumulation at other places.

Despite these setbacks, scientists continued to search for patterns in the occurrence of small, medium, and large earthquakes and in other earthquake-related phenomena which might lead to predictions. With the increasing sensitivity and accuracy of seismic measurements, new pattern recognition methods have been developed. These have facilitated the statistical search for patterns in the fast-growing data stream for signals or precursors that might be common to large earthquakes. Nevertheless, progress continues to be meager, at least regarding the goal of issuing earthquake warnings that could help mitigate causalities.

1.3 EARTHQUAKE HAZARD ASSESSMENT

Earthquake hazard assessment is practiced all over the world to determine the seismic character of every region. These assessments suggest which earthquake effects (such as ground acceleration, intensity, etc.) can be expected in a given region during a specific length of time. The term commonly used for this method is "standard hazard assessment", indicating that it is based on generally accepted procedures for such assessments, which are still mostly based on statistical evaluation of the history of earthquakes in the given region. This history is by and large much shorter than the earthquake cycle there and varies according to the size of the regions considered. But the consideration of regions large enough for repetitions in time to be seen has the effect of lowering resolution. What is more, these large regions may vary widely in crustal conditions. The relative homogeneity assumed by such assessments thus becomes problematic. Knowledge of the near-surface structure is of course gradually being added to the general assessment. As knowledge about tectonics increases, it gradually finds its way into assessment procedures.

In his book *Earthquake Prediction*, Tsuneji Rikitake points out that even if stable periodicities have been found in some cases, "it is in many ways doubtful that periodicity study can be applied to earthquake prediction. It may be that statistical study of large earthquakes possibly enables us to estimate, to a degree of approximation, a probable return period of large earthquakes in a certain region. Such a study on earthquake risk is certainly useful for planning urban and industrial development, dam construction, earthquake insurance and the like. But such a study is quite useless for foretelling the occurrence of a particular earthquake that will strike a certain region next time because the conclusion from statistics is valid only for the mean state of the set of earthquakes analyzed" (Rikitake, 1976).

Hazard assessment as described here is sometimes called "prediction of a possible hazard", but (as Rikitake states) it is certainly not a valid prediction method as to the severity and time of individual earthquakes. It is thus of limited value for enabling individuals and governments to take preparatory action ahead of

earthquakes. As a result of our limited understanding of crustal processes, hazard assessment based on the historical periodicity of events is only helpful to a point. It is the standard method used by engineers and politicians for establishing building standards and by insurance companies for setting insurance fees. In such cases it is better to reach a kind of a consensus about what in general can be expected from the Earth's crust rather than listen to speculative theories about the crustal beast lurking beneath the surface. Lack of knowledge reduces the responsibility on our shoulders to provide warnings and prepare responses. Deeper knowledge of seismic behavior, on the other hand, puts responsibility on the shoulders of those scientists who think it is indeed possible to provide useful warnings about impending earthquakes.

Timeless (or time-independent) and time-dependent hazard assessments are better described in Appendix A.1, especially as practiced in Iceland.

1.4 PREDICTIONS "NOT IN THE MODE"

As a result of the inconsistency in prediction efforts, seismologists and other geophysicists concentrated on the release mechanisms of large earthquakes rather than on pre-earthquake processes. In any event, signals from pre-earthquake processes were often too small to be detected by the available monitoring technology and, most significantly, earthquake prediction was not the remit given to scientists by their funders.

The introduction of broadband seismometry and digital recording late in the 20th century added significantly to a better understanding of the release mechanisms of earthquakes in general. New ways of studying land deformation by GPS measurements and InSAR satellite radar images of the Earth's surface added considerably to our knowledge. This gradually led to better models for predicting the likely intensity and nature of potential earthquake hazards and thus for estimating the effects of probable large earthquakes on man-made structures in various places.

However, there has been little progress in estimating when and where individual earthquakes will occur. Moreover, the progress in predicting the effects of individual earthquakes was and still is meager. The Mexico earthquake of 1985 (Lomnitz, 1994), the Armenia earthquake of 1988 (Philip *et al.*, 1992), the Kobe earthquake in Japan (1995) (Dapeng Zhao *et al.*, 1996), and the great Indian Ocean Earthquake (the Sumatra–Andaman earthquake) in 2004 (Lay *et al.*, 2005) all had unexpected effects. The combination of the unexpected source functions of these earthquakes and unexpected surface responses led to their unexpectedly high destructive power. The same can be said about the magnitude-7 strike slip earthquake in Haiti in January 2010, which killed 230,000 people. The magnitude-8.8 earthquake, 10 km off the shore of Chile in February 2010, caused enormous material destruction and unleashed a tsunami. Half a million homes were damaged. The magnitude-9 earthquake near the east coast of Japan in March 2011 showed just how vulnerable highly

industrialized societies are to major earthquakes. In spite of progress in risk mitigation efforts, disastrous earthquakes still occur without prediction of their time of occurrence, location, and likely effect. This calls for international efforts, not only in preparation and rescue, but also in various preventative measures, including earthquake prediction research.

1.5 NEW MULTINATIONAL PREDICTION RESEARCH PROJECT IN ICELAND, STARTED 1988

In light of the harsh criticism of earlier methods and at a time when some claimed that earthquake prediction had reached a dead end, a decision was made to establish a multinational earthquake prediction research project in Iceland.

Instead of limiting our efforts to pattern recognition procedures and the study of observable phenomena without understanding well the physical significance of these phenomena, it was decided to concentrate on studying the physics of potential pre-earthquake processes. We assumed that such an approach would not only help us to provide useful short-term warnings, it would also give us better information about the source processes of the impending hazard, and thus the effects and destructive potential, before it occurred.

Increasing our knowledge of pre-earthquake processes would also help us to understand better the underlying causes of many other phenomena that have been observed before the occurrence of large earthquakes. We could thus make good use of them in our warning practices.

Further recommended reading about earthquake prediction research in general and about the Parkfield prediction in particular, besides what has been referred to in the text are Sykes (1971), Rhoades and Evison (1993), Ellsworth (1990, 1993) Kagan and Jackson (1995), Segall and Yijun Du (1993).

1.A APPENDIX

Seismic hazard assessment is used to indicate the probability of specific earthquake effects (acceleration, intensity) during a given length of time. Mostly it is based on historical documents about earthquake occurrence, at least regarding large and rare earthquakes. As our knowledge of tectonics increases, so will seismic hazard assessment.

Seismic hazard assessment is used to describe the character of a region (i.e., which earthquake effects can be expected in a specified region regardless of when). In many cases it is better to use the term "standard hazard assessment", indicating that the method is based on a generally accepted procedure for such assessments, which even today is based on statistical evaluation of the history of earthquakes in a region, a history of large earthquakes that is mostly much shorter than the

earthquake cycle there, depending of course on the size of regions being considered. However, by considering regions that are large enough for repeatability to be seen over given time periods has the effect of lowering resolution and—what is worse—may include significantly variable crustal conditions within the considered region. Relative homogeneity is implicitly assumed in such assessments.

A commonly used method to evaluate the seismic history of a region is the so-called Gutenberg and Richter relation $\log(N) = a - bM$, where N is the annual number of earthquakes larger than or equal to M (the magnitude). The constant $a = \log N$ is (as seen from the formula) the number of all earthquakes larger than or equal to 0. Thus b is an estimate of the relation between size and magnitude, while a is an estimate of the total number of earthquakes produced in a region. As we have an abundance of measurements of small earthquakes, it looks an easy matter (based on this formula) to find the frequency of large earthquakes by extrapolating the straight line of this linear relation. However, observations show deviations from a straight line when approaching larger earthquakes, for which observations are few. Moreover, we know from tectonics that there is an upper limit to the size of earthquakes in any area. In the South Iceland Seismic Zone (SISZ), magnitude 7.2 (M_s) is assumed to be the upper limit. This assumption of an upper limit of magnitudes is based on the size of the crustal volume where stress is being built up, the thickness of the elastic/brittle crust, and the possible length of a zone that may be activated in one earthquake. However, the Gutenberg–Richter method would indicate unlimited size, and thus is not realistic for expressing the number or probability of occurrence of large earthquakes. So, based on the data, some other methods expressing distribution with upper bounds of observations of large earthquakes have been used (i.e., a statistical extreme value method), like applying Gumbel's third distribution method of extreme values (as developed for earthquake hazard assessment by Burton, 1979).

Halldórsson (1992), applying Gumbel's third distribution in Iceland by using only the extreme value of magnitudes for every 10-year interval, gives the following distribution of magnitudes:

$$M = w - (w - u)(-\ln(P(M)))\exp(1/k)$$

The parameters used in this formula are adapted interactively to fit the real distribution of observed magnitudes. The parameter w indicates the upper limit of the distribution. An important part of hazard assessment is (interactively with the distribution of magnitudes) to estimate attenuation with distance of the intensities observed in the historical data. For further discussion see Burton *et al.* (1985).

Results indicating the largest probable intensities (accelerations or velocities of ground motion) are then put on a hazard assessment map such as the map of Iceland shown in Figure 1.4.

Besides the references given so far, I recommend Lomnitz (1994) for further study of hazard assessment procedures.

Standardized hazard assessment is a kind of a "techno-economic" procedure that standardizes the best possible use of generally accepted knowledge and includes a simple model for crustal behavior. It is a basis for worldwide engineering efforts to carry out risk analysis in a uniform way, to create standards in building regulations,

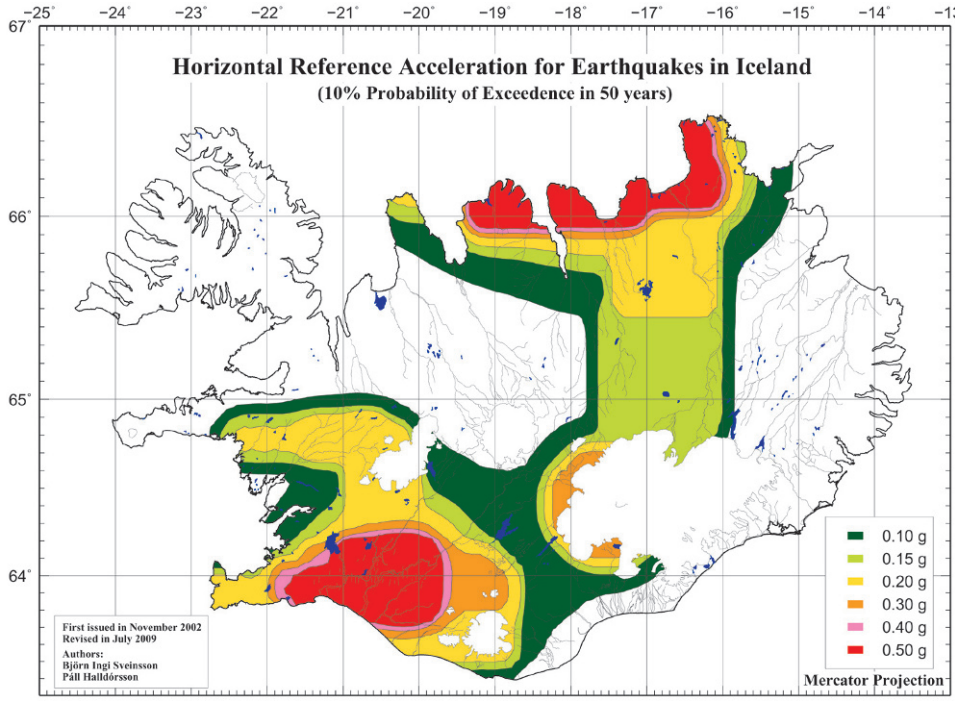

Figure 1.4. Division of Iceland into areas of probable maximum horizontal ground acceleration every 500 years. There is a 10% probability that the acceleration indicated in this map will be exceeded over a 50-year period. This map forms part of EUROCODE 8 for Iceland. Red indicates areas where gravitational acceleration may reach 40% (g) or higher (published by Staðlaráð Íslands).

and for insurance companies to decide the insurance rates for various sites and various types of man-made structures. Gradually a greater understanding of fault characteristics, crustal structure, and surface response will be built into standard hazard assessment, increasing information on the probable effects at any spot on Earth.

As is the case for many kinds of law-making, conservatism or adherence to standard methods tends to prevail over desires to increase our understanding of crustal behavior, although in time new results from earthquake prediction research and other geoscience research will find their way into standard earthquake assessment, but only when they have been proven beyond any reasonable doubt. This conservatism is understandable from the point of view of builders, who follow building regulations strictly, and do not like any scientific data that would devalue their houses. However, from the point of view of those who live in these houses this conservatism must not hinder further studies and the issuing of useful warnings.

Despite the limitations, such assessments are significant, especially if they are understood for what they are (i.e., indicating which hazards are probable in light of

our present knowledge). They help to tell engineers and builders where and how to construct houses and other facilities. They are taken into account in making building standards and regulations. Every site on Earth destined for building undergoes hazard assessment. This assessment will change with time, but only very slowly and only if any new understanding is generally accepted.

Standard hazard assessment will not change with time unless any new understanding can be proven. Conservatism enjoys the benefit of the doubt. When I was in Japan several years ago, as part of a group of seismologists and engineers, I visited an earthquake museum. It was a house built on the fault of a recent large earthquake—with the purpose of being able to look into the fault. An American engineer in the group was shocked. "How can you do such a thing? This house will collapse in the next large earthquake occurring on this fault." The Japanese guide answered: "It is not such a big problem, the next large earthquake on this fault will occur after about 800 years." "But the probability of such an earthquake is the same now as it was before this earthquake occurred," the American engineer responded. "In the standard hazard assessment procedure every earthquake is independent of another even if it occurs in the same place," he proceeded. "You see," the Japanese guide replied, "if we would follow your rule we would build no houses in Japan."

The fact of the matter is that in classical hazard assessment (i.e., the assessment used for building regulations and for insurance) every earthquake is treated as independent of other earthquakes in the area in question. The brief earthquake history that is avilable to us limits hazard assessment procedures to identifying places that have suffered destructive earthquakes during the last hundred or few hundred years. From a very few events we try to assess the expected repeatability period for destructive earthquakes for a given site and make the assumption that tectonic conditions remain as they have been during this short period of time.

1.A.1 Time-dependent hazard assessment

Standard hazard assessment is sometimes called "timeless hazard assessment". In contrast, time-dependent hazard assessment involves the assessment of hazard for a given timeframe. The probability of having an earthquake of given intensity or magnitude within a given time changes with changing conditions in the crust. The usual assumption is that overall differential plate motion velocity is constant and rheological conditions or other conditions influencing strength also stay constant. If this can be assumed, and if we know the recent history of large earthquakes in the zone, we may be able to estimate with some confidence the time and size of the next earthquake in the zone. If we can assume that the largest possible earthquake for the zone has recently occurred it is probable that another earthquake in the same place and of similar size would be delayed, compared with what would be expected from timeless standard hazard assessment—that is, a protracted interval since the last earthquake in a given place would make it likely for an earthquake to occur within a relatively short time. A typical example of time-dependent hazard assessment is the forecast probabilities of occurrence of large earthquakes in California for a 30-year period starting in 1988 (as described in Section 1.2.4).

Time-dependent hazard assessment is made under the plausible assumption that the stress and strain that result in earthquakes is released in each earthquake and it will take some time for ongoing plate motion to build up the same conditions for a renewed earthquake at the same place (say, on the same fault). In time-dependent hazard assessment we take into account the velocity of strain buildup and time elapsed since the last earthquake. On the basis of a few hundred years of known earthquake history, we can assess the time of the next earthquake (i.e., by assuming that strain energy was totally released in the last large earthquake, by assuming constant plate straining velocity, and by assuming knowledge of crustal rheology). This is sometimes called ''long-term prediction''. Such a prediction contains many uncertainties. One of the uncertainties lies in the fact that historical statistics rely on very few events, and on events that occur under variable conditions and even on different faults. Of course, these facts also weaken timeless hazard assessment. In trying to use the same data as for time-dependent assessment, the number of unknown parameters for calculations is increased. Such assessments are in general too weak to be a basis for changing building regulations or for alerting people to earthquake effects. Moreover, such predictions cannot predict individual earthquakes. At the most they can predict the general probability of occurrence of earthquakes in the area. Time-dependent hazard assessment is significant for selecting places that warrant scientific concern and intensified watching, and much more so when more information is gathered and when we understand better the ongoing processes in the area.

Time-dependent hazard assessment has been routinely carried out in Iceland by the staff of IMO in the following way (Páll Halldórsson, pers. commun.). Let us assume the zone in question is the SISZ, that it was totally relaxed after the last large earthquake in 1912, and that straining of the zone increased linearly by plate motion of 2 cm/year after that. In practice we always calculate the probability of an earthquake to occur during the next 20 years by calculating the probability of an earthquake occurring during a period of time which was 20 years plus the time from the last large earthquake in the region. Time-dependent hazard assessment calculated in this way for the SISZ just before the 2000 earthquakes showed a 95% probability that an earthquake of magnitude 6 or larger would occur in the SISZ during the next 20 years.

Other more sophisticated methods for time-dependent hazard assessment are described by Lomnitz (1994) and Stein (2006). However, in their cases the underlying simplifying assumptions are basically the same: constant strain rate and constant rheological conditions.

Time-dependent hazard assessment even if it is too uncertain to use for building regulations and issuing warnings to people has been shown to be very useful for making choices about the monitoring and scientific efforts necessary to pave the road to improved information services and warnings.

2

A new approach to earthquake prediction

The decision to set up an international earthquake prediction research project in Iceland was taken in the 1986–1988 timeframe, a period characterized by growing pessimism worldwide about the possibilities for earthquake prediction research.

In the early 1980s the Council of Europe decided to encourage research into earthquake prediction in the European area. As part of this it allocated a few test areas, known for major earthquakes, where cooperative multinational research efforts could be concentrated. The South Iceland Lowland (SIL), with its history of hazardous earthquakes, became one of these areas (Figure 2.1). It is a highly productive farming area and, relative to the rest of Iceland, a densely populated region.

The 70 km long South Iceland Seismic Zone (SISZ) extends from east to west through this area (Figure 2.2).

The Nordic countries (Iceland and Scandinavia) took up the challenge posed by the Council of Europe. Since 1988 Iceland, especially the SIL, has been a European test area for earthquake prediction research. The basis for the creation of this test area and its value to research is fourfold: high earth activity, many favorable natural conditions, the gradual buildup of high-level geophysical monitoring systems and other forms of scientific expertise, and the quality of the science undertaken (Stefánsson *et al*., 1993).

2.1 ICELAND AS A NATURAL LABORATORY

Most earthquakes around the world occur at plate boundaries in zones that can be several kilometers to tens of kilometers wide called ''seismic zones''. Shearing strain builds up in response to plate motion and is mostly released during small and large earthquakes, when stress has exceeded the fracturing resistance of the crust at

R. Stefánsson, *Advances in Earthquake Prediction: Seismic Research and Risk Mitigation*,
Springer Praxis Books, DOI 10.1007/978-3-540-47571-2_2, © Springer-Verlag Berlin Heidelberg 2011

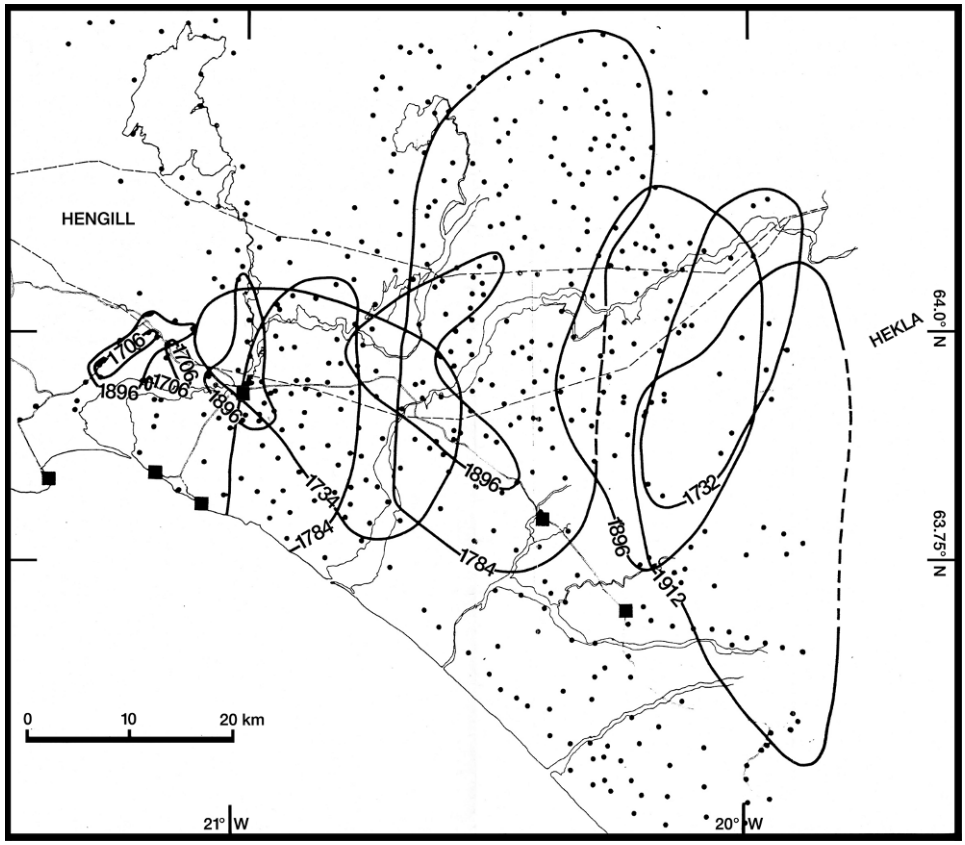

Figure 2.1. The contours show areas that suffered earthquake destruction in the SISZ of southwest Iceland between 1700 and 1912 (Figure 2.2 shows this area in relation to the SISZ and Iceland proper). Within the contours half of all farmhouses collapsed as a result of individual earthquakes. The year of occurrence is marked on the contours. The dots indicate the farms from which information was gathered. The squares show small villages. The epicenters of the earthquakes are along the SISZ which is oriented east–west and finds itself between two rift zones, with the frequently active Hekla volcano at the eastern end and the currently less active Hengill volcano at the western end (reproduced from Almannavarnaráð, 1978; see also Björnsson and Einarsson, 1981; basic data about the degree of destruction are from Thoroddsen, 1899, 1905).

various places within the zones. Ultimately the strain is released triggering large earthquakes with displacements across fault planes from the surface through the whole elastic/brittle part of the crust down to deep ductile levels, usually some 10 km to 30 km in depth. There are also much deeper earthquakes that extend a few hundred kilometers down in what is usually considered to be the uppermost part of the mantle. Their fault planes do not get near the surface and they are not as harmful, relative to their size, as shallower earthquakes.

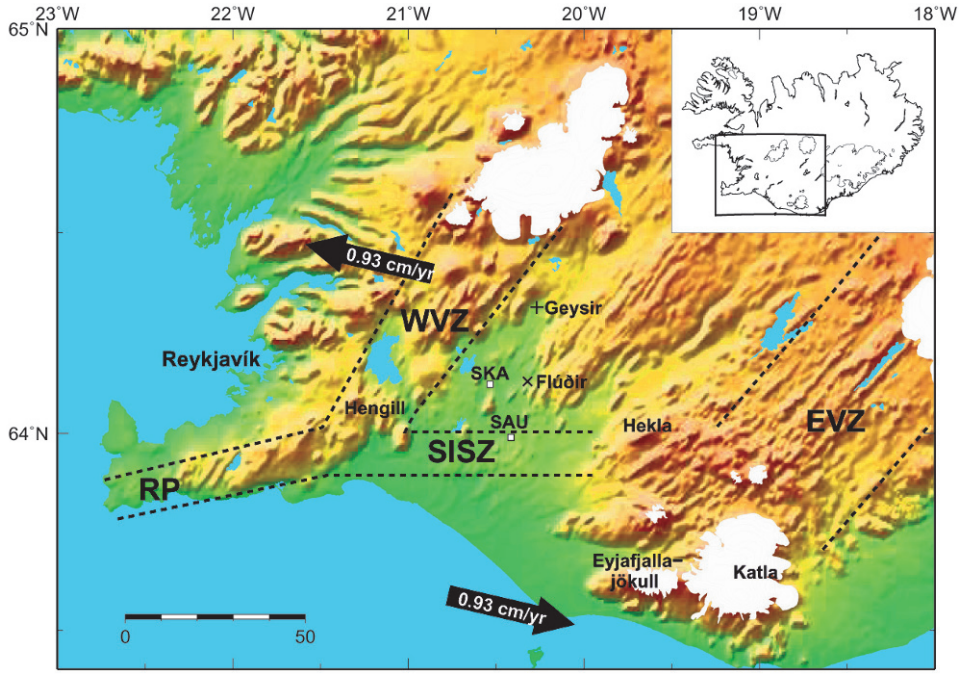

Figure 2.2. The southwestern part of Iceland. Dotted lines denote the Western Volcanic Zone (WVZ) and the presently more active Eastern Volcanic Zone (EVZ). The SISZ (a transform zone) is indicated along with its prolongation in the Reykjanes Peninsula (RP), considered to be a mixture between a transform zone and a rift zone. The direction of relative plate motion is shown by arrows. Hekla, Katla, Eyjafjallajökull and Hengill are volcanoes. SKA, SAU and Flúdir are measuring sites. Geysir is the site of the famous geyser and hotsprings.

With this seismological information in mind let us explore the reasons that Iceland, with its geological extremities, has been selected as a test area to study processes of large earthquakes in general.

What is common to large earthquakes in Iceland and in many other active tectonic regions is that large earthquakes cut through the whole elastic/brittle crust, from ductility at depth to the surface. This means that the fault environment is rheologically strongly heterogeneous. This is very significant especially when studying the faint pre-earthquake crustal processes that are expected in the vicinity of large earthquakes anywhere. The brittle/elastic part of the crust in Iceland is thin; that is, the depth down to the ductile part of the crust is shallower in Iceland than in typical continental areas or subduction zones. Hence it is easier to sense faint pre-earthquake processes in Iceland than in many other places.

Large earthquakes in Iceland, especially in the SISZ, are typically of the strike slip type (see Appendix 2.A about earthquake mechanisms). They occur by means of near-horizontal shear slip (strike slip) on a vertical fault plane. It has been claimed that the SISZ, with its earthquake magnitudes of 6–7, bridges the gap between

laboratory model zones and the huge transform (horizontal strike slip) fault zones of the world with their much larger earthquakes. But normal faulting is also common in the adjacent rift zones of Iceland. Even thrust (reverse) faulting appears in Iceland (as small earthquakes), but is mostly of secondary significance compared with strike slip and normal faulting.

Appendix 2.A contains some basic information on earthquake faults and the micro-earthquake technology used to study them. It gives a breakdown of how the mechanisms of small earthquakes are studied and of how technology is used for accurate relative location and absolute hypocenter location when swarms of micro-earthquakes occur.

The buildup time for large earthquakes can vary extremely. Intervals of the order of 100 years are typical for some zones although intervals of tens of years or thousands of years are also found. The length of time between earthquakes is related to regional velocity of strain buildup across plate boundaries as well as on material or rheological conditions in the crust and in the upper mantle near these boundaries. In general, a large compression across faults, such as occurs in thrust faulting (reverse faulting), would delay faulting compared with what is expected in normal faulting where earthquakes occur at lower compressional stress (i.e., at relative tension). But, as discussed in Chapter 1 (which dealt with the Parkfield earthquakes), the length of the time intervals between earthquakes also depends on the spatial and temporal pattern of recent earthquakes as well as on other kinds of strain release at nearby places.

The length of large transform zones, such as the San Andreas Fault zone in North America or the Anatolian fault zone in northern Turkey, are around 1,000 km. One of the largest single earthquakes on Earth since measurements began was the Sumatra–Andaman earthquake of 2004. Its fault was around 1,500 km long (Chieh, M. *et al*., 2007). This earthquake involved thrust-faulting caused by subduction of Indian Ocean crust under the continental crust of Sumatra. The length of subduction zones takes on the size of continents.

The length of the South Iceland Seismic Zone is less than one-tenth of the San Andreas or the Anatolian fault zones; it is only 70 km long. But, physically it contains many of the features of the larger zones and in many ways is easier to study. The Icelandic SISZ is a sharply defined transform zone linking together two rift zones: the EVZ and the WVZ of Iceland (as seen in Figure 2.2).

Rift zones (like subduction zones) extend across a large part of the globe. They are characterized by normal faulting, caused by general plate tension and local opening processes which are often volcanic. Relatively small earthquakes characterize rift zones. Basaltic fluids released from the mantle or from plume heads, at around a depth of 100 km, fill in fissures that open in the crust. Sometimes these magmatic fluids rise close to the surface, resulting in the extrusion of lava and volcanic ashes. Deep down in the ductile material the plates continuously drift apart. Looking at the wide span of rift zones, we find that the crust is continuously

being deformed, stretched by plates drifting apart. This eventually leads to local rifting episodes at the ridge itself, concentrated in the shallower elastic/brittle crust, resulting at times in large surface slips and eruptions. Large strike slip earthquakes occur at bends in rift zones, sometimes called transform zones, such as the east–west striking SISZ and the more complicated Tjörnes Fracture Zone off the north coast of Iceland (see Chapter 3 and Figures 3.1 and 3.2).

The relatively short ridge segments in Iceland possess all the main features of the huge rift zones of the globe. Much rift opening in Iceland today takes place in the Eastern Volcanic Zone (EVZ). Westward transform motion or horizontal shearing along the SISZ is left-lateral to comply with the opening of the EVZ. The Tjörnes Fracture Zone (TFZ), off the north coast of Iceland, is as a whole a right-lateral transform zone (Figures 2.2 and 3.2). Rift opening in Iceland interacts with the buildup of strain and stress in transform zones.

Below depths of 10 km to 20 km, continuous slip is expected across transform zones, but this is intermittently released as earthquakes in the brittle/elastic crust above. Iceland has sometimes been described as a test sample, intermediate in size between laboratory rock samples and the huge transform fault zones of the world. Here, the push or drag from rift zones creates input comparable with the input of pressure or shearing stress on a laboratory rock sample. The selection of the SISZ as a test area was influenced by this simple and clear configuration: the combination of a rift zone that is actively pushing or pulling and the shearing of a transform zone where large earthquakes occur. As we will see in later chapters, these relations are much more complicated than they may at first appear.

Another reason for selecting the SISZ as a test area was the expected return of large earthquakes or earthquake sequences every 100 years or so. The latest large earthquake sequence, before the 2000 earthquakes, occurred between 1896 and 1912, around 100 years earlier. So, renewed activity was expected to be imminent.

A further significant reason for proposing such a research effort in Iceland was the lack of sediments on the Earth's surface. The ice mass of the last ice age and the resulting floods leached soil from the surface while it receded around 10,000 years ago. In many places this left cracks and faults which can be seen at the surface of the bedrock. In addition, scant vegetation allowed for better observation of geological features and deformations.

When the Nordic countries—Denmark, Iceland, Norway, and Finland—took up the challenge of setting up an earthquake prediction research project in Iceland, based on the resolution taken by the Council of Europe, which proposed the South Iceland Lowland (SIL) as a test area, the SIL project was born. This initiative very naturally was led by scientists in Iceland, the only Nordic (Scandinavian) country where large earthquakes frequently occur. Iceland is traditionally considered by Nordic countries as a "natural laboratory in geophysics research", a phrase stemming from the famous Swedish seismologist Marcus Båth in a paper about the crustal structure of Iceland (Båth, 1960). Iceland has earthquakes, volcanic eruptions, and other geological processes that can be observed in real time. Processes that occurred millions of years ago in other parts of the world, lasting for thousands of years, have occurred in Iceland during the last 100 years of geophysical monitoring.

In the other Nordic countries, scientists taking part in ongoing high-level seismological research looked forward to testing their advances and hypotheses in the "natural laboratory" that is Iceland.

2.2 STATISTICS ON PHENOMENA PRECEDING EARTHQUAKES

SIL is the acronym adopted for the project, the full title of which was "Earthquake Prediction Research in the South Iceland Lowland".

As mentioned above, the SIL project was initiated at a time of growing skepticism about the possibilities of earthquake prediction. Seismologists were divided into two strongly opposed groups: one claiming that earthquake prediction was not possible and would never be possible; the other group claimed that at least some earthquakes could be predicted. In reality these disputes were about the validity or capability of the scientific method that was currently in use.

The method that was most commonly applied was a statistical approach to discovering, in time and space, typical patterns of medium and large earthquakes that might precede still larger earthquakes. The basis for these statistics came from earthquake lists in seismological bulletins from the prior century. Some other types of patterns had been observed before large earthquakes—such as changes in groundwater depth, tilting of the ground, and animal behavior—which also became targets for statistical analysis. All these patterns, including those described in seismological bulletins, have to be considered phenomenological as long as their physical connection to an impending earthquake is not well understood.

Statistical studies of such phenomena may be of great importance in predicting repetitive identical events. However, earthquakes are rarely if ever the same, even when they occur at the same place. During the past 100 years of reliable available observations, large earthquakes have hardly been repeated in the same place.

In order to use forerunners from one earthquake to help us predict another, we need a better understanding of the physics of the process leading up to them. The physics behind past and future earthquakes may well be similar, although the observed forerunners may be quite different, occurring as they have at different places and different times. Even if the place is the same the available observations may differ significantly.

Influenced by earthquake prediction research in many countries and also by critiques aimed at statistical studies of badly understood, but frequently observed phenomena before earthquakes, the SIL group decided to pursue the physical route. In other words, they aimed to concentrate their studies on the physics of the processes leading up to large earthquakes.

2.3 THE PHYSICAL APPROACH TAKEN BY THE SIL PROJECT

The SIL group sat on the fence in the ongoing dispute about whether or not it was possible to predict earthquakes. We admitted that some of the criticism of earlier

prediction work was well founded. However, we maintained that, for the sake of progress, we had to study the physical processes leading up to large earthquakes, applying all available and emerging technology.

The following guidelines were established from the very beginning of the SIL project:

(1) The fundamental requisite to predict earthquakes is understanding the physical processes leading up to them.
(2) The best way to study these processes is to retrieve information from very small earthquakes (down to magnitude 0). Small earthquakes occur all the time in seismic zones, near the plate boundaries, and can provide, in time and space, detailed information about the conditions below. If we can develop methods to retrieve information from the signals of small earthquakes, we might be able to assess prevailing stresses near their sources. We could also gather information about the nature of fractures at their origins and about variations in the velocities of their signals on their way to the surface, which reflect stresses along their paths.
(3) This task, which could involve monitoring thousands of micro-earthquakes per day, would require the development of new methods for automatic acquisition of seismic signals, and for automatic, real-time evaluation of the enormous amounts of information carried—almost continuously—up to us from deep in the crust. Automatic, real-time evaluation would also make it possible to provide short-term warnings if likely short-term pre-earthquake activity could be recognized from the data.

More about the basis and the first years of the SIL project can be found in Stefánsson *et al.* (1993).

2.4 THE HUMAN DRIVE TOWARD EARTHQUAKE PREDICTION

The drive to predict earthquakes in Iceland stemmed from the experiences of large earthquakes that caused widespread devastation in the SISZ 100 years ago. As a long-time earthquake watcher and an Icelander who has inherited this drive, I considered it most unsatisfactory to have to limit my activities to describing earthquakes after the fact. Volcanic eruptions could be predicted by observing small earthquakes and crustal deformations. This experience was significant in creating the SIL project. Could not earthquakes be predicted in ways similar to volcanic eruptions? By applying modern technology we might be able to record probable pre-earthquake processes. We expected that the pre-process of an earthquake would not be as easily observable as the penetration of volcanic material up through the crust before a volcanic eruption. Such penetration causes considerable strain changes, which are observable by conventional seismometers, strain meters, or tilt meters (Figure 2.3). We expected much weaker processes before earthquakes. We hoped that by increasing our sensitivity to detect very small earthquakes

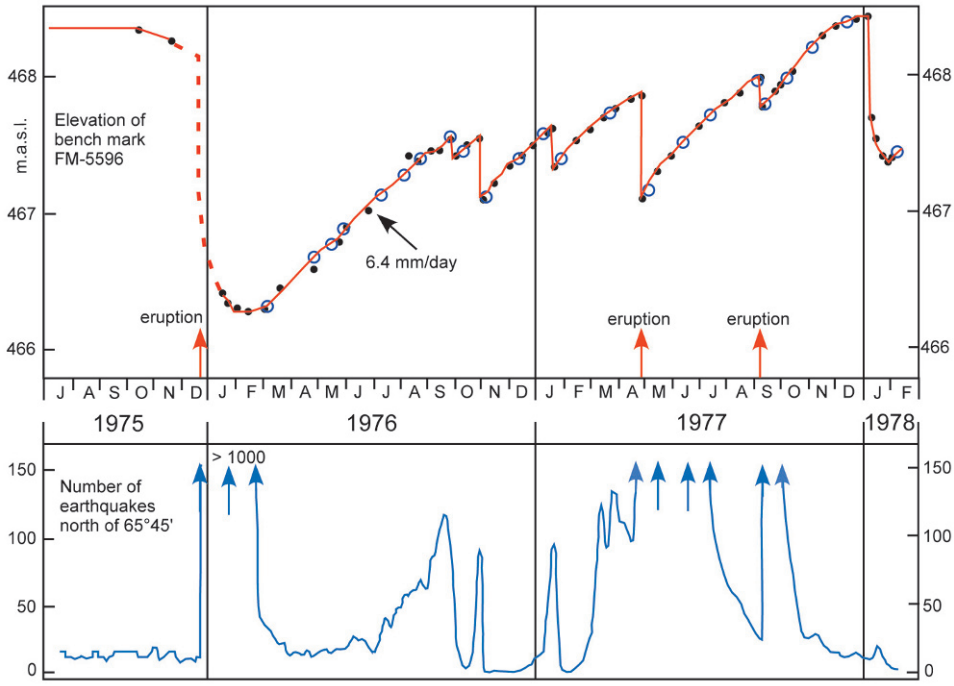

Figure 2.3. Monitoring in the first years of the Krafla rifting episode (1975–1984). The upper graph shows changes of land elevation in meters based on tilt measurements at the Krafla power station, 3 km south of the central volcanic activity. It also shows times of new eruptions. The lower graph shows the number of recorded earthquakes close to the volcanic caldera Krafla (from Björnsson *et al.*, 1979).

(micro-earthquakes) and by utilizing in full the information carried by them, we would be able to monitor and understand pre-earthquake processes as well.

By counting small earthquakes, studying their sizes, and observing strain meters and tilt meters, we have been successful in predicting eruptions in some cases. During the Krafla volcanic and rifting episode in north Iceland (NVZ in Figure 3.2) between 1975 and 1984, several eruptions were predicted on the basis of elevation changes and earthquake activity shortly before the eruptions (Figure 2.3). This activity was caused by the flow of molten lava up into the shallow part of the crust, resulting in measurable land elevation, high fluid pressure, and swarms of small earthquakes preceding the eruption.

According to many seismological studies around the world, typically occurring small earthquakes disappeared in many cases shortly before the occurrence of large earthquakes. Many studies based on seismological bulletins identified this phenomenon as "quiescence before large earthquakes". However, a period of quiescence did not warrant making predictions. It was a period when there was no information, at least no seismic information. What was the quiescence telling us? Was it simply because the sensing system was not sensitive enough?

It was considered probable by many scientists that unusual seismic activity patterns, often noticed before earthquakes, were caused by the beginning, or acceleration, of slow slip motion across the fault, at a depth below the brittle–ductile transition (e.g., see Tse and Rice, 1986). This slow slip would in turn cause a relocation of stresses in the elastic/brittle part of the crust and thus variations in micro-earthquake activity. To be able to give useful short-term warnings ahead of earthquakes we would have to take such stress relocations onboard. We assumed that any acceleration of deformation would be expressed in micro-earthquakes above the brittle–ductile boundary if our measuring facilities were sensitive enough.

We further assumed a period of quiescence only meant that there were no earthquakes recorded that were larger than 3 to 4 in magnitude, which during the 20th century was the typical lower limit of sensitivity reported by worldwide seismological bulletins. We expected 100 times as many earthquakes of magnitude 0 than of magnitude 2 and 10,000 times as many earthquakes of magnitude 0 than of magnitude 4. All observable seismic activity contains information, almost continuous in time and space, of changing conditions in the crust.

2.5 DESIGNING A NEW TYPE OF SEISMIC SYSTEM

Modern technology should make it possible for us to resolve and extract information from the steady stream of small earthquakes and to understand the significance of the messages we were getting. Of course we could not be sure that we would find seismic premonitory activity that would directly help us to make useful warnings ahead of earthquakes. Even if that were not the case, micro-earthquakes held the potential of offering us the information necessary to better understand conditions deep in the crust and for creating more Earth-realistic models of its behavior. By Earth-realistic models I mean models that take into account all known and relevant rheological parameters of the crust.

We would need to run operations for a long time before we could show that we were on the right track. Funding for projects is often generous at the beginning, but the funders get impatient if costs add up over time without any publicly observable results. So the operational cost of the system had to be low. Much effort in designing the system was concentrated on keeping the operational cost as low as possible without cutting down on the information we wanted.

We could also build up public support and funding if our research yielded a by-product that was immediately useful even if we could not get information to help us predict earthquakes for some time to come. One such by-product could be the location of fissures down in the crust that are often conduits for hot water. Since work in the field of hazards and warnings involves the negative task of bringing bad news, the ability to find sources of energy, with immediate financial benefits, could help bring the project into a more positive light.

Designing of the new seismic system, the SIL system, took into account the consideration above. In theory it was possible to become more sensitive to small

seismic signals than before and to extract more information about these signals than had been possible before. But would this be possible in practice?

Two key individuals—in cooperation with us in Iceland—handled the tasks of building a monitoring and evaluation system that fulfilled our objectives: Reynir Böðvarsson (see Appendix 2.B), at that time a research engineer at the University of Uppsala in Sweden, and Ragnar Slunga (see Appendix 2.B), a physicist then at FOA (later FOI), the Research Defence Institute in Sweden. Böðvarsson is Icelandic and had demonstrated great expertise at monitoring volcanic activity in Iceland. Ragnar Slunga is Swedish and, at the beginning of the SIL project, already had 15 years of experience in developing methods for finding the source mechanisms of very small earthquakes. These two were influential within the Nordic group in designing the SIL project and have since that time (1986) been principal cooperators with the IMO group in earthquake prediction research efforts in Iceland.

Appendix 2.B is a short report about the IMO group (the Icelandic Meteorological Office group) as well as about some of the other scientists mentioned in this book.

2.5.1 Realization of the SIL system

The SIL Monitoring and Evaluation System was the most significant outcome of the SIL project. We succeeded in meeting the design criteria above, both as concerns sensitivity as well as the ability to evaluate a huge amount of high-quality data in near–real time, providing information about their sources.

The problem of extracting good micro-earthquake data, down to magnitude 0, is largely to identify the weak signals of seismic waves through the disturbing noise that prevails near to the Earth's surface. Another problem is to extract useful information from the huge number of micro-earthquakes that are expected when the magnitude level is so low. And we had to be fast. The system had to provide information of significance for short-term watching within seconds and minutes. The system was designed to cope with all these problems. We showed our design ideas for the SIL system to some high-level seismologists at the American Geophysical Union (AGU) Fall Meeting in San Francisco in 1986. Besides generating very fruitful discussion, the general response was that such a system was what all seismologists dreamed of but it did not seem attainable in reality.

Getting the SIL system working the way we wanted was certainly difficult and the input of seismologists and electronic engineers alike was tremendous. But as soon as the basic system was working it gave us valuable new data and information about the crust that encouraged future work and secured funding and continuity.

The SIL system was from the outset limited to eight stations in the South Iceland Seismic Zone. The distance between stations varied from 25 km to 30 km (Figure 2.4). Seismic detectability was possible down to magnitude 0 in this area. High crustal noise in the zone due to the proximity of the ocean certainly made it difficult to get down to this level of detectability, but it was not impossible. Through the facilities of the SIL system the dense stream of micro-earthquakes provided

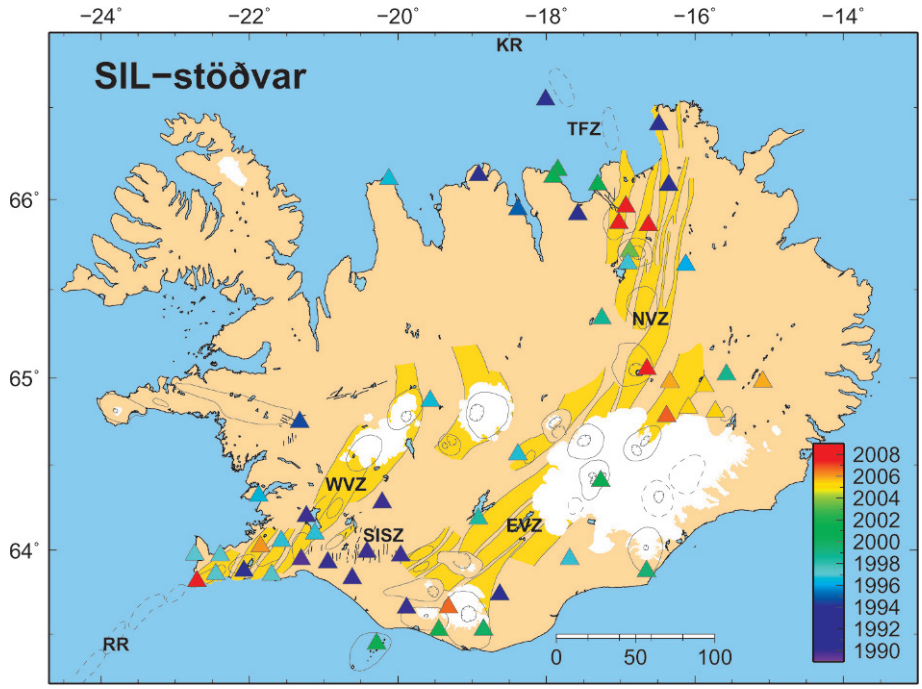

Figure 2.4. Triangles show the positions of SIL stations as the system developed between 1990 and 2008. Rift zones are in yellow. The east–west elongation of the stations in the north and in the south marks the transform zone areas (modified from Jakobsdóttir, 2002).

high-level information about the crustal structure, fissures, and dynamics within the zone as expected. The success of the SIL system in the SISZ paved the way for a gradual increase in system coverage of Iceland (Stefansson *et al.*, 1993; Jakobsdóttir *et al.*, 2002).

2.6 FROM TECHNOLOGICAL DEVELOPMENT TO RESEARCH AND WARNINGS

The success of the SIL project has been the ability to use micro-earthquakes to record crustal processes in real time and at high resolution in time and space. The project has also paved the way for new projects in the area of earthquake prediction research and gradually, as new patterns have been discovered, paved the way for new multinational earthquake prediction research projects. We are also confident that the SIL system could be extended to other areas subject to geohazards, as already is the case in other parts of Iceland (Figure 2.4).

2.6.1 Overview of research projects

Appendix 2.C contains a list of international research projects concerned with earthquake prediction and warnings (especially in Iceland). Many significant results of these have been described in numerous magazine articles and reports. In the list you will find keys to these results—both as they appear in internationally available papers and as reports directly on the webpages of the various participants.

The first project, the SIL project, created the SIL micro-earthquake system, which is the basis for all the other projects. The two next projects, the PRENLAB and PRENLAB II projects, were basic research projects involving the application and testing of data from the SIL system for learning about crustal processes. The PRENLAB projects also involved a more multidisciplinary approach, incorporating geology, seismotectonics, earthquake history, deformation from GPS, InSAR, and dynamic crustal modeling based on a multiplicity of data. In Section 2.6.2 the PREPARED project is presented.

2.6.2 The 2000 earthquakes represented a test for our efforts

Two large earthquakes occurred in the South Iceland Seismic Zone and coincided with the end of the PRENLAB projects in 2000, at places that were predicted to be the sites for the next large earthquakes in the zone (as described in Chapter 4). The 2000 earthquakes represented a good opportunity to evaluate the progress that had been made and to take new research steps forward. A new project, the PREPARED project, was created to learn from the experience of the 2000 earthquakes and to try and predict still more aspects of expected future earthquakes.

As seen in more recent projects (listed in Appendix 2.C), the scope has been widened to include volcanic prediction research, especially as concerns geohazard watching. Steps have been taken to develop multidisciplinary geohazard-watching practices and a system to merge together all the results of the research work for the purpose of practical information service and warnings (as more fullly described in Chapter 7).

2.6.3 Significance of the results for other earthquake areas

The period of project development described above has also been a period of worldwide doubt about the prospects of earthquake predictions. The prevailing idea in many countries has been that the only thing that can be done is to build better houses, an idea that is especially popular in many developed countries where good and earthquake-resistant houses already exist. The successes of Icelandic projects, not only the SIL micro-earthquake system but also research experience in Iceland, have led to much interest in their application at other places. It is of course often claimed that the conditions in Iceland are so different from anywhere else in the

world that direct export of Icelandic systems and expertise would not be helpful, and this is fair comment. However, common to all areas is the physics behind earthquake phenomena, and the methods that have been developed for monitoring and modeling can be applied elsewhere. What Iceland can export is its expertise in establishing the necessary infrastructure to initiate research and warning activities. This is much more significant in the long run than providing equipment. Moreover, most of the hardware equipment we have used is available off the shelf.

For further reading about the design and function of the SIL system see Stefánsson *et al.* (1993), Bodvarsson *et al.* (1999), and Jakobsdóttir *et al.* (2002). For more about its evaluation qualities see Slunga (2001, 2003).

Appendix 2.A further treats micro-earthquake technology that is currently being applied, while Appendix 2.C contains a list of major international earthquake prediction research projects carried out in the Iceland test area between 1988 and 2009, with links to webpages for further information.

2.A APPENDIX: EARTHQUAKE FAULTS AND MICRO-EARTHQUAKE TECHNOLOGY FOR THEIR STUDY

Appendix 2.A is not an in-depth treatment of earthquake faults or micro-earthquake technology. However, it does explain some basic features and recommends further reading. As for micro-earthquake technology, I describe at first hand the technology applied in the multinational earthquake prediction research projects in Iceland.

2.A.1 About the main fault types

Definition of three characteristic types of faults is demonstrated in Figure 2.5. Large faults cutting through the whole crust like those shown in Figure 2.5 are created over the course of hundreds to millions of years, through earthquake release, complemented by slow slips across them at some places. In reality the mechanism of individual earthquake faults may involve slip motion, which is a mixture of the slip motions shown in the figure. However, one of these types will be characteristic of any particular region and express the general long-term stress field that prevails there.

Individual earthquakes along individual faults may be mostly one type, but a small number could be of another type. In short the creation of such faults as shown in the figure takes place during long periods of time by processes that involve small earthquakes on the faults or in their surroundings, culminating in large earthquakes cutting through the whole crust. The prevailing mechanisms of small earthquakes are mostly of the same type as expressed by the main faults of the region, but some may be of significantly different type. Individual small earthquakes on a normal fault may be of the strike slip type or of the reverse fault type reflecting local variations in the stress field with time. But even if they are of the same type, the directions of faults of individual small earthquakes may deviate significantly from the main faults

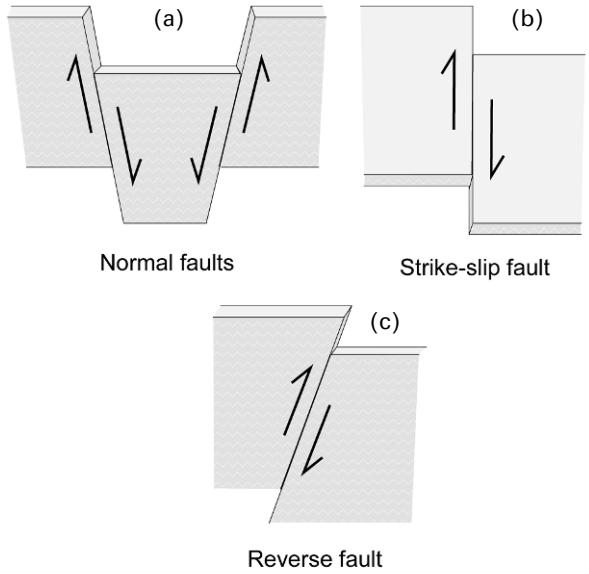

Figure 2.5. The main types of earthquake faults. (a) *Normal fault* shown in cross-section through the crust, typical direction of faults in tensional regions like rift zones (such as those in Iceland). Normal faults, at 45° slope from the surface as in the figure, prevail where the vertical stress component is larger than the horizontal components of stress, and the fault is created between the maximum stress, the vertical stress, and the minimum horizontal stress across the fault (this is frequently described as horizontal tension in the direction of the lowest stress). (b) *Strike slip fault* (horizontal view), vertical fault in the figure, is created where both the largest and the smallest stress components are horizontal. Strike slip faults are typical of nearly vertical boundaries of plates which slip horizontally towards each other, such as the transform faults or transform zones that are found in the main earthquake zones in Iceland. The slip shown by the arrows is right-lateral, indicating that if you stand at one side of the fault you see the other side move to the right. This is also often named "dextral". The opposite slip would be left-lateral also often named "sinistral". (c) *Reverse fault*, as demonstrated in the figure, both horizontal components of stress are larger than the vertical, typical of the thrust faulting that occurs at plate collision, such as in the Himalayas and subduction of ocean crust below the continental crust.

depending on loading stresses and fault conditions. This is of significant help in monitoring crustal conditions and crustal processes. Small earthquakes are released all the time in earthquake zones, and from the position of their origins and the mechanisms of their individual release processes we are able to map deep faults in the crust and their development as well as the variable stresses and crustal stability (or instability) in the faults and in their surroundings.

2.A.2 Micro-earthquake mechanisms

To study the preparatory process of an impending large earthquake it is important to find the micro-faults involved in the release of individual micro-earthquakes in

the area and the direction of fault slips along these faults (i.e., their fault plane solutions). The deviations found in micro-earthquake fault plane solutions from large-scale fault planes give valuable information about the dynamics of the surroundings of main fault planes. Mapping micro-earthquake sources and finding their fault plane solutions is a good way to understand what is going on in the crust, what stresses and instabilities are prevailing and being built up, and how this can lead to their release in large disastrous earthquakes. Because of how frequent small earthquakes are in time and space they can be expected to give a good picture of ongoing processes.

Methods to understand the mechanisms of micro-earthquakes have developed fast during the last 40 years. The terminology used here is based on the original terminology used when fault plane solutions were found using graphical methods.

Fault slips during earthquake release give rise to quadrantal distribution in the amplitudes of the seismic waves transmitted from them. This distribution is used to find the fault plane and direction of the slip. Earlier, mainly the polarities of the first motion of *P*-waves, compressional waves, are used for this. Compression (up or away from the source) or dilatation (down or towards the source) at the onset of the *P*-wave was observed at seismic stations in various directions and distances from the source. According to the geographical position of each seismic station and based on crustal velocity along the wave path it was calculated where the seismic rays would reach a virtual homogenous sphere surrounding the fault, sometimes called "the focal sphere" (Figure 2.6).

The polarity of the initial recorded motion of *P*-waves divides the focal sphere (represented by large circles) into four parts: the plus parts are where the initial motion of the *P*-wave is push (compression, away from the source), and the minus parts are where the initial motion of the *P*-waves is pull (dilatation or towards the source). The two flat planes which divide the focal sphere in this way are called "nodal planes". They are at right angles to each other, if we assume a balanced double couple point source to describe the fault motion at the origin, which is a fair assumption as long as local conditions are homogeneous. These planes armed with knowledge of which quadrants are positive or negative define the so-called "fault plane solution". One of the nodal planes is the real fault plane; the other is called "the auxiliary plane". The direction of fault slip can be ascertained from this by assuming that one of the nodal planes is the fault plane. The method usually applied to identify the appropriate fault plane is to observe aftershocks, which are then assumed to line up along the real fault plane. This had long been the main method of finding fault planes and slip directions from large earthquakes observed all around the earth. It was also used for small earthquakes, although it was difficult because measurements at local stations only covered a small part of the virtual focal sphere. The results are usually demonstrated as positive and negative parts in stereographic projections of the lower half of the focal sphere in case of distant earthquakes (Figure 2.6). The results are the two-colored balls (often named "beach balls") frequently seen in maps (like those shown in Figure 2.7).

This way of finding fault plane solutions is valid as long as the size of the fault and the slip across it are small compared with the distance from observing stations.

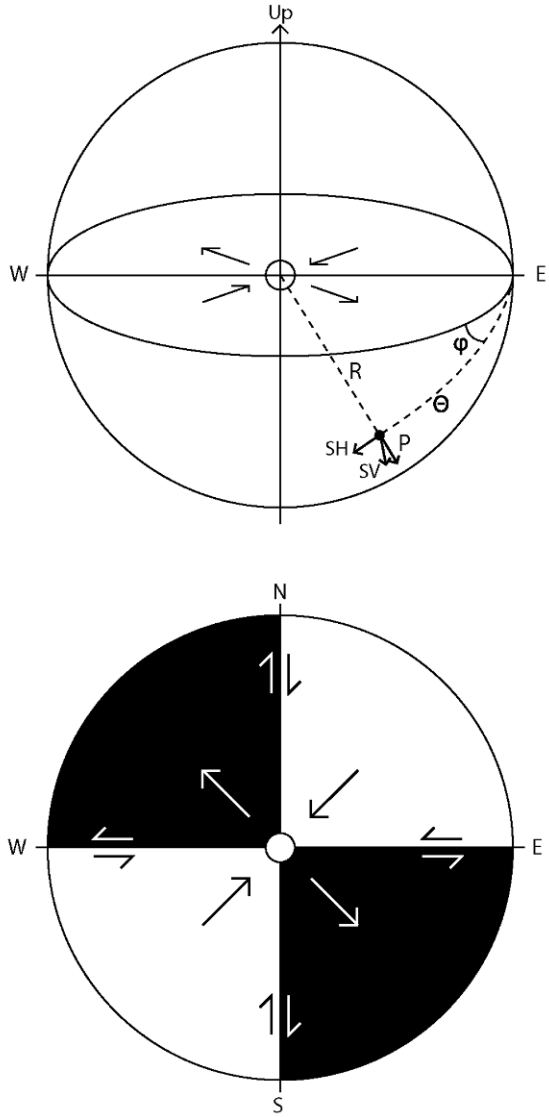

Figure 2.6. The focal sphere. *P*-waves oscillating along the ray of the wave (*R*) and cause push or pull on the surface. The amplitudes of the two components of the *S*-wave are indicated in the figure (i.e., the S_H that is perpendicular to the ray *R* from the source and along the surface, and the S_V component that is perpendicular to *R* and along the plane that the ray has with the vertical). Observations are plotted on the surface of the focal sphere after they have been corrected for ray path effect at a point that has spherical coordinates φ and θ. The circle below denotes the stereographic projection of the lower part of the focal sphere on the horizontal surface. White denotes areas where the pull of *P* is observed, while black denotes areas where the push of *P* is observed. Nodal planes are between these areas. This is a simple case where both nodal planes are vertical, and thus they are presented as straight lines in this projection.

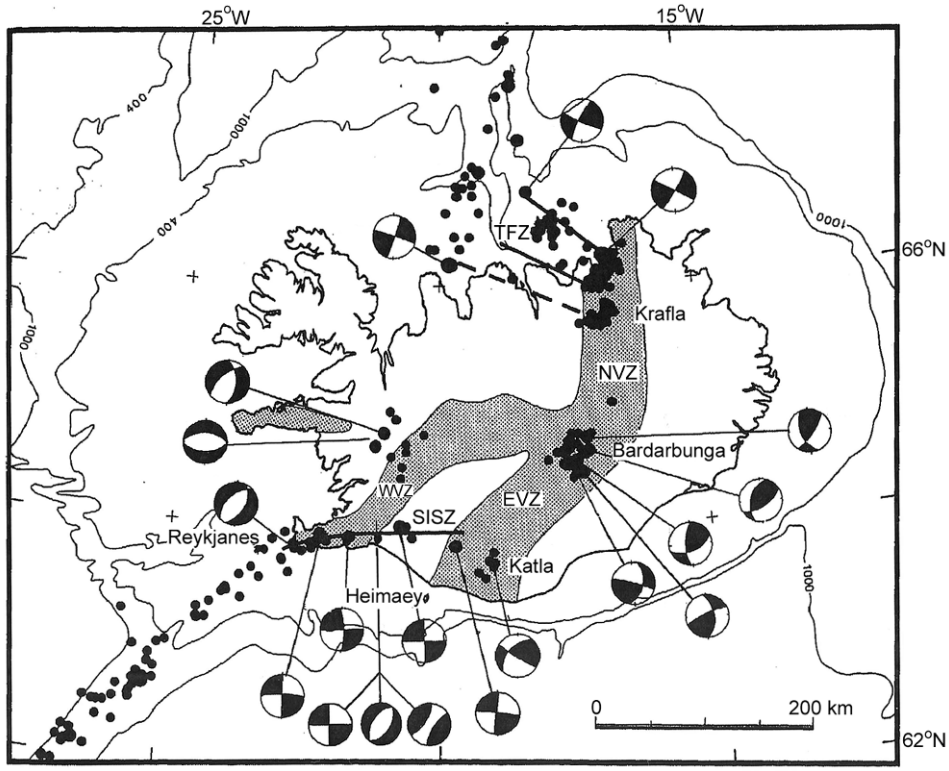

Figure 2.7. Fault plane solutions and epicenters of earthquakes larger than magnitude 5 (mb) between 1963 and 1987. Focal mechanisms are shown by stereographic projection of the lower hemisphere of the focal sphere. Compressional quadrants are shown in black (i.e., the initial motion of *P* in these quadrants is push). The vertical nodal planes of strike slip earthquakes prevail in the seismic zones to the north and south. Normal faults (white lozenge in the middle) are found in the western part, and thrust faulting (black lozenge in the middle) in the central part of Iceland (based on Einarssson, 1991).

Most of the time this is the case for small earthquakes, which we can expect to give us useful information ahead of large, dangerous earthquakes, which are the main concern in this book. Typical dimensions of small earthquake faults which we can easily observe in the crust are from a few tens of meters to a few hundred meters, while distances from observing stations are of the order of 10 to a few tens of kilometers. When observations are made at distances that are large compared with the dimension of the fault planes we talk about "point sources".

Another way of presenting fault plane solutions is by showing the direction of maximum stress released by the earthquakes—the *P*-axis—and the direction of minimum stress—the *T*-axis—which in an isotropic medium are perpendicular to each other. At some places in this book we present this by calculating the so-called horizontal compression direction (i.e., compression along the horizontal, calculated

from the angles of both the *P*-axis and *T*-axis). This must not be confused with the general rock stress tensor in the crust, which because of the orientation of earlier cracks and other heterogeneities may be significantly different from stresses which are released in individual small earthquakes.

This traditional method was and still is in many cases a satisfactory way of finding fault planes and the slip across faults (especially of large earthquakes, which are recorded by a large number of seismic stations all over the world). There were of course other patterns in the wave train that could be used to get the requisite solution, which, however, basically relied on the polarities (the push or pull) of the initial *P*-waves. Among the main problems with the method was that under Earth-realistic conditions it was very difficult to decide whether faint signals close to the nodal planes were plus or minus. This was especially difficult in the case of high-frequency waves from small local earthquakes which were significantly disturbed by local heterogeneities at the place on the surface where recording took place. Another problem was that observations only covered a small part of the Earth's surface and thus a small part of the virtual focal sphere around the source.

Gradually, methods emerged which applied the observed amplitudes of seismic waves to fault plane solutions, instead of just their polarities. A method was found for this information from a large number of stations to be inverted in order to find the source parameters. The theoretical basis for such a method can be found in a number of textbooks (e.g., Aki and Richards, 1980).

However, studies of the fault plane solutions of small earthquakes had long been difficult and tedious in practice. The technology that has been applied in Iceland since commencing the SIL system to study the mechanics of small earthquakes, which are only recorded locally, was based on the spectral amplitudes of *P*-waves and *S*-waves, a method developed around 1980 by Ragnar Slunga (Slunga, 1981), a leading member of the SIL group. In his method, the Fourier spectra of amplitudes *vs.* frequency are calculated from the initial part of incoming waves. The Fourier spectra provide a better estimation of the energy emitted by the various waves than by reading the amplitudes from the initial part of waves, which are greatly disturbed by surface heterogeneities and especially so by small seismic signals. Besides this, Fourier spectra provide information on the relationship between high and low frequencies and thus on the size of the source volume or fault length. This method was further developed and tested by Rögnvaldsson and Slunga (1993). It has been shown to be a fast and robust method for focal mechanism studies.

By the initial part of incoming *P*-waves and *S*-waves we mean a timelength of the order of seconds, depending on distance from and size of the earthquake, sufficient to give an option to minimize the effects of surface reflections and other disturbances to the clean signal. The DC level of the spectra is applied as amplitudes to find the nodal planes by inverting observations from many seismic stations. Figure 2.8 shows the expected radiation patterns of amplitudes of compressional waves (*P*) and shear waves (S_V and S_H) for strike slip faulting and for normal faulting. Well-observed signals of the initial motion of *P*-waves are used to discover which parts of the focal sphere, divided by the nodal planes, are positive and which are negative. The size of amplitudes and the frequency of waves together with an Earth-realistic

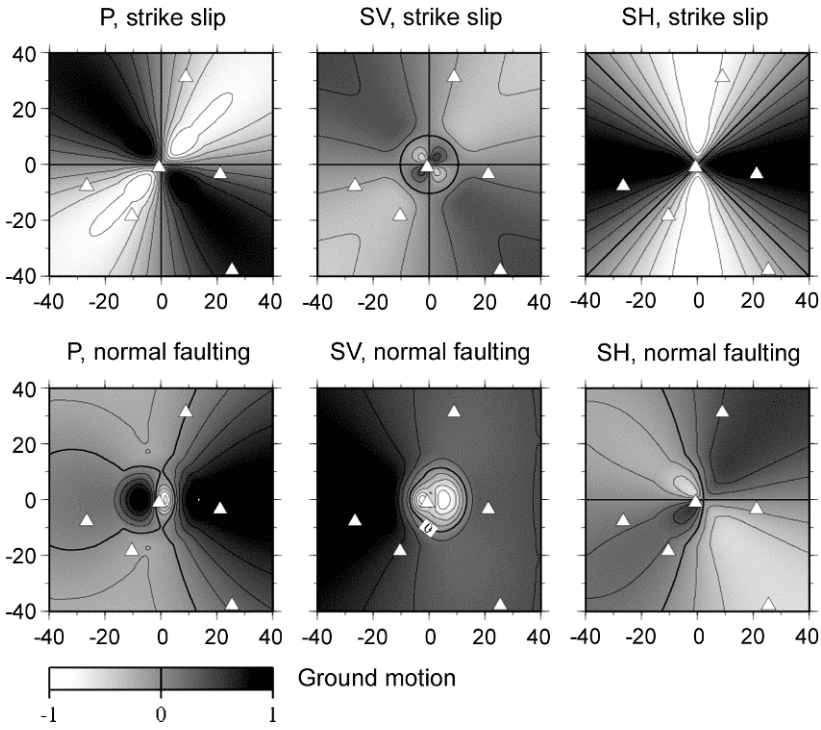

Figure 2.8. The radiation pattern for P, S_V, and S_H waves for two different earthquake mechanisms. The origin of the coordinate system is at the epicenter of the earthquakes and the numbers are in kilometers. The seismic stations in the SISZ, the closest SIL stations, are marked with triangles in the same coordinate system. The mechanism in the upper row corresponds to right-lateral strike slip on a vertical fault, striking due north (up in the figure) (see also Figure 2.6). The lower row is for normal faulting, which involves dip slip on a north–south striking fault, dipping (down-sloping) 60° to east (to right). The grayscale bar shows (in arbitrary units) the expected absolute amplitudes of P-waves and of two components of S-waves, the S_V and the S_H, at the seismic stations. To find the mechanism (the fault plane solutions) from observations, we search the nodal planes and slips, which best fit the ground motion amplitude fields of the P and S seismic waves (Bödvarsson *et al.*, 1996).

assumption about the source function are routinely used to estimate fault slip, fault size, moment of release, and moment magnitude.

The printout given in Figure 2.9 shows part of a result of automatic evaluation of the source mechanism of one micro-earthquake in Iceland. The basic mechanism solution shown in Figure 2.8 indicates the range of values that can be fulfilled by the data other than the optimal solutions. Besides what is seen in the figure the automatic mechanism solution also includes discussion of the statistical significance of the obtained solutions by graphically describing the fit and lack of fit between the solution and observations, which is especially significant when using many earthquakes to map active faults and fault processes. Besides the conventional fault plane

Dynamic source parameters			
Size measures			
Seismic moment			$0.245 \cdot 10^{12}$ Nm
Local magnitude			1.4
Shear wave corner frequency range at close distances (900 km)			4.2–4.8 Hz (5.8 Hz)
Fault radius range			143–164 m (118 m)
Stress drop range			0.024–0.036 MPa (0.064 MPa)
Range of peak slip at the fault			0.1–0.2 mm (0.2 mm)
The orientation of relaxed stress			
	Azimuth	*Dip*	
P-axis	52°	68°	
T-axis	137°	−2°	
Horizontal deviatoric stress as given by the P- and T-axes			
The azimuth of compression			47°
Relative size			0.57
The two possible fault planes			***O***
	Strike	*Dip*	*Slip*
Plane a	248°	47°	121°
Plane b	207°	129°	−61°
The normal directions of the fault planes			
	Azimuth	*Dip*	
Plane a	338°	43°	
Plane b	117°	39°	
Normal faulting dominates			

Figure 2.9. An example result after automatic earthquake mechanism analysis in the SIL system of a small earthquake in Iceland. The ***O*** stands for optimal. Besides the parameters of mechanism that are presented in this figure, the automatic solution contains more information than can be shown here on their statistical significance such as a graphical representation demonstrating the fit and lack of fit between the obtained solution and the data (for more information see Rögnvaldsson and Slunga, 1993).

solutions the inferred mechanism contains estimated seismic moment and peak slip, based on the DC level of the spectra corrected for geothermal spread, as well as the fault radius based on the corner frequency of the spectra and an assumption of a spectral source model to fit with the data (Rögnvaldsson and Slunga, 1993).

In making use of fault plane solutions to study the pre-earthquake and interseismic processes that may help us to predict earthquakes, a huge number of solutions must be applied to get the best possible resolution of the ongoing process. Simplifying assumptions are made about rock homogeneity and elasticity in the immediate vicinity of the small source area. In addition, spectral amplitudes are not exactly definable as the amplitude of a seismic wave. Such simplifications are necessary because of the huge number of cases to be treated and the need for fast results. On the other hand, the method is based on both *P* and *S* waves and they can be used to provide estimates of the stability of the obtained solutions. This together with the huge number of earthquakes that can be evaluated helps us to monitor real ongoing processes and to map faults.

The following papers are good guides to the methodology necessary to find mechanisms, including the fault plane solutions of micro-earthquakes, by using spectral amplitudes of micro-earthquakes from many stations, the basis of the method and testing: Slunga (1991), Rögnvaldsson and Slunga (1993, 1994). Shomali and Slunga (2000) compares application of the full waveform of body waves for moment tensor inversion with the application of spectral amplitudes.

The question of displaying or assembling descriptively the huge number of solutions to understanding micro-earthquake mechanisms in order to compare them with observable faults or other processes can be done in different ways. Figures of the virtual focal spheres cut by the great circles of nodal planes, as we saw in Figure 2.7, can be useful in the case of a small number of earthquakes.

Ragnar Slunga developed a method of visualizing a large number of fault plane solution data utilizing the fact that any fault plane solution is completely defined by two force dipoles of unit magnitude, the axis of maximum compression (the *P*-axis) and the axis of tension (the *T*-axis). The two axes are by definition 45° from the nodal planes of the point source. Maximum horizontal compression and tension can be calculated from *P*-axis and *T*-axis orientations towards the horizon. He introduced the "stress" square of a unit dimension for displaying fault plane solutions by plotting horizontal maximum compression *vs*. the horizontal minimum compression or tension (Figure 2.10) (for the methodology see Rögnvaldsson and Slunga, 1994). The stress square is very useful to see which type of faulting is prevailing within defined volumes (see Figure 4.32 for an application of the stress square).

A simple way of visualizing micro-earthquake mechanisms, especially when fault planes are vertical (as is the usual case in the SISZ) is to plot horizontal compressions only and estimate their frequency in different directions by means of rose diagrams (as seen in Figure 4.19).

Another way of utilizing the fault plane solutions of large groups of micro-earthquakes, to describe crustal conditions and processes in the crust, is to estimate the absolute stresses released by small earthquakes in a small volume. The method is described in Section 4.9.3. This is based on fault plane solutions that only provide relative stresses in three directions and by assuming that the vertical stress equals the lithostatic pressure at the site. This is an approximation and, significantly, is not what is usually defined as the rock stress tensor. This is an estimation of the absolute stress that is released in individual earthquakes and is useful in expressing changes in

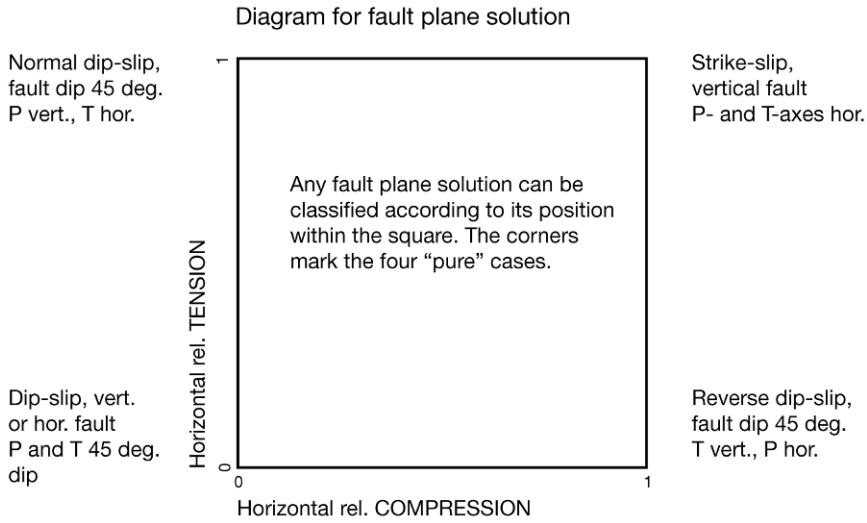

Figure 2.10. The stress square diagram for displaying the fault plane solutions of individual earthquakes (i.e., a plot of minimum *vs.* maximum horizontal compression in the release of individual earthquakes). So, for a large number of earthquakes with small or large seismic volumes, the stress diagram gives a good overview of the prevailing mechanisms useful for mapping changing crustal conditions. This diagram is frequently used in practice to characterize seismic volumes. An example demonstrating its use is given in Figure 4.28.

a heterogeneous environment, as can be expected during the preparation period of a large earthquake. A regional rock stress tensor for the crust is estimated on the basis of a large number of earthquake mechanisms and locations in volumes that can be assumed to be stress-homogeneous (as described in more detail in Section 4.9.2).

2.A.3 Absolute and relative locations of similar events

Comparison of the arrival times of seismic waves from a group of nearby earthquakes has long been applied to locate earthquakes relative to a so-called "well-located earthquake" in the group. The location of earthquake epicenters, which is ascertained by comparing the arrival times of waves from them at various seismic stations, is based on knowledge of the velocity of elastic waves in the crust, which is often incomplete. For a group of earthquakes whose origins are nearby their seismic waves travel nearly the same path as the well-located earthquake. This reduces errors in assumed wave velocities, which helps to locate members of the group relative to the well-located earthquake. However, the absolute position is based on knowing the location of one of the earthquakes. This is usually a relatively large earthquake in the group and as a result has been thoroughly observed by many seismic stations at various distances.

In the SIL project a different method for relative location was described by Slunga *et al.* (1995). It has been applied to enhance both relative and absolute

determination of hypocenters for groups of small earthquakes. The method does not assume *a priori* that the position of any of the earthquakes is known. It locates all the earthquakes relative to all the others. In addition, this has the effect of enhancing the accuracy of absolute location. It can be explained in the following way. The time difference between observations at nearby stations is affected by the position from which the earthquake source is viewed, in much the same way as our eyes manage to estimate distances because of the distance between the eyes. The relatively located group is thus moved to a position which minimizes the difference between expected and observed distance between any two earthquakes in the group. This calls for high accuracy in reading the onsets of waves to be able to see small time differences. Cross-correlating arriving waves having similar signals recorded at each observing station is carried out to increase the accuracy of reading the time of arrival of similar signals at the same station as well as to estimate the degree of similarity between them. Clearly, to achieve good accuracy in reading signal onsets in this way, the signals must be very similar and of similar size; thus, relatively large events would be excluded from the group that is to be used in the relative location procedure to achieve the best accuracy.

This represents a significant part of the micro-earthquake technology applied in Iceland. It has made it possible to achieve relative accuracy of similar nearby events down to 10 meters and absolute accuracy to a few tens of meters. This, together with fault plane solutions, enables mini-faults within the fault zones and the direction of slips on them to be mapped (as will be seen at several places in Chapter 4).

The methodology for absolute and relative locations of micro-earthquakes applied in the SIL system is described in Slunga *et al*. (1995).

A similar method for joint hypocenter location is the so-called double-difference method described by Waldhauser and Ellsworth (2000).

For further reading about the design criteria and functioning of the SIL system see Stefánsson *et al*. (1993) and Bödvarsson *et al*. (1999) and about its evaluation qualities see Slunga (2001, 2003).

2.B APPENDIX: PARTICIPANTS IN THE RESEARCH AND DEVELOPMENT THAT FORMED THE BASIS OF THIS BOOK

2.B.1 Icelandic Meteorological Office

The most significant institution in carrying out the earthquake prediction research described in this book is the Icelandic Meteorological Office (IMO). It was set up in 1920 as a weather watch institute. Since 1950 a small section of IMO has concentrated on monitoring seismic and volcanic hazards and providing a warning service. This group currently consists of 15 geophysicists and technical engineers, who have been responsible for coordinating internatioal earthquake prediction research in Iceland since 1986, together with geohazard watching. In 2009 the Icelandic Hydrological Survey (formed in 1948) merged with IMO. As a consequence IMO

is now responsible for watching and studying natural hazards in Iceland in a much broader sense than earlier.

2.B.2 Staff at IMO who directly or indirectly contributed to the book (in alphabetical order)

Ágústsson, Kristján (b. 1951, geophysicist, Fil. Lic.). Worked at IMO from 1987 to 2007. Apart from regular work on seismic monitoring he was responsible for the operation of IMO's volumetric strainmeter and gravimetric networks as well as modeling crustal deformation. Presently he is working at Iceland GeoSurvey (ÍSOR) with focus on microearthquakes in geothermal areas.

Ármannsdóttir, Sigthrúdur (b. 1951, geographer, B.Sc.). Worked part-time at the Geophysical Department of IMO from 1990 and full-time since 2007. She is working on monitoring, evaluation, and mapping.

Bergsson, Bergur (b. 1966, electronics engineer, B.Sc.). Between 1991 and 2000 he worked on the development and operation of the SIL seismic system, the strainmeter system, and the continuous GPS system of IMO. After several years abroad on international projects, he returned to IMO in 2009.

Skaftadóttir, Thorunn (b. 1949, geologist, B.Sc.). Her main field of work since 1973 has been monitoring and interpretation, based on old seismic systems. Since 1991 her work has mainly been based on evaluation of data in the SIL system and geowatching.

Geirsson, Halldór (b. 1976, geophysicist, M.Sc.). He commenced work at IMO in 1999. His main contribution has been buildup of the Iceland continuous GPS system for real-time monitoring of crustal deformation, research based on these data, and geowatching.

Guðmundsson, Gunnar B. (b. 1955, geophysicist, B.Sc.). He has been very active in earthquake perediction projects since 1988. His main contribution, besides daily responsibilities for evaluation of geophysical data and geowatching, has been development and operation of the SIL seismic system, especially software development and visualization of results.

Halldórsson, Páll (b. 1950. physicist, Dipl. phys.). He came to IMO in 1979 and was active there untill 2008. His main scientific contribution concerns the earthquake history of Iceland and seismic hazard assessment. After increased administrative responsibilities during his last years at IMO, he left to become president of the Icelandic Scientists Trade Union.

Hjaltadóttir, Sigurlaug (b. 1976, geophysicist/seismologist, M.Sc.). She has worked at IMO since 2003 in monitoring and evaluation of seismic data. Her speciality during recent years has been detailed mapping of subsurface faults and magma movements using microearthquake technology.

Hólmjárn, Jósef (b. 1946, electronic and machine engineer). He came to IMO in 1997 after working as a geophysics engineer at the National Energy Authority between 1974 and 1997. At IMO his work involves installation and operation of seismic and other geophysical monitoring systems.

Jakobsdóttir, Steinunn S. (b. 1953, geophysicist/project manager, Cand. Scient.). She came to the Geophysical Department of IMO in 1987 after two years of research at the Geological Survey of Greenland in Copenhagen. Since that time she has been among the main developers of SIL system facilities and responsible for its operation. She has been responsible for geophysical monitoring at IMO since 2004.

Kjartansson, Einar (b. 1952, geophysicist, Ph.D.). He has worked at IMO since 2007 and between 1996 and 1998. After his Ph.D. he participated in various projects on seismic wave propagation, reflection seismology, and development of computer technology. His contribution to research projects at IMO covers a number of fields from visualization of real-time data streams and buildup of the database to producing real-time maps of expected seismic effects.

Ólafsson, Sveinn (b. 1962, electronic engineer, B.Sc.). He carried out innovative work at IMO between 1989 and 1990 in software development and data transfer in the early buildup phase of the SIL system in Iceland.

Pálsdóttir, Gudrún (b. 1949, librarian, M.A. in information science). She has worked at IMO since 2000 and is responsible for the library as well as information science and related work.

Pálsson, Sighvatur, K. (b. 1957, electrical engineer). He has worked at IMO since 2001 on maintainance and technical development of the SIL system.

Roberts, Matthew (b. 1976, geologist/glaciologist, Ph.D.). He joined the Geophysical Department in 2002. Besides the everyday geohazard watch, his specialities are glacial outburst floods, glacial and volcanic hazards, GIS science, information and warning systems for geohazard watching.

Rögnvaldsson, Sigurdur Th. (b. 1964). He sadly died in a car accident in October 1999. His Ph.D thesis focused on developing and testing geophysical algorithms implemented as part of the SIL seismic network to monitor and analyze information carried by micro-earthquakes. Working with Ragnar Slunga, his most important contributions to prediction research were in automatic estimation of fault plane solutions for micro-earthquakes based on the spectral amplitudes of *P*-waves and *S*-waves, and in the relative locations of micro-earthquakes and the mapping of faults deep in the crust. Sigurdur joined IMO in 1995 and took part in daily monitoring and evaluation as well as ongoing research projects.

Sveinbjörnsson, Hjörleifur (b. 1971, geologist, B.Sc.). Since 2000 he has worked on maintainance and further develoment of the SIL system, in addition to monitoring and evaluating seismic data.

Thorbjarnardóttir, Bergthóra S. (b. 1955, geophysicist, M.Sc.). She has worked at IMO since 1998 in seismic monitoring and evaluation. Besides the everyday geohazard watch, she develops and maintains the geophysical database and is responsible for making it available.

Vogfjörd, Kristín S. (b. 1956, seismologist/Director of Research, Ph.D. in geophysics). She joined IMO in 2000. Her research work spans microseismicity, relative earthquake location, subsurface mapping of active faults and magma pathways in volcanoes, crustal wave propagation, earthquake source mechanisms, seismic tremors from volcanic eruptions, glacial floods (*jökulhlaups*), and seismic early warning.

Thorkelsson, Bardi (b. 1952, geologist). He joined the Geophysical Section of IMO in 1978 and took part in monitoring and evaluating old and new seismic data. Gradually, he became more involved in publishing work, organization of meetings, and coordination of large EU projects in earthquake prediction research.

2.B.3 Scientists from other institutions who contributed significantly

Angelier, Jacques (b. 1947, Professor at the University "Pierre et Marie Curie"). He sadly died on January 31, 2010. He participated in Icelandic prediction projects in 1996 and continued his studies of Iceland's brittle tectonics until his death. His main contribution to earthquake prediction research in Iceland was the reconstruction of stress fields based on geological fault slip data and the focal mechanisms of micro-earthquakes.

Árnadóttir, Thóra (b. 1963, Ph.D., Senior Research Scientist, Nordic Volcanological Center), Institute of Earth Sciences, University of Iceland. She joined IMO in 1998 and moved to NVC in 2000. Since 2000 she has participated in earthquake prediction projects or related research projects. Her main contribution is in crustal deformation monitoring and modeling of the plate boundary in Iceland, as well as crustal rebound studies.

Bergerat, Françoise (b. 1949, Research Director at CNRS—National Center of Scientific Research). Since 1996 she has been involved in multinational prediction research projects in Iceland. Her specialities (as applied to Iceland) include ancient and active brittle deformation, reconstruction of stress tensors by inversion of fault slip data, and seismotectonics.

Bonafede, Maurizio (b. 1949, Chair professor in Geophysics, Department of Physics, University of Bologna, Italy). His main field is the theoretical physical modeling of tectonic processes. He has been involved in earthquake prediction research projects in Iceland since 1996. His main contribution to the projects is in the application of the theoretical studies of fracture mechanics to model faulting and magma intrusion processes. Of especial significance are his studies on the role of fluids and related thermo-poro-elastic effects in triggering instability in tectonically active zones.

Bödvarsson, Reynir (b. 1950, research engineer and seismologist, Director of the Swedish National Seismic Network of Uppsala University). At the outset of the SIL project in 1986 he was a senior research engineer at the University of Uppsala and was from the very start of the project one of its three main leaders. He led the technical design of the SIL seismic system and is still in the forefront of ongoing software development; he also contributes to the development of other geophysical algorithms.

Crampin, Stuart (b. 1935, seismologist, honorary research associate of the British Geological Survey, and between 1992 and 2008 professor at Edinburgh University). He began participating in Icelandic prediction research projects in 1996 and is still active in such projects. His main contribution is in studying and modeling shear wave splitting (SWS) and seismic anisotropy in efforts to forecast earthquakes and volcanic eruptions.

Einarsson, Páll (b. 1947, professor of geophysics, University of Iceland). He was one of the founders of the SIL project in 1986 and since then has actively participated in multinational prediction research projects, contributing to the mapping and modeling of faults of historical earthquakes, deformation and seismicity related to large earthquakes and volcanic eruptions, and studies of radon anomalies.

Gudmundsson, Ágúst (b. 1953, geologist, professor at the University of London Royal Holloway). He took part in earthquake prediction research projects in 1996 by studying and modeling seismotectonics, volcanotectonics, rock fracture mechanics, and fluid transport in rock fractures.

Linde, Alan T. (b. 1938, Senior Research Staff Member, Department of Terrestrial Magnetism, Carnegie Institution of Washington). In cooperation with IMO he participated in the development and installation of a network of borehole strainmeters in the SISZ in 1979 and actively followed up its operation. His main contribution to prediction research efforts in Iceland is in studying and modeling crustal deformation related to earthquakes and volcanic activity.

Lund, Björn (b. 1965, researcher at the Swedish National Seismic Network). He has worked on Icelandic prediction-related projects since 1995. His main contribution has been in crustal stress estimation and modeling based on micro-earthquakes and on glacially induced deformation.

Roth, Frank (b. 1951, Prof. Dr. head of the Modeling Group "Earthquake Risk and Early Warning" of GFZ in Potsdam, and Professor of Geophysics at the Ruhr-University Bochum, Germany). His main research field is seismotectonics. His most significant contribution to Icelandic projects is in modeling deformation and stress changes as a result of single earthquakes and earthquake sequences.

Sacks, Selwyn I. (b. 1934, Senior Research Fellow of the Department of Terrestrial Magnetism, Carnegie Institution of Washington). In 1979, in cooperation with IMO, he led construction of a network of Sacks–Evertson borehole strainmeters (co-invented by him) in the SISZ. His main contribution to prediction research

efforts in Iceland has been in monitoring and studying crustal deformation, based on the strainmeters and broadband seismometers he invented and had installed in Iceland in 1972.

Sigmundsson, Freysteinn (b. 1966, geophysicist at the Nordic Volcanological Center, University of Iceland). Before 2004 he was Director of the Nordic Volcanological Institute, which subsequently integrated with the University of Iceland. His main field of study is in crustal deformation inferred from space geodesy, using GPS and satellite radar interferometry. He has studied strain accumulation across seismic zones, earthquake deformation, volcanic unrest, and magma movements.

Slunga, Ragnar (b. 1943, Executive Manager of QuakeLook in Stockholm). When prediction projects first started he worked at the FOA (later FOI) in Stockholm, and was for 17 years a part-time research professor at the University of Uppsala working on prediction research. He had a leading position in the SIL project from the very start in 1986, especially in defining its physical design criteria. He is currently working on prediction research in Iceland. His main contribution is in using micro-earthquakes to study the *in situ* stress field and stability of fractures for the purpose of earthquake warning.

Tryggvason, Ari (b. 1967, Docent in geophysics, Uppsala University). His speciality is local seismic tomography and inversion of geophysical data. He first participated in prediction research projects in 1996 by studying the detailed crustal structure in the SISZ, using SIL micro-earthquake data; he has continued on and off with this work ever since.

2.C APPENDIX: RESEARCH PROJECTS IN THE FIELD OF EARTHQUAKE PREDICTION

There now follows a list of international multidisciplinary research projects in the field of earthquake prediction research and warnings in which Icelandic scientists participated. The South Iceland Seismic Zone was the test area for most of the projects:

- Earthquake Prediction Research in the South Iceland Lowland (SIL, 1988–1995), cooperative project of the Nordic countries. For information about the project see the report: Seismic Datasamlingssystem för Södra Islands Lågland, 1986, mostly in English (*http://www.vedur.is/media/vedur stofan/utgafa/greinargerdir/1995/SeismDatSIL1986.pdf*). See also Stefánsson *et al.* (1993) (Icelandic coordination).
- Earthquake Prediction Research in a Natural Laboratory (PRENLAB, 1996–1998), an EC project (ENV4-CT96-0252). For information see *http://www.vedur.is/media/vedurstofan/utgafa/greinargerdir/1998/98023.pdf*, PRENLAB Report, 1998 (Icelandic coordination).

- Earthquake Prediction Research in a Natural Laboratory-2 (PRENLAB II; 1998–2000), an EC project (ENV4-CT97-0536). For information see *http://www.vedur.is/media/vedurstofan/utgafa/greinargerdir/2001/01001_1.pdf* and *http://www.vedur.is/media/vedurstofan/utgafa/greinargerdir/2001/01001_2.pdf*, PRENLAB II, final report, April 1, 1998–June 30, 2000, published in 2001 (Icelandic coordination).
- Application of practical experience gained from two recent large earthquakes in the South Iceland Seismic Zone in the context of earthquake prediction research to develop technology for improving preparedness and mitigating risk (PREPARED, 2003–2005). For more information see *http://www.vedur.is/skjalftar-og-eldgos/skyrslur_og_rit*. Several reports can be found there, see, for example, PREPARED Third Periodic Report, 2006 and PREPARED Final Report, 2006 (Icelandic coordination).
- Realistic Evaluation of Temporal Interactions of Natural Hazards (RETINA, 2002–2005). For information visit *http://www.acri-st.fr/retina/*. An EC project (French coordination).
- Early information and warning systems for geological hazards (EWIS, 2002–2005), see *http://gis.vsb.cz/webcastle/doc/Iceland_CaseStudy1_QV3.pdf*. See also *http://www.vedur.is/skjalftar-og-eldgos/skyrslur_og_rit*, Icelandic scientific and risk mitigation report.
- Frequent, Observation-driven, Realistic Evaluation and Simulation of Interacting Geophysical Hazard Triggers (FORESIGHT, 2004–2006). For information visit *http://www.acri-st.fr/foresight/*. An EC project (French coordination).
- Tsunami Risk and Strategies for the European Region (TRANSFER, 2006–2009). For information visit *http://labtinti4.df.unibo.it/transfer/index.php*. An EC project (Italian coordination).
- Seismic Early Warning for Europe (SAFER, 2006–2009). For information visit *http://www.saferproject.net*. An EC project (German coordination).

3

The test area

The South Iceland Seismic Zone (SISZ), tectonics, and measurements

The multiplicity of observable crustal processes in Iceland has made the country a good natural laboratory for multinational earthquake prediction research. Using Iceland as a natural laboratory for such research is based on the favorable geological or tectonic conditions found in Iceland. Little by little, the availability of the necessary technology for observations and the high level of geological and geophysical research is being built up to complement the natural facilities.

The SIL micro-earthquake system set up two decades ago as the initial part of multinational earthquake prediction research in the SISZ is still the most significant basis for earthquake prediction research in Iceland and is significant for understanding the tectonics of Iceland. But there are other systems and observations available for studying the test area that are also of enormous value. I mention here the deformation measurements made by volumetric strainmeters and precise GPS measurements. There is also a system of radon monitoring. Geological mapping of faults of earthquakes that have occurred over the centuries is significant. Intensive and multidisciplinary studies of the structure of the crust and of the upper mantle are also a significant part of earthquake prediction research in the SISZ.

In this chapter I give a short insight into the tectonic framework and status of research and observations in the test zone and refer to some papers that are key to the search for deeper knowledge.

3.1 THE TECTONIC FRAMEWORK

Iceland is situated on the Mid-Atlantic Ridge (Figure 3.1). The speed of opening as a result of plate motion across the Mid-Atlantic Ridge in Iceland is, on the basis of global plate motion modeling, estimated to be around 2 cm/year.

Extending through Iceland, the Ridge plate boundary is deflected toward the east by the Iceland Mantle Plume (Figure 3.2) the roots of which reach more than

R. Stefánsson, *Advances in Earthquake Prediction: Seismic Research and Risk Mitigation*,
Springer Praxis Books, DOI 10.1007/978-3-540-47571-2_3, © Springer-Verlag Berlin Heidelberg 2011

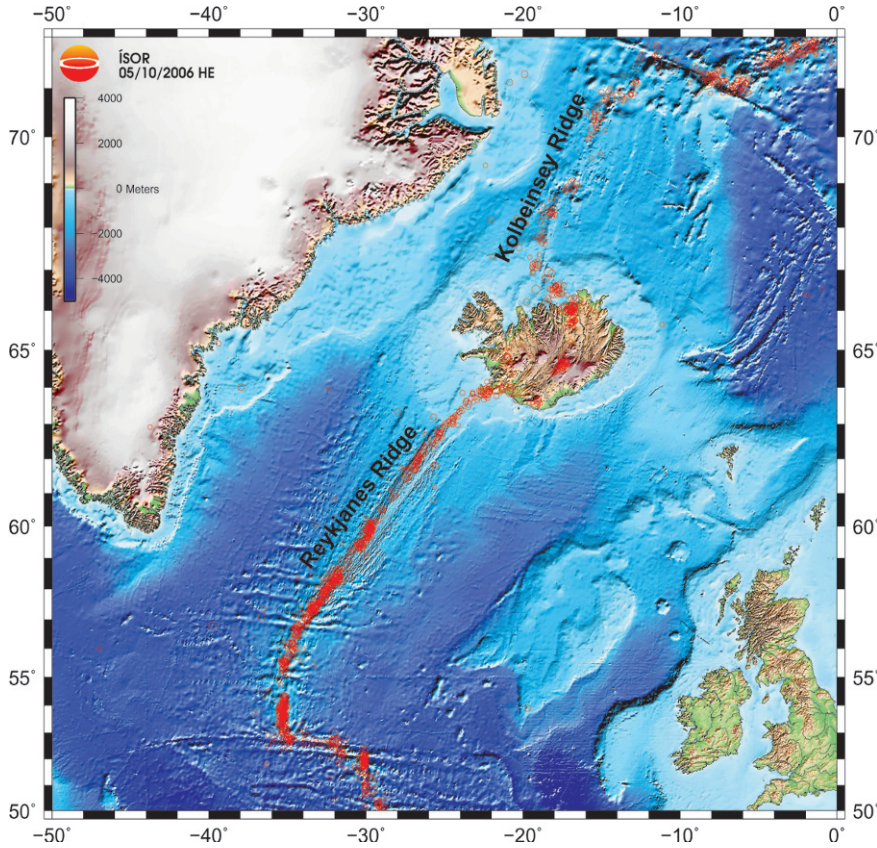

Figure 3.1. The map shows the North Atlantic Ocean and parts of the American and Eurasian continents on both sides. The active Mid-Atlantic Ridge plate boundary is shown by the epicenters of earthquakes (red dots) between 1964 and 2006, based on data from the U.S. Geological Survey (USGS). Extending through Iceland the ridge boundary is deflected to the east by the Iceland Hot Spot (mantle plume) (reproduced from Einarsson, 2008).

400 km in depth. The global plate tectonics hypothesis that emerged in the 1960s did not at its early stage incorporate the existence or significance of such plumes. Wilson (1963) and Morgan (1972) explained such a landmass anomaly in Iceland as the surface expression of a deep mantle plume. Tryggvason *et al.* (1983) used teleseismic *P*-waves to map such a plume down to a depth of 400 km (the results are shown in Figure 3.2). To study the seismic velocity below Iceland they used readings of *P*-wave onsets at a large number of local seismic stations in Iceland. They found a seismic anomaly which could only be explained by an upwelling plume from the mantle. It had a lower velocity of *P*-waves than the surroundings. From the observed 4% velocity contrast they estimated the ascent rate of the plume to be 1.7 m/year by assuming a viscosity of 10^{19} Pa s in the uppermost mantle below Iceland. If 10^{20} Pa s is correct for the viscosity, the ascent rate would be 10 times smaller.

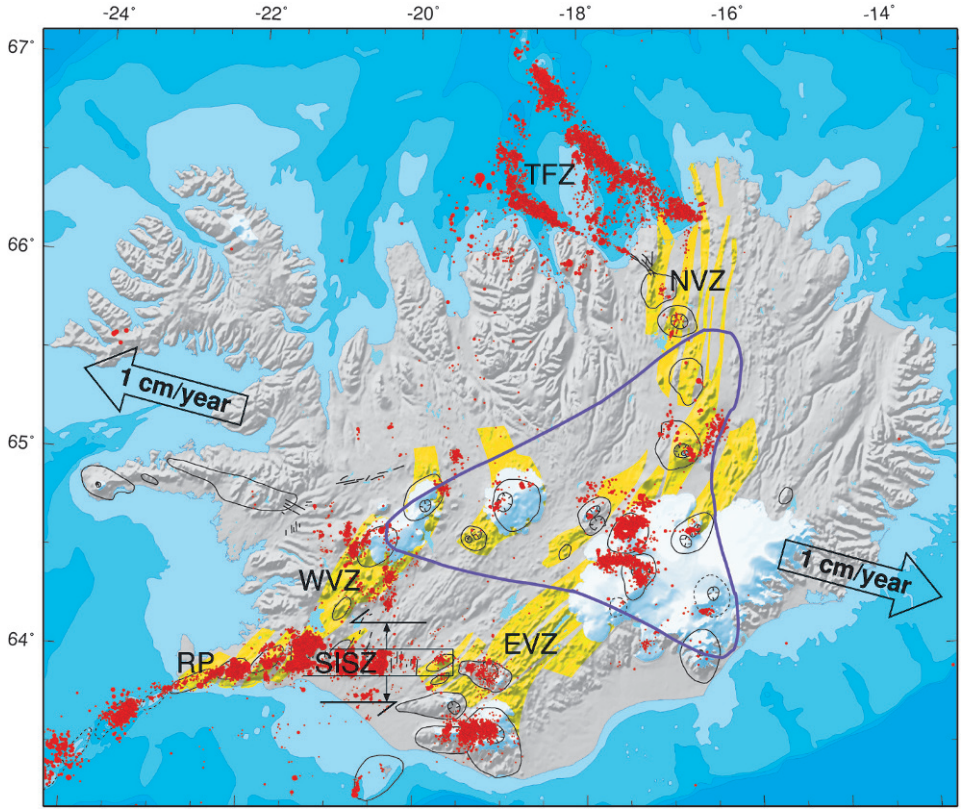

Figure 3.2. Iceland: the South Iceland Seismic Zone (SISZ), Reykjanes Peninsula (RP), plate motion directions, transform motion along the SISZ, and rift openings. Dots indicate small earthquakes occurring between 1994 and 2004. The outlines of the Iceland Plume at a depth of 300 km to 400 km are shown by the central large contour (Tryggvason *et al*., 1983; Stefánsson and Halldórsson, 1988). The weaker and smaller contours indicate central volcanoes. The volcanic rift zones WVZ, EVZ, and NVZ are indicated in yellow. TFZ and RP are shear zones experiencing volcanism (reproduced from a map by Einarsson and Sæmundsson, 1987).

Here and in the following when describing seismic structure, I often use the terms "teleseismic" and "local seismic" observations. Teleseismic is a term used for seismic observations at great distances from the source, usually more than 1,000 km away (i.e., covering the whole globe). The waves, at long teleseismic distances, travel through the deepest parts of the globe. What is meant by local seismic observations are observations made at less than 1,000 km distance from the source. On their way from source to receiver the waves only travel through the crust and the uppermost mantle (i.e., they only penetrate down to depths smaller than 100 km).

Intensive studies of the Iceland Mantle Plume have been ongoing during the last two decades. Through the application of newer technology and multidisciplinary modeling there is general agreement on its existence (Wolfe *et al.*, 1996; Ito *et al.*, 1999; Allen, 2002; Foulger *et al.*, 2001; Bjarnason, 2008; Bjarnason and Schmeling, 2009). Some results indicate that the plume's roots reach the lower mantle but others claim the roots are in the uppermost 400 km or so of the mantle.

Interplay is expected between the upflow of basaltic fluids from the mantle plume and local plate movements in the seismic zones. The upflow of basaltic material into the crust is episodic and appears as dyke injections in fissures, frequently with a strike that is almost north to south, and as volcanic eruptions.

The opening across the Mid-Atlantic Ridge to the south and to the north of Iceland, and the opening across the volcanic zones of Iceland, are connected by east–west shearing or transform zones, experiencing no or little volcanism in present times, but where earthquakes up to 7 in magnitude can occur. The South Iceland Seismic Zone (SISZ) has a strike that runs due east–west and is 70 km to 80 km long. Across this part of the plate boundary, horizontal left-lateral shearing predominates. The plate to the north of the SISZ is moving west compared with the plate to the south. There are active volcanoes near both ends of the zone (Figure 3.3).

According to a global model of plate motions by DeMets *et al.* (1990, 1994), relative plate motion opening across this part of the ridge is estimated at 18.9 ± 0.5 mm/year at a heading of 105° east of north (Figure 3.3). Plate spreading observed by repeated GPS surveying since 1992 is in good agreement with this (Árnadóttir *et al.*, 2008; Geirsson *et al.* 2006). The SISZ's strike is almost due east–west, so the plate motion vector indicates movement of 1.8 cm/year parallel to the zone and approximately 0.4 cm plate opening across the zone, assuming a negligible opening across the WVS. The earthquake zone at the north coast of Iceland is more complicated (as seen in Figure 3.2). This is called the Tjornes Fracture Zone and connects the NVZ to the Kolbeinsey ridge segment of the Mid-Atlantic Ridge, 120 km farther west (Figure 3.2).

Studies of the mechanisms of many small earthquakes in the SISZ indicate that they are dominated by strike slip earthquakes with a *P* (compressional) axis N45°E and *T* (tensional) axis N135°E. This is in good agreement with left-lateral transform motion from east to west (Angelier *et al.*, 2008). Inversion of the mechanism to obtain the general rock stress tensor for the area yields a tensor with maximum compression in direction N50°E and minimum compression (or tension) N140°E and the intermediate axis is close to vertical (Angelier *et al.*, 2004b).

Plate motion proper (i.e., well away from the plate boundaries of the brittle crust) is supposed to be uniform and continuous. Near the plate boundaries, plate motion is hampered by the effective strength of the crust which reacts differently at different places and at different times. At rift opening boundaries and horizontal shearing or transform boundaries there are local differences in the speed of deformation and its direction.

The interplay between the variety of earthquake zones and ascending magma, especially above the center of the Iceland Mantle Plume, makes Iceland a significant natural laboratory for earthquake prediction research. When studying the rheology

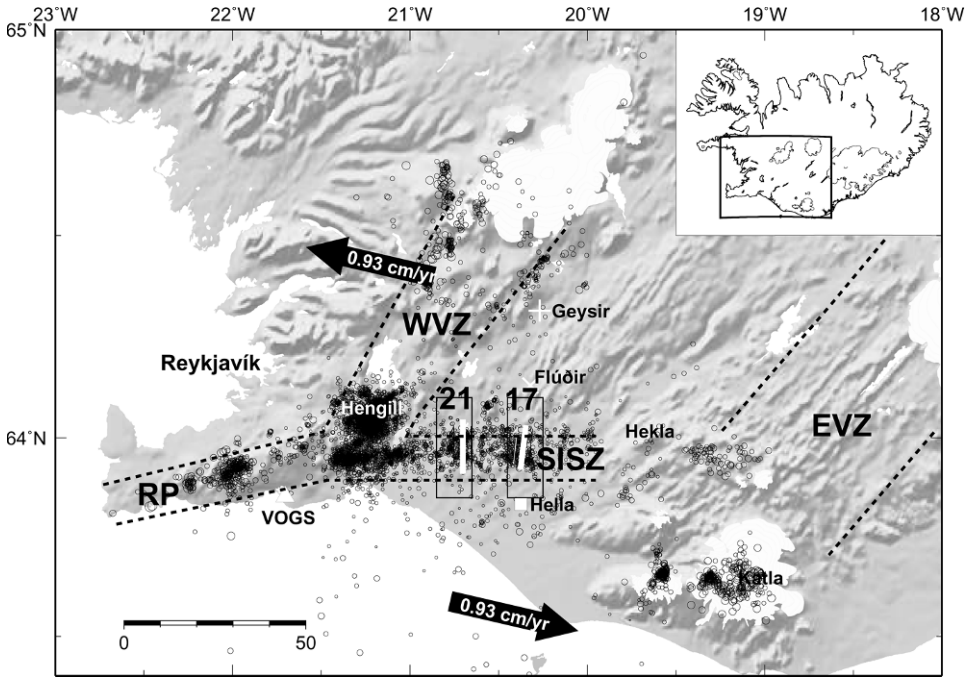

Figure 3.3. The southwestern part of Iceland. Dotted lines denote the Western Volcanic Zone (WVZ) and the presently more active Eastern Volcanic Zone (EVZ). The South Iceland Seismic Zone (SISZ) is indicated as well as its prolongation in the Reykjanes Peninsula (RP). The direction of relative plate motion is shown by arrows. Locations of the faults (in white) of the two large earthquakes that ruptured on June 17 and 21, 2000 are indicated by 17 and 21. Small dots (circles) show the epicenters of small shocks that occurred between 1991 and 1994 and delineate the SISZ and the RP. There was high seismic activity between the two zones at the Hengill volcano, where seismic activity started in 1994. In the southernmost part of Iceland, below the icecaps Katla and Eyjafjallajökull (white) there was high seismic activity between 1991 and 1994 as well.

of a rock sample, or propensity to cracking or yielding, we exert a known stress to a small sample and observe the resultant deformation and cracking. In Iceland's natural laboratory we can observe input stress as well as output stress in an Earth-realistic test sample. The transform zones of Iceland can be used to bridge the gap between laboratory experiments and the huge transform zones of the world, like the North Anatolian Fault Zone and the San Andreas Fault.

Because of scant vegetation and the absence of sediments, tectonic processes are relatively transparent in the geology of Iceland, The country was totally covered by an icecap in the last ice age, which ended between 10,000 and 15,000 years ago, digging up and flushing away older sediments. The vegetation layer which has built up after the ice age is thin.

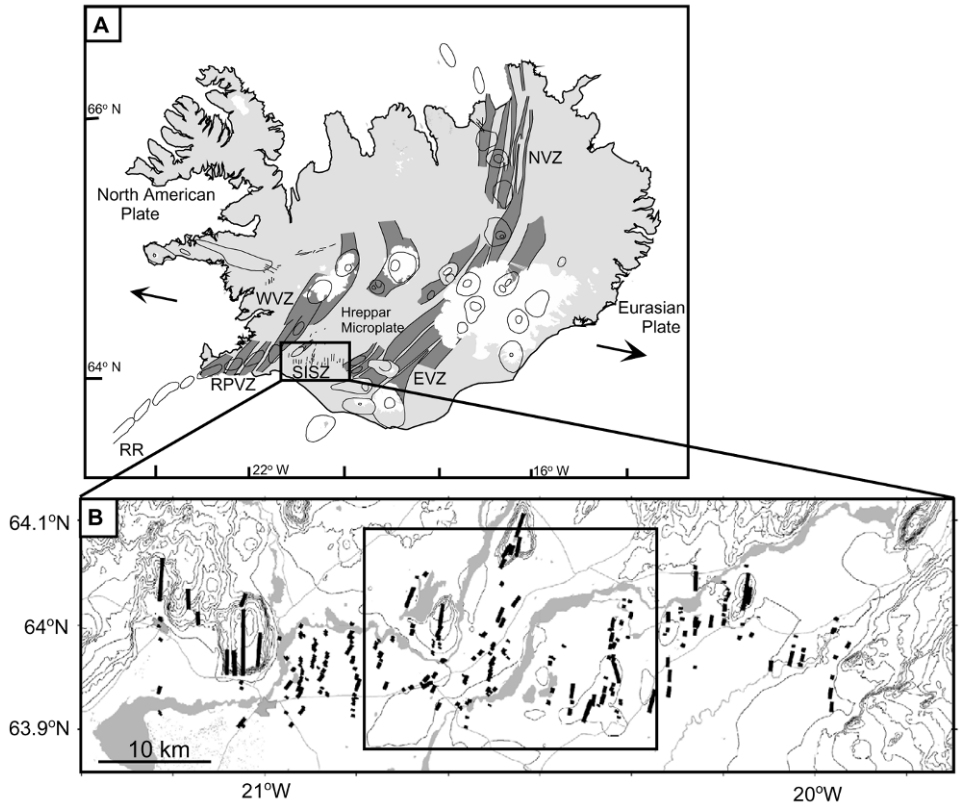

Figure 3.4. Iceland with its rifts (see caption to Figure 3.2). Part B of the figure is a simplified map of the surface fractures associated with north–south striking strike slip faults in the South Iceland Seismic Zone (SISZ) (from Clifton and Einarsson, 2005).

The observed fault segments of recent earthquakes in the SISZ outline a zone that is only 10 km to 15 km broad (Figure 3.4; see also Einarsson, 1991; Clifton and Einarsson, 2005). This is in good agreement with the everyday micro-earthquake distribution in the zone (as demonstrated in Figure 3.3, see also other figures of micro-earthquake locations in Chapter 4).

This indicates that the SISZ is a well-defined zone of weakness some 10 km to 15 km wide between the stronger and less fractured crust to the north and south. However, it is not quite as simple as that. The fault planes of some of the large earthquakes in the area reach much farther to the north and south of this narrowly defined zone.

For further reading on Iceland's tectonic framework see Sigmundsson (2006) and Einarsson (2008).

3.2 THE CRUSTAL STRUCTURE OF THE SOUTH ICELAND SEISMIC ZONE (SISZ)

Knowledge of the rheological conditions of the crust and uppermost mantle of the SISZ are significant for understanding the dynamics of the zone and ongoing rupture processes. There has been much dispute about the thickness of the crust in the SISZ as is the case for the rest of Iceland. The dispute concerns two main models of the crust: the thin crustal model and the thick crustal model. The thin model indicates the crust to be around 10 km thick in the SISZ and the thick model assumes a thickness of more than 20 km. This is to some extent a matter of how the crust is defined. I will not involve myself here in this dispute, instead—as at other places in this book—I will concentrate on observable features that can be expected to influence rupture processes in the crust. For other information I will point the reader to some further readings.

The elastic/brittle crust in Iceland is around 10 km thick and is most significant for earthquake release. This is where most plate motion strain builds up only to be released later in earthquakes. In a large part of the SISZ—the eastern and central part—the depth is around 10 km, becoming a few kilometers shallower in the western part. I will come to this later.

Figure 3.5 schematically shows some of the most significant features of the SISZ crust. For the structure of seismic velocity the figure is based on the active refraction/

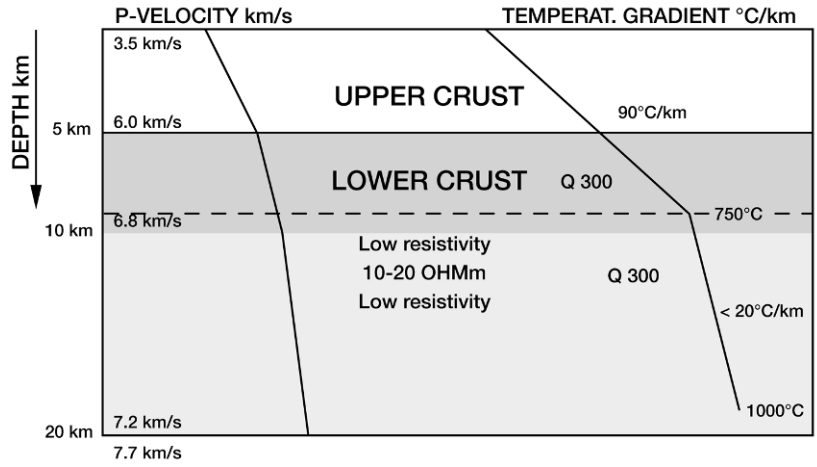

Figure 3.5. A schematic vertical cross-section showing some of the most significant features of the crustal structure of the SISZ down to a depth of 20 km. It shows *P*-wave velocities, the temperature gradient, and values of the quality factor *Q*. This high value of *Q* reflects the good transmission of elastic waves from distant earthquakes (i.e., the crust responds elastically to high strain rates, produced by elastic waves, all the way through it). However, ductility toward slow strain rates, as caused by slow plate motion, is indicated by lack of earthquake release. It is shown here as being below the 750°C temperature level, which defines the brittle–ductile boundary or brittle–ductile transition (the dashed line).

reflection seismic methods outlined in Pálmason (1971), Flóvenz and Gunnarsson (1991), and Bjarnason *et al.* (1993). Resistivity information comes from the magnetotelluric observations outlined in Beblo and Björnsson (1980), Hersir *et al.* (1984), and Eysteinsson and Hermance (1985). The depth of the brittle–ductile boundary is based on the local and teleseismic earthquake observations given by Stefánsson *et al.* (1993).

3.2.1 The detailed seismic velocity structure in the SISZ

The seismic velocity structure shown in Figure 3.6 is based on three-dimensional inversion of the travel times of *P*-waves and *S*-waves from earthquakes and explosions along the SISZ and its east and west prolongations (Tryggvason *et al.*, 2002). Cross-sections of the velocity distributions shown in the figure are representative in a 20 km wide area along the SISZ.

Of especial interest for dynamic processes in the SISZ is the relatively low value of the ratio of *P*-wave velocity to *S*-wave velocity, V_P/V_S, below a depth of 3 km to 4 km in the SISZ (see Figure 3.6c). This may reflect relatively high pore fluid pressures below 3 km to 4 km. It is of especial interest in connection with the discussion (later in the book) about modeled high pore fluid pressures at the bottom of the brittle crust of the SISZ which, in response to plate motion strain, is expected to cause the upward flow of high-pressure fluids into the seismogenic (elastic/brittle) crust and hydro-fracturing.

As pointed out by Tryggvason *et al.* (2002), detailed information about velocity and velocity ratios in the area is highly dependent on the number of local small earthquakes available for velocity inversions. Within the SISZ the number of micro-earthquakes was low and there were very few of them below a depth of 8 km to 9 km, which limited the resolution of velocity inversions. We only see the ratio V_P/V_S at a good enough resolution some 7 km to 8 km deep along the SISZ (as seen in Figure 3.6).

Figure 3.7 shows the velocities in a three-dimensional view of the Hengill volcanic complex at the western end of the SISZ. Clear low-velocity anomalies are indicated at seismogenic depths (i.e., at depths between 4 and 6 km) both for *P*-waves and *S*-waves, but relatively lower velocities for the *P*-waves—as shown by the low V_P/V_S ratios in panel (c). This anomaly is not caused by partial melt (Tryggvason *et al.*, 2002), it is interpreted by the authors as being local heavily fractured crust and the low velocities as being caused by supercritical fluids—involving meteoric water and fluids of magmatic origin—present in the crust.

Similar conditions regarding the V_P/V_S may well prevail below the whole of the SISZ, but they could not be proven as the resolution of velocity information is much lower in the SISZ than in the Hengill area because of far fewer micro-earthquakes and thus fewer ray paths that could be used for velocity inversion. Anyhow, as already stated, the authors see a relatively low V_P/V_S velocity ratio below a depth of 3 km to 4 km in and around the SISZ and even down to around 7 km—the limit at which data can be resolved satisfactorily.

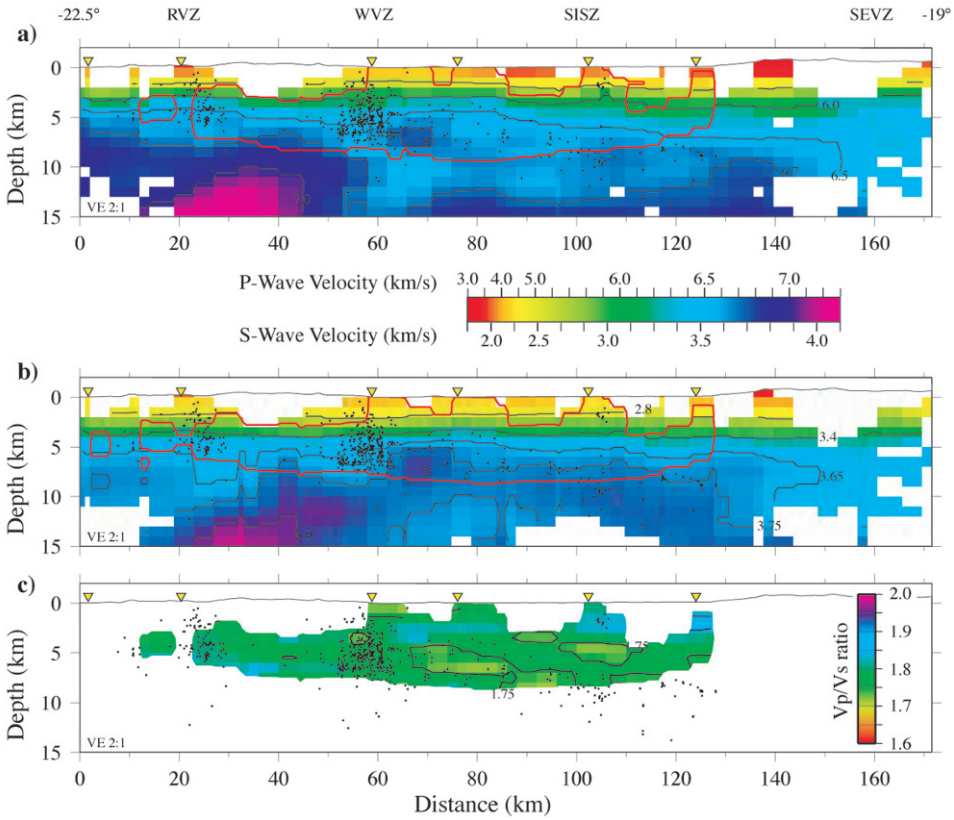

Figure 3.6. Velocities of *P*-waves and *S*-waves—(a) and (b)—in a vertical cross-section around 20 km thick from the Reykjanes Peninsula to the East Volcanic Zone. The SISZ is between 60 km and 130 km in the maps (areas with insufficient information are white). The cross-section (c) shows the V_P/V_S ratio. Seismicity within 2 km of the cross-section is shown as black dots, and triangles indicate the projected positions of SIL seismic stations. The thin red lines seen along (a) and (b) indicate the upper and lower limit of well-resolved values for the *P* and *S* velocities (i.e., where values for the V_P/V_S ratio are significant). Panel (c) only shows significant values for V_P/V_S (i.e., results from in between the two red lines; Tryggvason *et al.*, 2002).

Another interesting feature of the velocity distribution in the SISZ is that depth down to the lower crust (i.e., to velocities of 6.5 km/s) increases from less than 4 km in the west to more than 5 km in the east (Tryggvason *et al.*, 2002). An explanation of this could be that deposits from recent volcanic activity are thicker in the eastern part of the SISZ, nearer the presently more active Eastern Volcanic Zone, than in the western part.

3.2.2 The brittle–ductile boundary

The depth to ductility, i.e. to a depth where earthquakes normally do not occur varies with the strain rate. The crust responds as elastic/brittle to large strain rates

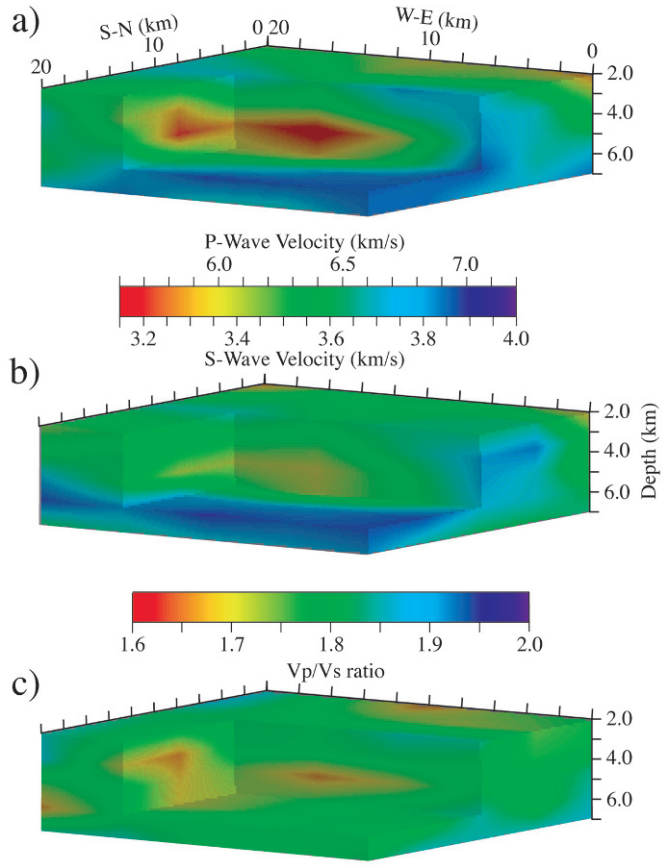

Figure 3.7. A three-dimensional view of velocities below a 20×20 km rectangular area of the Hengill volcanic complex at the western end of the SISZ. Because of the higher microseismic activity below this area, resolution is better than in the adjacent SISZ as a whole (as demonstrated in Figure 3.6). Spatial variations of P, V_P, are shown in (a), S velocities in (b), and the V_P/V_S ratio in (c). The greater reduction in P velocity than S velocity is well demonstrated in the velocity ratios. The view is from the northwest (from Tryggvason *et al.*, 2002).

but as ductile to low strain rates. Figure 3.8 shows local depths to this boundary in everyday seismicity, as evaluated by Tryggvason *et al.* (2002). They conclude that the depth is 5 km in the young crust at the western end of the SISZ deepening to 12 km at the older eastern end of the zone, in agreement with Stefánsson *et al.* (1993). The deepest aftershocks of the two earthquakes of year 2000 indicate 1 km greater depth for the brittle behavior than indicated in Figure 3.8, reflecting higher local strain rates accompanying the earthquakes.

Comparison with temperature gradients from boreholes indicates a temperature of 580°C to 750° at the brittle–ductile boundary, depending to some extent on the amount of fluids in the rock. Björnsson (2008) advocates that the higher value is most probable.

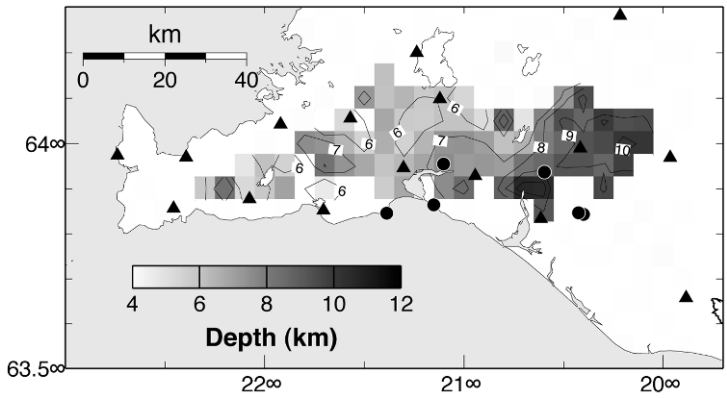

Figure 3.8. Depth to the base of the brittle crust, defined as depth to the deepest everyday seismicity. The black circles mark the locations of the boreholes used to measure geothermal gradients and the triangles are the seismic stations used for depth determination of earthquakes (from Tryggvason *et al.*, 2002).

3.2.3 High pore fluid pressures near the top of the ductile layer

A significant step forward for understanding the dynamics of a zone was taken when very low electrical resistivity was found below the crust. Magnetotelluric measurements indicate a layer of low resistivity underlying large parts of Iceland. The layer is expected to be around 5 km to 10 km thick and the resistivity to be between 5 Ω/m to 10 Ω/m. The depth to the center of this layer varies but is expected to be around 15 km in the SISZ (Björnsson, 2008). Figure 3.9 shows the depth to this layer of high conductivity.

A probable explanation of this high conductivity is the high density of fluid-filled pores and fractures in the rock at these depths. Moreover, there is good transmission for short-period shear waves down to 20 km according to Menke and Levin (1994). To explain both (i.e., the low resistivity of the layer below the brittle–ductile boundary and the good transmission of shear waves), Stefánsson *et al.* (1996) proposed the following structure for this layer: a crystal matrix of olivine-rich peridotite close to dunite (responsible for the good transmission of seismic shear waves) with intergranular fluids composed of water and carbon dioxide (responsible for the low resistivity).

Recommended further reading regarding the crustal structure of the SISZ includes Bjarnason (2008), Bjarnason and Schmeling (2009), Brandsdóttir and Menke (2008), and Darbyshire *et al.* (1998).

3.3 GEOLOGICAL MAPPING AND MODELING OF EARTHQUAKE FAULTS IN THE SISZ

Since 1966–1967 the belief that the SISZ was a zone of left-lateral shearing or transform motion elongated east to west has predominated (Stefánsson, 1967;

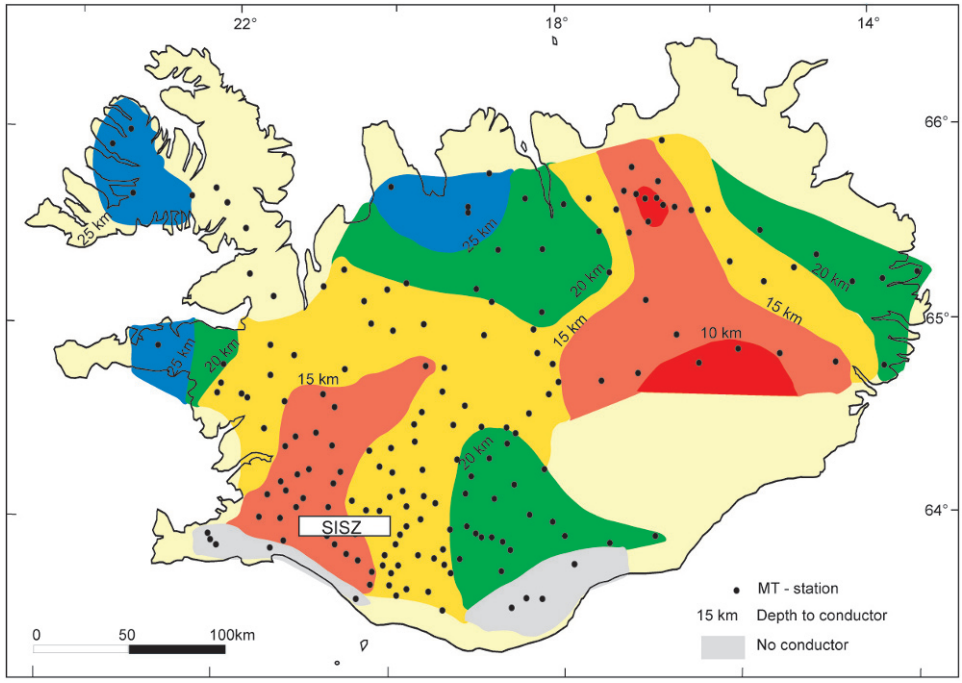

Figure 3.9. Depth in kilometers down to the center of the electrical conductor at the base of the Icelandic crust. The depth is less than 15 km beneath the major developed rift zones in SW and in NE Iceland. The depth thickens with age to 20–25 km beneath the older Tertiary areas in W. and E. Iceland (modified from Björnsson *et al.*, 2005).

Ward, 1971). This was in good agreement with the then emerging hypothesis of global plate tectonics.

Surface mapping of Holocene earthquake ground ruptures has been ongoing in the SISZ since the late 1970s—the time of pioneering work led by Páll Einarsson (see Appendix 2.B). In some cases, ground ruptures could be identified with known historical earthquakes. At an early stage it was discovered that individual faults took on a north–south direction (i.e., perpendicular to the strike of the SISZ) and they indicated right-lateral horizontal slip. The distance between individual earthquake faults appeared to be no more than 5 km, even though total fault lengths appeared to be between 10 km and 20 km (Einarsson and Eiríksson, 1982; Einarsson, 1991; Clifton and Einarsson, 2005).

The north–south configuration of the faults was explained by so-called ''bookshelf faulting''. The zone was expected to be around 15 km wide and the north–south segments between faults would fall to the sides like books on a bookshelf. Books falling to the left would be caused by general left-lateral motion across the westward-striking SISZ, and segments between the faults (the books) would have right-lateral displacement toward each other.

The bookshelf tectonics concept for SISZ, originally suggested by Páll Einarsson, has been explained in detail in *Geodynamics of Iceland* (Sigmundsson, 2006).

To explain the dense fabric of faults, Stefánsson and Halldórsson (1988) suggested the so-called ''dual-mechanism model''. This model assumes that zone faults break along existing north–south faults in the interplay between dyke injections into cracks elongated north–south and horizontal shearing motion caused by differential left-lateral motion across the plate boundary. They assumed the predominant energy rising from depth (i.e., carried in mantle fluids) governed where individual earthquake faults would occur (i.e., fluid intrusions at depth into a dense system of available fissures). Otherwise, it would be impossible (according to the authors) to explain why these long earthquake faults were so close to each other.

There was no contradiction between these two hypotheses. The bookshelf model was a kinematic model reflecting the fault pattern. The dual-mechanism model was put forward on the basis of historical earthquake data, known features of Icelandic geology, and the newly suggested existence of a layer of low resistivity below the brittle–ductile boundary, and to explain the dense fabric of active north–south earthquake faults.

Both models were criticized by some geologists who claimed that we would see northeast–southwest fault strikes in the geology if the ''books were falling'' to the left. However, in *Geodynamics of Iceland* Sigmundsson defends the idea, claiming that if the distance between active 40 km long earthquake faults were small enough (i.e., of the order of 0.5 km) they would still be striking north–south after only a few earthquakes on each fault during the postglacial time of 10,000 years. But he does not try to explain rheologically how they can be so close to each other. He only assumes stiff segments (i.e., books). In reality, crust stress anomalies after each earthquake would quickly dissipate into nearby areas and then out into gradually larger areas. Moreover, 10,000 years is a short time for this area when compared with it being sheared in a similar way for 2 million years.

The dual-mechanism model was criticized by pointing out that magmatic intrusions in the zone would be expressed in higher temperature gradients than observed, and remnants of recent volcanism would be seen in the zone as, for example, in the Reykjanes Peninsula (RP) zone (see Figure 3.3). In the RP long periods of rifting (of the order of 500 years) with large dyke injections are separated by earthquake periods of comparable duration.

The discussion on models of SISZ dynamics will be continued in Chapters 5 and 6 on new modeling.

3.4 THE AVAILABLE TECHNOLOGY TO OBSERVE CRUSTAL PROCESSES

For Iceland (as for other countries) seismological observations started less than a century ago, and since then the information provided by such observations has been

growing. When studying the crustal processes linked to large earthquakes it is important to make use of all available information, from historical descriptions to modern geophysical information. The mapping of active earthquake faults enables us to increase the length of seismic history, reaching back hundreds to thousands of years.

3.4.1 Evolution of the SIL system

In Sections 2.3 and 2.5, I described design criteria for the new seismic system that was earmarked for creation in 1986. Creation of this system was the most significant part of the first multinational earthquake prediction research project in Iceland: the SIL project, 1988–1995 (Appendix 2.C). SIL stands for South Icelandic Lowland, the test area of the project. The SISZ extends from east to west through this area. The seismic system to be created was called the SIL system or the SIL network.

The design criteria had already been fulfilled and operation of the system had become automatic in the SISZ by 1991. Since that time the evaluation capacities of the system have gradually been enhanced, and automatic operation gradually became safer as a result of experience gained in hazard watching and warnings in Iceland. The operation of the system now applies to all the seismic and rift zones of Iceland. During this time the system has become paramount for earthquake prediction research in Iceland.

The SIL system is a network of triple-component (i.e., vertical, E–W, and N–S) digital seismic stations and a data-processing system, created around 1990. For the purpose of recording earthquakes down to magnitude 0 in this area a dense network was needed. The distance between stations in the SISZ is 25 km to 30 km (Figure 2.4). Gradually, more stations were added along geologically active zones of the country as shown in Figure 2.4, and the density of stations varied according to scientific needs and financial constraints. Now there are more than 50 stations under centralized automatic operation.

When the SIL system was designed and automatic operation started (i.e., 20 years ago), it was in many ways at the scientific forefront worldwide in detecting and evaluating micro-earthquakes, and remains so to this day. Although there are now many digital seismic systems available, which in many ways are comparable with it, the SIL system is still at the forefront because of its sensitivity, flexibility of operation, and openness to new applications. Based on 20-year operational experience in Iceland new applications have gradually been added to the system, ranging from an enhanced capacity to extract information on crustal conditions from micro-earthquakes to gradually safer operation.

The buildup and operation of the SIL system has been a major achievement. The story behind SIL and how it developed into what it is now is interesting. In fact, despite still being based on the 20-year-old design it has gradually been enhanced by major developments in computer and communication technology.

In order to fulfill the design criteria for sensitivity and to avoid the huge cost at that time of transmitting the 19,200-baud data stream continuously to the evaluation

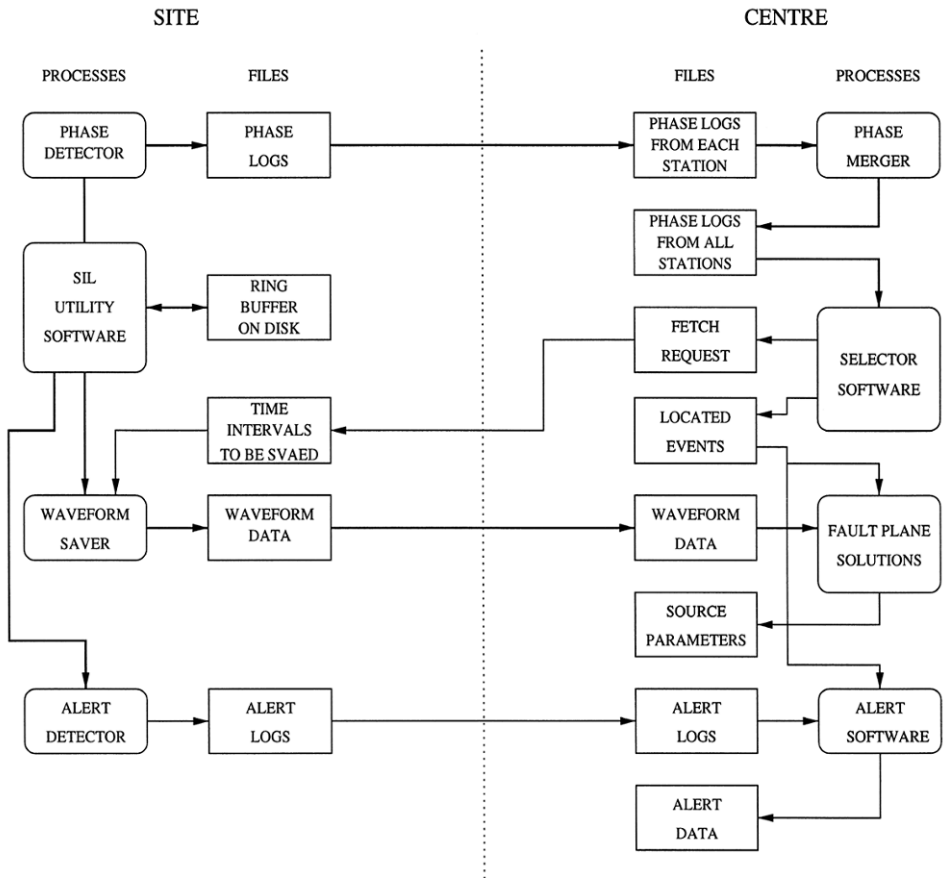

Figure 3.10. Flow chart of SIL processing. A phase detector in the computer at a remote seismic station produces phase logs that are transferred to the center. At the center a program merges phases from all stations into one file which is input to the "selector" software. The selector software defines the possible seismic events of earthquakes through a phase association procedure and determines time intervals of waveform data to be retrieved from the remote stations. At the remote stations a net saver program copies the data from the ring buffer system to local files and transfers them to the center. The alert software works in parallel with the acquisition system using information from the selector software and from the alert detector at each site (from Bödvarsson *et al.*, 1999).

center at the IMO, it was decided that every remote seismic station should automatically perform significant evaluations (Figure 3.10). In those days phone lines simply could not cope with the baud rate needed to carry the necessary data stream continuously. So, every seismic station was equipped with a 32-bit computer running a UNIX operating system for local automatic evaluation. Significant analysis was carried out at the remote stations, and short messages were transmitted to the system center and back to the stations before complete data streams of detected seismic

events were sent over. The seismic system worked as a distributed UNIX computer system.

So, during regular operation of the SIL system very little of the continuous data stream released by the seismometers ever got to the center. The computers at the remote stations analyzed every signal that exceeded some low predefined level. Information about every sensed pulse including its onset time, spectral amplitude and corner frequency, coherence between components, and incoming azimuth were packed into a 128-byte message and sent through a communication link (mostly X.25 links at that time) to a computer at the central station. The central computer compared the information from the various remote stations, localized the origin of the signals, and stated whether the signals were caused by real earthquakes or by some local disturbance, like traffic near the sensors or animals. On the basis of the information in this 128-byte signal from some stations, the central computer produced a preliminary report giving a detailed description of any seismic events. After this analysis, the central computer fetched the total waveform data of earthquakes from all stations capable of observing them and created a new report with better constrained results about the earthquakes. However, the complete data stream from the sensors was preserved on a ring buffer in the computer of the remote station so that it could be retrieved later for further analysis.

The detection method that was (and still is) used was called a ''net detection'' method. It is a means of ascertaining how sensitive the system is at detecting small, but real earthquakes. High sensitivity meant that any ''suspicious'' small signal was considered by the site computer to be possibly an earthquake until it was rejected by the central computer as a local disturbance, sometimes because it was only seen by one station or because the character of the signal excluded it. The net detection facility of the SIL system is still, after almost two decades of operation, at the forefront worldwide in detecting those small seismic signals that are the most significant for earthquake prediction.

As already stated, the main reason for getting much of the analysis of the system done at the remote sensor stations was that it was so expensive to hire lines for transmission of the full data stream from the seismic sensors to the center of the system for the whole analysis to be carried out there. With new communication technology it is now possible at a relatively low price to transmit the whole data stream in real time to the SIL center and this is already the case for many of the seismic stations. However, the method used for evaluation at the remote sites is still valid and secures the data when communication failures occur. Automatic analysis at remote stations is also significant for detecting and analyzing individual earthquake signals when activity is almost continuous or when there are swarms of earthquakes. In a hazard situation it is necessary to make use of all the information coming to the system. Experience shows the system capable of automatically managing high-level analysis of thousands of earthquakes per day.

In most cases, when continuous data are transmitted from stations to the center they go to a ''station computer'' there, and communication between station computers at the center and the main central computer is practically the same as when

the local computers were remote. In each case the method selected for transmission and communication is a matter of what best fulfills the operational needs.

3.4.2 How the SIL system works

A final automatic report on earthquakes is ready in a few minutes, depending on the distance to the stations used in the location procedures. The system also reports detected phases of earthquakes within a second, which has major importance for early warnings.

The sample frequency of waveform data that are preserved is set to 100 per second. Experience shows this sample frequency is enough to record even the smallest micro-earthquake signals. Of course, this can be set higher. However, the main frequency of earthquake waves down to magnitude 0 hardly ever exceeds 20 Hz. For this purpose, 100 samples/s is good enough to get the main observable features of the wave. However, the system can be modified to record at much higher sample frequencies, which might be needed in a very dense network to securely record micro-earthquakes down to magnitude -1 or so.

The sensitivity of the system is extraordinarily good. For example, in some areas of the SISZ it can detect all micro-earthquakes down to magnitude 0 and can extract significant information from earthquakes down to -1 in magnitude.

The general features of the SIL system have led to many significant applications being developed and introduced and many more are under development. The enormous number of small earthquakes recorded and the time accuracy of one millisecond makes the mass evaluation of information on seismic waves coming from dense origins possible. This can be applied to very precise locations with relative accuracy down to 10 meters and an absolute accuracy of the order of a few tens of meters. Work is ongoing at automatizing such location procedures.

The capacity of the system to find automatic fault plane solutions on the basis of both *P*-wave and *S*-wave amplitudes coupled with the ability to locate micro-earthquakes with error limits down to 10 meters makes the system useful to accurately map small faults at depth as well as ongoing slip across them. Many other applications will be discussed in Chapter 4. The SIL system is more than just a useful tool to monitor processes in the crust and to increase understanding of them. Geologists have found the ability of the SIL system for detailed fault mapping very useful at discovering probable water conduits in the crust. This can be used to select sites to drill for hot water. It is not an easy task to operate an observational system for the length of time necessary for real warnings and for studying long-term processes. Those who pay the operational costs easily become impatient with the passage of time. Application of the system to other fields which can help in paying the operational cost is therefore significant.

The above description of the SIL system is based on Bödvarsson *et al.* (1996, 1999), Bödvarsson and Lund (2003), Jakobsdóttir *et al.* (2002), Slunga (2003), and Stefánsson *et al.* (1993), all of which are recommended for further reading.

3.5 OLDER METHODS OF SEISMIC OBSERVATION

A conventional seismic system was continuously run in Iceland from 1927 by the Icelandic Meteorological Office. Although sensitivity was low in the beginning (around magnitude 4 over the whole country), gradually it was upgraded to be sensitive to magnitudes around 3 in some areas. The seismic signals then recorded by instruments could not be viewed in real time, they were recorded on photographic paper which was sent to the Meteorological Office on a weekly bases for evaluation. In 1973 the Science Institute of the University of Iceland started work on a seismic system that could directly record signals on paper. As this system was being built up Iceland underwent increased volcanic activity. This system significantly increased the ability to detect small earthquakes in Iceland. However, it was still not possible to record earthquakes with magnitudes down to 0 until the advent of the SIL system in 1990, which being digital could collect more detailed information from each earthquake. However, information from the older networks is enormously useful for studying the long-time evolution of seismicity (e.g., related to pre-hazard processes in volcanic and seismic areas) and for studying seismic structure. Mapping of the hypothesized mantle plume and the root of the Iceland Hot Spot some 400 km deep (see Section 3.1) is an example of significant research achievements based on systems pre-dating the SIL system (Tryggvason *et al.*, 1983) .

3.6 STUDYING HISTORICAL EARTHQUAKES AND THEREBY EXTEND EARTHQUAKE HISTORY

Seismic networks built up over the last 100 years reveal very little of how seismicity varies with time. Historical documents that describe the effects of and destruction caused by earthquakes help us to go beyond the 100-year history and get a better handle on its variability and thus of its causes. These documents are extremely significant for understanding the dynamics of the Iceland plate boundary. Very good information on large earthquake effects is available (starting in 1700) for the SISZ and there is also useful information from as early as 1200.

Significant information about historical earthquakes can be found in a detailed report by geologist Thorvaldur Thoroddsen (1855–1921). The Danish king, who was also king of Iceland at the time, sent this researcher from Copenhagen to Iceland to study the destruction caused by the 1896 earthquake sequence. The aim was not to study the cause of earthquakes or their nature, but the destruction caused by them. Thanks to his good scientific work, albeit for a different purpose, we now have these data available. They are extremely significant for earthquake prediction research. Figure 2.1 shows a map compiled by Sveinbjörn Björnsson for a report (Almannavarnaráð, 1978, which was partly reproduced in Björnsson and Einarsson, 1981). The basis of this report was the work of Thorvaldur Thoroddsen on destruction caused by historical earthquakes. A detailed description of the destruction is provided in his books on earthquakes in Iceland (Thoroddsen, 1899, 1905).

Figure 2.1 shows areas where 50% of all houses have collapsed as a result of earthquakes in the SISZ since 1700.

This information about destruction was the basis for allocating magnitudes and places of origin (i.e., epicenters) to these earthquakes. Instrumental information which was available for the last of these earthquakes (i.e., the 1912 earthquake) also helped in this. As a global network of seismic stations was available at this time, its instrumental magnitude could be determined. The internationally based M_s magnitude of the earthquake in 1912 was 7.0. By comparing the areas of destruction of other earthquakes since 1700 with the destruction area of the 1912 earthquake, and knowing the M_s magnitudes of the last one, the magnitudes of all historical earthquakes could be estimated.

The large attenuation of intensity of observed earthquakes with distance indicated a very shallow origin (i.e., faults open to the surface) and thus the largest surface effects would indicate the epicenters, which were simply put in the middle of destruction areas that were elongated north–south (Figure 2.1), and thus could be located with good accuracy.

The catalog of destructive earthquakes computed in this way has been much used for hazard assessment and for studying strain buildup and strain release along the SISZ. Benioff's formula of the relation between magnitude and strain release in earthquakes (Benioff, 1951) has been used to calculate strain release along the SISZ (as will be described in Chapter 4).

3.7 OBSERVATIONS OF DEFORMATION

3.7.1 Volumetric borehole strainmeters

Monitoring volumetric crustal strain in boreholes started in the SISZ in 1979 with the installation of seven Sacks–Evertson type strainmeters. The installation was carried out by the Icelandic Meteorological Office and the Department of Terrestrial Magnetism, Carnegie Institution of Washington. The inventor of the instrument, Selwyn Sacks (see Appendix 2.B), led the installation work. It was hoped that this extremely sensitive instrument could detect the small deformation expected to occur before large earthquakes and thus could be of help in their prediction.

The instrument consists of a cylinder that can be 3 m to 6 m long, with a diameter depending on the width of available boreholes. The main part (i.e., the lower part of the cylinder) is filled with a special oil of low compressibility. At the top it is connected to a small linearly expandable bellows (Figure 3.11). When the large sensing volume in the cylinder is deformed by pressure changes, the oil in the large container flows out of or, respectively, into the small bellows which thus deforms uniaxially, proportional to the volume change in the large container. The lengthening or shortening of the bellows is measured by a differential transformer (i.e., basically a rod at the end of the bellows penetrates the transformer and changes its capacity accordingly). In this way a large hydraulic amplification of strain

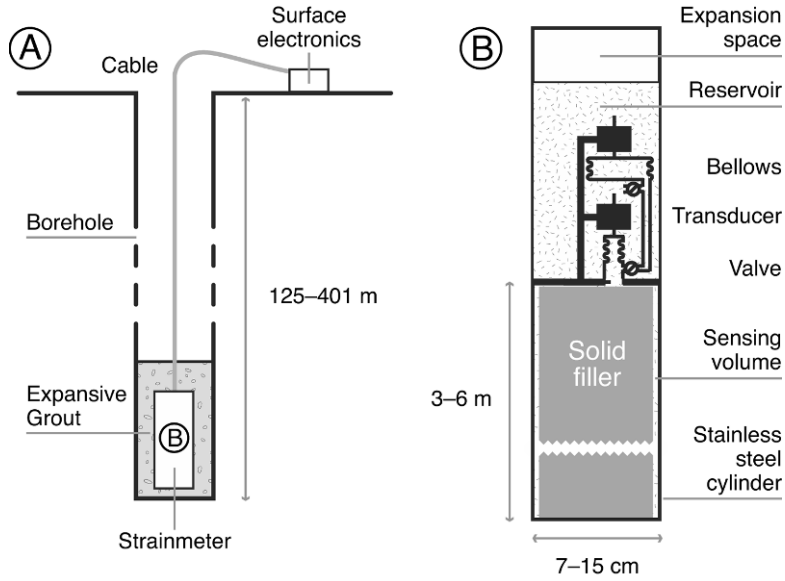

Figure 3.11. The construction of a Sacks–Evertson volumetric borehole strainmeter. It is cemented to a borehole wall by means of an expansive grout, which securely connects it during large rock deformations. The depths indicated (125–401 m) are the depths of the various strainmeters in Iceland. These depths are limited by the depths of the boreholes. The fluid in the large sensing volume in the cylinder goes into a small bellows which expands relative to the volumetric strain exerted by the surrounding rock, as measured by a differential transducer. The instrument in the figure has an extra bellows, larger and less sensitive, to take over when the pressure gets too high in the small bellows, useful for keeping track of long-term strain changes.

signals is obtained, which is very difficult if not impossible to obtain with electronic amplification only, because of electrical noise.

As strainmeters are cemented under pressure in boreholes, they can measure both compression and expansion of the surrounding borehole rock. They can measure strain of the order of 10^{-12}, which is dimensionless, but expressing in this case volume change divided by volume. In boreholes the conditions are usually so good that this makes them the most sensitive deformation measurements available worldwide. In this connection the depth of the boreholes and the condition of the rock is significant. For the installations in Iceland in 1979 it was considered too expensive to drill special holes, so old holes, drilled for other purposes, were used.

The effective sensitivity of the instrument is extremely good at short time intervals (i.e., of the order of seconds to days). Earth and ocean tides are about 10^{-8} in volumetric strain. Such noise can be predicted to some degree and thus removed. This is also true for the effects of atmospheric pressure lows which exert much larger strain changes than tides. Various effects of meteorological origin on the surface of the Earth have, during longer recording periods, less predictable influence over effective sensitivity. Most significant in this connection is change in groundwater level.

Strainmeters are still used in the SISZ and have provided extremely significant information especially about eruptions in the Hekla volcano at the eastern end of the zone. Such information has been used for dynamic modeling of the eruptions and their preparatory stage (Linde *et al.*, 1993; Ágústsson *et al.*, 1999). Monitoring and modeling were used for a very successful and useful short-term prediction of the Hekla eruption in 2000. This is described in Chapter 7 ''Warnings''.

Strainmeters and seismometers showed signals 2–3 hours before a magnitude-5.8 earthquake in the easternmost part of the SISZ, the Vatnafjöll earthquake in 1987. These signals were modeled as reflecting magmatic intrusion at depth in the crust, possibly triggering the earthquake.

For further information about strainmeters, observations, and modeling see Sacks *et al.* (1971, 1980), Linde *et al.* (1993), and Ágústsson *et al.* (1999).

3.7.2 Repeated and continuous GPS measurements

Deformation has been subject to repeated GPS measurements since 1986. A nationwide network of stable benchmarks (Figure 3.12) for repeated GPS measurements is an important tool for monitoring long-term deformation in Iceland and deformation due to isolated events such as earthquakes and magmatic movements. Significant papers based on episodic campaign measurements on these points include Heki *et al.* (1993), Sigmundsson *et al.* (1995), Hofton and Foulger (1996), LaFemina *et al.* (2005), and Árnadóttir *et al.* (2008, 2009).

Continuous GPS measurements in Iceland began in 1995 when the first station was set up in Reykjavík. In 1997 a second station was added in Höfn in southeast Iceland. The buildup of networks of continuous GPS measurement stations has generally followed increase in seismic and deformation activity in different parts of the country (Geirsson *et al.*, 2006). In 2008 over 60 continuous GPS measurment stations were running nationwide (Figure 3.12).

When the large earthquakes occurred in the SISZ in 2000 there were no continuous GPS measurement sites near the epicenters, but those to the west and east of the SISZ provided information that was used for modeling earthquake ruptures (Árnadóttir *et al.*, 2001). In May 2008 a large double-earthquake occurred in the western part of the SISZ. At this time the network was better placed to observe co-seismic deformation (see Chapter 4). In this case some continuous GPS measurement stations sampled at a high-rate (1-second sampling), enabling direct observations of displacement wave coda from an earthquake for the first time in Iceland (Hreinsdóttir *et al.*, 2009).

For further reading about this see Sigmundsson *et al.* (1995), Hreinsdóttir *et al.* (2001), and Árnadóttir *et al.* (2006).

3.8 OBSERVATIONS OF GROUNDWATER

Drilling holes to increase monitoring sensitivity is not feasible in Iceland. Boreholes would eat up much of the budget earmarked by the government for running a warning service. However, there are many boreholes in Iceland that have been

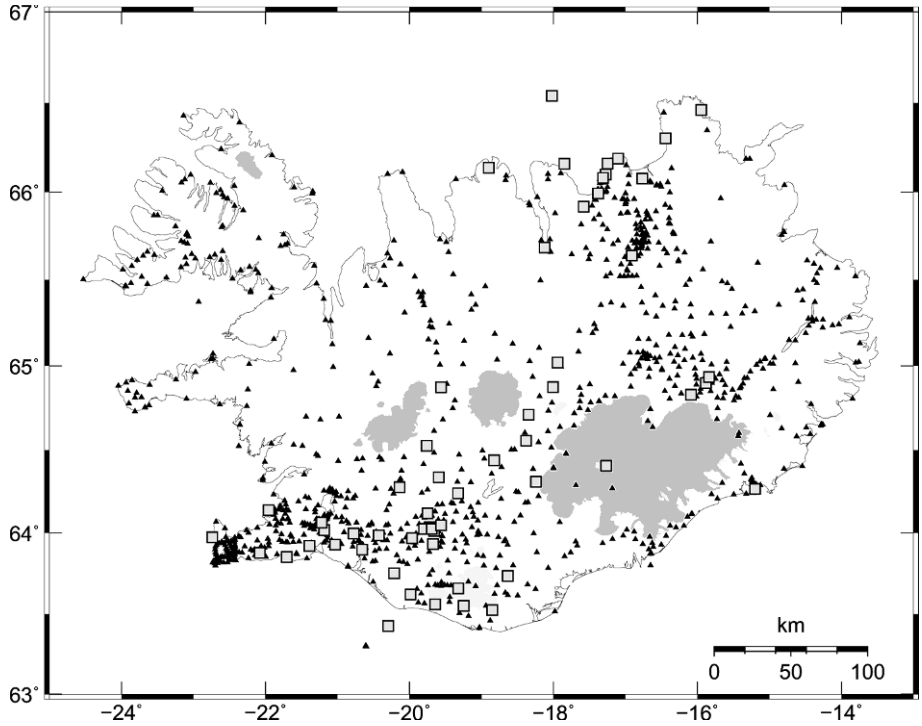

Figure 3.12. A map showing the locations of GPS benchmarks in Iceland (black triangles) and continuous GPS measurement stations (gray boxes).

drilled (a few hundred meters deep) for the purpose of extracting hot water. Such holes have in some cases been used for volumetric strainmeters. Other holes where the water supply is deep can be used to monitor deformation, by measuring changes in water height and chemical content.

3.8.1 Observations of groundwater level changes in boreholes

Borehole water levels are monitored at several sites in the SISZ, not for monitoring crustal pre-earthquake processes but to extract geothermal heat from depth for domestic and business usage. The purpose is to monitor the condition of the holes and to be alerted to the possibility of dry pumping when the water level drops. Experience shows that upgrading such facilities for continuous and high-frequency monitoring of water height can be of use in monitoring crustal pre-earthquake processes (Björnsson *et al.*, 2001). Such monitoring could take place regularly at selected holes in cooperation with borehole owners at several places in Iceland. The existence of boreholes near the plate boundaries in Iceland that could be used for this purpose is something that needs to be further investigated.

3.8.2 Observations of geochemical changes in well water

Radon (^{222}Rn) is a chemical element, a gas, which is a by-product of the radioactive decay of radium in Earth rocks. It has a half-life of only 3.8 days. Because of this short decay time the amount of it in wells is evidence of the speed of changes in its production from the rock. The likely reason for these changes is that the opening or closure of cracks in the rock, due to straining in the rock, increases or decreases the surface that is in contact with the well water we are observing. This fluid–rock interaction takes place at a shallow depth in fractured rock close to the surface but is probably related to deformation deeper down.

Observations of radon in borehole wells began in Iceland in 1977 (Hauksson and Goddard, 1981; Hauksson, 1981; Jónsson and Einarsson, 1996). The purpose was to monitor possible pre-earthquake processes. Several indications were found in that early dataset that related anomalies in radon to earthquakes in the SISZ.

This program was discontinued in 1993 because of lack of funding. A new radon-monitoring program with improved technology started in 1999, fortunately just a year before the 2000 earthquakes. The program picked up clear anomalies at six out of seven stations prior to the earthquakes (Einarsson *et al.*, 2008).

The findings have brought about further technological development that will make radon much more feasible as a tool to monitor crustal strain changes (Theodórsson and Gudjónsson, 2003). It is now possible to carry out continuous radon observations. However, further work is needed to better understand radon anomalies and to explain the science underlying their occurrence.

Geochemical observations with the purpose of discovering whether there are connections between the concentrations of heavy metals and seismicity were carried out in 2002 in a 1,500 m deep borehole on the Húsavík–Flatey fault in the Tjörnes Fracture Zone in north Iceland. Changes were observed shortly before a magnitude-5.8 earthquake 100 km to the north of the observing site (as reported by Claesson *et al.*, 2004). These results and later continuation of these studies resulted in recent plans to build a facility at this site for continuous monitoring of geochemical changes, with the purpose of contributing to geohazard warnings.

3.8.3 Building the infrastructure to predict geohazards

Earlier Icelandic experience at providing information about Earth hazards is a significant facility for Iceland as a test area. The positive attitude of people to Earth monitoring and prediction has helped to create the human and technological infrastructure necessary for practical warnings. Successful eruption warnings during the last 30 years as well as the establishment of a useful pre-earthquake warning service during the last 10 years have had the effect of creating a positive attitude among people. Icelandic geoscientists cooperate closely with civil protection authorities and are always available to give advice on impending hazards and warnings. By explaining the science they have also played a significant role in calming down fears that small but felt earthquakes sometimes cause. Developing a state-of-the-art practical warning service will be treated in Chapter 7 "Warnings".

4

Observable crustal processes preceding two large earthquakes in the SISZ test area

This chapter comprises 11 sections describing large earthquakes that occurred in the South Iceland Seismic Zone in 2000. The chapter looks at how they were predicted and how they could have been predicted. Section 4.12 describes an earthquake in 2008 also in the SISZ.

Section 4.13 contains a summary of observations of pre-earthquake processes that may be of value for predictions.

Multinational earthquake prediction research projects in the South Iceland Seismic Zone (SISZ) started in 1988 and were still proceeding when two large earthquakes occurred in the zone.

Right at the end of the PRENLAB 2 project (see Chapter 2) two large earthquakes occurred in the zone. They could be considered a timely test to verify and modify the results of 12 years of earthquake prediction research in the area. The earthquakes were anticipated. That was the reason for selecting the SISZ as a multinational earthquake prediction research area in the first place. The public and emergency services were well prepared and the area was instrumentally well equipped to observe the process and preparatory processes that are vitally important for issuing warnings of earthquakes in the area or at other earthquake-prone sites. The scientific groups involved in earlier earthquake prediction research projects got together in a new project, one that would make use of the experience gained from the 2000 earthquakes. The full name of this new project was "Application of practical experience gained from two recent large earthquakes in the South Iceland Seismic Zone in the context of earthquake prediction research to develop technology for improving preparedness and mitigating risk." As this was a bit of a mouthful, it was given the acronym PREPARED (see Chapter 2 and Appendix 2.C).

The two magnitude-6.6 ($M_s = 6.6$) earthquakes seriously rocked the inhabitants of the SISZ in June 2000 for the first time in almost a century (Figure 4.1). The first

R. Stefánsson, *Advances in Earthquake Prediction: Seismic Research and Risk Mitigation*, Springer Praxis Books, DOI 10.1007/978-3-540-47571-2_4, © Springer-Verlag Berlin Heidelberg 2011

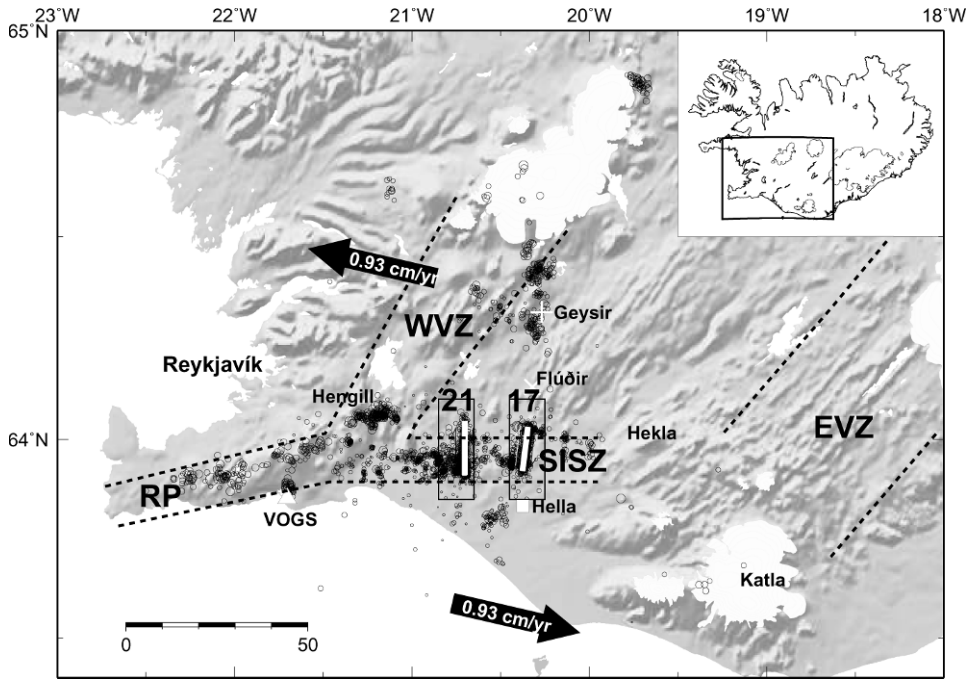

Figure 4.1. The southwestern part of Iceland. Dotted lines denote the Western Volcanic Zone (WVZ) and the presently more active Eastern Volcanic Zone (EVZ). The South Iceland Seismic Zone (SISZ) is indicated as well as its prolongation in the Reykjanes Peninsula (RP). The direction of relative plate motion is shown by arrows. The faults of the two large earthquakes that ruptured on June 17 and June 21 in 2000 are indicated by the labels "17" and "21". The epicenters of the small shocks that followed the large earthquakes (dots and small circles) show the extent of the seismically active area during and after the 2000 earthquake episode.

occurred on June 17, 2000 and the second three and a half days later on June 21, 2000 at a site 17 km farther west in the zone.

The last large earthquakes to strike in the SISZ were a sequence of six earthquakes which occurred in the zone around 100 years ago: five occurred in 1896 and the sixth one in 1912. The last was the largest. It was instrumentally recorded worldwide and reached magnitude 7 (M_s).

4.1 SOME BASIC INFORMATION ABOUT THE 2000 EARTHQUAKES

4.1.1 The June 17, 2000 earthquake

The first of the two earthquakes occurred on June 17, 2000. According to the Icelandic Meteorological Office (IMO) the origin time of the earthquake was 15:40:40.94 GMT, the epicenter was at 63.97°N, 20.37°W, and the depth of the hypocenter was 6.3 km (Stefánsson *et al.*, 2003). Aftershocks indicated a

12.5 km long vertical fault from the surface to a depth of 10 km striking N7°E (Hjaltadóttir and Vogfjörd, 2005). Surface fissures showing right-lateral motion on an underlying fault were found along the fault (Clifton and Einarsson, 2005). This agreed well with the USGS Rapid Moment Tensor Solution which showed a nodal plane striking N4°E and a dip of 84° to the east. The moment calculated by the USGS was 6.0×10^{18} Nm, assuming a best-fitting double–couple solution. The preliminary magnitudes estimated by the National Earthquake Information Center (NEIC) in the U.S.A. were $m_b = 5.7$ and $M_s = 6.6$. The Harvard CMT Solution (the global Centroid Moment Tensor project) indicated a scalar moment of 7.0×10^{18} Nm and magnitude of $M_w = 6.5$. An average right-lateral displacement of 2 m (Árnadóttir *et al.*, 2001) was inferred from GPS inversion.

4.1.2 The June 21, 2000 earthquake

The second earthquake occurred three and a half days later and 17 km farther west along the SISZ. The IMO determined the origin time of the June 21, 2000 earthquake as 00:51:46.95 GMT, the epicenter was at 63.98°N, 20.71°W, and the depth of the hypocenter was 5.1 km (Stefánsson *et al.*, 2003). Aftershocks (Hjaltadóttir and Vogfjörd, 2005) indicated a vertical fault, 16.5 km long, striking 1°NW. The depth to the brittle–ductile boundary as indicated by the distribution of microearthquakes increased from around 7 km in the northern part to 10 km at the southern margin (figure 3 of Hjaltadóttir and Vogfjörd, 2005). Surface fissures indicated right-lateral motion (Clifton and Einarsson, 2005). The USGS Rapid Moment Tensor Solution gave a moment of 5.2×10^{18} Nm, assuming a best-fitting double–couple solution. Preliminary magnitudes by the NEIC were $m_b = 6.1$ and $M_s = 6.6$. An average right-lateral displacement of 1.5 m (Árnadóttir *et al.*, 2001) was inferred from GPS inversion. The Harvard CMT Solution indicated a moment magnitude of $M_w = 6.4$, a scalar moment of 5.4×10^{18} Nm, a strike of 2°NE, and a dip of 85° of what we assume to be the fault plane.

4.2 DISTRIBUTION OF AFTERSHOCKS AND SLIPS ON THE TWO FAULTS

Aftershocks provided significant information about the size of the faults and, indirectly, information about how stresses were released along them. In general, there would be more aftershocks at the hard cores, ends, and near the bottom of faults (i.e., where slip motion on faults encounters a hindrance). GPS measurements several days before and repeated after the earthquakes sensed deformation related to them. Seismic strong motion instruments directly recorded instantaneous fault movement in the earthquakes and could be inverted to estimate slip on the faults.

Figure 4.2 (top panel) shows the distribution of aftershocks in a vertical north–south cross-section within a couple of kilometers from the north–south striking

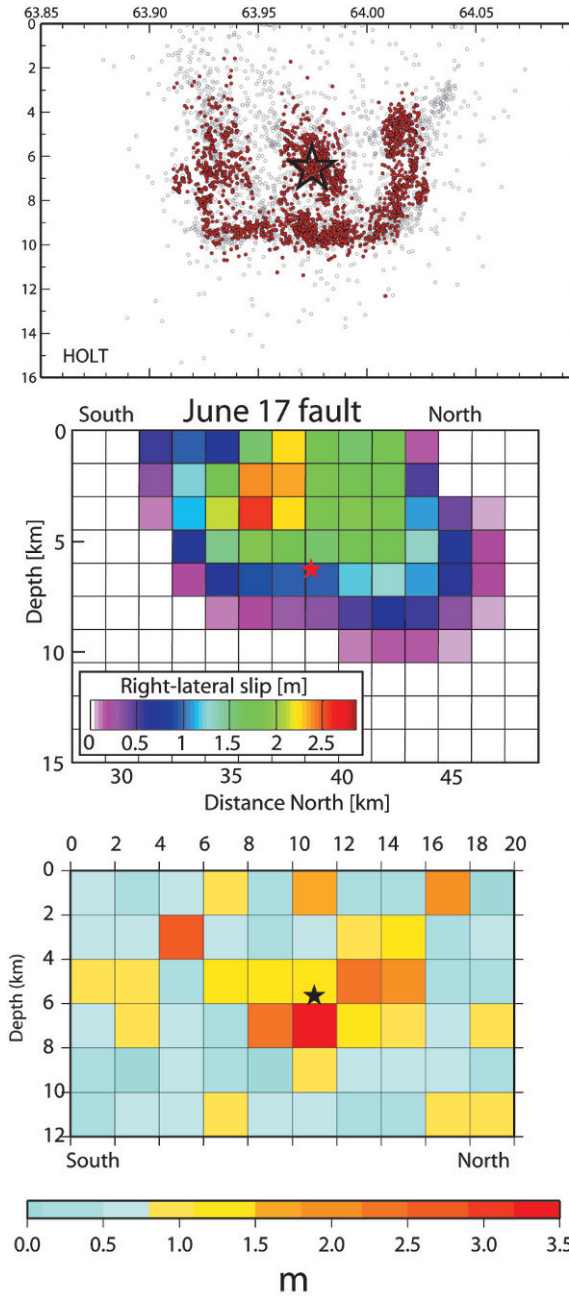

Figure 4.2. The two faults—June 17, 2000 on this page and June 21, 2000 on the opposite page. (*Top*) Relatively located aftershock distribution of fault planes in a vertical view from east to west. Events on identified faults are in red. (*Middle*) Right-lateral fault slip models for the June 17, 2000 and June 21, 2000 main shocks derived from joint inversion of InSAR and GPS data.

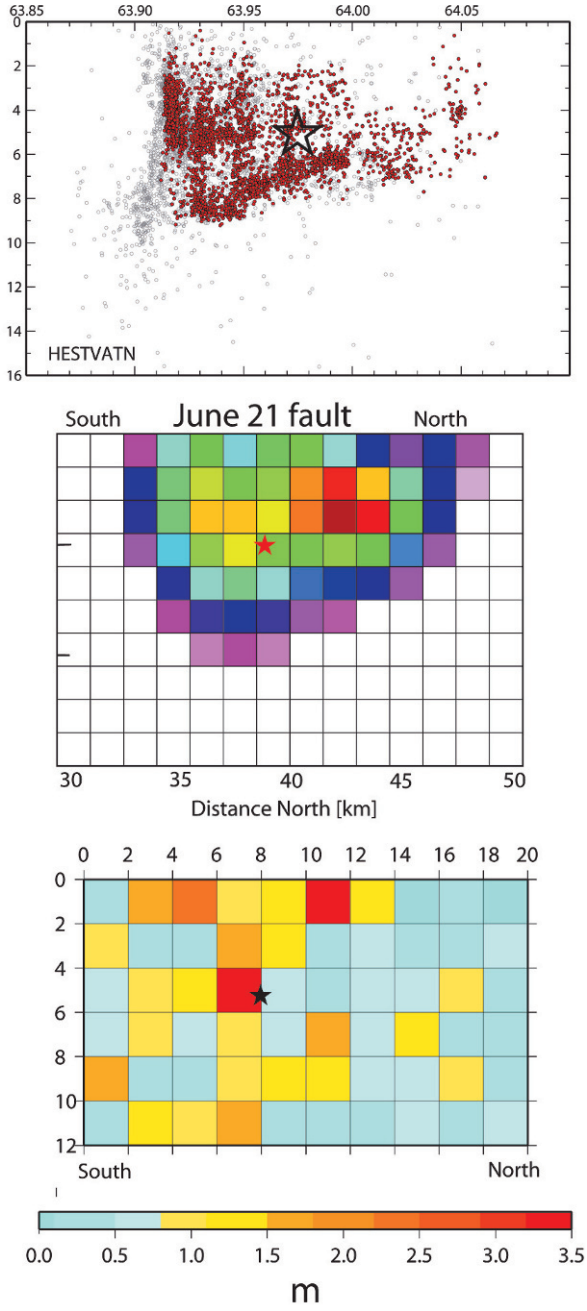

Figure 4.2 (*cont.*). The size of each grid cell is 1.5 × 1.5 km. (*Bottom*) Slip distribution obtained from strong motion data. The value for each grid cell is plotted in a discrete colored scale of intensities. The size of each grid cell is 2 × 2 km. Stars show main shock hypocenter locations (from Hjaltadóttir *et al.*, 2005).

faults, looking from the east. We see a concentration of aftershocks at the southern and northern ends of the rupture. They reflect high stresses where fault slip stopped (Hjaltadóttir *et al.*, 2005). A similar effect is observed at the bottom of the fault (i.e., at the brittle–ductile or B-D boundary, described in Section 3.2.2). Aftershocks were also concentrated close to the hypocenter of the initial large shock, suggesting that this was an earthquake asperity, a hard core in the fault, approximately 3 km in diameter.

The middle part of Figure 4.2 is based on joint inversion of InSAR and GPS data for the area (Pedersen *et al.*, 2003). The bottom part of Figure 4.2 displays the distribution of seismic moments on the fault plane, as inverted from seismic strong motion data. In this case the sum of the total moment has been constrained by the observed teleseismic moment (i.e., moment calculated from the worldwide network of seismic stations; Hjaltadóttir *et al.*, 2005; Stefánsson, 2006).

Figure 4.3a shows in geographic view, seen from above, the rupture of the June 17, 2000 earthquake. Aftershocks, which occur mainly below a depth of 3 km, display clustering in the middle and toward both ends of the fault comparable with what is seen in the vertical cross-section. Geologically mapped surface fissures deviate somewhat from the fault as expressed by aftershocks and as seen in the figure. Aftershocks have a tendency to occur along north–northeast striking left-stepping *en echelon* segments within a 2 km wide zone (i.e., expressing right-lateral slip of the large fault below).

From the geographic view of the distribution of aftershocks of the June 17, 2000 earthquake we can see the following (Figure 4.3a): the deepest part of the fault at or below the brittle–ductile (B-D) boundary (i.e., below a depth of 8 km) has evenly distributed activity indicating, however, that the fault slip consists of at least three main slip patches at an angle to each other. It apparently expresses that motion is forced by north–south right-lateral slip deeper down. At depths of 3 km to 8 km (i.e., in the elastic/brittle part) the three patches of the fault are still more clearly expressed. Surface mapping shows a complicated fissure arrangement. It expresses response to slip across faults in the uppermost kilometers of the crust, which is also expanded by cracks filled with meteoric water, generally the result of variable strength because of heterogeneities close to the surface.

Studying aftershocks in more detail than can be resolved in Figure 4.3a shows that aftershocks in the first 24 hours were more evenly distributed over the entire fault than later aftershocks.

Figure 4.3b shows the rupture of the June 21, 2000 earthquake from above as expressed by aftershocks in the 6 months following the earthquakes and by surface fissuring.

In the first 24 hours following the June 21, 2000 earthquake, aftershocks were distributed over the entire main fault up to a depth of about 1 km. Afterwards, activity was concentrated along the bottom of the fault, except at the southern end where it was distributed over the whole depth range and continued in this way throughout the year. Aftershocks defined the overall fault length as 16.5 km and its strike as 179°. Fault depth increased southward, from ~7 km in the northern half to ~10 km at the southern margin—see Figure 4.2 (top panel) on the right-hand

page. South of the hypocenter, aftershocks were evenly and densely distributed over the fault, while north of the hypocenter activity was less and mostly concentrated near the bottom.

Figure 4.3b displays an apparently straight fault plane of the June 21 earthquake with conjugate faults at shallower depths. However, looking closer at the distribution it becomes obvious that the fault plane is composed of a few distinct faults. North of the hypocenter two fault segments can be identified as having different dips although their strike is the same. Near the hypocenter and south of it, fault segments stick out of the main fault, extending a few kilometers to the west of the main fault (Hjaltadóttir and Vogfjörd, 2005).

The sketch in Figure 4.4 summarizes schematically some features of the two faults and the differences between them (seen in geographic view and as a vertical cross-section). The June 17, 2000 earthquake contains an asperity (i.e., a hard core in the middle) where the hypocenter is (i.e., where earthquake rupturing starts). It is surrounded by a weaker material, probably long eroded by fluids from below. The fault can be roughly divided into three subfaults oblique to the main fault strike. The second June 21, 2000 earthquake has a northern part which is weak and a southern part that is stronger; the start of the earthquake is at the boundary between the strong and weaker parts of the fault. It does not have a hard core like the first earthquake. The whole fault has long been weakened by fluid erosion, the northern part has been weakened more. As concerns micro-earthquake aftershocks the bottom is 2 km to 3 km shallower at the northern end than at the southern end (i.e., it appears that in the northern part of the fault, slip occurs without earthquakes below a depth of around 7 km—at the shallow B–D boundary). Although aftershocks express roughly one main fault, a closer look indicates that it is composed of a few distinct fault segments, having the same strike, however, as indicated in the sketch.

4.2.1 Why study old faults to predict future earthquakes?

Sections 4.1 and 4.2 describe some features of the 2000 earthquakes. Some might question what this has to do with predicting earthquakes because these two have already occurred. In our approach to earthquake prediction finding the faults of future impending earthquakes and studying their nature is fundamental. Many features of the faults and processes that appeared clearly in the 2000 earthquakes and in their aftershocks could have been studied to some extent from much fainter signals before the earthquakes occurred. Possibly this could have helped us to make an even better prediction than we did. But, what is more significant now is that the 2000 earthquakes taught us a lesson about fault release that will help us to understand better faint pre-earthquake signals at other sites.

From this point of view the mechanism behind the release of the 2000 earthquakes should be studied in greater depth. I have done so here by referring to other people's work combined with my own speculations.

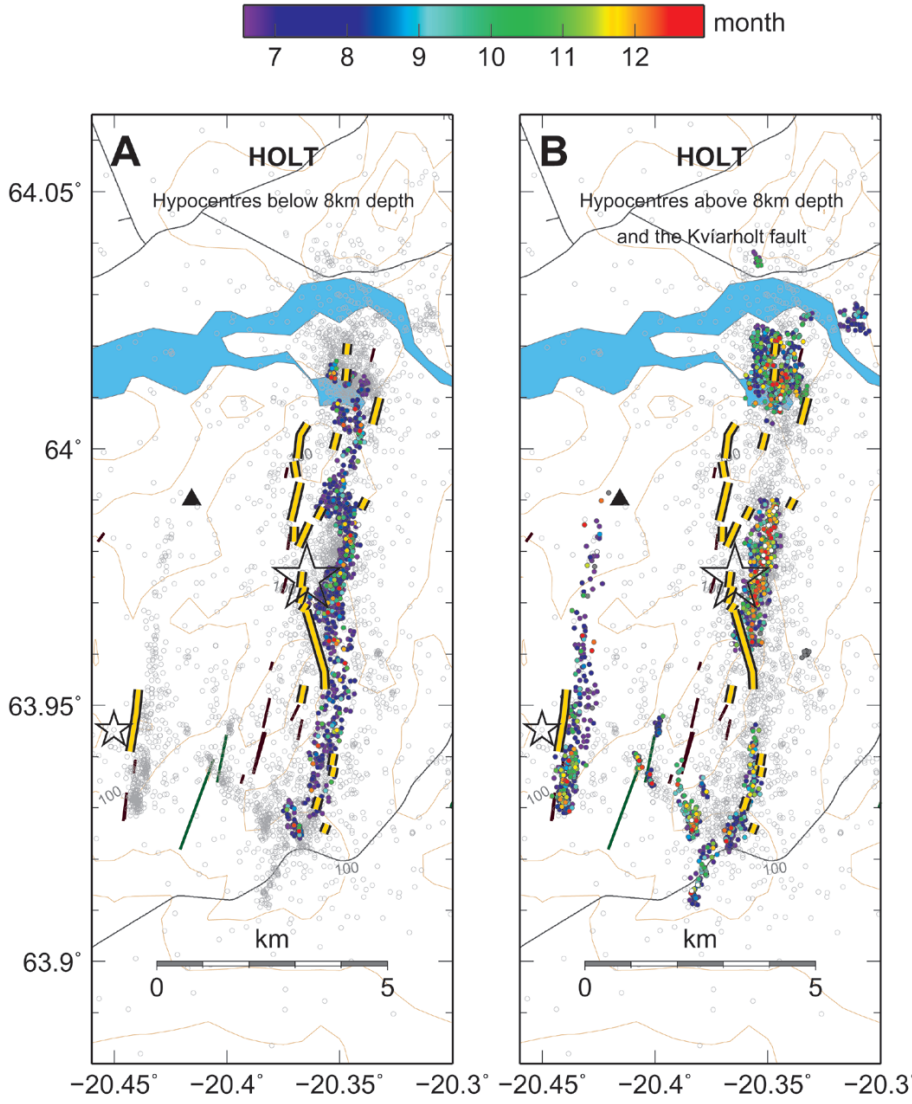

Figure 4.3a. Aftershocks and surface ruptures on the Holt fault (i.e., the first earthquake, June 17, 2000). The hypocenter of the magnitude-6.6 (M_s) earthquake is denoted by a star. The hypocenter of a smaller earthquake occurring roughly 2 minutes later is marked by a smaller star. All events are shown in the background in gray. Events on identified faults are displayed in color, according to age (from June 17 to December 31) and for different depth ranges below and above the 8 km depth, respectively. Yellow lines display surface ruptures from 2000. Brown line segments are older fissures (Hjaltadóttir and Vogfjord, 2005).

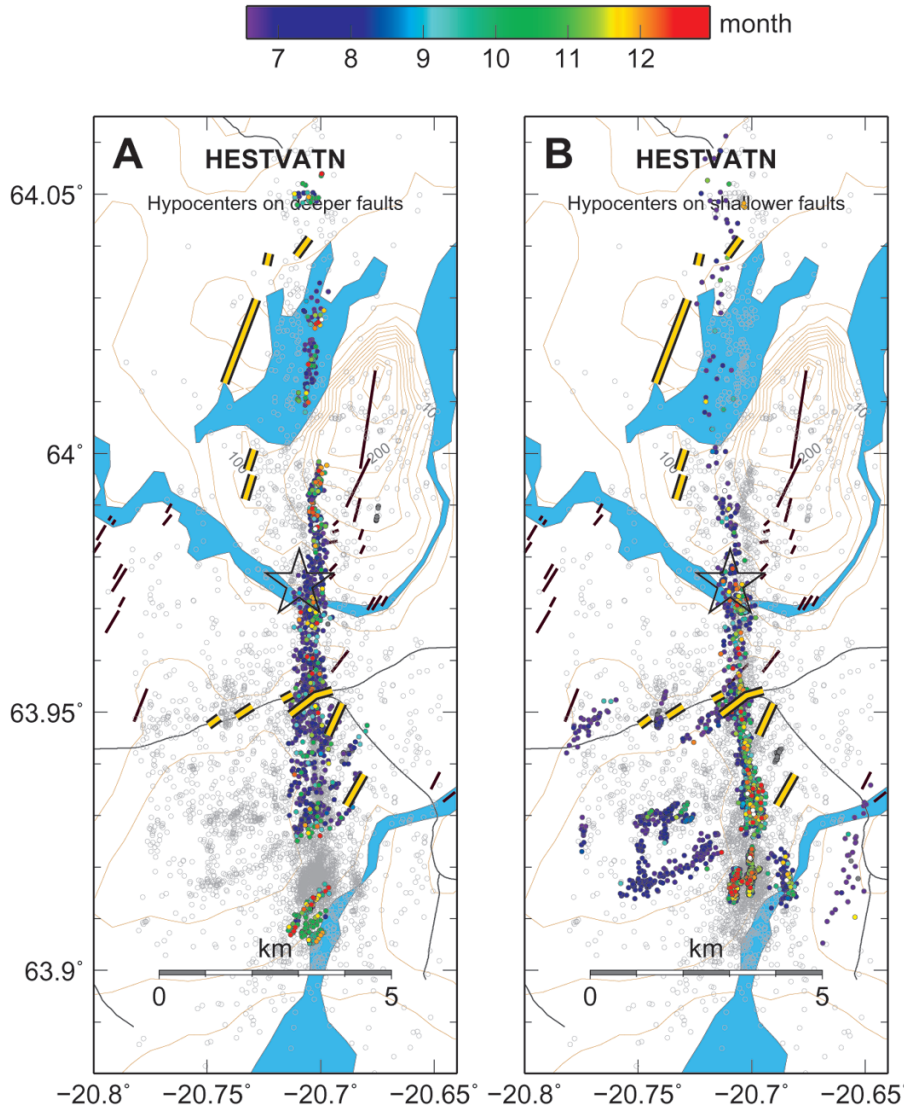

Figure 4.3b. Aftershocks and surface ruptures on the Hestvatn fault. The hypocenter of the June 21, 2000 magnitude-6.6 (M_s) earthquake is denoted by a star. All events are shown in the background in gray. Events on identified faults are displayed in color, according to age (from June 21 to December 31) and for different depth ranges. Yellow lines display surface ruptures from 2000. The brown line segments denote older fissures (Hjaltadóttir and Vogfjord, 2005).

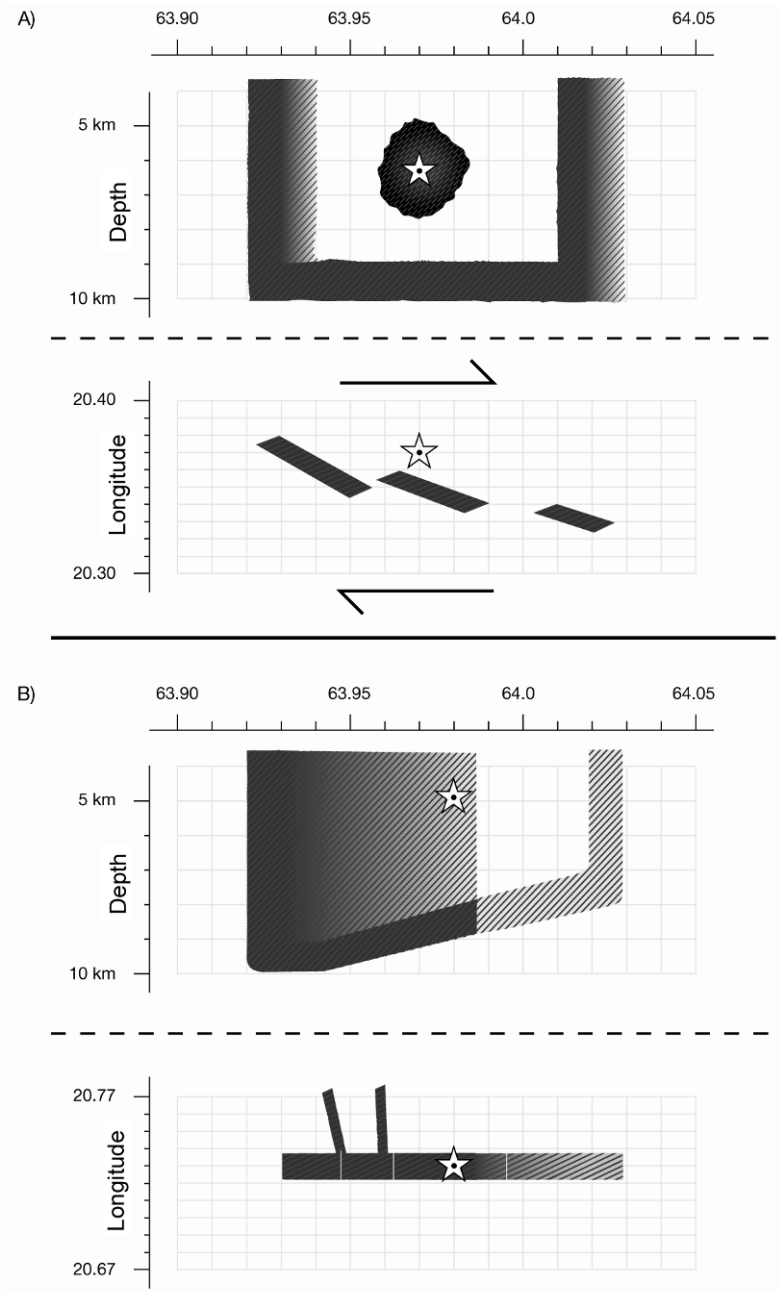

Figure 4.4. Some features of the two faults (black means dense seismic activity, gray and white less activity): A) is the June 17, 2000 earthquake fault, and B) the June 21, 2000 fault, in vertical (resp. horizontal) view, as expressed by the distribution of aftershocks (Figures 4.2 and 4.3). Comparison has also been made with deformation modeling and modeling based on strong motion data (as expressed in Figure 4.2).

4.3 IMMEDIATE TRIGGERING OF DISTANT EARTHQUAKES

Sections 4.1 and 4.2 described aftershocks that occurred mostly within a kilometer of the fault planes of the two earthquakes, which is usual for aftershocks. The initial earthquake (on June 17, 2000) triggered activity at a much greater distance. Within less than a minute to a few hours after the earthquake, seismic activity began in several areas up to 90 km to the west and north of the June 17, 2000 main shock (Figure 4.1). Three earthquakes of magnitudes 3.5–5.5 occurred within a few tens of seconds on the Reykjanes Peninsula, at distances between 60 km and 85 km from the June 17, 2000 earthquake. This has been interpreted as dynamic triggering by waves from the first earthquake because of closeness to failure at these sites, because of high shearing stresses, or because of high pore fluid pressures (as explained by Antonioli *et al.*, 2006). Besides being of general geophysical interest, these events strongly made the case for the necessity and possibility for prediction and warning before coupled events as a part of warning before a main earthquake.

4.4 PREDICTION OF THE 2000 EARTHQUAKES

The crustal processes preceding these earthquakes had been observed for long and short periods of time before the earthquakes. Long-term processes are sometimes described in terms of timeless historical hazard assessment while by short-term pre-earthquake processes we mean an observed process taking place minutes to weeks before an earthquake. As will be made clear in the following sections, both earthquakes were preceded by observable crustal processes or characteristics related to the particular fault, decades before they struck. In the following sections I will describe some processes and the way in which they were observed and interpreted in real time.

4.4.1 Hazard assessment and long-term prediction

A so-called ''time-dependent hazard assessment'' or long-term prediction was made 15 years ago for the area, suggesting that there was more than an 80% probability that large earthquakes would occur in the SISZ during the next 25 years. It was predicted that the earthquakes would probably start in the eastern part of the seismic zone, with an event of magnitude between 6.3 and 7.5 and that in the next few days or months a sequence of earthquakes would follow farther west in the seismic zone (Einarsson, 1985). This was based on historical documentation. Later revisions of magnitudes and hazard assessments assumed that the largest possible earthquake in this zone could not exceed magnitude 7.2 (M_s) (Halldórsson, 1987; Stefánsson and Halldórsson, 1988). Time-dependent hazard assessment was made routinely on the basis of earthquake history and assuming a continuous buildup of strain by known general plate motion (Halldórsson *et al.*, 1992). Such an assessment for the SISZ just before the 2000 earthquake showed that there was a 95% probability that an earthquake of magnitude 6 or larger would occur in the zone during the next 20 years (see

description in Appendix 1.A about time-dependent hazard assessment routinely studied in Iceland).

4.4.2 Predicting the site of the two earthquakes

A decade before the 2000 earthquakes occurred, their sites were indicated in papers published in the journal *Tectonophysics* (Stefánsson and Halldórsson, 1988; Stefánsson *et al.*, 1993). In the papers, their origins along the SISZ were indicated to be within a couple of kilometers of where they actually occurred and their size approaching magnitude 7 (M_s) as among the largest in the zone (i.e., not as precise as the origins). Both earthquakes had a magnitude of 6.6 (M_s) and were among earthquakes which historically were called "large South Iceland earthquakes". Prediction was based on lack of earthquakes in strain release history, micro-earthquake distribution, and a tentative idea of the significant role played by fluid intrusion from below into a dense fabric of north–south faults in interplay with earthquake strain release.

4.4.2.1 Strain release history

As described in Section 3.6, historical documentation was used to study the long-term seismicity of the SISZ and how the release of strain energy in large earthquakes would be distributed along the zone.

In this study, it was assumed that strain release in the earthquakes would be proportional to the release of plate motion strain at each site along the transform zone. Figure 4.5 shows accumulated earthquake strain release in different parts along the zone since 1700. Plots are made in such a way that half of the strain allocated from earthquakes at each site was distributed at both sides of it, to allow for probable errors in locating the earthquakes on the basis of historical data. The figure also shows microseismicity since the start of the SIL micro-earthquake system and until 1999.

As a result of studying Figure 4.5 the following very significant observations can be made:

(1) Strain release in earthquakes appears to be generally less in the western part of the zone than in the eastern part. This can be explained by thinning of the brittle uppermost part of the SISZ crust from east to west, as discussed in Section 3.2.2—that is, less of the energy built up by plate motion is released by earthquakes in the western part than in the eastern part because the depth to ductility there is less and thus the strength of the brittle crust is also less (Stefánsson *et al.*, 1993; Tryggvason *et al.*, 2002).
(2) There appears to be a lack of strain release, compared with the surroundings, around west longitude 20.3° and 20.7°, indicating that there might be seismic gaps at these longitudes. Significantly, clusters of micro-earthquakes can be seen at these gaps.

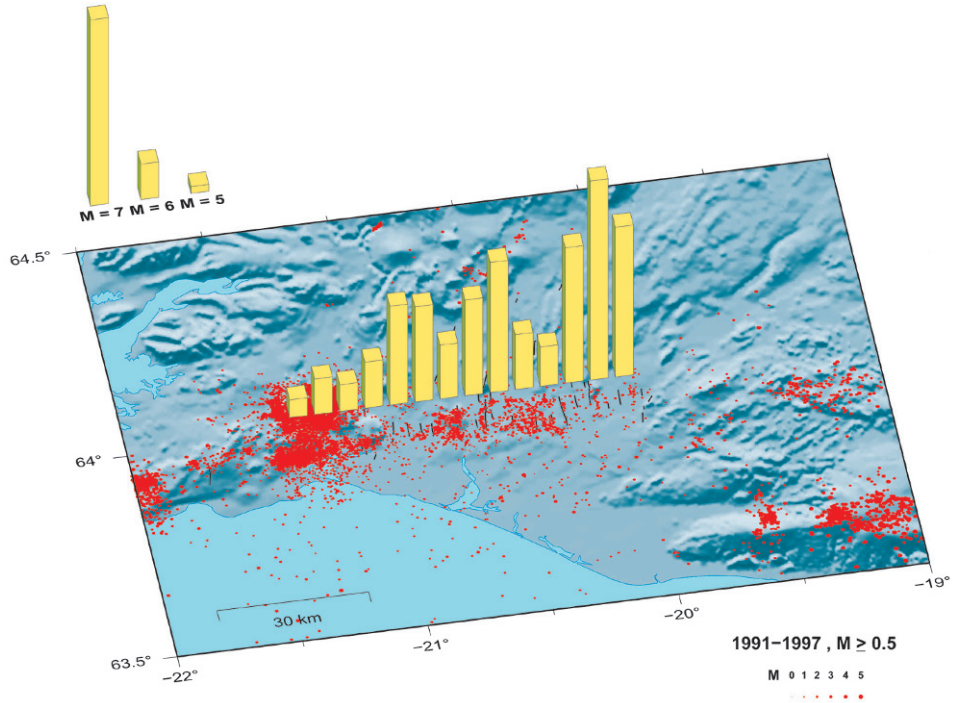

Figure 4.5. Pillars arranged along the SISZ in southwest Iceland indicate release of strain energy in historical earthquakes from 1700 to 1999. Here Benioff strain (Benioff, 1951; Stefánsson and Halldórsson, 1988) is calculated from the magnitudes of each historical earthquake. Half of the strain released by each earthquake is put at the most probable site, while one quarter is put at each side to try to allow for probable location errors. Dots show microearthquakes larger than magnitude 0.5 between 1991 and 1999. Black lines indicate the position of known earthquake faults. Historical earthquakes tend to be larger in the eastern part than in the western part of the zone, which has been explained by the thicker and stronger brittle/elastic crust in the eastern part.

Based on geological mapping of earthquake fissures in the zone, a new understanding of the release of earthquakes in the zone emerged in the 1980s (i.e., that earthquakes occurred on a dense fabric of north–south faults). It appeared that the distance between parallel faults of successive earthquakes was less than 5 km (Einarsson, 1991). This agreed well with the north–south elongated form of destruction areas (see Figure 2.1).

Based on the magnitudes of historical earthquakes, the moment release of earthquakes was calculated using the following formula of Purcaru and Berkheimer (1978): $\log Mo = 16.1 + 1.5M_s$ (where Mo is the moment and M_s is the surface wave magnitude). This is an empirical formula based on studying earthquakes at several places around the world, and can be considered a good estimate for the relation between magnitudes and moments of earthquakes in the magnitude

range 5–7 (M_s). This was compared with the total buildup of strain moment in the zone by differential plate motion along the zone, which was assumed to be 2 cm/year with an assumed crustal plate thickness of 15 km. Comparison showed the same value for moments released by earthquakes as for the calculated moment of plate motion strain buildup (Stefánsson and Halldorsson, 1988). By adding scant information of historical earthquakes between 1200 and 1700 to the good historical information since 1700, the authors concluded that the zone had a total breakthrough at intervals of 140 years. These crustal breakthroughs for total strain release of the zone occurred in clusters lasting several years, as demonstrated by the long sequence of releases between 1732 and 1784 and the shorter sequence from 1896 to 1912.

Comparison between moments released in earthquakes and moment buildup by plate motion seems to be in a very good agreement. However, the authors concluded that they should have obtained less moment from earthquakes than from plate motion. The reason, they surmised, was that the elastic brittle crust on average appeared to be only about 10 km thick—not 15 km as had been assumed—and it would be natural to expect that a part of the strain buildup by plate motion would be released aseismically below 10 km. In short, the earthquakes were stronger than expected from the velocity of differential plate motion in South Iceland.

Two reasons were suggested to explain this. One was that historical magnitudes were overestimated; another that some energy was acquired by the zone as a result of upward migration of hot fluid, which would add further energy to the release of individual earthquakes.

4.4.2.2 The dual-mechanism model and site prediction

Upward migration of fluids or dyke injections into the zone was considered necessary to explain how close to each other successive historical earthquakes were (i.e., local fluid inflow from below would help to create conditions that would govern selection of the site of each earthquake, when a certain level of straining was achieved in the zone overall). This was named the ''dual-mechanism'' model for earthquake release in the zone. In this model there is an assumed interplay between the strain caused by upwelling of fluids and plate motion buildup of strain energy (Stefánsson and Halldórsson, 1988).

As detailed in Chapter 3, micro-earthquake distribution in the South Iceland Lowland defines the SISZ plate boundary as a seismic zone only 10 km to 15 km broad (Figure 3.3). It has been estimated that depth to the brittle–ductile boundary is 5 km to 6 km at the western end of the zone whereas in the east it reaches depths of 10 km to 12 km. This estimate is based on the depth of microseismicity. However, most micro-earthquakes occur in or near active faults, so what seems to be the bottom of the brittle crust may reflect depths to ductility in individual faults (as discussed earlier).

After installation of the SIL seismic system and before the 2000 earthquakes, micro-earthquakes clustered in the strain release lows left by large earthquakes, in much the same way as shown in the earthquake history of Iceland (Figure 4.5). Long

before the 2000 earthquakes it was assumed likely that these micro-earthquakes reflected high stress in preparation for a large earthquake although it could not be excluded that they involved aseismic release of stress in the seismic zone (Stefansson *et al*., 1993).

Seismic gaps in the release of large earthquakes as described above, clusters of micro-earthquakes at the same sites (Figure 4.5), and new ideas about how earthquakes are released in the zone led to the following indications about the sites of the 2000 earthquakes years before they occurred. A paper in *Tectonophysics* (Stefánsson and Halldórsson, 1988) stated: "there are strong indications that the next large earthquake of a size approaching 7 in the zone will take place near longitude 20.30–20.40." This assumed it to take place on the east–west oriented SISZ at around 64°N (Figure 4.5). In a paper in the *Bulletin of the Seismological Society of America*, Stefánsson *et al*. (1993) pointed out the significance of low strain release at longitudes 20.3° and 20.7°, and that such strain release lows coincided with high seismic rates. The basis for these indications of the site of the next large earthquake was, besides strain release gaps and microseismic clustering, the new understanding that earthquakes in the zone occurred on a dense fabric of consecutive north–south faults, separated by distances less than 5 km.

So, the next two large earthquakes in the zone (i.e., the 2000 earthquakes) had their hypocenters at longitudes 20.37°W and 20.71°W (i.e., within 2–3 km of the positions indicated 10 years before they occurred).

4.4.2.3 Further considerations about prediction of the site

The vague formulation used to predict the sites of the two earthquakes reflected doubts among scientists. We needed a very strong basis to definitively allocate the site of the next large earthquake in this way. But, what is the point of these indications if we are not 100% sure? This is the dilemma facing earthquake prediction and earthquake hazard assessment, in general. Is it not the duty of scientists to say what they themselves believe to be true even though such "knowledge" cannot be proven? My view is that this is a duty incumbent of scientists to society, despite some claiming that if a "truth" cannot be proven it should be kept in the minds of the scientists—and not scare the public or investors in real estate. Such considerations will be left for Chapter 7 on warnings.

A 140-year cycle of total strain release or complete breakthrough of the whole SISZ was also postulated on the basis of historical magnitudes (Stefánsson and Halldórsson, 1988). The total strain release of the zone as a whole is demonstrated according to this hypothesis by the high rate of large earthquakes occurring in sequences lasting 10 to several tens of years. This was based on good historical documentation since 1700 and some scanter information between 1200 and 1700. Two strain release episodes, breaking through the whole zone, match this hypothesis well—one from 1896 to 1912, the other from 1732 to 1784—and fulfill the strain energy considerations necessary for total strain release. A strain release period centered around 1620 is indicated though not as well constrained, but fits in the 140-year timeframe (Stefánsson and Halldórsson, 1988).

In support of this hypothesis, a 140-year period was found many years later in bouts of major volcanic activity above the Iceland Mantle Plume (Larsen *et al.*, 1998). At present this does not have a predictive value as we do not yet understand the connection. But this and other similar possible couplings or interactions should be included in, or explicable by, overall modeling of the dynamics of the Iceland Mantle Plume–Ridge and thus little by little become part of future warning procedures.

4.4.3 Short-term warning before the June 21, 2000 earthquake

On the basis of historical evidence (see, e.g., Einarsson, 1985) it was considered probable that another earthquake would follow farther west along the zone after the June 17, 2000 earthquake. Late in the evening of June 19, 2000 a special warning was issued by IMO personnel to state and local Civil Protection groups. In the warning it was stated that the most likely hazard area of a probable impending earthquake would be as indicated by the boxes in the upper panel of Figure 4.6. In a follow-up telephone call it was explained that the larger box was the more likely location. The magnitude would be similar to the first earthquake on June 17, 2000 (i.e., $M_s = 6.6$) or slightly smaller. It was advised that preparations should be made for an earthquake occurring "at any moment".

The warning was based on the following evaluation by IMO seismologists:

(1) The north–south micro-earthquake distribution (Figure 4.6) along the expected fault plane direction.
(2) The historical indication that large earthquakes in the SISZ are followed by earthquakes farther to the west.
(3) The site was within a couple of kilometers of the place long predicted for the next large earthquake in the zone (Stefánsson and Halldórsson, 1988).

Backing up this evaluation was the hypothesis that the fault motion of large earthquakes may start as stable slip without seismic activity below the brittle crust. In modeling this, based on the rate/state-dependent constitutive relationship, Tse and Rice (1986, p. 9469) assumed that: "Inelastic crustal deformation during the

Figure 4.6. The *upper map* of this figure, not including the red line, was sent to the Iceland Civil Protection, including the National Civil Protection Agency (NCPA), shortly before midnight on June 19, 2000, 26 hours before the earthquake on June 21. Red dots indicate the location of automatically located small earthquakes, which were the basis for the short-term warning. The symbol "q" is a measure of the quality of automatic locations. Green boxes show probable hazard areas of the impending earthquake (*Líkleg umbrotasvæði* is Icelandic and means "probable hazard areas"). An accompanying telephone report explained that an earthquake of similar size to the June 17 earthquake or slightly smaller was to be expected to occur within either of the green boxes, more likely within the larger one. A strictly defined time window was not given, but advice was given to prepare for an earthquake of this size and at this location to

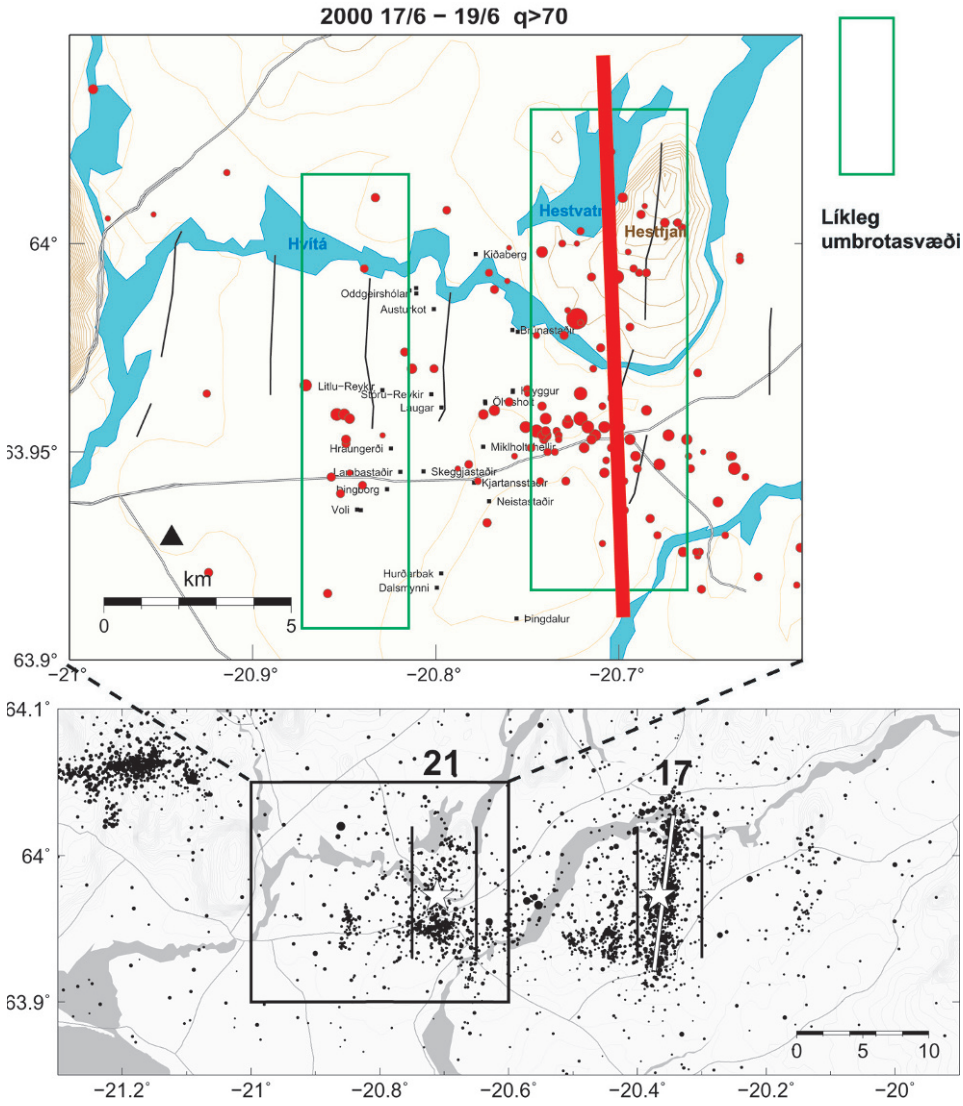

occur "anytime soon". The red N–S line, which was later put on the warning map, shows the real fault plane of the June 21 earthquake which occurred 26 hours later. The small letters, hardly legible on this original map, are names of some of the farms in the region. A triangle denotes a close seismic station of the SIL type. The *lower map* shows the seismic situation in the SISZ as a whole between the onset time of the two large earthquakes. The rectangular box indicates the area of the warning map above. The stars below the numbers 17 and 21 indicate the epicenters of the two earthquakes, and the fault plane of the June 17 earthquake is shown by a white, nearly N–S, line a couple of kilometers east and west of the epicenters indicate areas of microseismic activity close to the faults often referred to in the text. The dots show seismic activity in the whole zone between the two earthquakes, after manual control of automatic evaluations.

earthquake cycle can be idealized as being localized to a fault surface which penetrates deeply below the depth of the seismogenic zone.''

The immediacy of the warning was also based on the speed of westward migration that was experienced. A rule of thumb had been suggested and discussed among scientists, although nowhere reported in papers, saying that earthquakes might migrate at a speed of approximately 5 km/day along the SISZ (see discussion about migration velocity in Section 4.10.4).

This warning became a reality 26 hours after it was issued (i.e., with a magnitude-6.6 earthquake at 00:51 GMT on June 21, 2000). The location of the earthquake is shown by the thick red line in Figure 4.6, which indicates the real fault plane of the earthquake. This line was added to the warning picture afterwards (Stefánsson *et al.*, 2000).

4.4.4 Partly successful warnings and research for further success

Because of long-term predictions and warnings indicating the immediacy of large earthquakes in the SISZ, local Civil Protection groups and the scientific community were in many ways well prepared for the earthquakes. Several scientific initiatives were taken to enhance monitoring and research, to bring about earthquake prediction research projects, like the multinational SIL and PRENLAB projects, which included setting up a micro-earthquake monitoring system in the area, the SIL system (Stefánsson *et al.*, 1993; Bödvarsson *et al.*, 1999), and to monitor crustal deformation on a continuous basis. This meant significant observations could be made before, during, and after earthquakes, of great value to understanding the crustal processes that preceded them. I will now describe some of these observations and some results of the intensive research work that was carried out after the 2000 earthquakes. Long-term warnings motivated various types of earthquake preparatory actions to mitigate risks. National and local Civil Protection groups took significant measures to mitigate risks in case of destructive earthquakes especially by strengthening public awareness and preparedness.

However, long-term warnings were put forward simply as an indication and were not intended to lead to direct governmental actions as would be expected in response to classical earthquake hazard assessment, leading to modifications of building regulations, etc. Better understanding of the physical processes leading up to earthquakes would have made such predictions more significant and made it possible to predict more aspects of earthquake effects and coupled earthquakes.

The short-term warning of the second earthquake helped local Civil Protection group and community leaders set in motion previously planned preparations; it also had the effect of motivating scientists to get involved in earthquake prediction research.

4.4.5 Could we have done better before the first earthquake?

There was no short-term warning of the first earthquake, although it was obvious from later detailed studies of some observations that the SIL system monitored faint

signals shortly before it. Had there been an active warning system to automatically utilize such information, it might have been possible to use these signals to issue warnings.

The instant (dynamic) triggering by the first earthquake of magnitude-5 earthquakes some 85 km to the west (i.e., on the Reykjanes Peninsula) had not been foreseen. Hence, no warning of such a consequence of a large earthquake in the SISZ was given.

A multidisciplinary, multinational research program (the PREPARED project) was set up to study the physical processes leading to the earthquakes. It is described in the *PREPARED Final Report* (Stefánsson, 2006). The report claimed that better understanding of the processes underlying the earthquakes would increase the significance of earthquake warnings and lead to warnings of more aspects of earthquakes before they occur. This applies to warnings about basic earthquake processes, warnings about expected earthquake effects before the earthquakes, and for nowcasting. Warning practices will be further described in Chapter 7.

Some significant results from the PREPARED project regarding pre-earthquake processes of relevance for the issuance of warnings are given in the following sections.

4.5 MORE ABOUT THE LONG-TERM PATTERNS THAT PRECEDED THE EARTHQUAKES

Section 4.4 dealt with the real predictions and warnings made before the 2000 earthquakes and the basis for making them. Sections 4.5–4.12 will focus on what we learned from observations of the 2000 earthquakes, and their forerunners, as well as about earthquake prediction research that was carried out after the 2000 earthquakes. The focus of these sections will be the knowledge that has been gathered and how it can be used to better prepare us for future earthquakes.

4.5.1 The regular historical fault pattern

Figure 4.7 shows positions, directions, and estimated lengths of historical earthquake faults in the South Iceland Seismic Zone since 1700, including the 2000 earthquakes. Recent detailed mapping of faults (Clifton and Einarsson, 2005) made epicenter determination of historical earthquakes more accurate than determinations only based on the descriptions of destruction. On the basis of magnitudes estimated from historical earthquakes and known rheological parameters, the lengths of the fault planes have been estimated (Roth, 2004). Figure 4.7 reveals some significant features of the seismic zone:

(1) As seen in Figure 4.7 the damage width of the SISZ may be considered to be around 30 km. Micro-earthquakes appear within 10 km of the zone (see Figure 3.3) which thus probably only involves a distinctly weak part of the zone, weakened by hydrofracturing and expansion.

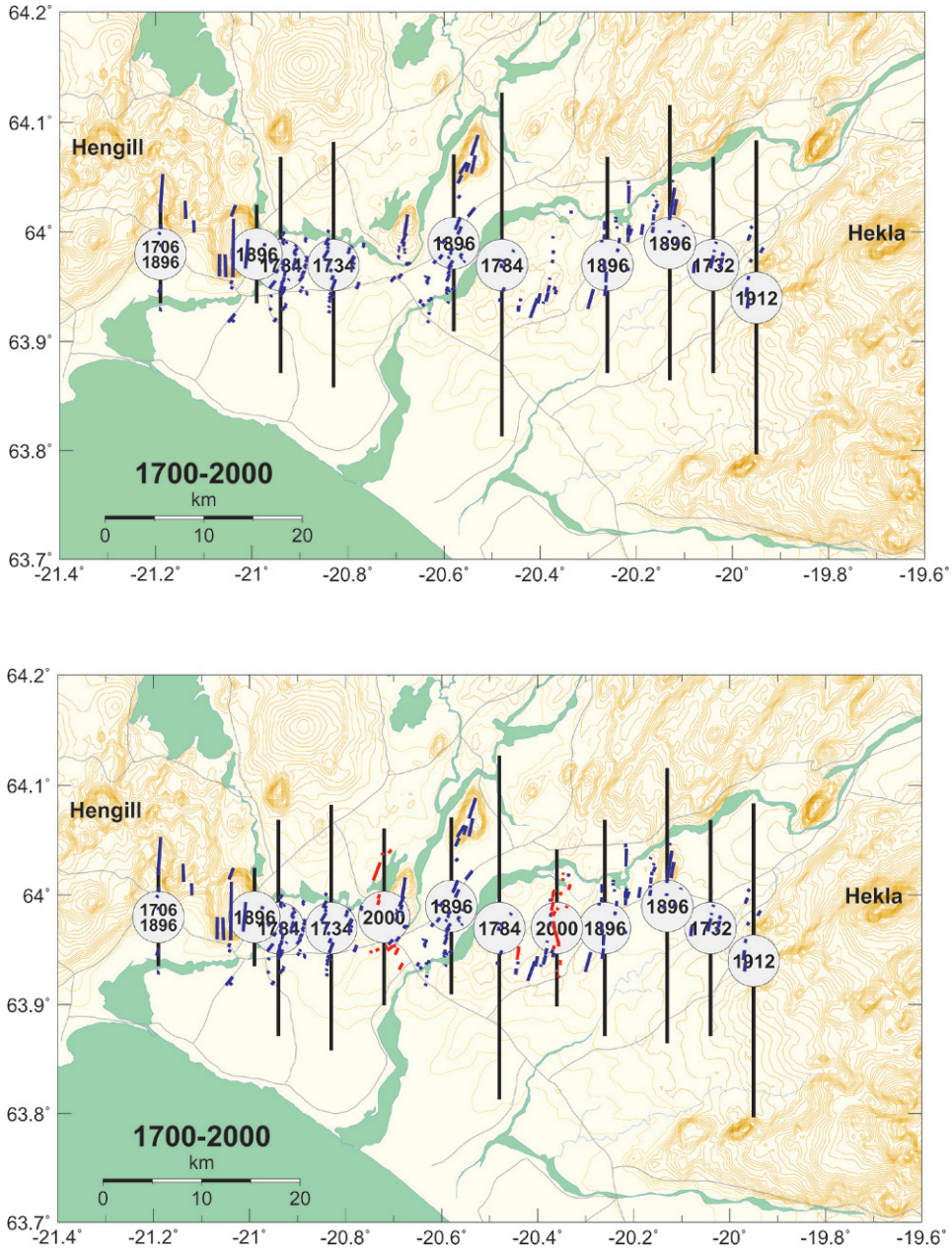

Figure 4.7. Earthquakes in the SISZ since 1700: (a) before the 2000 earthquakes and (b) where both the 2000 earthquakes are included. The earthquakes are arranged side by side and have right-lateral slip on north–south faults. Fault epicenters and magnitudes (Stefánsson *et al.*, 1993; Clifton and Einarsson, 2005) are estimated from historical data, and fault lengths are from Roth (2004).

(2) The 2000 earthquakes fill in gaps in the historical pattern of epicenters (i.e., the gaps mentioned in Section 4.4). However, they certainly do not fit well with the idea that earthquakes are larger in the east than in the west. This was especially true of the first of the 2000 earthquakes, which was far too small to be comparable with the relatively large earlier earthquakes in the eastern part of the zone.
(3) A third gap is indicated between 21.0°W and 21.2°W, which was filled by a twin-earthquake in 2008.

Figure 4.7 gives the impression that it is easy to predict the site of the next earthquake in the SISZ. In fact, in 2003 a warning was sent to the Iceland Civil Protection Agency (ICPA) informing them that a dangerous earthquake was expected in the westernmost part of the zone, approximately where the 2008 earthquake occurred. This will be described in Section 4.11. Since 2008 it is unclear whether there is a lack of earthquakes in this regular pattern. However, historical information before 1700 indicates at least two large earthquakes in the central and eastern part of the zone which occurred in between the earthquake faults shown in Figure 4.7. So, to predict the sites of the next large earthquakes in the zone, mainly on the basis of gaps in earlier activity, the situation is not as clear as it was before the 2000 and 2008 earthquakes. Hopefully, the situation will be clearer well before the next large earthquake in the zone.

4.5.2 Long-term time patterns preceding the 2000 earthquakes

Figure 4.8 is an overview of seismic activity since the large 1896 sequence of earthquakes. The 1896 earthquakes together with the 1912 earthquake involved a complete breakthrough of the entire zone (i.e., near-total strain relaxation of the zone; Stefánsson *et al.*, 1993).

Hekla is a volcano at the eastern end of the zone, with eruptive times in the 19th century as shown in the figure. The Hengill volcano-seismic area is at a triple junction to the west and northwest of the zone. It had intensive volcano-tectonic episodes between 1994 and 1998 as well as between 1953 and 1955, but these are just examples of the most recent episodes.

After the earthquake sequence of 1896 there appears to have been an 8-year seismically silent period in the SISZ. This silence was broken in the following 8 years by a series of earthquakes (Figure 4.8) which were felt in the easternmost part of the SISZ, preceding the large 1912 earthquake there. This pre-earthquake activity in the focal region of the 1912 earthquake is extremely interesting in our efforts to understand the pre-processes of SISZ earthquakes (discussed in Chapter 6).

The following conclusions can be drawn from observed earthquake activity from 1896, 1912, 2000, and the intervening years:

(1) The SISZ was pretty much strain-relaxed after the 1896 earthquakes, except the easternmost 25 km of the zone.
(2) Strain buildup in this part was apparently accelerated until the 1912 earthquake released it. This was reflected in five earthquakes with magnitudes estimated

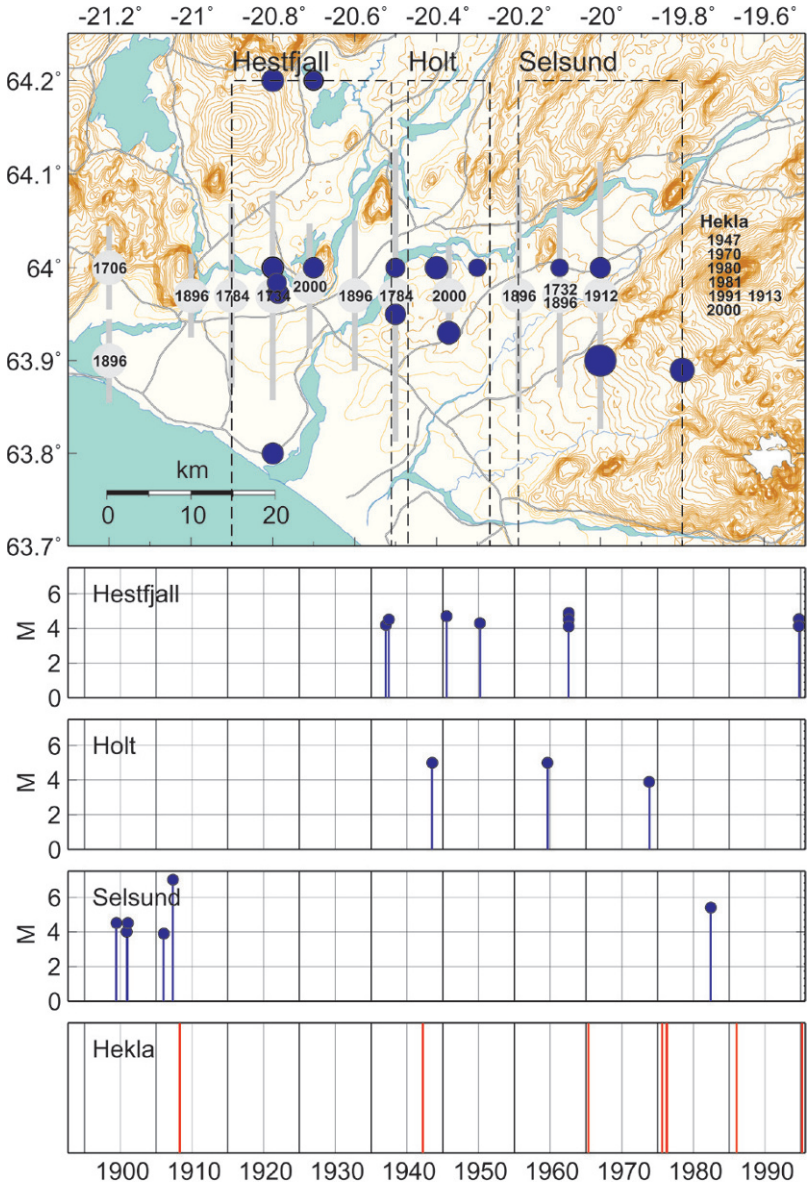

Figure 4.8. (*Upper*) Filled circles show earthquakes with magnitudes around 4–5 in the SISZ since the sequence of 1896 until shortly before the two large SISZ earthquakes in 2000. The faint lines in the background indicate the faults of historical large earthquakes. (*Lower*) In the time graphs of the figure, the vertical lines to the left of year labels mark the start of the year. Hestfjall marks the area where the second 2000 earthquake occurred, Holt marks where the first 2000 earthquake occurred, and Selsund where the magnitude-7 1912 earthquake occurred. The eruptions of Hekla at the eastern end of the zone are shown as red lines (from Stefánsson *et al.*, 2006a).

between 4.0 and 4.5 in the 8 years before the 1912 earthquake, which were both felt and observed by people (Figure 4.8).

(3) After the 1912 earthquake (i.e., after complete crustal breakthrough by the 1896–1912 series), there followed more than 30 seismically silent years in the SISZ. These silent years were followed by two to three decades in which a few magnitude-4 to magnitude-5 earthquakes occurred in the Holt and Hestvatn areas and then relative silence until the 2000 earthquakes broke out in these areas (Figure 4.8).

4.5.3 Coupling between the 2000 earthquakes and volcanic activity

Statistical analysis of historical events in Iceland reveals a weak but significant relationship between large earthquakes and volcanic eruption, with the eruptions occurring first (Gudmundsson and Sæmundsson, 1980). However, there are no historical examples indicating that eruptions of Hekla have triggered large earthquakes in the SISZ in the short term (Stefánsson *et al*., 2010).

The following volcano-tectonic processes may possibly have helped to build up tectonic conditions for earthquakes in the area before the 2000 earthquakes, although any such relation is currently poorly understood (see Figure 4.1):

(1) Hekla is at the eastern end of the fault zone. It erupted big time in 1947 and has erupted every 10th year since 1970, an unusually dense period in its history. The last eruption started only three and a half months before the 2000 earthquakes.
(2) The Hengill volcanic complex at the western end of the zone had a large seismotectonic episode between 1994 and 1998, involving (besides plate motion) upward fluid migration into the system, but no effusive activity.
(3) Probable major intrusive activity preceding the large eruption below Iceland's largest icecap Vatnajökull in 1996 (the Gjálp eruption) may have led to increased release of micro-earthquakes in the SISZ (precisely where the initial June 17, 2000 earthquake occurred). A seismic swarm occurred in that part of the zone for a few months before the large eruption 150 km away. After that swarm period there was a general increase in seismicity in the SISZ, especially at the site of the June 17, 2000 earthquake before the 2000 earthquake sequence started there (Figure 4.10, see Section 4.6.2). Seismologist Stuart Crampin (see Appendix 2.B) reported at a workshop in Iceland a month before the eruption of Gjálp that shear wave splitting in seismic stations in the SISZ and at some other seismic stations showed increased stress (Volti and Crampin, 2003; see also Figure 4.10).

It is likely that these volcanic processes helped to create the conditions for the 2000 earthquakes, but the physics underlying the connection is not clearly understood at present. It is important that the coupling between such events is subjected to intensive study and is then introduced into an Earth-realistic physical model of the region, taking onboard all available multidisciplinary observations.

4.6 INFORMATION FROM MICRO-EARTHQUAKES ON LONG-TERM PROCESSES BEFORE THE 2000 EARTHQUAKES

The most significant pre-earthquake activity before the 2000 earthquakes was revealed by the SIL micro-earthquake system, whose sensitive equipment had been operational for 9 years before the earthquakes occurred. It is difficult to identify such activity as precursors of large events on the basis of statistical significance by comparing them with precursors of other large earthquakes. The best way to relate possible pre-earthquake activity to an impending earthquake is to explain physically the possibility of such a relationship.

4.6.1 Micro-earthquake distribution before the earthquakes

Micro-earthquakes before the 2000 earthquakes had a significantly different spatial distribution from the micro-earthquakes that followed the 2000 earthquakes.

Figure 4.9 shows the distribution of micro-earthquakes (down to magnitude 0) in the 9 years leading up to the 2000 earthquakes (Stefánsson and Gudmundsson, 2005). Two distinct clusters can be seen in the epicentral areas of the earthquakes. Careful search through the seismological data available between 1926 and 1989 indicates that the main characteristics of the seismicity may have changed little from that of 40 years earlier, although sensitivity was too low to detect in the same way as after 1991, when the sensitive SIL system came into operation.

As discussed before, the two clusters of microseismicity in the center of the SISZ coinciding with the lack of release of historical earthquakes indicated the sites for the next large earthquakes in the SISZ. Based on older seismic monitoring, micro-earthquake activity was relatively high at these sites in the 30–40 years before the 2000 earthquakes. Although these clusters were considered likely forerunners of large earthquakes that could occur at these locations, the explanation of them was somewhat diffuse at that time, and it could not be ruled out that they were representative of slow or aseismic strain release (i.e., they might indicate release of strain without large earthquakes occurring).

The release of the two large earthquakes in 2000, subsequent change in the configuration of seismic clusters, and constraining a model about the interaction of strain buildup with upward fluid migration from below the crust in these areas confirmed that the clusters were forerunners to the 2000 earthquakes.

Such an interplay between fluid upwelling from the mantle and plate motion strain buildup had been suggested before, as part of the dual-mechanism model, to explain large-scale dynamic features of the SISZ (Stefánsson and Halldórsson, 1988), especially the observations that parallel north–south faults of historically recent large earthquakes were so close to each other (as discussed in Chapter 3). This model was revived in a PRENLAB workshop in 1999 in discussion about how the model might explain these micro-earthquake swarms and discover whether they could be pre-earthquake processes. Maurizio Bonafede (see Appendix 2.B), a member of the PRENLAB group, undertook the challenge to work on an Earth-realistic model that could answer this question.

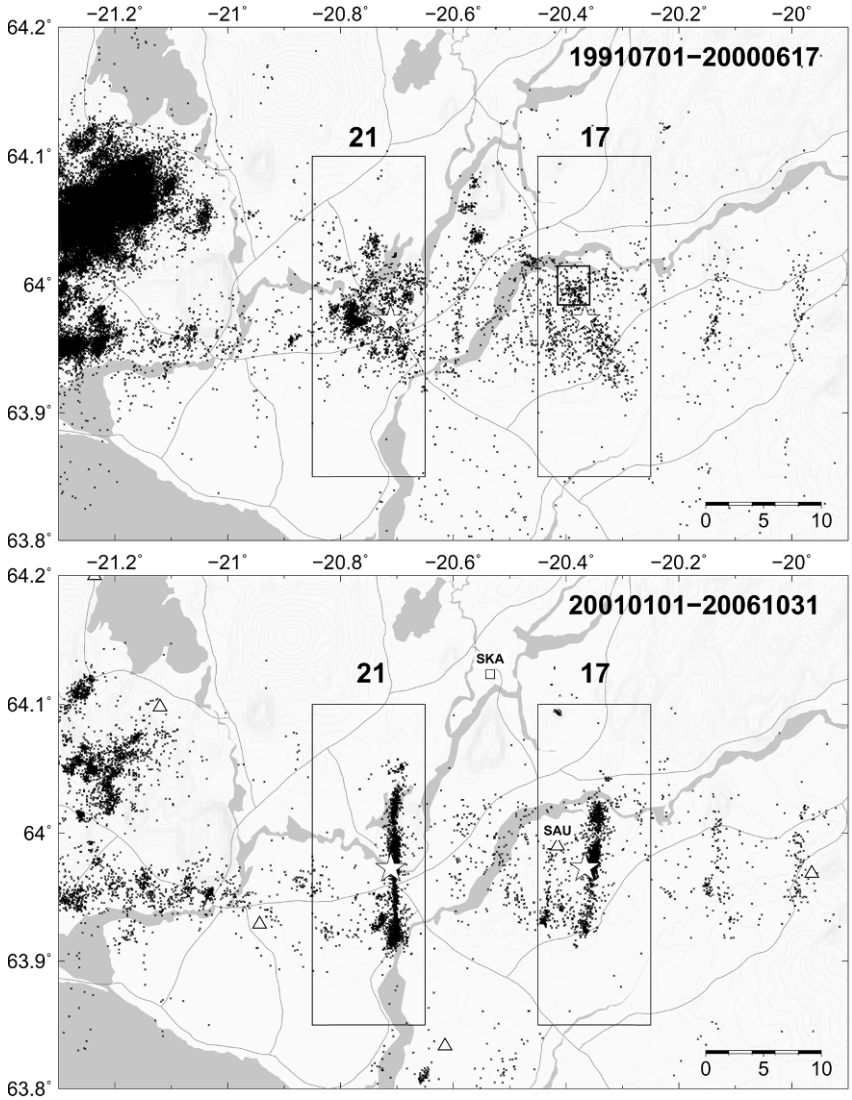

Figure 4.9. The upper map shows seismicity (indicated by dots) along the east–west elongated SISZ before the 2000 earthquakes, and the map below shows seismicity after the 2000 earthquakes. See periods of time in upper right corners. Boxes labeled 17 and 21 enclose micro-earthquakes at the sites of the June 17, 2000 and June 21, 2000 earthquakes. The epicenters of the two large earthquakes are shown by stars. Two faint clusters to the east of the two boxes show some remnants of micro-seismicity from two large earthquakes 100 years ago in the eastern part of the SISZ. The area of dense seismicity at the western end of the SISZ is a volcano-tectonic swarm around the Hengill volcano, at the junction between the SISZ and the Western Volcanic Zone. It is displaying the high seismic activity that occurred there during a volcano-tectonic episode between 1994 and 1998. At the eastern end of the SISZ we are close to its junction with the Eastern Volcanic Zone.

As will be discussed in Chapter 5, such a model was successfully created. It answers many questions about micro-earthquake swarms. These micro-earthquake swarms, sometimes called "dilavolume" (Stefánsson and Gudmundsson 2005), were central to the new "fluid–strain model" (sometimes abbreviated as the F-S model). The fluid–strain model is physically better constrained than the dual-mechanism model. It explains the large earthquake patterns in much the same way as the dual-mechanism model, but adds many features relating to micro-earthquake–pre-earthquake patterns (Zencher *et al.*, 2006; Bonafede *et al.*, 2007).

In hindsight, it is now clear that these micro-earthquake swarms occurring at the sources of both earthquakes were indicative of where the next large earthquakes in the zone would occur.

4.6.2 Increased micro-earthquake activity preceded the first 2000 earthquake at its source

Figure 4.10 shows the cumulative number of earthquakes in two areas inside the SISZ between 1991 and 2000. The thicker curve is from the area of the initial 2000 earthquake on June 17. It shows high earthquake activity starting in May 1996 only to fade out in the autumn. From that time on, there is a gentle increase in activity until the occurrence of the first large earthquake. Such a gentle increase in seismicity can be interpreted as general stress increase ("gentle increase" means that it does not consist of swarms or aftershocks, which may involve local stress release). It is of interest that the fast buildup in 1996 may be attributed to magmatic intrusive activity in the Vatnajökull area, 150 km away toward the northeast, in preparation for the large eruption that started there 4 months later (i.e., at the end of September 1996). Based on shear wave splitting, stress increase was discovered at a few seismic stations some 150 km distant in different directions from the volcano, starting 3–5 months before that eruption (Volti and Crampin, 2003).

The thinner curve of Figure 4.10 shows seismicity evolution farther west (i.e., at the site of the June 21, 2000 earthquake). It shows no such gentle micro-earthquake increase that can be explained by general stress increase. It can be straightforwardly explained in such a way that additional strain buildup in this part of the zone is continuously released in small earthquakes instead of building up stress (i.e., a balance is reached where stress release is just as fast as stress buildup). This balance continued until release of the first earthquake, which dynamically started a process reflected in micro-earthquakes along the whole June 21, 2000 fault, which led to the earthquake there a few days later. It may be speculated that when the first earthquake occurred its dynamic impact at the site of the second earthquake (Árnadóttir *et al.*, 2003) started a strain–fluid process there, instability along a large deeper part of the fault, and slow shearing motion across it, which created enough stress at some part of it to trigger the second earthquake. To release a large earthquake we need both instability along the major part of a large fault as well as a strong stress-releasing trigger.

Counting the number of small earthquakes and other methods that show general stress increase in a fault area is significant to understanding what is going on, and an

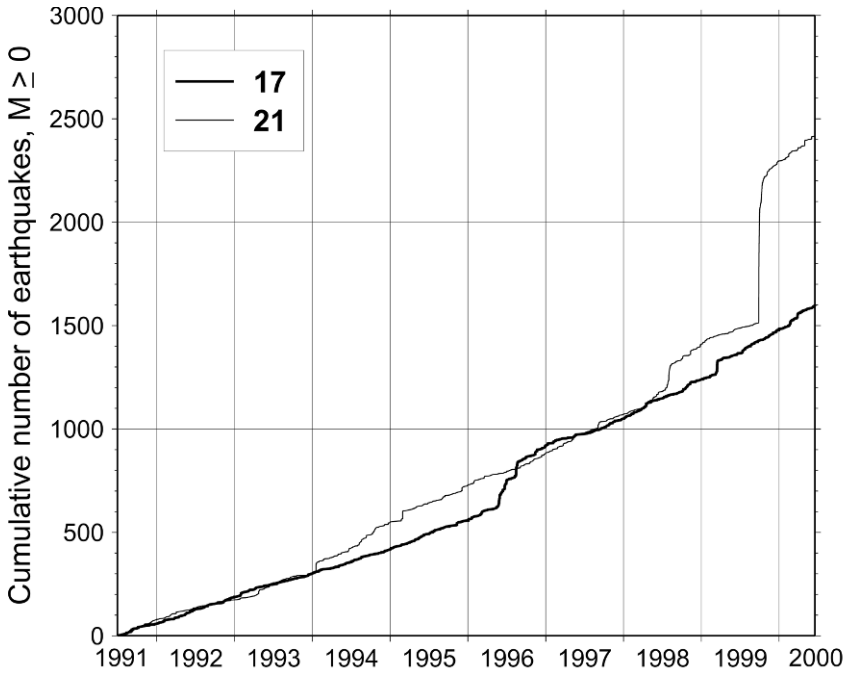

Figure 4.10. Cumulative number of earthquakes larger than magnitude 0 from 1991 to 2000, just before the first earthquake on June 17, 2000. The graph line labeled 17 is based on the earthquakes in box 17 in Figure 4.9. The other line is based on earthquakes in the focal area of the June 21, 2000 earthquake. By carefully studying the graph line labeled 17 we can see that it indicates a concave upward increase in the number of earthquakes after the substantial swarm activity in 1996. The graph line labeled 21 shows linear increase over time, intermittent with substantial swarms like those in 1999.

indication about what may be on its way. However, alone it is of limited value for short-term prediction because we do not know with certainty what level of stress increase and closeness to fracturing conditions has to be reached before a large earthquake will be released. However, by means of modeling and more physically based information about the source area, it will help our understanding of the ongoing process and help in efforts to extrapolate the process into the near future.

4.6.3 Mapping hard cores in a seismic zone

The character of a seismically active volume is often described by the so-called "*b*-values" of the formula $\log N = a - bM$ (Ishimoto and Iida, 1939), where N is the cumulative number of earthquakes above some magnitude M, and a and b are constants characterizing each site—a representing total earthquake production of the volume and b expressing the relation between the number of large and small earthquakes during the study period.

Large values of *b* represent an area or volume with many small earthquakes compared with large earthquakes (i.e., a volume where the mean magnitude of earthquakes is low). Experience also shows that volumes of high *b*-values are characterized by high pore fluid pressures and hydro-fracturing, making them weak as far as straining is concerned, while volumes of low *b*-values express a volume that is less fractured. Thus, if we have recorded enough earthquakes in a volume, *b*-values can be used to study the heterogeneity of the mechanical strength of the medium (e.g., to find the hard core of an earthquake fault or hard cores in a seismic zone). Such hard cores, often called "asperities", have frequently been found in the release process of large earthquakes. When the hard core breaks, fault motion will proceed in a larger part of the fault, possibly along the whole old fault, and thus possibly to a large earthquake.

Mapping the *b*-values of micro-earthquakes along the SISZ before the two large earthquakes (Figure 4.11) indicate their asperities as limited volumes with low *b*-values. The tendency for there to be high *b*-values at the bottom of the seismogenic crust supports evolving ideas of high pore fluid pressures there and correlates well with the thickness of the brittle crust in the middle of the SISZ (Wyss and Stefánsson, 2006; see also Chapter 3 on seismic structure).

We should not expect *b*-values to provide a clear image of the structure. One of the reasons is that they were probably undergoing changes during the time period studied, but if we make the periods shorter we do not have enough *b*-value data for a

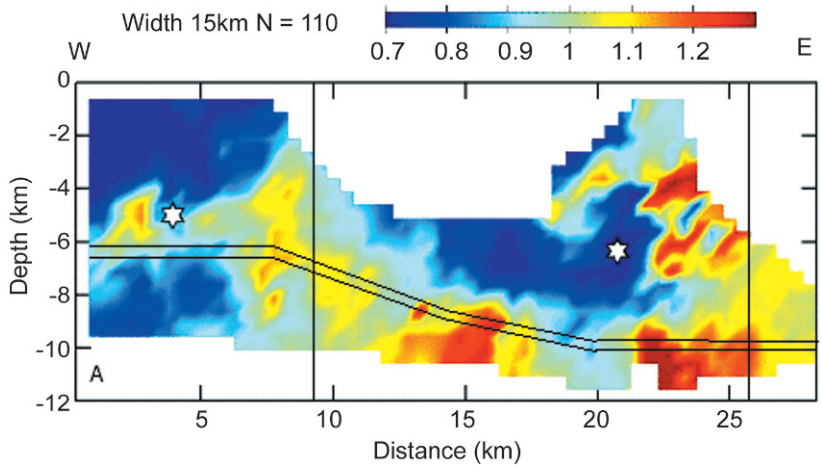

Figure 4.11. Map of *b*-values in cross-sections (color bar) along a 15 km wide east–west strip inside the SISZ. The two hypocenters of the large earthquakes are marked by stars. The initial earthquake is the star farther to the east. The double line indicates the bottom of dense seismic activity (i.e., approximately the brittle–ductile boundary). The vertical lines in the figure mark the faults of two of the largest earthquakes in 1896. The data period for *b* evaluation is 1991 to 2000 and before the June 17, 2000 earthquake. The magnitude-7 earthquake of 1912 and the initial 1896 earthquakes occurred slightly east of this figure (modified from Wyss and Stefánsson, 2006).

stable result. It is interesting to note the high *b*-value volumes at seismogenic depths in Figure 4.11 slightly to the east of the hard core of the first 2000 earthquake (i.e., where two of the largest earthquakes occurred during the last sequence before 2000: the 1896–1912 sequence). The magnitude-7 earthquake in 1912 and the initial 1996 earthquake (Figure 4.7) occurred east of where there is good resolution of *b*-values in the study. We also see high *b*-values 5 km to the east of the second earthquake, at a site close to one of the largest 1986 earthquakes. These volumes of high *b*-values were probably much fractured and corroded by that earthquake sequence and its pre-earthquake activity 100 years ago and have not yet fully consolidated in the intervening time.

Another significant outcome of this study of *b*-values (see Wyss and Stefánsson, 2006), but not expressed in Figure 4.11, is that it indicates the very dense structural fabric of the order of 2 km in the SISZ, supporting earlier ideas that in the long run earthquakes in the zone may repeat on faults so close to each other (see Clifton and Einarsson, 2005). It also supports the idea that local fluid pressure at depth may determine the exact site of earthquake nucleation among those sites that have similar and uniform straining caused by continuous plate motion.

Figure 4.11 also indicates that a volume 5 km to the west of the June 17, 2000 earthquake could be a strong (i.e., a high-stress) asperity of a large future earthquake there. However, it is possible that *b*-values there have changed now as a result of the large earthquake. This has not been studied so far with the *b*-value method.

Figure 4.11 and the discussion above reveal some of the problems of mapping the brittle–ductile boundary (transition) when only small earthquakes are counted. The boundary defined in this way apparently moves with time depending on the release of large earthquakes.

4.6.4 The SRAM procedure to find the probable epicenter of an impending earthquake

In the SRAM procedure all possible earthquake faults in the SISZ are assumed to have north–south strikes and right-lateral slips across them. Any grid point of the dataset is assumed to be a possible center of such a north–south striking fault. When an earthquake occurs on the fault with right-lateral slip the crust will compress in the southeast and northwest quadrants, but expand in northeast and southwest directions (i.e., in tensile quadrants). For the whole dataset (i.e., for the 9-year period of pre-earthquake micro-earthquakes) the method calculates the ratio between the number of earthquakes in compressive quadrants and the number in tensile quadrants for any given point of the grid assumed to be the center of the coordinate system. The result is shown in Figure 4.12, as are the epicenters of the impending large earthquakes. So, there are many more micro-earthquakes in the two quadrants of impending large earthquakes destined to be compressive quadrants. This configuration is in agreement with slow slip proceeding across the faults long before the occurrence of large earthquakes and in agreement with hard cores in the middle of fault planes hampering the slip. The method is an effective way of quantifying and visualizing the distribution of seismicity around the most likely earthquake fault

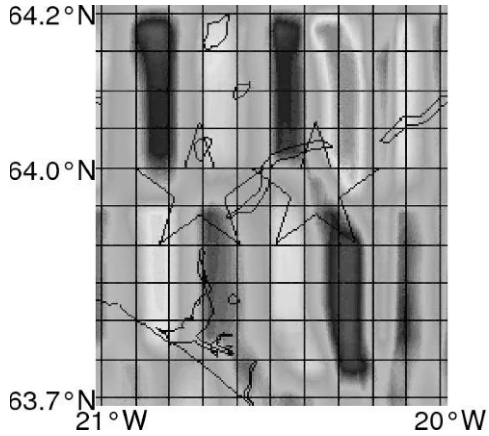

Figure 4.12. Results of the SRAM analysis in the SISZ 9 years before the 2000 earthquakes. A grayscale indicates increase (from light gray to dark gray) in the ratio between number of micro-earthquakes in compressive parts to number in tensile parts of quadrants of the assumed fault plane solution. The centers of the stars are the epicenters of the two large earthquakes in 2000.

direction in the area (Bödvarsson *et al.*, 2005; Stefánsson *et al.*, 2006a). To put it more concretely, the method indicates the north–south faults that best fulfill the observed distribution of seismicity, given the quadrantal distribution of earthquakes around a nucleation point in the preparation period of earthquakes in the zone.

Why the number of earthquakes is higher in the compressive quadrants of impending earthquakes is explained by modeling in Section 5.2 (see also Figures 4.9 and 4.20). To reiterate: long before the occurrence of an earthquake low crustal pressures are created in the northwest and southeast quadrants around the hard cores of old faults in the SISZ, because of east–west shearing of the weak SISZ which deforms between harder boundaries. These low crustal pressures favor upward migration of high-pressure fluids into the seismogenic part of the crust causing micro-earthquakes triggered by pore pressure in the northwest and southeast quadrants. When right-lateral earthquakes occur on north–south faults they compress these quadrants.

Reynir Böðvarsson (see Appendix 2.B) told me that he discovered this while evaluating the micro-earthquake sequence in his computer, without really realizing the significance of this observation until later. The strain/fluid modeling described in Chapter 5 provides a good explanation.

4.6.5 Nucleation of the June 17, 2000 earthquake based on micro-earthquake information

The preparatory processes for the two earthquakes can be observed in seismicity 30–40 years before they occurred (as already mentioned). The seismic rate at the two earthquake sites has also been discussed.

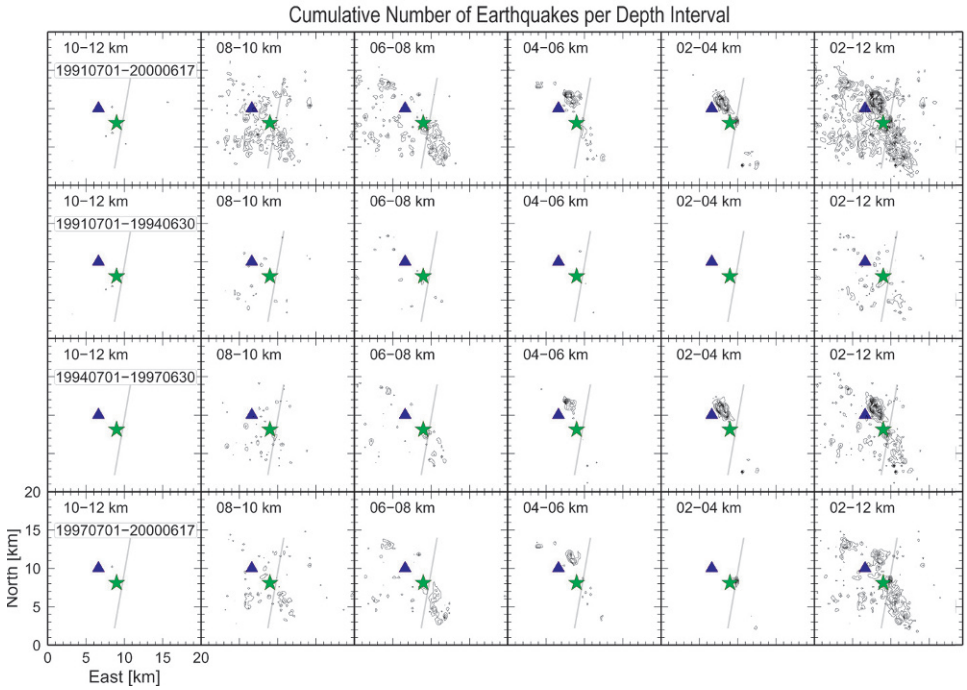

Figure 4.13. Distribution of small earthquakes (down to magnitude 0) at various depth intervals in 20×20 km areas around the epicenter of the June 17, 2000 earthquake. The top row contains seismicity for the entire 9-year period at various depths. The three other rows show activity during equal periods of time (3 years each). The four time intervals are indicated in the upper left corner of each row (yyyymmdd). The epicenter of the impending earthquake is shown by a star; a weak line striking nearly north–south indicates the fault plane of the impending earthquake.

In the following I will discuss the development of seismicity in the volume around the initial earthquake (the June 17, 2000 earthquake) since the advent of the SIL system in 1991. The SIL system made it possible to detect seismicity down to magnitude 0 across the entire SISZ. Figure 4.13 shows the distribution of micro-earthquakes horizontally and vertically and how they changed with time around the fault of the initial earthquake in the 9 years leading up to it.

As demonstrated in Figure 4.10, the rate of seismicity increased gradually in the focal area of the first 2000 earthquake 4 years before it occurred. Analyzing the spatial distribution of these earthquakes in Figure 4.13 we can see that seismicity at depths of 10 km to 12 km is unchanged with time while at depths of 8 km to 10 km it increases slowly and gently with time without clustering. In contrast, seismicity at shallower depths develops from being minor during the first period to becoming greater with clustering in space in later periods, clearly seen at depths of 2 km to 6 km.

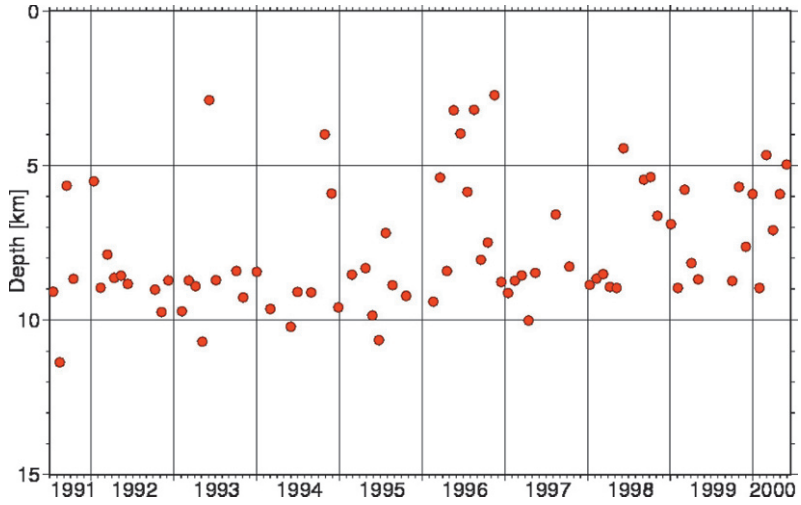

Figure 4.14. Depth of micro-earthquakes with time: 30-day median values of micro-earthquake depths in the seismically most active area around the epicenter of the June 17 earthquake (i.e., to the northwest of the center of the fault).

The nature of depth distribution with time is better demonstrated in Figure 4.14, where each point denotes a median depth during a 30-day period. Micro-earthquakes have a tendency to stay close to depths between 8 km and 10 km most of the time, but do appear at shallower median depths for short periods (i.e., of the order of days to weeks). These shallowings increase in number, especially after 1996, toward the time of occurrence of the large earthquakes. On the other hand, activity near the bottom of the brittle crust is almost continuous.

It is difficult to describe the spatial pattern of micro-earthquakes with time at the requisite resolution. The reason is that earthquakes interact with each other, back and forth, in the small volumes considered, and much of the activity may involve the release of earthquakes that are smaller than we can observe.

Figure 4.15 demonstrates more quantitatively but with lower resolution the long-term development of seismicity with time and depth before the June 17, 2000 earthquake, close to its fault. The top row shows background seismicity at various depths in the 9-year period of micro-earthquake monitoring before the earthquake. In the lower rows we see the percentage level of this background distribution in different time periods. The second row (time period mid-1991 to 1994) indicates relatively low activity at medium depths, possibly reflecting high seismic release and relaxation in the SISZ just before this period. Hekla erupted near the eastern end of the SISZ on January 17, 1991, lasting 7 weeks. A flurry of small earthquakes followed it westward along the SISZ until May/June, releasing stresses and high pore fluid pressures at seismogenic depths, locally along the zone. The activity shown in the second row is thus mostly deep (i.e., at the brittle–ductile boundary). For the next period 1994–1996, there is a tendency toward shallower depths of seismicity, and in 1996–1997 still shallower depths prevail, involving the large swarm in mid-1996 (see

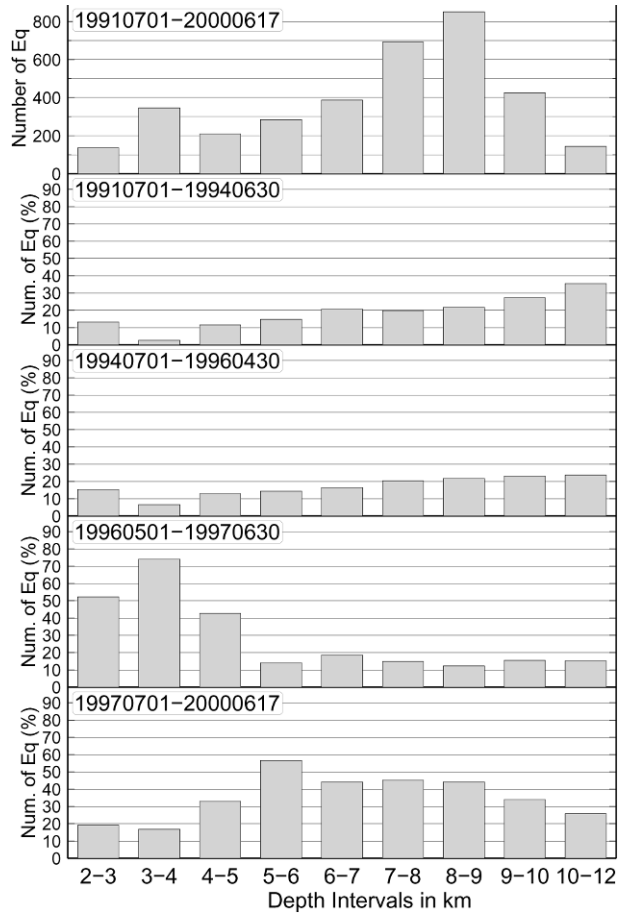

Figure 4.15. Distribution of micro-earthquakes per depth interval in the 9 years before the June 17, 2000 earthquake, within a couple of kilometers of the fault. The top row shows the total number (i.e., the background). The four lower rows show total number expressed as a percentage during different periods of time before the earthquake on June 17, 2000.

also Figure 4.10). The last period, 1997–2000, just before the 2000 earthquakes, again exhibits high mid-depth activity possibly reflecting upflow of high pore fluid pressures to these depths just below the asperity of, and in preparation for, the large earthquake that occurred after this period (i.e., on June 17, 2000) at this site of the SISZ.

The spatial development of microseismic activity described above has a tendency toward episodic shallowings. This can be explained by emerging ideas that high (near-lithostatic) pore/fluid pressures can in response to strain be brought upward with time to modify fracturing conditions at medium depths in the crust. This is discussed and modeled in Chapter 5 (see also Zencher *et al.*, 2006; Stefansson *et al.*, 2006b). The bottom row of Figure 4.15 would then express high pore fluid pressures

and stresses at medium depths before the release of the June 17, 2000 earthquake, with its 6 km deep hypocenter breaking upward through the whole crust. If this is the right interpretation, it would represent a new method of discovering pre-earthquake activity comparable with seeing the upflow of magma through the eruption column toward the crater (of paramount value in predicting an eruption). Of course, it would depend on there being a tendency toward high pore fluid pressures at the bottom of the brittle/elastic crust.

4.6.6 Episodic upwelling of fluids in response to buildup of strain

As stated in Section 4.6.5 and discussed further in Chapter 5, episodic shallowing of earthquakes in the SISZ can be explained by episodic upward fluid migration from below the brittle–ductile boundary. Episodic upward fluid migration itself can be explained in the following way: when pore fluid pressure at depth and plate motion strain have between them reached a fracturing level somewhere along the bottom of the brittle seismic zone, pressure is released by upwelling that is usually limited to a small volume of the deformed zone—especially volumes whose confining pressures are relatively low. The fluid carries the high near-lithostatic pressure upward and in so doing helps to release micro-earthquakes on its way.

Figure 4.16 is an example of what probably is a fluid-driven micro-earthquake upwelling lasting 10 days. This swarm occurred to the northwest of the epicenter of the June 17, 2000 earthquake between March 7 and March 16, 1999. The speed of upward migration was of the order of half a kilometer per day and reached a depth of about 3 km.

Figure 4.16 shows a causal relationship over time for such a process from the bottom to the top of the seismogenic crust. In the fault zone of the June 17, 2000 earthquake this was the best example expressing such a process.

But how do we know that this is caused by upwelling of high-pressure fluids?

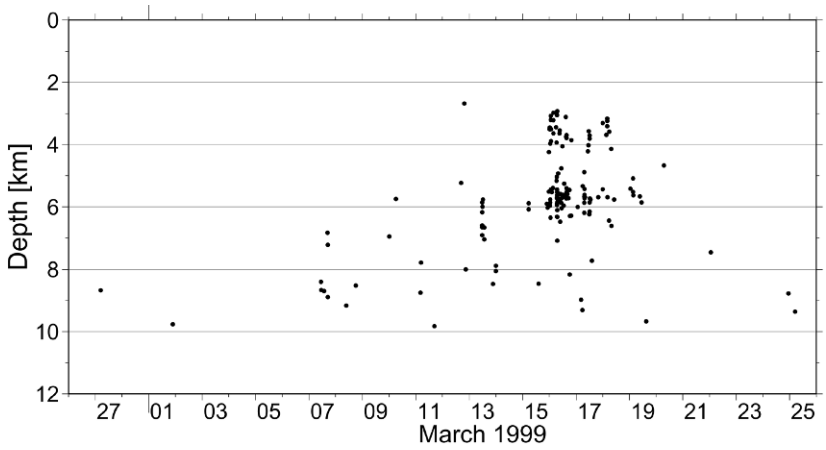

Figure 4.16. How micro-earthquake depths changed with time between March 7 and March 16, 1999, near the epicenter of the June 17, 2000 earthquake.

At present, the only way to monitor such fluid upwelling is indirect (i.e., by watching small earthquakes assumed to be fluid-driven). Such an upwelling probably only consists of compressible fluids that are not measurable even by high-sensitivity deformation measurements at the surface. The fluids cause only infinitesimally small strain changes. Any new micro-earthquake releases fluid pressure locally, so the small faults created don't grow, but a new micro-earthquake fault is created at a new place (Stefánsson *et al.*, 2010). It is expected that most fluid-triggered earthquakes are so small that they cannot be detected. The flow migrates in a step-like manner, each new pressure front breaks out somewhere else, possibly after having long been sustained at the same place. In volumes of small-scale heterogeneities of strong internal coupling, downward jumps should also be expected as part of normal upward fluid migration. Moreover, many jumps should be expected to result in earthquakes no larger than magnitude 0 and thus not easily detected by the seismic system.

So maybe we should not expect many upflows all the way from the brittle–ductile boundary to be expressed in the 9 years of seismic recording. It is a fact that the example in Figure 4.16 is the only "complete" one in the preparation volume of the June 17 earthquake. There are others "half complete', as seen in Figure 4.21. The detection of such processes may be of extreme interest for earthquake prediction research and for the study of such possibilities. At sites where earthquakes are likely to occur, sensitivity should be increased as much as possible to try and detect such upwelling.

Doubts about the existence of such a stress-modifying fluid upwelling was the catalyst for Earth-realistic modeling of the fluid upflow by the PREPARED group. Among the most significant modeling results is that such an upwelling of stress-modifying and fracturing fluids from below the brittle crust is a necessary corollary to the existence of the Iceland Hot Spot. This modeling work resulted in the fluid–strain model, which will be more thoroughly discussed in Chapter 5. Shallowing episodes of small earthquakes in the preparation zone of the first 2000 earthquakes (as demonstrated in Figures 4.13–4.16) suggest a slow but measurable modification of fracturing conditions, involving hydrofracturing and locally high pore fluid pressures, at depth in the zone where large earthquakes are expected to nucleate. As to whether this can be utilized for prediction of earthquakes in the short term can be answered in the affirmative: as a part of other studies investigating slow changes in physical conditions in the preparation zone.

Studies of the spatiotemporal distribution of micro-earthquakes during the 9-year period suggests a slow but episodic and observable preparation period, starting many years before the 2000 earthquakes.

4.7 SHORT-TERM PROCESSES BEFORE THE FIRST EARTHQUAKE IN 2000

This book generally concentrates on the crustal activities that preceded the initial 2000 earthquake, while basic multinational research concentrated on the initial

earthquake. The reasons are twofold. First, it made more sense to use the limited funds available to discover underlying processes facilitating prediction of the first earthquake in a sequence. Secondary earthquakes triggered by the first would then be easier to foresee, as our experience shows. The premonitory activity before the second earthquake was dominated by the first earthquake and its aftershocks, so it was more difficult to see and understand in detail the multiplicity of crustal processes preceding it.

4.7.1 Observations that might have led to short-term warnings preceding the initial earthquake

Figure 4.9 shows how the volumetric distribution of micro-earthquakes preceding the first 2000 earthquake (i.e., the June 17, 2000 earthquake) changed to activity along the vertical plane after the earthquake. Did this change occur before the earthquake? In other words, did the earthquake process start shortly before the real earthquake was released?

Figure 4.17 shows how small earthquakes were arranged along the plane of the impending earthquake 2–3 weeks before the earthquake, on the basis of routine seismic evaluation. During the earlier part of this period there was a relatively high number of micro-earthquakes near both ends of the fault. Only a day before the earthquake, small earthquakes clustered densely around the epicenter of the fault; this was at the asperity, the hard central core of the earthquake fault. The day before the earthquake, the central core started to break.

This cluster of small earthquakes moved from being along the fault 2 weeks before it to a point just before it. This suggests the following process. Slow slip started across the deeper parts of the entire north–south fault, shortly before the earthquake. This slow slip was hampered by a hard core (an asperity) in the middle of the fault. The slow fault slip put a strain on this core, stress levels rocketed, and micro-earthquakes started inside it the day before its release. The hard core broke and thus triggered the earthquake along the entire length of the 10 km fault.

Such a pattern of earthquake nucleation is physically understandable. It is difficult to say in hindsight whether this could have led to some kind of short-term warning. This pattern was observed as a result of automatic evaluation in the SIL system, but only partly constrained by seismologists before the earthquake occurred. In any event, the earthquakes were small (<1) and the pattern was not adjudged safe until manual evaluation confirmed it, shortly after the magnitude-6.6 earthquake occurred.

In hindsight, it is possible that this pattern would have led to a pre-earthquake warning if

- the old long-term prediction of the site of the next large earthquake in the zone had been taken into consideration in our warning procedure and was exactly there;
- an early information system had been available to highlight the ongoing pattern

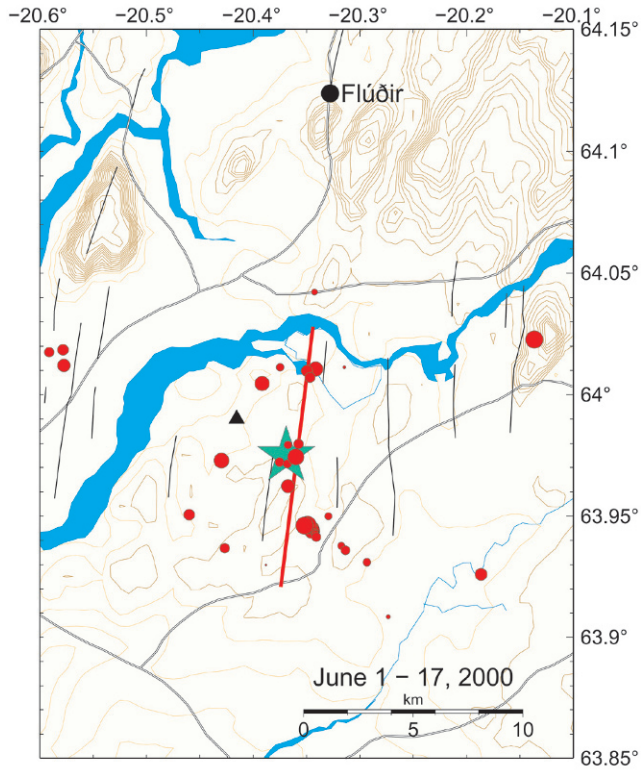

Figure 4.17. The area surrounding the June 17, 2000 earthquake. The epicenter is shown by a triangle and the fault of the impending earthquake is indicated by a straight line that is striking close to north–south. The other north–south striking line segments indicate some old earthquake faults observed on the surface. Dots show micro-earthquakes (36 in number, $M_L = -1$ to 1), during the 17 days before the earthquake. They were mostly concentrated near the ends of the fault, until the last 1–2 days when they clustered in the middle of it (the epicenter). Hydrological changes were observed in the village of Flúðir (as reported in the text).

of clustering based on evaluated and automatic data (before the earthquake the alert system should have been better focused on the expected earthquake fault, but at that time the alert system was only based on the number and magnitudes of micro-earthquakes in a much larger area);

- algorithms been available to quickly carry out evaluation and modeling based on the information carried by micro-earthquakes to detect physically expected pre-earthquake processes in light of earlier results and understanding.

Had all of this been prepared beforehand (i.e., in an active information and warning system) we might have been able to issue a low-order warning to the ICPA and might have taken it on ourselves to enhance monitoring in the area. Later sections reveal much more of the pre-earthquake process as a result of hindsight.

At a geothermal borehole at Flúðir, a village 10 km to the north of the fault and in line with the north–south striking fault plane (Figure 4.17), a water level drop of 6 m was noted by staff 24 hours before the earthquake. Unfortunately, this signal is not seen in the preserved record (i.e., records of signals kept at the borehole) which is based on taking measurements of the water level at 15-minute intervals. A higher frequency record was not preserved. It must be noted that this is a commercial hole used for providing hot water—not for watching pulses in the crust and predicting earthquakes—hence there is little need to keep high-frequency records. Water level monitoring is used to alert staff when the water level in the borehole drops below a certain point to avoid dry-pumping, which can seriously damage the pump, if not destroy it. During 5 years of continuous operation this was the first time the alarm sounded (Björnsson *et al.*, 2001). This alert was not reported until after the earthquake. Had this alert caught the attention of scientists along with other signals from the borehole this may well have been enough to issue a low-order warning to the ICPA.

Although the recording of this water level signal was not preserved it has to be considered significant. It occurred at a time of micro-earthquake activity near the asperity. A physical explanation of it may be that it was caused by a temporary deformation across the fault and its surrounding, caused by an abrupt cessation of deep fault motion at a hard and undeformable shallower asperity, which could have expanded the crust at seismogenic depth near to the borehole. Such an expansion of an asperity near the water at the bottom of the borehole would have led to abrupt lowering of the water level. In this way the borehole acted in much the same way as a volumetric strainmeter with a huge sensing volume (see Section 3.7.1). Such a signal can be short-lived either because of not being static or because water is quickly diffusing from the surrounding cracked volume into the holes that open up as a result of the asperity and thus is not seen even in a 15-minute record (Stefánsson, 2006).

4.7.2 Short-term pre-earthquake patterns in seismicity and fault plane solutions

The way in which the distribution of pre-earthquake seismicity went from being volumetric to planar is described in Figure 4.18. The figure shows the distribution of seismicity from 1991 until just before the earthquake by projecting the sites into a three-dimensional box around the hypocenter of the first 2000 earthquake. Steady activity can be seen near the boundary of the elastic/brittle crust and the ductile layer below it, probably expressing high pore fluid pressures there. Upwelling into the upper crust has occurred episodically (as discussed in Section 4.6.6). We can see a tendency toward planar seismicity in the 2–3 weeks leading up to the earthquake in Figure 4.18c and the planar distribution after release of the earthquake in Figure 4.18d.

An effort to quantify changes in directivity of micro-earthquake sources along the fault and of the fault plane solutions is demonstrated in Figure 4.19 (Stefánsson and Gudmundsson, 2005). The upper part of the figure shows the frequency of changes in direction of individual earthquake epicenters from the center of the

main earthquake fault. In the lower part of the figure, the most significant directions taken by horizontal compressions of the fault plane solutions of individual earthquakes are demonstrated by rose diagrams (Stefánsson and Gudmundsson, 2005; see also discussions on horizontal compressions in Chapter 2 and Appendix 2.A).

Although this is not a strong indication of pre-earthquake changes or good precursors to the first large 2000 earthquake, it nevertheless complies with ideas about nucleation of the earthquake.

A tentative interpretation of the observations shown in Figure 4.19 is summarized schematically in Figure 4.20 (based on Stefánsson and Guðmundsson, 2005 and Stefansson *et al.*, 2006a). It shows volumes of long-term seismic activity, created by accumulated episodes of micro-earthquake upwelling to the northwest and southeast of the asperity of the earthquake. This activity fades out just before occurrence of the earthquake as seen in the upper part of Figure 4.19. Figure 4.20 also shows the directions of micro-earthquake faults, as indicated by horizontal compressions of the fault plane solutions seen in the lower part of Figure 4.19. In general, micro-earthquakes in the area tend to have fault directions that are close to north–south, expressed in horizontal compressions that by definition are at an angle of 45° to the fault direction. The rotation of horizontal compressions as seen in Figure 4.19 from around 50°–55° northeast in much of the time preceding the earthquake to around 65°–70° northeast just before it probably expresses *en echelon* cracking 15° oblique to the nearly north–south right-lateral strike slip across the deeper part of the fault.

4.7.3 Short-term spatiotemporal patterns preceding the first 2000 earthquake

Figure 4.21 shows variation with time in depth and north–south positions along the fault of micro-earthquakes in the 20 days leading up to the June 17, 2000 earthquake. The data are from a rectangular area around the fault, 20 km in the north–south direction along the fault and 5 km in the east–west direction across the fault. Increased variability of position along the fault is indicated in the 10–15 days leading up to the earthquake, compared with the relative stability of positions over longer periods of time (better demonstrated in Figures 4.22 and 4.23).

What happens can best be explained by commencement of fault slip at depth (i.e., below 8–10 km). Microearthquakes occur all along the fault plane in the 2 weeks leading up to the earthquake and concentrate in a cluster 24 hours before it (as seen in Figure 4.21).

A simple algorithm describes the observed process (Figure 4.22). It adds up the distances between consecutive micro-earthquake hypocenters over a period of time, along the depth axis and horizontally along the fault. It expresses planar spreading of seismic sources along the fault in the 2 weeks leading up to the initial June 17 earthquake. It finally changes to clustering at a point (i.e., the hypocenter) 24 hours before the earthquake (see also Figure 4.21 for short-time resolution).

The pre-earthquake increase shown in Figure 4.22 is larger as a result of a slight increase in frequency before the earthquake. Therefore, in Figure 4.23 the accumulated distances have been normalized with the number of recorded earthquakes in

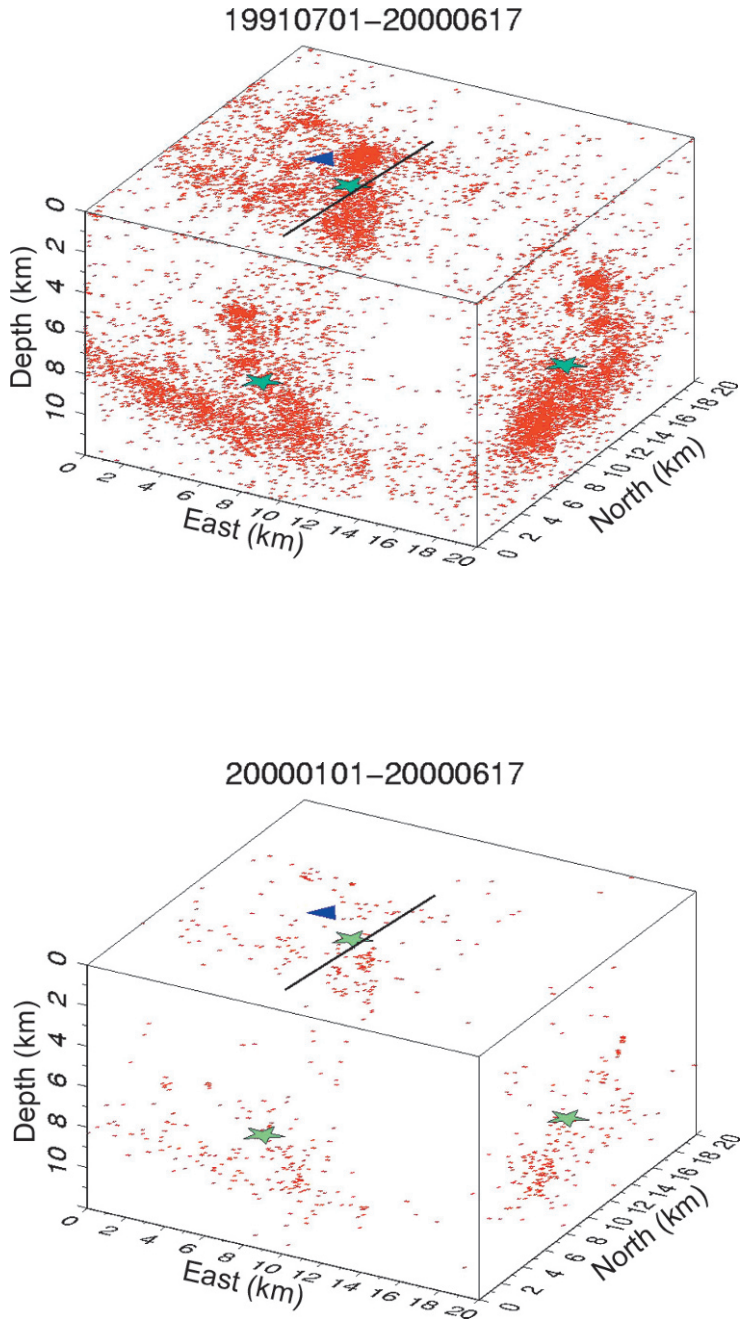

Figure 4.18. A three-dimensional look along the June 17, 2000 fault at seismicity changes in the pre-earthquake to post-earthquake situation, in a box of the crust which is 20 km^2 in size and 12 km deep. The time periods for plotted data are indicated as yyyymmdd.

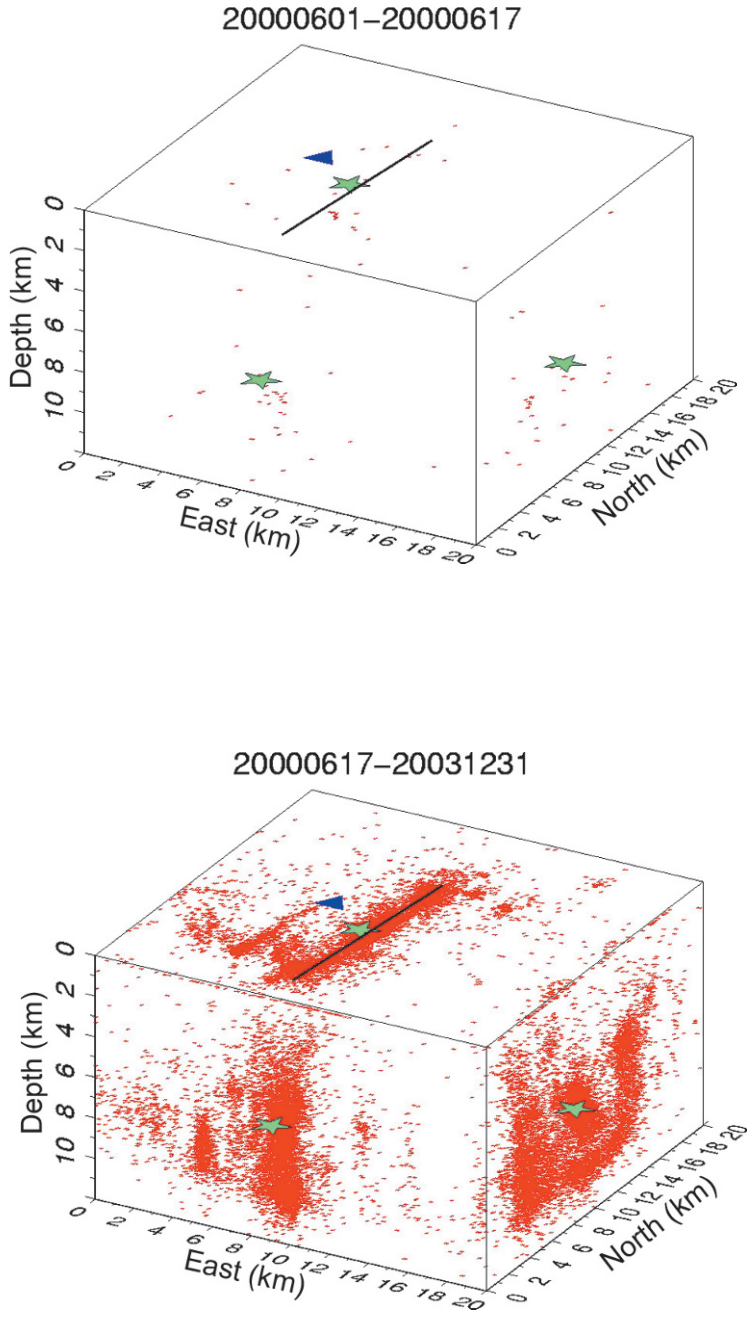

Clear orientation toward the fault direction is seen during the last 17 days before the earthquake. After the earthquake, seismicity is oriented along the fault and the W29°N dilavolume (i.e., micro-earthquake swarms) has disappeared.

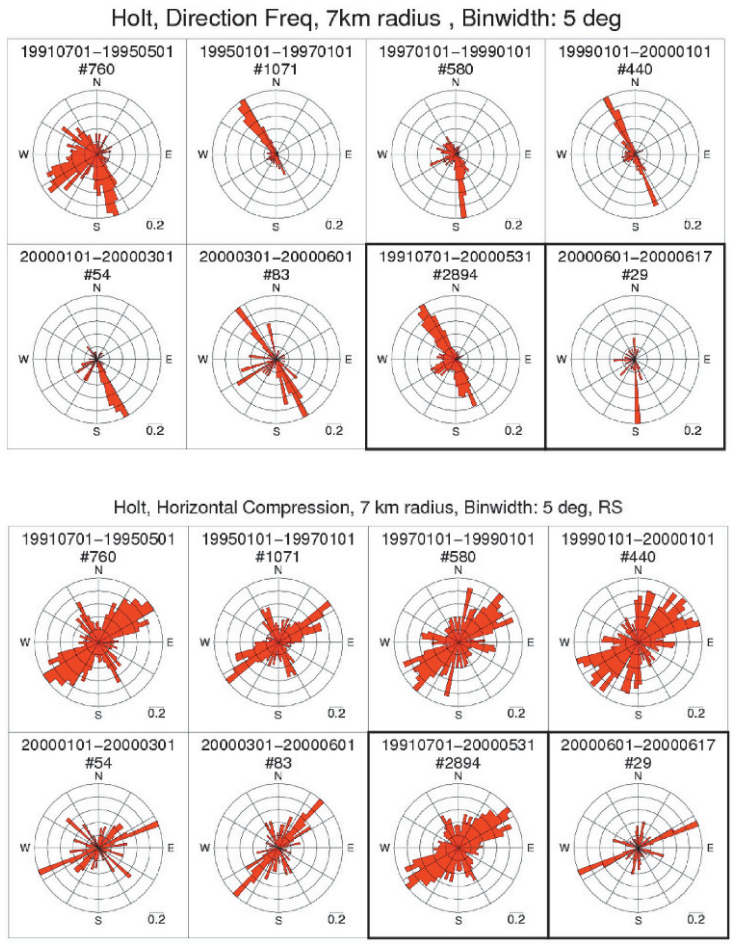

Figure 4.19. (*Upper*) Rose diagrams expressing the frequency of directions of micro-earthquakes as seen from the hypocenter of the developing June 17 earthquake. The first six diagrams are for various periods from 1991 to June 1, 2000. The diagrams inside the dark frames denote, respectively, the frequency of directions for the whole period and the frequency of directions during the last 16 days before the June 17 earthquake, when they were very close to the NS fault plane. (*Lower*) The frequency of horizontal compressions (HC) calculated from the fault plane solutions of individual micro-earthquakes. The HCs calculated here are by definition 45° from fault planes. The first six diagrams are for various periods from 1991 to June 1, 2000. The last two (in the dark frames) denote respectively the whole period and the last 16 days before the June 17 earthquake. For most of the time HCs strike 50–55° east from north. During the last period a 65–70° strike is most frequent. So a rotation of around 15° to the right is seen in the fault planes of the micro-earthquakes when they move above the main fault. This could possibly express *en echelon* cracks, striking 15°—above and oblique to the 5° east-of-north strike-slip—on the deeper part of the main fault (modified from Stefánsson and Gudmundsson, 2005). Each rose involves a 5° angle, 0.2 is the fraction of the radius length in the diagrams, and # indicates the number of earthquakes used in the solution.

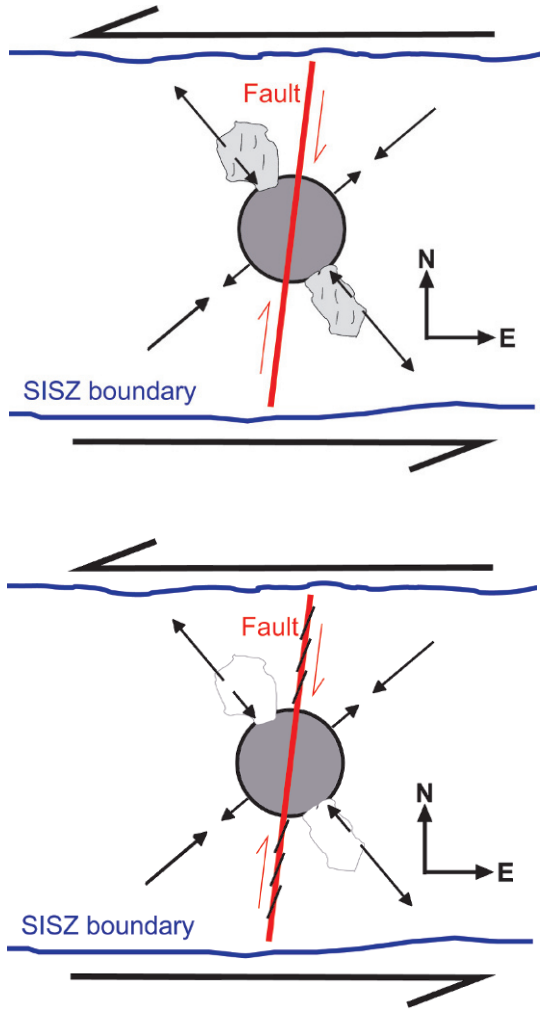

Figure 4.20. Conditions around the fault of the June 17, 2000 earthquake before its occurrence. East–west motion across the SISZ is shown by left-lateral arrows, and boundaries of the 10 km wide SISZ are shown by wavy lines. The June 17, 2000 fault has a strike of 5°NE. Red arrows show the expected slip across it. An asperity 3 km in diameter is shown in dark gray. Regional horizontal stress axes are shown by arrows, and maximum horizontal compression is here taken as 50°NE. The local field heterogeneity caused by left-lateral steady motion across the hard core is indicated by opposing short arrows. In the top diagram, the dilavolumes of premonitory seismic swarm activity that endure for decades are in light gray and contain line segments indicating the fault planes of frequent micro-earthquakes. The bottom diagram describes the last 17 days before the earthquake. Micro-earthquakes are now clustering near the plane of the main fault (mostly below 6 km). The fault planes of micro-earthquakes are now *en echelon*, complying with the proposed right-lateral slip motion that has started across the fault at depth (from Stefánsson and Gudmundsson, 2005; Stefánsson *et al.*, 2006b).

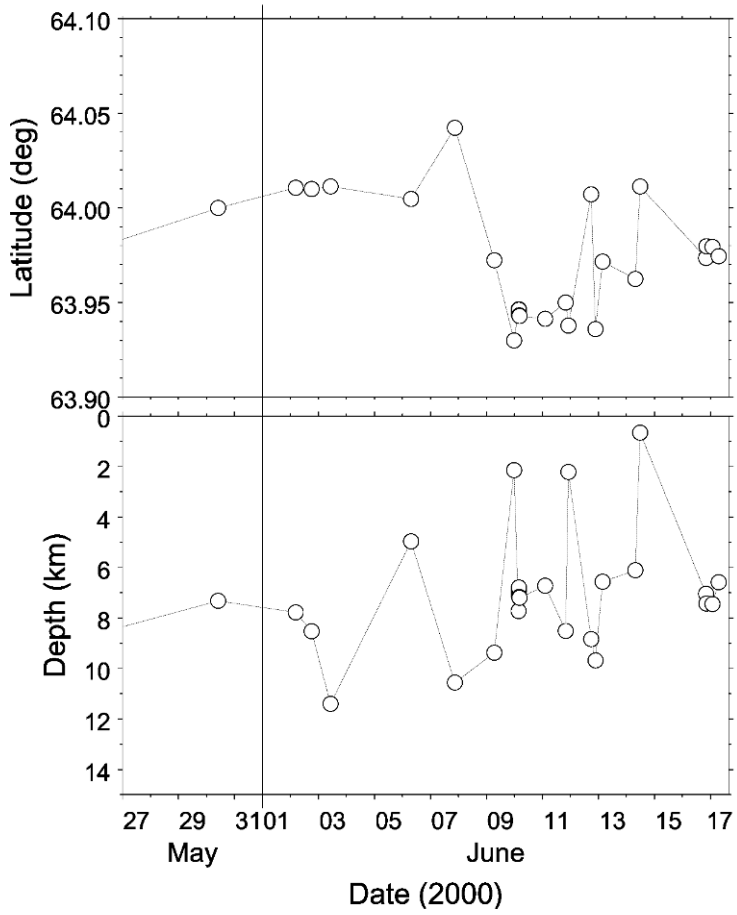

Figure 4.21. Depths and north–south positions (along the fault) of micro-earthquakes (minimum magnitudes −1) in the 20 days leading up to the June 17, 2000 earthquake in a rectangular area 5 km across the fault and 20 km north–south along the fault.

the area surrounding the fault. So, in this case it is assumed that the impending fault plane is known (in fact, exactly as predicted). So, Figure 4.23 adds the effects of a clustering of widespread activity to a plane spread along the plane.

By studying Figures 4.21–4.23 and keeping in mind the volumetric distribution of seismicity in the area long before the earthquakes, we observe the following seismic pre-processes preceding the initial (i.e., the June 17, 2000) earthquake: the distribution of cumulative long-term seismicity was volumetric for a long period of time and changed to planar along the plane of the impending large earthquake 10–15 days before it occurred. Densely clustered activity in the hypocenter of the impending earthquake started 21 hours before it (i.e., at 20:19 on June 16, 2000) at a depth of 7 km, indicating where the asperity started to break up (i.e., less than a kilometer

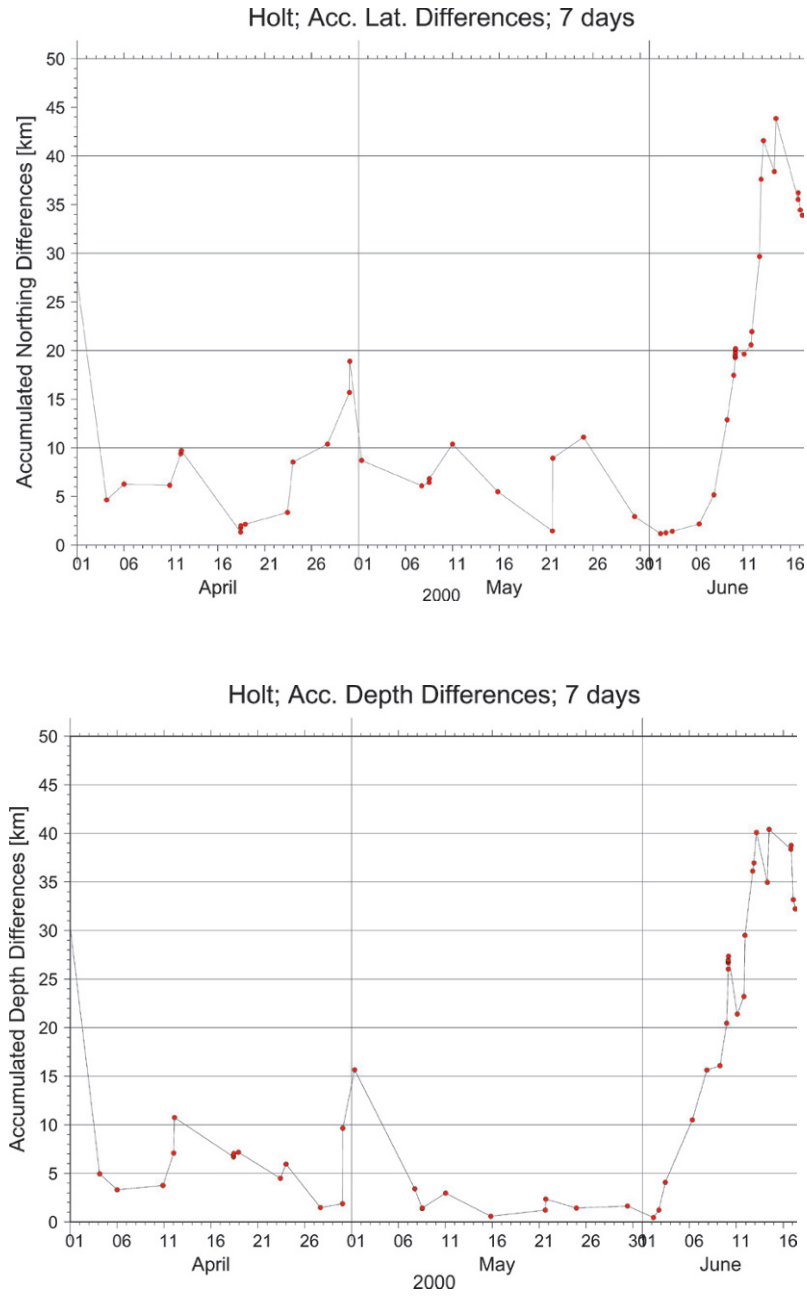

Figure 4.22. Accumulated distances between consecutive micro-earthquake sources along the depth axis and along the north–south axis, respectively, in the 2.5 months leading up to the earthquakes in a 5 km wide strip across the fault (as in Figure 4.21). Each point in the figure is based on data (distance sums) from the preceding 7 days.

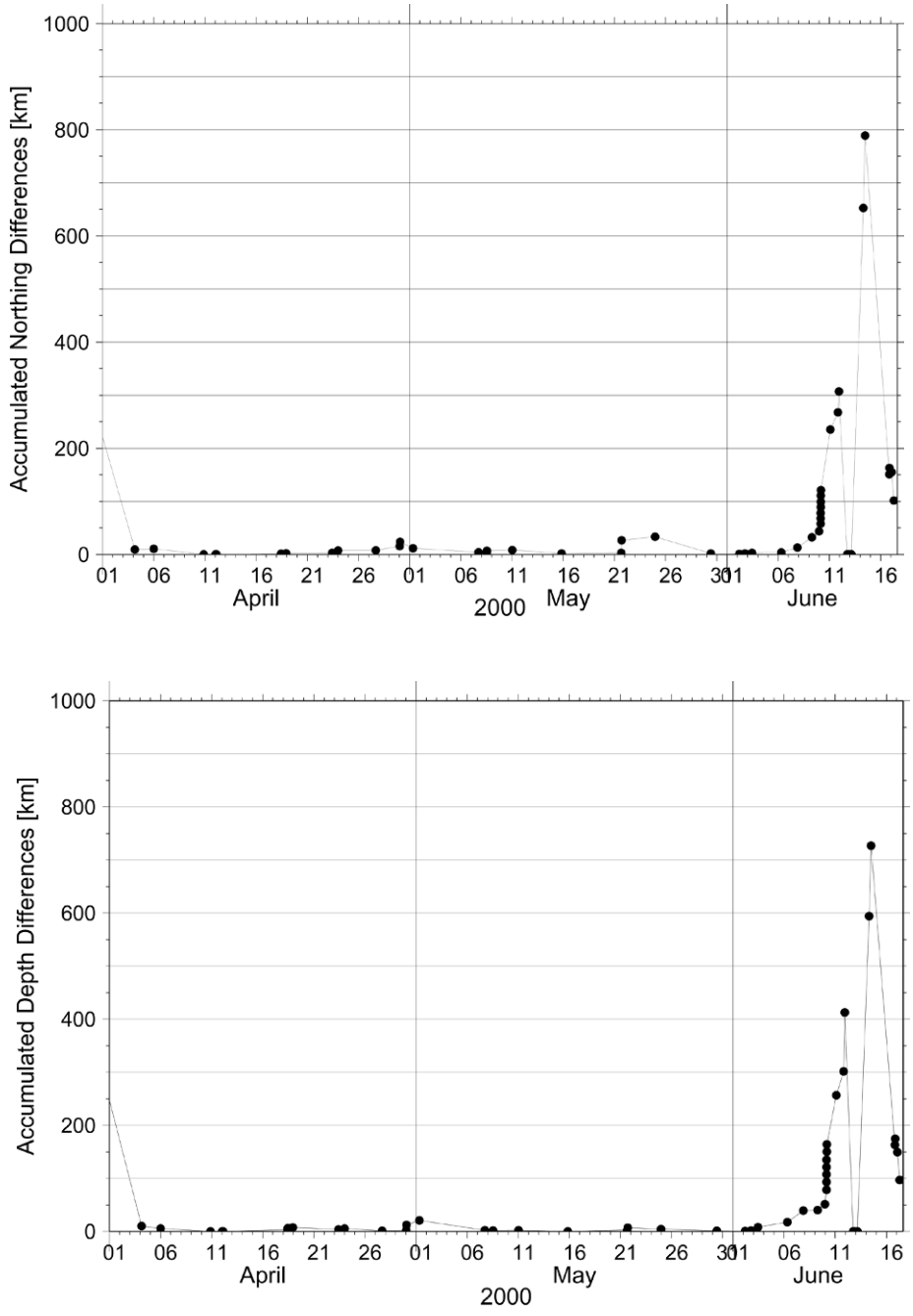

Figure 4.23. Same as Figure 4.22, but here the cumulative sums have been normalized by dividing by the number of micro-earthquakes in a 20 km wide strip outside the 5 km wide fault strip (i.e., normalized by the surrounding background seismicity).

below the calculated hypocenter of the earthquake). A closer look at the time patterns (Figure 4.21) reveals that slip motion started at the bottom and at the northern end of the fault. It must be added here that over the 9 years of micro-earthquake recordings there have been two to three events similar to this, although none appear in the last part (i.e., clustering at the hypocenter and breaking through the hard central core). This indicates that earlier in this period of time there may have been fault slip motion at depth without leading to the asperity breaking and to a large earthquake.

It is worth noting that if earthquakes larger than magnitude 0 had only been used the pattern above would not have been discovered.

4.7.4 Significant observations from Sacks–Evertson strainmeters

Since 1980, six Sacks–Evertson volumetric borehole strainmeters have been continuously operated in the SISZ (see Section 3.7.1). The main reason for this was to study in detail the spreading process of the diverging crustal plates in Iceland (Sacks *et al.*, 1980). The technology and instruments have been extremely valuable in recording and modeling the eruptions of Hekla at distances of 15 km to 45 km from the volcano (Linde *et al.*, 1993) and facilitated release of a short-term warning of Hekla's latest eruption in February 2000.

On May 28, 19 days before the first large 2000 earthquake, a strainmeter at a depth of 180 m in a borehole at the SAU station, a couple of kilometers from the epicenter of the June 17, 2000 earthquake, showed a 400-nanostrain contraction signal (Figure 4.24). A similar signal had not been seen at the SAU station since 1982 when several such signals occurred in a single year (Stefánsson and Halldórsson, 1988). The signal was not seen on other strainmeters 15 km to 20 km away, and therefore had to originate from a local source (i.e., only a few kilometers from the SAU station and at a shallow depth—less than 3 km). The closeness in time and space relates it to a pre-earthquake process. As can be seen in Figure 4.21, microseismic activity started approximately at a depth of 12 km five days after this strain signal started. But the 2–3 week long slip process, which the micro-earthquakes indicate, was not directly observed in the strainmeter record. However, the relatively low compression which the strainmeter shows after the so-called "big bump" and leading up to the earthquake (Figure 4.24) is of interest. It indicates expansion compared with the period before the bump. This may express the opening of shallow micro-cracks during accelerated slip motion indicated by micro-earthquakes in the 10–15 days leading up to the earthquake.

This strainmeter signal (i.e., the big bump) probably reflected some kind of very shallow fluid–rock interaction, as it was not recorded by other strainmeters in the SISZ. Being so shallow such a fluid–rock interaction probably only involved meteoric water. It was possibly triggered by strain changes at depth. It started only a couple of days before the deep crustal slip reflected by micro-earthquakes. The expansion, probably also in the shallow crust, which was seen after the big bump might express crustal expansion at a greater depth shortly before the release of the earthquake. The release of the bump and the expansion following it might be an

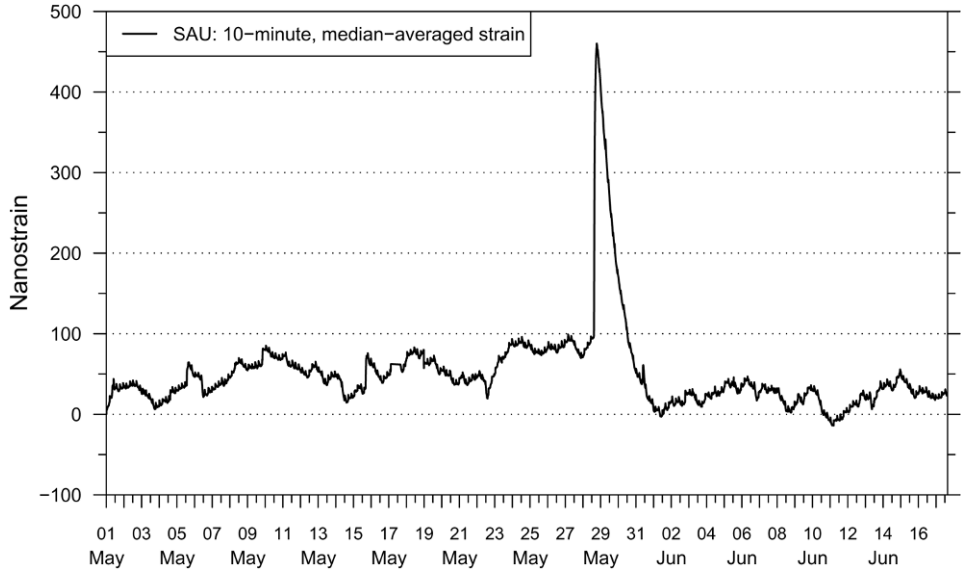

Figure 4.24. The large signal (termed the "big bump") given by a borehole strainmeter at Saurbær (SAU) a few kilometers from the epicenter of the June 17, 2000 earthquake. The data have been filtered to give 10-minute median values. Upward movement of graph lines in the diagram means compression (i.e., the strainmeter has been compressed). The start of the earthquake is right at the end of the graph. The situation indicates relative calm on this frequency scale except for this one signal. Also, it is interesting that there seems to be a general lowering of compression from the start of June. Such an indication of crustal straining, as suggested, may be significant for earthquake warnings even if it is not understood how this is related. The possibility that it may reflect unusual crustal straining should be taken into account in monitoring procedures and merged with physically understood signals and other unusual phenomena that may be related to local and fast strain buildup preceding an earthquake. However, there is the possibility that it was caused by stress buildup in an asperity at seismogenic depths, or related to fast-developing instability around the deep part of the fault caused by increased pore fluid pressure there.

instability process in the shallowest part of the crust as a response to deformation around the great depth of the fault immediately preceding the earthquake.

In spite of the isolated large-strain signal and possibly lower pressure near the fault of the June 17, 2000 earthquake, the deep crustal slip that micro-earthquake information implied was ongoing during the 10–15 days leading up to this earthquake was not directly reflected in the strainmeter record at the SAU station, which was 2 km from the fault. Moreover, at other strainmeter stations within 20 km of the fault there was no observable signal. In a fortnight, strainmeters can be expected to sense continuous buildup or release of around 10 nanostrains. A fault motion of 0.1 mm at around a depth of 5 km would give an observable signal. Micro-earthquakes seen at such depths or deeper before this earthquake had slips of only 0.01 mm to 0.1 mm. They covered only very limited parts of the fault plane in the

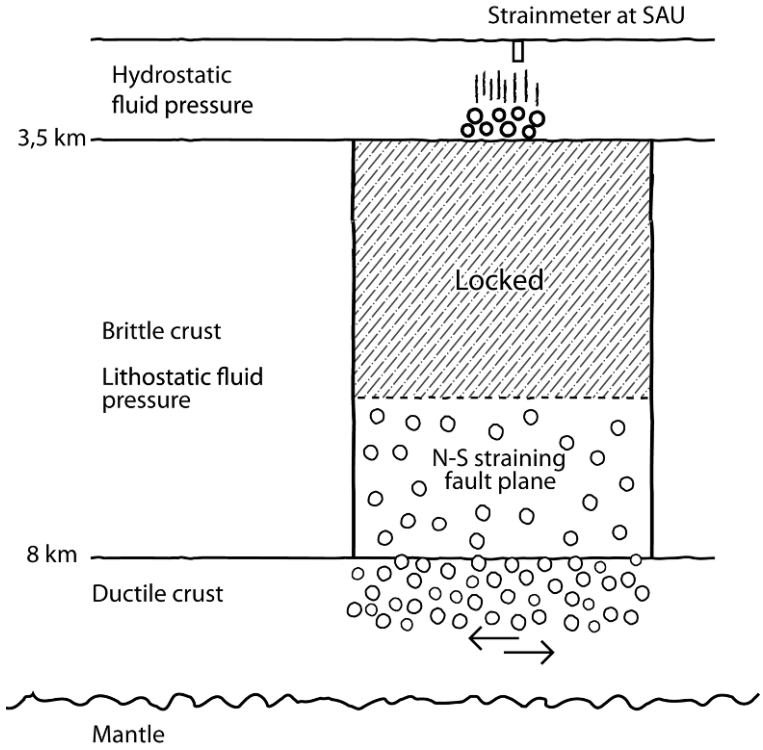

Figure 4.25. A north–south cross-section of the fault of the June 17, 2000 earthquake describing conditions in the fault leading up to it. Circles indicate the high density of fluid pores. Vertical line segments in the uppermost layer indicate the high density of cracks.

brittle crust during this time, so total slip expected at a depth of 5 km in the fortnight leading up to the earthquake was less than this. Note that fault slip at greater depths, especially below the brittle–ductile boundary at a depth of around 10 km, was probably much more, of the order of 2 cm per year (i.e., comparable with plate motion velocity, which would mean a slip of 0.5–0.8 mm across the fault during the 10–15 days). The fact that no pre-earthquake strain signals were picked up by the very sensitive strainmeters indicates that fault slip, which seems to have started 2–3 weeks before the June 17, 2000 earthquake, was infinitesimal (only 0.01 to 0.1 mm or even less) at a depth of around 5 km, so the fault was practically locked at medium depths (i.e., a few kilometers below the hydrostatic/lithostatic pressure boundary). Had there been slow slip at very shallow depths (i.e., near the hydrostatic/lithostatic boundary), it would probably have caused disturbances in the rock–fluid equilibrium in the cracked surface layers and slow quakes or short-term rock–fluid pulses, which would be better detected by the closest strainmeter.

For more about the strain changes in Figure 4.24 see Figure 4.25. They probably reflect processes in the shallowest 2 km to 3 km of the crust. In the long run

hydrostatic fluid pressure always prevails. However, this pressure can increase locally for short periods of time, especially in the deeper parts of this layer where upward fluid migration can be expected. High fluid pressure and strain changes may release a fluid-fracturing and rock slip process. The SAU strain station is on or near the top of a fault that was starting to move at depth, causing shearing in a large area around it, and at the same time upward fluid migration was increasing in the fault. So, the big contraction bump of Figure 4.24 may reflect upward release of fluid (water) from a local water container at a depth between 2 km and 3 km inside the crust (Figure 4.25). This would cause the old fault system to expand at shallower depths toward the surface, which is a possible explanation of the other significant pattern seen in Figure 4.24 (i.e., the general extension in the record resulting in the trace being lowered that persisted right up to the June 17, 2000 earthquake), while micro-earthquakes were reflecting fault slip at great depth just above the brittle–ductile transition (as explained in Section 4.7.3).

4.7.5 The signal detected in the 2-second period before the onset of main slip of the June 17, 2000 earthquake

About 2 seconds before the onset of main slip of the June 17, 2000 earthquake, volumetric strainmeters in the SISZ sensed the start of its breakup as a relatively small signal, but one that was observed at all strainmeter stations in the SISZ. Figure 4.26 (Alan Linde, pers. commun.; Stefánsson *et al.*, 2006a) is a typical example of the records. This signal could also be identified as the first part of the *P*-wave record made at short-period seismic stations. The local magnitude determined from this first seismic *P*-wave and the source radiation pattern (based on spectral amplitudes) was between 5 and 5.5, indicating a fault length of the order of 3 km in this nucleation source. This was in agreement with the assumption of a 3 km diameter asperity at a depth of 6 km at the hypocenter of the earthquake, as also indicated by aftershocks (see Figure 4.2, and Stefansson *et al.*, 2003; Hjaltadóttir and Vogfjörd, 2005). So, the earthquake started as a result of the 3 km diameter asperity breaking up 2 seconds before the onset of slip along the major part of the fault.

4.8 RADON ANOMALIES PRECEDED THE EARTHQUAKES

The earthquakes in June 2000 were preceded by radon anomalies sensed at seven radon-monitoring stations spread throughout the SISZ (see Section 3.8.2). Radon-monitoring and subsequent studies imply, like seismic studies, that there is an observable pre-earthquake process. Radon is released by crustal rocks and dissolved in water. The increase in its concentration in well water can be explained in terms of there being an enlarged surface area for rock and water to interact at

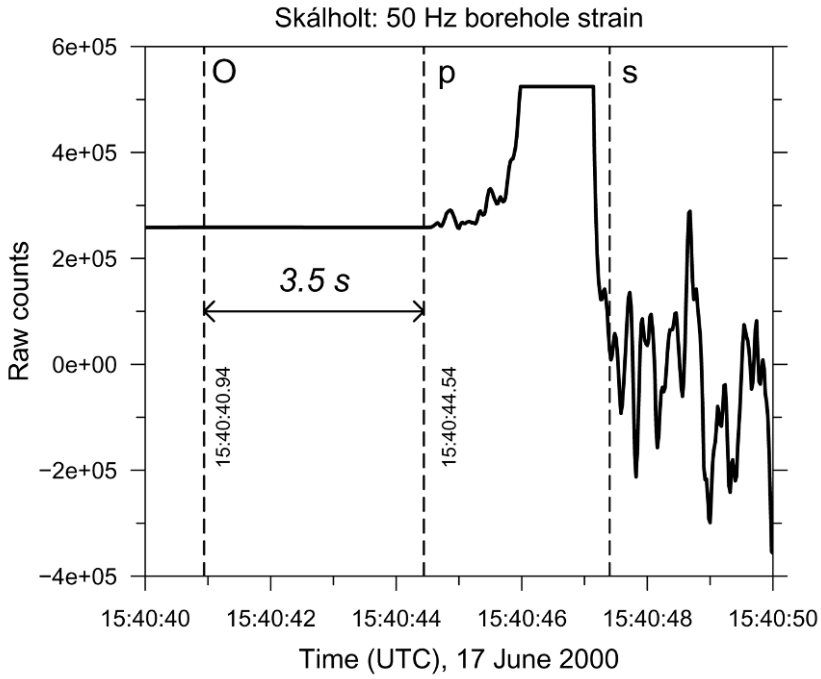

Figure 4.26. A strainmeter record from station SKA, 20 km to the northwest of the June 17, 2000 earthquake. Only the first 2 seconds of the signal are useful because the record was clipped (saturated), as seen at the top. But these 2 seconds are significant. They show a nucleation phase that began 1.8 seconds before the onset of slip along the major part of the fault plane. Afterwards, the record became saturated because of the size of the signal. In the vertical scale 100 counts are equal to 500 nanostrains, and up indicates contraction at the instrument site. The figure also shows the origin time of the earthquake and onset times of *P*-waves and *S*-waves at SKA (modified from Alan Linde, pers. commun., Stefánsson *et al.*, 2006a).

shallow depths in the crust or there being increased fluid flow through pre-existing fractures, both caused by crustal deformation.

The most significant finding from studying radon before the 2000 earthquakes was the high correlation in the time patterns of radon over the entire area between 1999 and 2001 (Einarsson *et al.*, 2008). Stations that are tens of kilometers apart show similar fluctuations in radon concentrations. Considering the short half-life of radon these fluctuations most likely have a common origin in a shallow part of the crust. In the uppermost 2 kilometers of the crust there is an abundance of water-filled cracks, which may widen and create connections with other cracks, thus increasing the flow of water, rock–water interaction, and fluctuations in water flow. Such fluctuations may be very sensitive to regional strain changes, originating deeper down in and near the SISZ, even more so than can be picked up by the most sensitive deformation monitoring. Such strain changes may have a common origin in the SISZ.

The strain change that caused these radon anomalies may be a large-scale strain change that helped to trigger both the eruption of Hekla, which started February 26, 2000, and the two large earthquakes in June 2000.

Observed radon fluctuations can certainly be counted among pre-earthquake processes. At the moment, however, we do not have a causative model to link radon observations to a physically well-based crustal process that leads to earthquakes. However, the probable connection between these fluctuations and strain changes deeper down in the crust certainly makes it useful in Earth observation, just like some of the other observable processes in the uppermost part of the crust that have already been discussed.

4.9 MONITORING STRESSES TO PREDICT EARTHQUAKES

Earthquakes—large or small—generally occur when deviatoric stresses are high at their origin. Stresses that are built up by stable large-scale plate motion can be assumed to be homogeneous or uniform in the long term, especially well away from plate boundaries. Pushes or pulls from outside would disturb this homogeneity, but be quickly relaxed depending on the pliability of the crust. The Earth's crust can withstand a limited amount of stress before it breaks. If we knew this breaking strength and the amount of stress we should be able to predict the time and site of earthquake occurrence. However, we don't know the breaking strength with sufficient accuracy, neither for that matter can we measure stress at the necessary accuracy for that purpose. Information on both these parameters is indirect and based on assumptions that limit their reliability for such a purpose. In order to ascertain these parameters, science adopts a gradual approach by studying interactions between these features and trying to get results that are in agreement with the constantly increasing amounts of observational data available.

However, current knowledge about the general stresses and breaking strength of the crust, which in some applications is assumed to be homogeneous on a large scale, is not enough to predict the site, time, or magnitude of an earthquake.

The crust is not even homogeneous on a small scale. Old earthquake faults exist and there are parts and particles that have a significantly different rheology from the average large-scale rheology. Among these small-scale heterogeneities are fluid-filled pores evenly distributed on a large scale that may become interconnected because of strain buildup and disturb large-scale homogeneity, now that fluids can move around.

It is these rheological heterogeneities, which may even be time-dependent, that stop us from estimating the general stress field with the necessary accuracy. Nevertheless, methods to estimate the stress field (especially seismic methods) do take account of such anomalies and try to correct for them. However, when trying to predict the site, time, and magnitude of earthquakes, scientists can make use of the anomalies instead. In fact, such anomalies based on their estimated effect on stress may form the basis for earthquake prediction.

Stresses in the crust that are significant for earthquake prediction can best be estimated on the basis of

- measured deformation on the surface of the crust by making use of our knowledge of rheological properties in the crust and the upper mantle;
- using information from micro-earthquakes with sources at the same depths as expected large earthquakes, either based on source mechanisms or ray path effects;
- the history of earthquake release.

There now follows a brief description of the methods used to estimate stress which have been applied in SISZ earthquake prediction research projects, based on history and the information carried by micro-earthquakes.

4.9.1 Stress estimations based on historical seismicity

Earthquakes cause anomalies in the stress field on both the large scale and the small scale, in space and time. One way of studying the stress field is to look for changes during a sequence of earthquakes that rupture the full length of existing faults. Modeling these stress changes and including our present knowledge of crustal structure and average crustal plate velocity in the model results in a stress field that could serve as a basis for predicting events after the sequence. By studying the buildup and release of many events interactively, we hope to be able to ascertain the absolute stress level at which earthquakes are released.

A study to reveal the stress field around the SISZ was carried out by seismologist Frank Roth (see Appendix 2.B) and co-workers (see Richwalski and Roth, 2008). They used a layered elastic/viscoelastic half-space model to obtain shear and Coulomb stress changes due to events with magnitudes $M \geq 6$ since 1706. Figure 4.27 shows an estimation made of the stress field immediately before the 2000 earthquakes.

After studying the maximum shear stress levels reached during the whole series of historical earthquakes, the authors concluded that immediately before a new event the estimated maximum stress was only reached in 50% of the cases (i.e., many earthquakes still occurred before breaking strength was reached).

The most likely explanation of this is that many historical earthquakes were triggered by local inhomogeneities before the stress reached the level necessary had the crust been homogeneous. A likely candidate is upward migration of high-pressure fluids into the seismogenic part of the crust at these locations.

4.9.2 Stress estimations based on micro-earthquake fault plane solutions

Micro-earthquakes almost continuously carry messages from great depth in the crust packed full of significant information about conditions and changes in conditions that prevail at these depths.

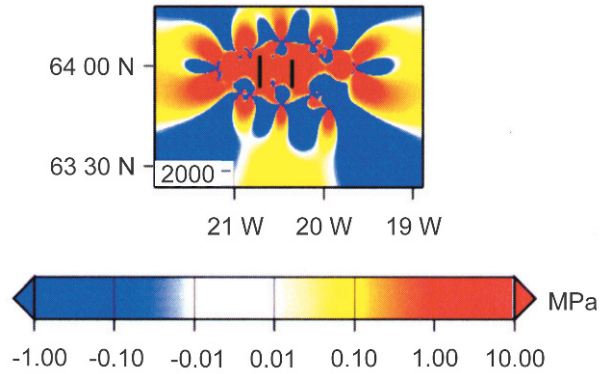

Figure 4.27. Horizontal shear stress near the SISZ just before the 2000 earthquakes estimated from historical seismicity in the area since 1700 using an Earth-realistic viscoelastic layered model. The two black line segments show the faults of the two earthquakes (modified from Richwalski and Roth, 2008).

There are various ways of using information from micro-earthquakes to estimate stress at depth in the crust. This has been done extensively in earthquake prediction research projects in Iceland. The high density in time and space of micro-earthquake sources makes them particularly useful at detecting small-scale anomalies and their changes over time, especially those that show up in stress release in small earthquakes. As said before, small-scale heterogeneities may lower the breaking strength across a fault under strain by plate motion and cause nucleation of a large earthquake long before the time expected in a hypothetically homogeneous crust. This is significant for earthquake prediction both in the long and short term.

Extensive studies have been carried out into stress fields in the SISZ based on the fault plane solutions of many micro-earthquakes. In such inversions, stress homogeneity must be assumed in the volume under investigation. This is done by selecting volumes for observation inside the zone where stress homogeneity is fulfilled, and where we have a sufficient number of widely distributed micro-earthquakes within the selected volume to constrain a good solution. The main conclusion is that the SISZ and its environment is dominated by horizontal strike slip with compression trending N45°E and tension N135°E (Angelier *et al.*, 2008). Basically such solutions express only the directions of the different components of the stress tensor—not the absolute stress. They are significant but they do not tell us much about how close we are to the breaking strength of the rock. However, in Section 4.7.2 we saw how changes in directions of fault planes showed up shortly before the June 17, 2000 earthquake (i.e., change in the direction of horizontal compression released by micro-earthquakes leading up to the 2000 earthquakes).

The best method of finding the rock stress tensor for a region is to make stress inversions from the fault plane solutions of many earthquakes in a region where homogeneity of the stress field can be assured. This involves a thorough study of misfits or, as they are sometimes called, "variances" from stress homogeneity.

Moreover, such variances in time and space from general stress may give valuable information for earthquake prediction.

In an effort to study such heterogeneities in time and space, variances can be estimated for each earthquake mechanism from the direction theoretically expected (see Gephart and Forsyth, 1984).

Lund *et al.* (2005) studied pre-earthquake variances in the stress field between 1991 and 2000 in the area where the June 17, 2000 earthquake occurred. An anomalous stress field was indicated in the 1996–2000 period below a depth of 7.5 km. For the period as a whole mechanisms of strike slip type are most frequent in this area (Figure 4.28). However, during 1996–2000 the character of faulting in deep earthquakes (below a depth of 7.5 km) became much more like the normal faulting type than earlier (i.e., in the 1991–1995 period). Above a depth of 7.5 km strike slip faulting predominated throughout this time and did not change significantly between the two periods. It was suggested that these features were caused by dyke injection at depth (i.e., injection of an incompressible mass). It would lead to normal faulting prevailing at depth, as expressed by seismic data. The faulting anomaly below a depth of 7.5 km at this site was present in the 4 years leading up to the earthquake, but not after it (Lund *et al.*, 2005; Lund, pers. commun.; Stefánsson, 2006). If there was a dyke injection below this depth we can imagine that the dyke itself would send fluids up into the main seismogenic part of the crust and thus, in effect, increase the surface of ductile material emitting compressible fluids to the upper parts of the brittle crust. Observations supported this. Micro-earthquakes increased in number after this time right up to the large June 17, 2000 earthquake (Figure 4.10), but above this depth they continued to be strike slip in type and thus expressed upward migration of compressible fluids only, in agreement with the emerging F-S model.

Bellou (2006) studied variances in the stress field from micro-earthquake fault plane solutions for the SISZ area as a whole at depth and in the shallows. Lower variances were found inside the zone before the large 2000 earthquakes than after, indicating that the zone returned to higher levels of frictional strength after the 2000 earthquake crisis. This can be explained by the release of fluid pressures in the SISZ crust during release of the large earthquakes. Release of pore fluid pressure increased friction across faults in the zone and thus made slip across them more difficult. Therefore, higher stress was needed to release small earthquakes and this made release along new faults at an angle to the main fault direction more probable.

The work by Bellou and Lund and their co-workers contains more significant results than space allows here and interested readers are, in addition to the papers referred to above, recommended to study Stefánsson (2006) which is available on the Internet and Angelier *et al.* (2008).

4.9.3 Prediction based on estimation of local stress and instability

Seismologist Ragnar Slunga (see Appendix 2.B) (Slunga, 2003, 2007) studied in hindsight the stress and fracturing conditions in the SISZ between 1991 and 2000 using the available fault plane solutions of micro-earthquakes. The fault plane

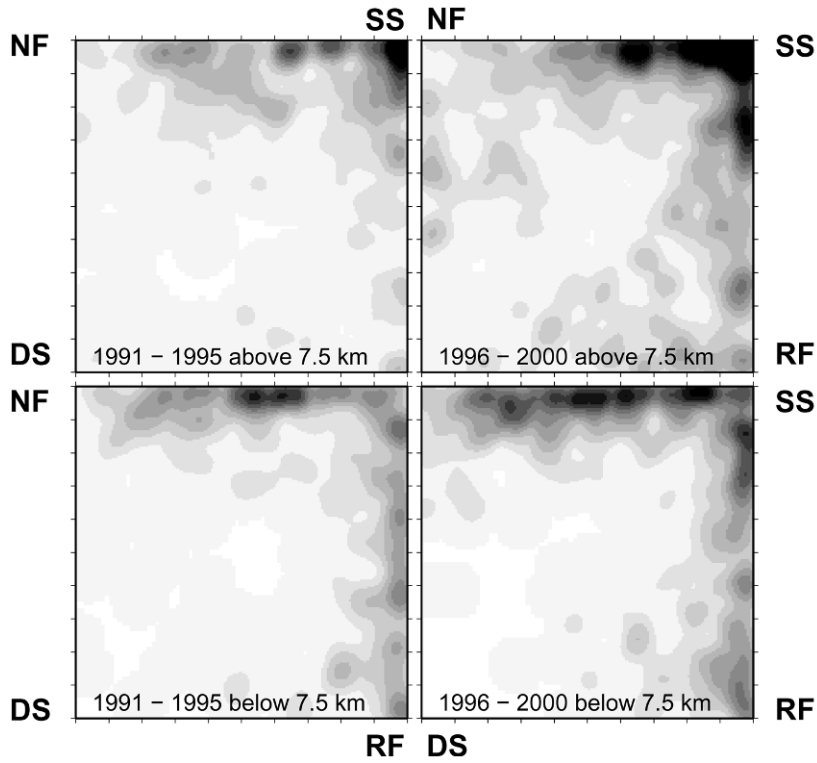

Figure 4.28. Fault plane diagrams based on the micro-earthquake fault plane solutions of earthquakes in the focal area of the June 17, 2000 earthquake from 1991 until just before the earthquake. The type of each earthquake is shown by its position in the diagrams (method proposed in Slunga, 1991; see also Appendix 2.A.2). The horizontal axes denote horizontal relative compression and the vertical axes show horizontal relative tension. The corners show the pure cases: the upper-right corner denotes pure strike slip, the upper-left normal dip slip, the lower-right reverse dip slip, and the lower-left vertical dip slip. The darkness of points inside the boxes expresses the frequency of relative sizes there (by so-called "kambcontours"). Any fault plane solution can be classified according to its position within the square. The two upper diagrams show the situation above a depth of 7.5 km in the 1991–1995 period to the left and the 1996–2000 period to the right. The two lower diagrams show the situation below a depth of 7.5 km in the 1991–1995 period to the left and in the 1996–2000 period to the right (based on Lund *et al*., 2005 and Lund, pers. commun.).

solutions of earthquakes provide the direction of stresses released by the earthquake, but not their absolute values. By assuming that vertical stress equals lithostatic pressure, which is plausible under the horizontal shearing conditions prevailing in the SISZ, he calculated the complete stress tensor that was released at the time and at the hypocenter of individual earthquakes. The fault plane solutions for individual earthquakes give two possibilities for nodal planes that are perpendicular to each other (see Chapter 2 and Appendix 2.A). One is the real fault plane for the

earthquake. The distribution of small earthquakes following the studied earthquake reveals which of the nodal planes is the fault plane as aftershocks tend to occur along the real fault plane. Then the plausible assumption is made that the CFS (Coulomb Failure Stress) at the fault plane of individual micro-earthquakes is zero at the time they are released. By means of such assumptions, the complete stress tensor (i.e., the six components) is estimated for the release of individual micro-earthquakes. Note that this is not the rock stress tensor characterizing the region near the fault—it is just the stress energy emitted during the release of individual micro-earthquakes.

Based on such results from the many micro-earthquakes in a given volume it is possible to estimate pore fluid pressure. Deviations of fault planes of individual micro-earthquakes from the main fault directions of linear earthquake swarms is a measure of pore pressure. Knowing pore fluid pressure in the volume in question means that the degree of instability of the impending earthquake fault can be estimated (i.e., the CFS for such a fault; Slunga, 2007; Figure 4.29).

In short, from the fault plane solutions and fault plane directions of many small earthquakes in a small volume it is possible to estimate the stress near an impending earthquake and the CFS along the assumed fault direction.

Figure 4.29 shows calculation results of absolute stresses carried out in this way for the 9-year period leading up to the 2000 earthquakes. The upper part of the figure shows the median values of stresses of individual micro-earthquakes in 2×2 km horizontal units in the SISZ for the entire 1991–2000 period. It indicates relatively high stresses (around 5 MPa) near the asperity of the June 17, 2000 earthquake, and much lower stresses near that of the second earthquake on June 21, 2000. The lower part of the figure shows the CFS calculated by Earth-realistic assumptions of friction and fracture shear strength. Low values of CFS (around -6) are shown by small circles indicating stability, while high negative values (i.e., close to zero) are shown by large circles indicating closeness to instability on north–south aligned faults, the assumed fault direction in the area. The closeness to instability indicated on the fault of the second earthquake explains the relatively high seismicity between 1991 and 2000 and why it did not build up stress. The same is indicated in the discussion of seismic rate (see Figure 4.10). Stress did not exceed a certain level, instead the continuous strain that had built up there as a result of plate motion was immediately released by small earthquakes. Moreover, this instability partly explains why it was so easily triggered by the first earthquake.

According to GPS modeling by Árnadóttir *et al.* (2003) the June 17, 2000 earthquake increased the CFS at and south of the hypocenter of the June 21, 2000 earthquake by 0.1 MPa at a depth of 5 km, bringing it closer to instability. The closest value to instability according to Slunga's results on north–south faults at the site of the June 21, 2000 earthquake was CFS -0.7 (Figure 4.29). The contribution from the June 17, 2000 earthquake would have lowered it to -0.6 (i.e., closer to instability which is 0, but not all the way). However, we must be mindful that Slunga's CFS values are average values calculated during the 10-year period. It may have been closer to 0 at the time of the initial large earthquake. Estimations by Slunga of the CFS at the fault of the June 21, 2000 earthquake shortly before the

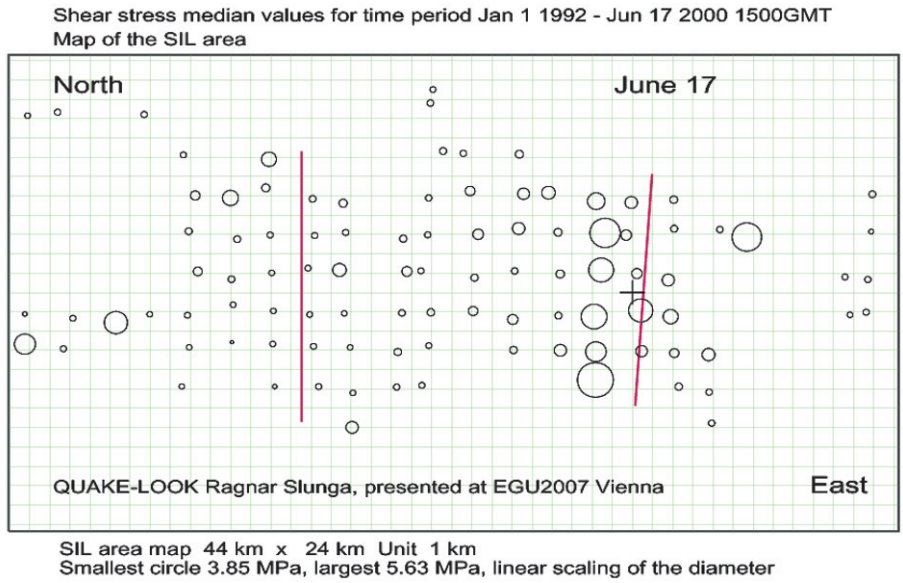

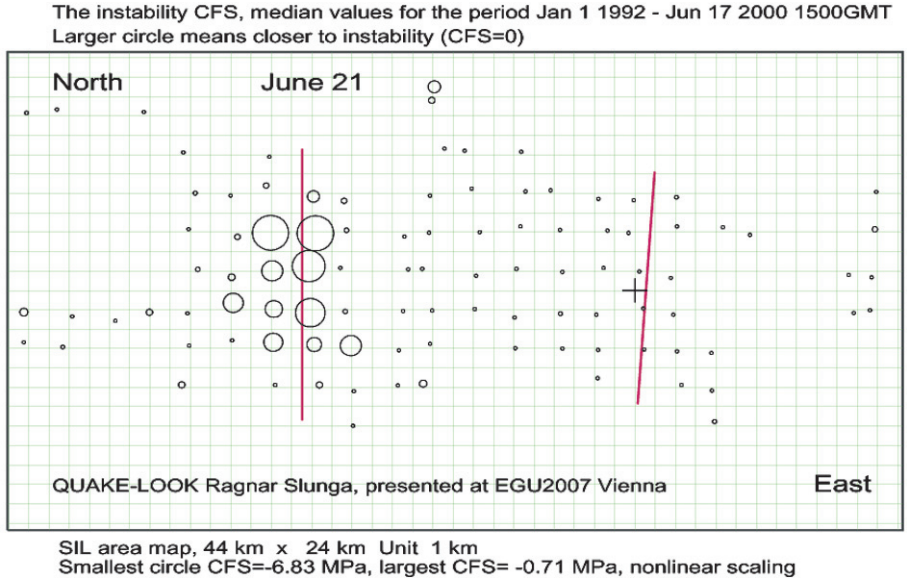

Figure 4.29. Circles in the upper panel indicate median values of stresses at the release of micro-earthquakes with epicenters in 2×2 km areas. The maximum value is 5.6 MPa and the minimum is 3.8 MPa. Circles in the lower panel show CFS as negative values. The largest circle indicates a value of -0.7 MPa (i.e., very close to instability which is 0). The other points indicate more negative values (i.e., more stability). North–south lines indicate the fault planes of the two earthquakes (from a poster by seismologist Ragnar Slunga presented at *EGU 2007*, see abstract in Slunga, 2007).

earthquake do in fact indicate CFS values much closer to instability. However, this is based on very few earthquake data and thus is not as well-based as the long-term average, nevertheless the indication is there and the earthquake really was triggered.

The delay of 3.4 days in triggering the second earthquake cannot be explained by the time it took for stress change from the first earthquake to reach the second only 17 km away. Dynamic triggering (i.e., triggering by seismic waves from the first earthquake) would only take a few seconds. Microseismic activity started to be well recorded at the fault of the second earthquake 2 hours after the June 17, 2000 earthquake. A triggered process may have started only a few seconds later, but this might be hidden on seismograms because of the enormous amplitudes recorded from the initial earthquake. A slow slip process may also have started at depth in the June 21, 2000 earthquake, well before the first micro-earthquakes occurred. Anyway, it is possible that the June 17 earthquake triggered local processes almost immediately below the brittle crust and in the fault of the second large earthquake, which in turn took 3.4 days to trigger the large earthquake there.

All of this is mostly based on micro-earthquake observations in the 9 years leading up to the 2000 earthquakes (median stress values). Slunga also calculated the CFS along the north–south faults of the two earthquakes for a few months before they occurred, but this was based on information from far fewer earthquakes and thus was not so well-constrained. However, these evaluations indicate that instability increased significantly, especially on the June 17, 2000 fault, in the 2–3 months preceding the earthquake. During this period the fault became the most unstable in the SISZ. Figure 4.29, which relates to the 9-year period before the earthquakes, shows that the highest stresses were observed 2 km to the west of the June 17, 2000 fault and that a relatively low CFS was observed there on average for the whole period. So, according to Slunga's estimations of the CFS shortly before the earthquake, significant changes in conditions occurred at the fault, in agreement with the plausible start of fault slip at depth during this period (as described in Section 4.7).

The question that arises from all this is whether changes that are based on a few data, as was the case in short-term estimations of the CFS from micro-earthquakes, are reliable. Such a question is perfectly reasonable. However, in practical efforts to issue warnings of earthquakes such indications must be used even though they are not as well constrained as we would wish. All information about processes in the crust are based on assumptions that are as Earth-realistic as our data allow them to be. No single method will give us totally inclusive information on every process. As will be discussed further in Chapter 7, practical warnings of earthquakes will be based on merging many methods and models to give warnings that satisfy a given degree of accuracy. In such an approach we do not have the time to wait until a method is developed whose results are beyond reproach. In practice, there will likely be a series of methods whose results will be combined to issue a warning to alert the scientific community and government bodies of an impending earthquake. In such a warning procedure Slunga's method for stress estimation will play a very significant role, from information indicating the site, fault length, and magnitude of the impending earthquake to short-term instability that is related to short-term nucleation

of the earthquake. The problem of scarcity of data during the short-term nucleation phase is common to all attempts at short-term prediction and can only be resolved by increasing the sensitivity of observations. In a practical warning service this would mean increasing observation sensitivity at the location likely to be the site of the next large earthquake. Another approach would be to apply all indications and give a warning as a percentage probability. This will be further discussed in Chapter 7 on warnings.

4.9.4 Stress changes preceding earthquakes as monitored by shear wave splitting

The shear wave splitting (SWS) method for monitoring stress changes is based on the splitting of shear waves (*S*-waves) into marginally faster or slower components when the wave passes through an anisotropic medium. The time difference between the fast component and the slow component depends on the stress applied to the medium, and this feature can be used to find stress changes.

As demonstrated in Figure 4.30 shear waves oscillate perpendicular to the direction of ray propagation. In an anisotropic medium such as rock with stress-aligned fluid-saturated micro-cracks, which is common in the crust, shear waves (*S*) split into two orthogonally polarized waves that propagate at slightly different velocities (Figure 4.30).

In contrast, *P*-waves are longitudinal waves that oscillate in the direction of ray propagation and are faster than *S*-waves. They travel faster through bodies with micro-cracks that are parallel to the ray than when the cracks are perpendicular to the ray. But, in uniform anisotropic media *P*-waves do not split into different phases and thus are not as useful for monitoring stress changes as *S*-waves.

Shear waves polarized in directions parallel to the face of micro-cracks are generally faster than those polarized perpendicular to the crack face. Figure 4.30 shows a shear wave propagating through a rock that has fluid-saturated stress-aligned pores, which is what is expected at depth in the crust. *S*-waves making their way to the surface from local earthquakes can be used to study anisotropy based on their splitting if they can reach the measuring station on the surface as an undisturbed direct wave. They must have an incidence angle to the surface that is steeper than 45°, which means that only earthquakes deeper than the epicentral distance from recording seismic stations can be used for such studies. This circle of incidence is known as the "shear wave window". For more about the method see Crampin and Lovell (1991), Crampin (1994), and Crampin and Chastin (2003).

Studies of the polarization angles of many earthquakes indicate that the direction of faster shear waves in the SISZ is around N45°E (Crampin *et al.*, 1999). Angelier *et al.* (2008) inferred this to be parallel to the largest horizontal compressional stress in the SISZ based on the fault plane solutions of micro-earthquakes. This was not only a beautiful fit, it also constrained high pore fluid pressures at medium depths in the crust. This immediately indicated that external stresses applied to such a medium could be monitored by observing how they change the aspect ratio of the pores. Directional force makes pores fatter or thinner, which

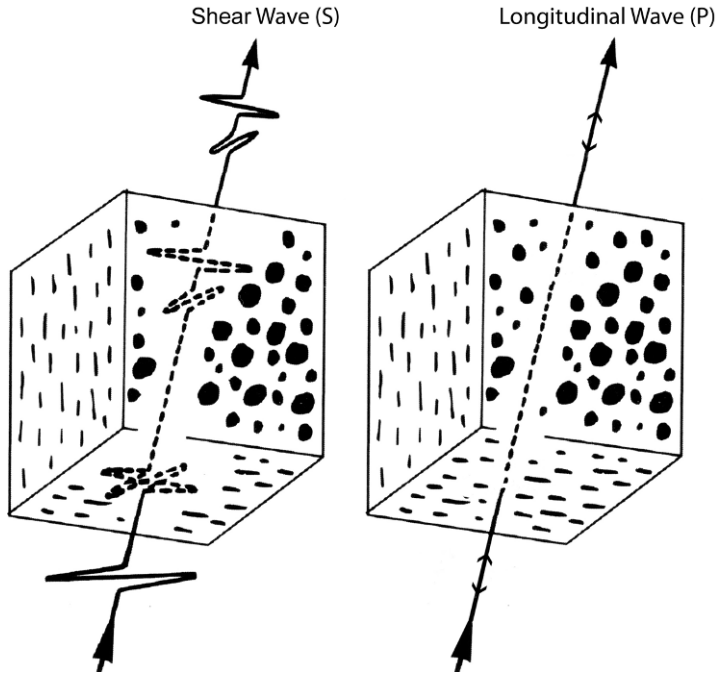

Figure 4.30. (*Left*) A seismic shear wave comes from below and through a cube that has many fluid-filled cracks. Wave motion is perpendicular to the ray path. It splits into a faster and a slower component because the velocity in different directions in the cube varies. Stress applied from outside deforms the cracks, makes them fatter or thinner, and thus changes the time difference between the two components. (*Right*) A longitudinal wave, a *P*-wave, goes through the cube. Its wave motion is along the ray path, as indicated by small back and forth arrows, and thus it does not split up. Therefore, a *P*-wave is not as useful as a shear wave at sensing stress-induced velocity changes in its wave path.

changes the time difference between faster and slower *S*-waves traveling through the medium.

In the SISZ the method has been applied to *S*-waves above swarms of small earthquakes. Based on modeling results (Zatsepin and Crampin, 1997), a long-term buildup of stress is proportional to the increase in time difference between the faster and slower split shear waves, making it possible to monitor stress accumulation in the medium above earthquakes. Observations also indicate stress relaxation shortly before impending earthquakes, which is interpreted by Crampin and co-workers as micro-cracks coalescing onto the eventual fault plane shortly before the release of a large earthquake (Crampin and Chastin, 2003; Crampin *et al.*, 1999; Gao and Crampin, 2004; Volti and Crampin, 2003).

Stuart Crampin (see Appendix 2.B) and colleagues started monitoring SWS above several SIL stations in Iceland at the beginning of 1996. At a meeting of the PRENLAB group in late August in 1996, Crampin reported a gradual increase in SWS time at stations at different places around the country. He suggested that this

might indicate that a large earthquake was imminent. A month later, at the end of September, a massive fissure eruption started in the Gjálp volcano beneath the Vatnajökul ice cap in the center of the Iceland Mantle Plume (Figure 3.2). A possible explanation of the increased SWS time, expressing stress changes, is that it was caused by upwelling of magma from below into the crust in preparation for the large eruption. A thorough description of the observations, interpretation of their meaning, and reporting of additional SWS results in Iceland can be found in the paper by Volti and Crampin (2003).

Figure 4.31 shows how stress change was monitored by SWS time at two seismic stations in the SISZ before the 2000 earthquakes. Rays having an incidence angle of 15°–45° (Band 1) are according to modeling results expected to be sensitive to stress changes (Zatsepin and Crampin, 1997). A gradual stress increase can be observed for several months and stress relaxations for days to weeks before the earthquake (as expected from modeling). Figure 4.31 shows that rays having an incidence angle of 0°–15° (Band 2) are sensitive to crack density, but consistent changes in Band 2 that can be related to earthquake preparation have not yet been constrained.

The 2000 earthquakes were stress-forecast by Wu *et al.* (2005) in hindsight on the basis of Figure 4.31.

Shear wave splitting was applied together with other information to successfully stress-forecast a magnitude-5 earthquake in southwest Iceland in 1998 (Crampin *et al.* 1999; see also Section 7.3.1 about warnings).

A very interesting result was obtained when shear wave polarizations around a large transform fault along the coast of North Iceland in the Tjörnes Fracture Zone (Figure 3.2) were studied. Close to the fault, polarization angles had flipped 90° compared with the general stress direction in North Iceland (Crampin *et al.*, 2002). This was interpreted to be the result of high pore fluid pressure in this seismically active fault zone.

4.10 EARTHQUAKE TRIGGERING BY ANOTHER OBSERVABLE CRUSTAL EVENT

In efforts to predict earthquakes it is important to keep in mind that they may be triggered by other earthquakes and possibly by volcanic eruptions. Knowledge of seismic history and pre-earthquake microseismic patterns made it possible to issue a short-term warning before the second large 2000 earthquake (as discussed earlier).

Figure 4.31. In the middle (Band 1) and upper (Band 2) panels, dots with error bars show observed values of SWS time delays (normalized to milliseconds per kilometer by distance in kilometers traveled) for shear waves from small earthquakes in the shear wave window below seismic stations in the 8 months leading up to the 2000 earthquakes at (a) Station SAU and (b) Station BJA (both in the SISZ). Wiggly lines are nine-point moving averages which are not used in the analysis but indicate the overall trend of the data. Straight lines are least squares fits to the

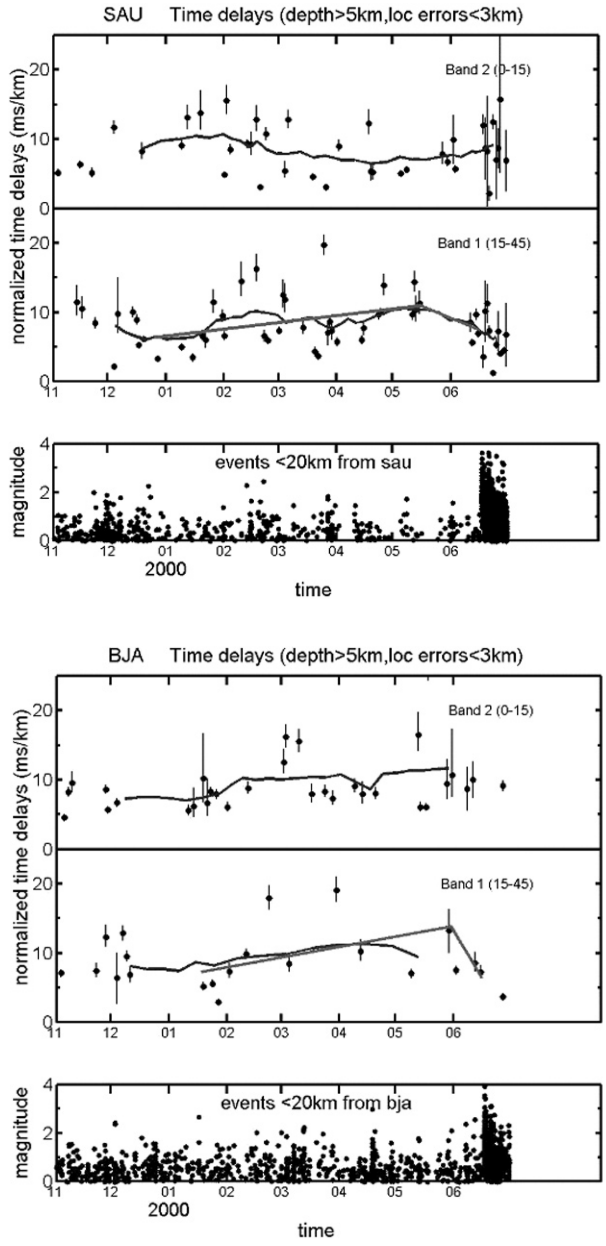

time delays in Band 1 showing the time trend of SWS time delays interpreted as stress accumulation. Station SAU (a) is within a few kilometers of the epicenter of the initial 2000 earthquake and (b) BJA is within 50 km. The bottom panels are the magnitudes of small earthquakes within 20 km of each station. Increased seismic activity marks the onset of the June 17, 2000 earthquake. A couple of weeks before the large earthquake ocurred, the Band 1 trace in both panels indicated stress relaxation (called by the author, crack coalescence).

4.10.1 Static and dynamic triggering

As described in Section 4.4.3, the process leading to the earthquake on June 21, 2000 started soon after the June 17, 2000 earthquake. Monitoring this process by means of micro-earthquake information and earlier models of the tectonics at the site made it possible to issue a useful warning before the second large earthquake. Triggering can be static or dynamic (i.e., either caused by static strain changes or dynamically by strong seismic waves from a first earthquake). In both cases the first earthquake may trigger a process near the source of the second earthquake which is then triggered after some delay.

Hindsight reveals that the change in static Coulomb Failure Stress (CFS) caused by the June 17, 2000 earthquake in the area of the June 21, 2000 earthquake could have been the trigger (Árnadóttir *et al.*, 2003). The triggering effect of an earthquake on another fault can be expressed as ΔCFS. In other words, the stress change as a consequence of a first earthquake may cause failure along part of the assumed fault plane of a second earthquake as long as this ΔCFS exceeds a given threshold value in that part. The June 17, 2000 earthquake caused a ΔCFS of about 0.1 MPa at a depth of 5 km along part of the fault of the June 21, 2000 earthquake (Figure 4.32). Experience tells us (see Toda *et al.*, 1998) this would be enough to cause failure and left-lateral slip on faults directed north–south (Árnadóttir *et al.*, 2003). However, triggering of the June 21, 2000 earthquake was not immediate. It took 3–4 days and happened 17 km west of the first one. This was far too slow for direct static triggering along the SISZ crust in light of its known viscosity. A possibility is that high pore fluid pressures near the brittle–ductile boundary may act as a low-viscosity layer by carrying stress changes at depth in a kind of pore-elastic process, which may be this slow. Jónson *et al.* (2003) stated in their study of water level changes, deformation, and aftershock decay in the SISZ following the 2000 earthquakes that they could not rule out long-term pore pressure transients at the depth of most aftershocks (i.e., near the brittle–ductile boundary). Another more likely possibility is that the first earthquake immediately triggered a dynamic slip process at the fault of the second earthquake below the brittle–ductile boundary, although this process did not show up in micro-earthquakes (i.e., with origins at shallower depth) until 2 hours later. It is most likely that the first earthquake triggered a strain release process in and near the fault of the second earthquake, possibly involving upward fluid migration and homogenizing the stress around the fault. Small earthquakes gradually covered a large part of the fault. This gradually caused instability in the fault as a whole. So, it seems a crustal process at the fault of the second earthquake which lasted for 81 hours after the first earthquake was the trigger (see Section 4.4.3 about prediction of the second earthquake).

Large earthquakes can also be directly triggered when conditions at faults are already unstable. Stress transfer (described in Section 4.3) is able to trigger earthquakes up to magnitude 5.5 from distances 85 km away. It takes less than a minute for stress from the triggering earthquake to be transferred to the triggered earthquake. The origin time of triggered events correlates well with the arrival of seismic

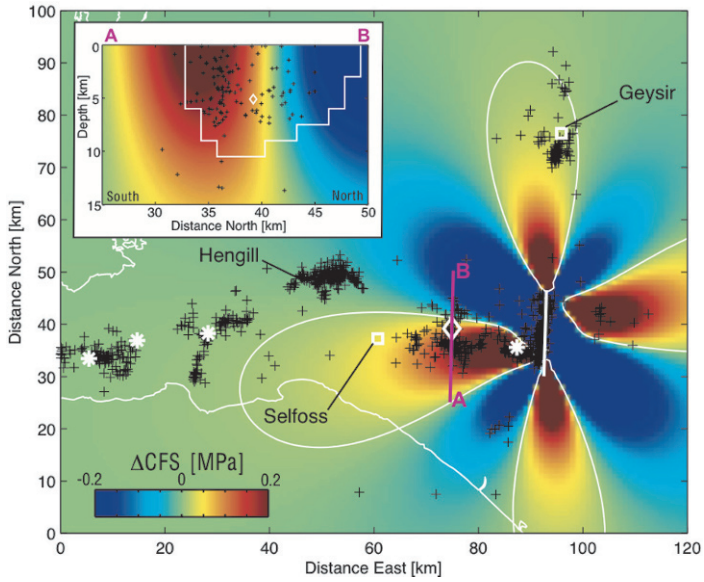

Figure 4.32. Static co-seismic CFS changes (ΔCFS in MPa) due to the June 17, 2000 fault slip, calculated at a depth of 5 km for vertical north–south faults with right-lateral strike slip motion. The contours surround areas where the CFS increased by more than 0.01 MPa (0.1 bar). The white diamond shows the location of the June 21, 2000 earthquake and white stars mark the largest aftershock on June 17, 2000. Note the three earthquakes triggered on Reykjanes Peninsula (see Section 4.3). Smaller aftershocks (location errors <2.5 km and <5 km vertically) with magnitudes greater than 1 between June 17, 2000 and June 21, 2000 are shown by black crosses. The location of the June 17, 2000 fault is shown by a white line. The white squares mark the Geysir geothermal area and the town of Selfoss. (*Inset*) The ΔCFS in a north–south cross-section along profile A–B is shown and the extent of the June 21, 2000 fault is indicated within the white-framed area. Aftershocks occurring between the dates of the two earthquakes, located within 2.5 km east and west of the profile, are shown with black crosses (from Árnadóttir *et al.*, 2003).

shear waves at a fault that is already very unstable. This is called "direct dynamic triggering".

4.10.2 Triggering by volcanic activity at Hekla and Hengill

Three and a half months before the 2000 earthquakes there was an eruption of Hekla, a volcano at the eastern end of the SISZ (Figure 4.1). Hekla has erupted on average once every 10 years since 1970, which is unusually frequent.

Between 1993 and 1998 there was tectonic activity involving intensive seismicity, land elevation, and intrusions in the Hengill volcanic complex at the western end of the SISZ (Figures 4.1 and 4.9). Closeness in time and space indicates that there was a connection between this volcano-tectonic activity and the release of the 2000 earthquakes in the SISZ. Based on mechanical modeling, involving rheological contrasts

between seismic and volcanic areas, Gudmundsson and Brenner (2003) suggested that volcanic unrest near the two ends of the SISZ was a precursors to the large earthquakes. Understanding how such events influence other areas should be priorities for research and modeling and should be added to the tools that are available for prediction.

A statistical study of large historical earthquakes and volcanic eruptions in Iceland reveals a weak but significant relationship between eruptions and earthquakes, with the eruptions leading (Gudmundsson and Sæmundsson, 1980). On basis of the data, the authors explain this relationship by a common source, i.e. plate motion affecting both, rather than eruptions leading to earthquakes.

However, the triggering potential of eruptions and other large events is not only based on the deformation or pore fluid pressure changes exerted by the event, but also on tectonic conditions in the seismic zone that are variable in time. Scientists at the IMO observed a clear difference between the micro-earthquake activity in the SISZ following the 1991 eruption of Hekla than that of the 2000 eruption, even though the eruptions were similar.

4.10.3 More about triggering by large events

Figure 4.33 shows the westward migration of seismic activity along the SISZ after large events, either eruptions of Hekla or large earthquakes in the eastern part of the zone. All triggering events in the figure are set at time 0 (see the starting event in the upper right corner).

A series of small earthquakes were triggered all along the SISZ by the Hekla eruption in 1991. However, the eruption in February 2000 did not cause any immediate increase in seismicity along the zone until the large earthquake occurred on June 17, 2000 (Figure 4.33). The difference between these two triggered processes can be explained as follows. The Hekla eruptions of 1991 and 2000 caused the crust to expand throughout most of the SISZ (i.e., at distances more than 10 km from the volcano). This was directly observed by volumetric borehole strainmeters in the area. The strainmeter station closest to the origin of the first large earthquake reported an expansion of 10^{-7} there in the 1991 eruption (Linde *et al.*, 1993). This was repeated in the February 2000 eruption. This expansion lowered friction on faults in the zone by reducing normal stress on them, thus triggering the release of small local earthquakes at sites where conditions were already near fracture criticality as a result of strain and local pore fluid pressures being high. This happened a matter of days after the 1991 Hekla eruption (Figure 4.33). After this eruption static expansive strain changes spread westward along the SISZ and encountered little resistance. After the February 2000 eruption of Hekla, the locked hard core (i.e., an asperity) of the June 17, 2000 earthquake created a hindrance (i.e., a stress shadow) to its west. When that asperity broke up and the first 2000 earthquake occurred, strain was easily carried westward and triggered small and large earthquakes, especially at sites where pore pressures had built up, not least because of the crustal opening caused by the Hekla eruption some months earlier.

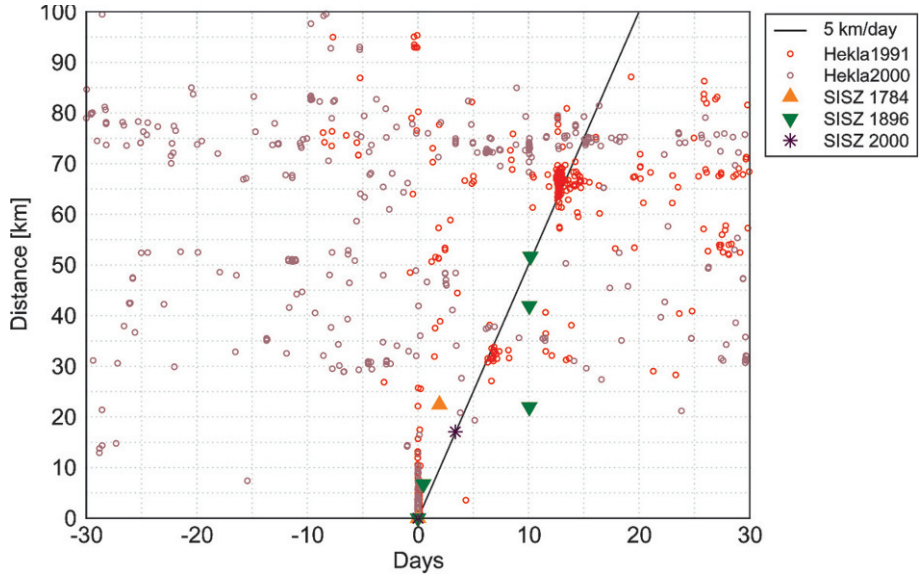

Figure 4.33. Westward seismic migration with time along the SISZ following large events in the central or eastern part of the zone. The small earthquakes that preceded and followed the Hekla eruptions of 1991 and 2000 migrated to the west along the SISZ. The figure shows 30 days before and after the eruptions. Three earthquakes in the SISZ have been put in at time 0. Distances from the original events are shown in a westerly direction (vertical scale). Both Hekla eruptions and the initial large earthquakes were followed by small or large earthquakes to the west or northwest along the SISZ.

4.10.4 The question concerning the 5 km/day migration velocity of seismic events throughout the zone

As mentioned earlier, there are some indications based on a few examples from seismic history and from recent observations that large seismic events in the SISZ migrate at a velocity of the order of 5 km/day from a triggering source in the eastern part of the zone (see Section 4.4.3). The time between the two June 2000 epicenters does in fact correspond with this migration rate. Figure 4.33 shows earthquakes following triggering events set at time 0. On the one hand, we see large earthquake sequences following a principal earthquake set at day 0. On the other hand, we see microseismicity throughout the SISZ following two recent eruptions of Hekla. The 5 km/day migration velocity is not well constrained. As indicated by Figure 4.33, the most likely explanation is that we are witnessing dynamic triggering of micro-earthquakes expressing processes that locally may lead to larger earthquakes after some time delay. Another explanation would be that, on the one hand, we have dynamic triggering (i.e., immediate triggering by large amplitudes of seismic waves) and, on the other hand, triggering by strain changes that traveled at a much slower velocity across the area after the large earthquakes, a so-called "strain wave" (Stefánsson *et al.*, 1993). However, a strain wave with a velocity of this order

would demand much lower viscosity than is the case below the SISZ. The question is whether strain steps can migrate at such velocities along the zone as a result of the interaction between rock and meteoric fluid in the fractured zone. Jónsson *et al.* (2003) concluded that deformation measured by InSAR and water level changes after the 2000 earthquakes in the zone "is consistent with rebound of porous elastic material in the first 1–2 months following the earthquakes." However, seismic activity continues for years at deeper sections of the fault and, with that in mind, Jónsson *et al.* (2003) concluded that they "cannot rule out a longer pore-pressure transient at the depth of the aftershocks." Such transients as a result of meteoric water in shallower parts or as a result of possible upward fluid migration into the crust in deeper parts may lead to pore pressure diffusion, which may migrate at the velocity suggested above and possibly trigger earthquakes.

Although the apparent 5 km/day migration velocity of seismic events in the SISZ is not well constrained by observations or by theoretical modeling, it is of value for observational procedures in earthquake prediction and when merged with other information.

4.10.5 Triggering at large distances by means of magma injection

It has been suggested that upwelling of magma in the buildup to the large Vatnajökull eruption of 1996 (the Gjálp eruption) triggered a seismic swarm and possible upward fluid migration into the seismogenic crust below the epicenter of the June 17, 2000 earthquake 150 km away.

As discussed in Sections 4.6.2 and 4.9.4 the seismic swarm during May to October 1996 at the site of the first 2000 earthquake in the SISZ may have been caused by the upwelling of magma from a great depth before the large Vatnajökull eruption of 1996. Compared with the time before this swarm, the seismic rate after the swarm up to the 2000 earthquakes was slowly but steadily increasing (Figure 4.10). This implies that a process of intrusion in the crust below Vatnajökull, which led to the huge Gjálp eruption there in 1996, may have triggered (by a process that lasted 4 years) the 2000 earthquakes in the SISZ at a distance of 150 km. Unfortunately, there were no observations close enough to the Gjálp volcano before the eruption to confirm such an upwelling or the depth of its origin. However, comparison with the process before the much smaller eruptions in Hekla and their impact on seismicity up to a distance of at least 30 km (Figure 4.33) suggests that this may be possible. It also suggests that long-range triggering or migrations should be subject to further study using modern seismic and deformation technology and emerging models so that such connections can be explained.

4.10.6 Triggering as a tool in earthquake prediction

As described in previous sections, the possibility of a large earthquake being triggered by another observable strain release event warrants intensive study and understanding the processes involved would be of great value for earthquake prediction. Even a weak possibility should immediately lead to increased monitoring

and modeling of crustal conditions and changes in them at the sites of concern, in an effort to establish their constitutional relationship and to merge them with other observations.

4.11 THE THIRD EARTHQUAKE: IN ÖLFUS 2008

We were very hopeful of being able to predict the next large earthquake in the SISZ after all the new findings that came out of earthquake prediction research projects. But we were only partly successful.

A magnitude-6.3 earthquake occurred in the westernmost part of the SISZ, in the Ölfus area, on May 29, 2008 (Figure 4.34).

The basis of this book has been earthquake prediction research in the South Iceland Seismic Zone. Studies of the two large earthquakes in the zone in 2000 constituted the final part of this research. We had hoped in light of all the good results obtained and new understanding gained that it would have been possible to issue warnings of the next large earthquake in the zone.

In fact, a low-order warning about the possibility of an earthquake in this westernmost part of the zone was issued in 2003. But it occurred without a short-term warning in May 2008. However, observable changes had been detected shortly before it. Probably a low-order short-term warning could have been issued if an active continuously operating Earth-watch system of the requisite standard had been

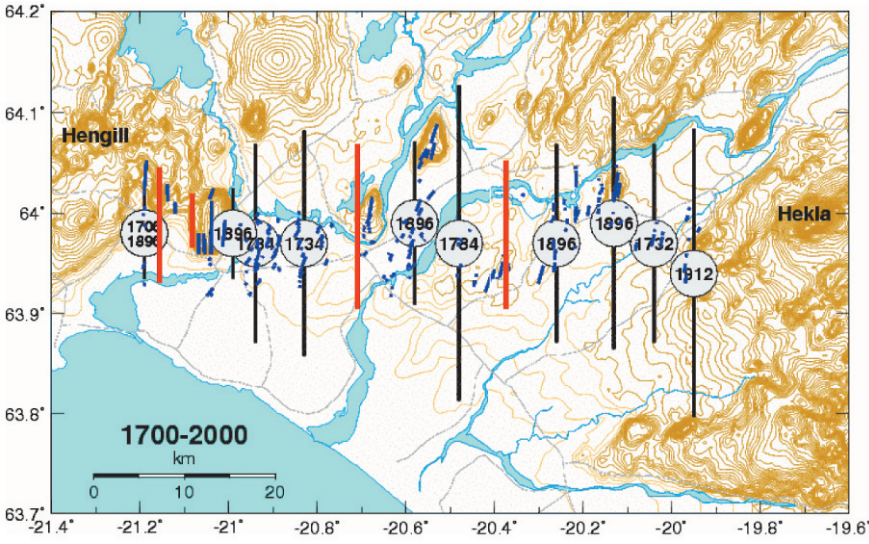

Figure 4.34. History and faults of large earthquakes in the SISZ from 1700 to 2008. The red lines in the center show the two 2000 earthquakes and the two shorter red lines near the western end of the zone are the two faults of a third earthquake that occurred May 29, 2008 (from Gudmundsson (see Appendix 2.B), pers. commun.).

available in Iceland at that time. Such an Earth-watch system continuously evaluates and merges observations from places of special concern, based on all available data, both real time and older. Unfortunately, this was not available. Sections 4.11.1–4.11.4 describe this earthquake and pre-earthquake processes in greater detail.

4.11.1 Basic information about the 2008 earthquake

An earthquake of magnitude 6.3 occurred near the western end of the SISZ on May 29, 2008. It had two main faults only 4 km apart (Figures 4.34 and 4.35). According to IMO the origin time was 15:45:58:91 UTC and the hypocenter was at 63.972°N and 21.072°W at a depth of 4.7 km. It was obvious from the first aftershocks that this was a double quake. The western fault started to slip only a few seconds after the first.

The IMO estimated the magnitude as 6.3 soon after the earthquake. A well-constrained magnitude provided by the U.S. National Earthquake Information Center (NEIC), based on global observations, came up with the same value: 6.3 (M_w GMT). In both cases the two earthquakes were treated as one and the same as they were so close to each other in time that they could not easily be resolved in the seismic records. According to evaluation of continuous high-frequency GPS measurements (1 Hz GPS), it is estimated that the second fault started to move 3 seconds after the origin time of the mainshock (Hreinsdóttir *et al.*, 2009). The length of the first as indicated by aftershocks was around 9 km and the depth limit around 6 km. The entire western fault was around 20 km long, and along a large part of it the depth limit seemed to be around 6 km. However, at the southern end of it, aftershocks occurred at a depth of 9 km. This fault may well consist of three distinct fault segments (Figure 4.35). This has not as yet been studied in detail.

It is difficult to estimate how much moment energy, as expressed in magnitudes, was released from each of the two main faults. Hreinsdóttir *et al.* (2009) estimate that the total moment released at both faults would correspond to $M_w = 6.2$, $M_w = 6.1$ on the eastern fault and $M_w = 6.0$ on the western fault, even though that fault is much longer overall.

4.11.2 Foreshocks

An hour and four minutes before the earthquake an intensive series of foreshocks started, the first one of local magnitude 3.5 (Figure 4.36). The foreshocks were in a dense group, only a few hundred meters in diameter and within a few hundred meters of the hypocenter (Figure 4.36).

The foreshocks occurred just below a depth of 5 km (as seen in Figure 4.36) and were on the 800 m long nearly north–south line seen in Figure 4.37. The figure also shows foreshocks moving back and forth with time, approximately north–south, along the strike of an apparent 800 m long fault at a depth of 5 km.

Figure 4.38 shows horizontal compressions caused by the release of 39 foreshocks that were well recorded before the earthquake and near its hypocenter.

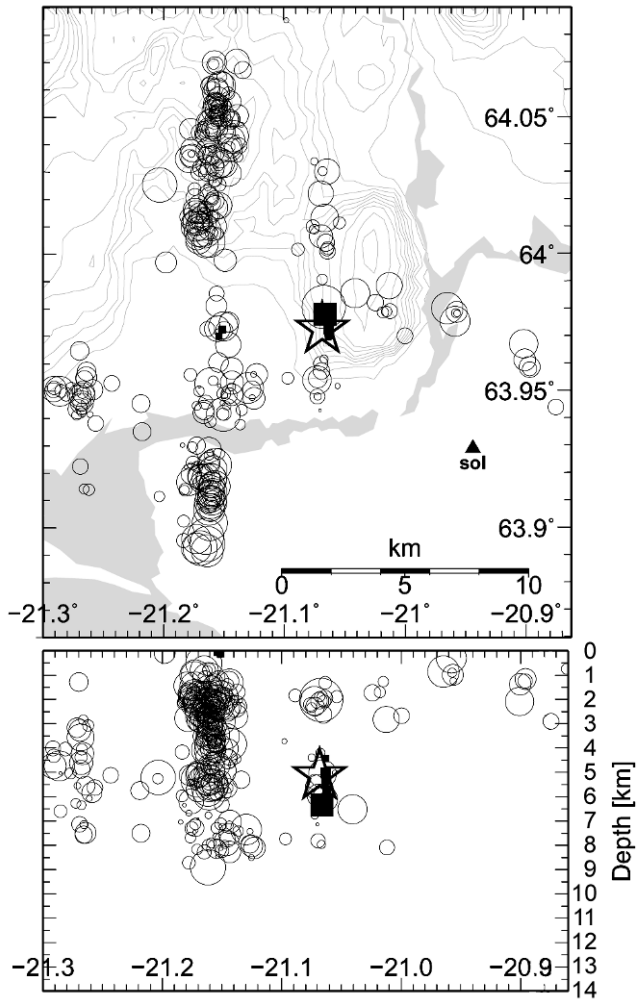

Figure 4.35. (*Upper*) A geographic view of the area where the May 2008 earthquake occurred (see for comparison Figure 4.34). The gray parts show the ocean in the south and the Ölfusá river flowing toward it. The earthquake occurred near the western end of the SISZ on two main faults which are shown by two north–south rows of mainly small aftershock epicenters. (*Lower*) An east–west cross-section at various depths of their sources. Circles are aftershocks in the two days following the earthquake, while squares are foreshocks one day before it. Foreshocks occurred almost entirely at the hypocenter of the earthquake, which is marked by a star obscuring the foreshocks. The north–south fault where the earthquake started (i.e., the eastern fault) was indicated as 9 km long by the aftershocks. The western fault, which started to slip just a few seconds after the first, is 4 km farther west and is 20 km long. The long fault could be considered two or three different faults, but as they are almost in the same north–south direction, I prefer to regard them as three segments of the same western fault. Some earthquakes on an old north–south fault even farther west are probably not part of the earthquake itself, rather they should be considered as being triggered by it.

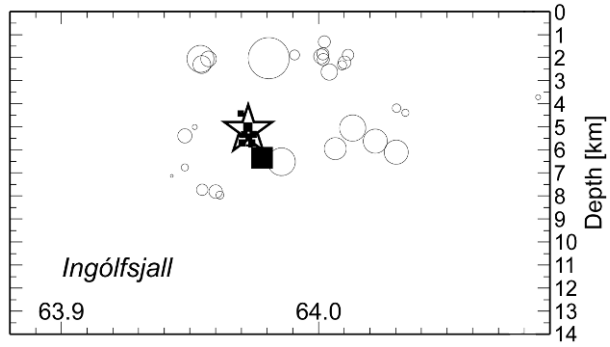

Figure 4.36. Earthquakes on a north–south cross-section along the fault of the first part of the earthquake (i.e., the eastern fault). The horizontal axis shows latitude in degrees north. Circles are aftershocks. Squares represent the 39 densely distributed foreshocks that occurred in a single hour close to the hypocenter which is indicated by a star.

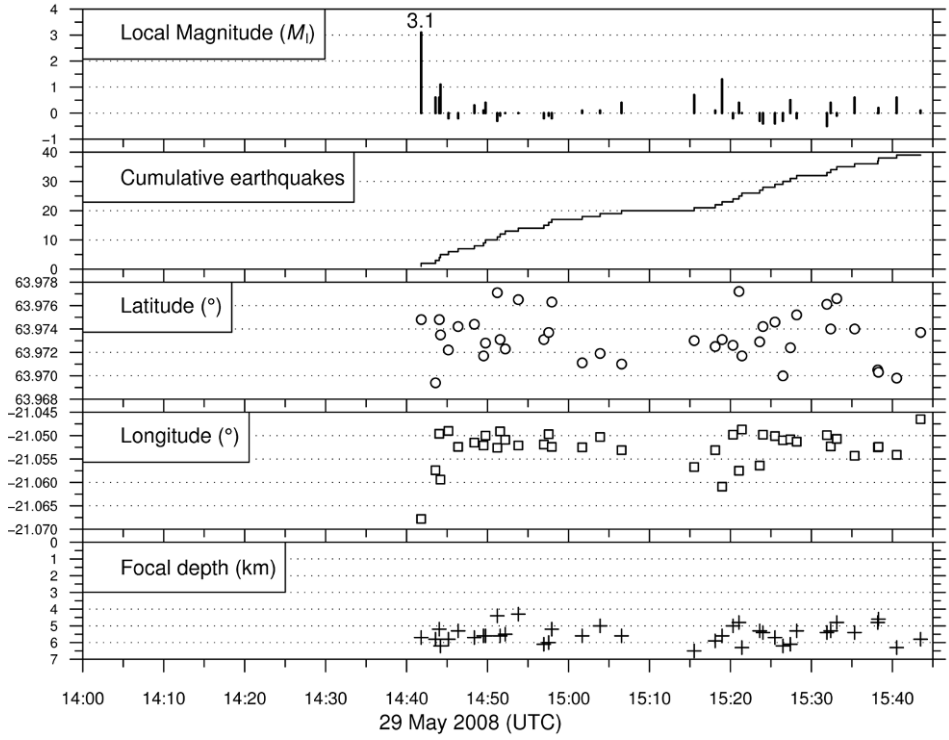

Figure 4.37. A time graph shows small earthquakes one hour before the first part of the Ölfus earthquake. In a single day before the double earthquake almost all foreshocks took place here, the exceptions being two small earthquakes near the surface above the second fault. Looking at the latitude distribution, you see north–south variability of the order of 800 m, while longitudes express a line distribution along the fault and at depths that is constant during this time (one hour) of the nucleation.

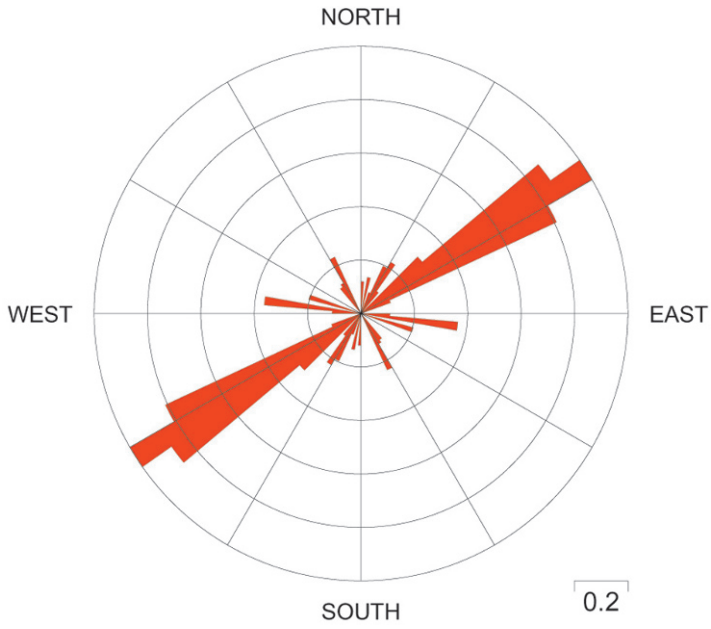

Figure 4.38. A rose diagram of the frequency of horizontal compressions in the fault plane solutions of each of the 39 foreshocks an hour before the earthquake. Frequency is counted within an angle of 15°. The main direction is very stable at around 59° east of north. This implies that almost all foreshocks had slips along small fault segments striking 14° east of north.

The stability of horizontal compressions at around 59°NE shows that most foreshocks followed a single main fault strike around 14°NE. This was roughly 14 degrees northeast of the strike of the main fault, which was due north according to the aftershocks. So, it looks as though the foreshocks followed an *en echelon* pattern forced by a north–south right-lateral slip deeper down. This is comparable to the process that took place 10–15 days before the initial 2000 earthquake. Earthquakes and faulting during these 10–15 days were apparently forced by a deeper slip.

Comparing the nucleation of the 2008 earthquake with the discussion about nucleation of the June 17, 2000 earthquake (Sections 4.7.2 and 4.7.3), it would appear that slow slip motion across the deepest part of the first 2008 fault, in the ductile crust, became gradually shallower and approached the brittle–ductile boundary. There it applied strain to the locked and brittle part of the crust to create small foreshocks and finally the main shock, which broke upward through the whole crust. This is in good agreement with results of stress estimations by Ragnar Slunga (see his report, Slunga, 2010) which used data to detect a high degree of crustal instability at around a depth of 7 km just below the hypocenter shortly before the earthquakes. Such instability is probably a sign of slow and stable slip motion which, based on other considerations, is expected at the deepest part of the fault leading up to an earthquake.

4.11.3 Long-term development leading up to the earthquake

The 2008 earthquake was a continuation of the two large 2000 earthquakes described in Section 4.5. Figure 4.34 shows the faults and history of large earthquakes in the SISZ from 1700 up to just before the 2000 earthquakes as black lines. The red lines near the center of the SISZ show the two 2000 earthquakes. The Ölfus earthquake of 2008 is indicated by the two short red lines near the western end of the zone.

4.11.4 Warning ahead of the 2008 earthquake

A low-order warning was issued by IMO staff to the Iceland Civil Protection Agency (ICPA) in 2003 pointing out the risk of a large earthquake on the western fault that almost directly passed through the village of Hveragerði. The reason for this warning was long-term expectations of an earthquake on this fault and minor seismic activity at the time of the warning. This warning was low key insofar as it simply advised the ICPA to consider how they would react to a short-term warning of a large earthquake on that fault and prepare the necessary planning to mitigate risks. This was discussed at a meeting of the Scientific Advisory Committee of the ICPA, which suggested some steps should be taken to increase observation. At the meeting it was also pointed out that the actual site of the earthquake could possibly be around 5 km farther east (i.e., the very site where the 2008 earthquake started).

Anyway, there was no short-term warning before the double earthquake in Ölfus relating to both these faults. A low-order warning would have been possible, but only at most an hour before the earthquake. The intensive swarm consisting of one micro-earthquake a minute at the site of the earthquake could have led to a low-order warning being issued to the ICPA, advising them to get ready for a large earthquake (i.e., magnitude 6–7). In fact, scientists at the earthquake section at IMO hurriedly discussed this possibility during this hour. They had also noticed a swarm of very shallow micro-earthquakes 4 km farther east 6 months earlier, which could have been an indication of generally high stress in the area.

In any event, there was not a geo-watching system available that contained all the necessary information and advised what to do in such situations (see Chapter 7 on warnings). Issuing a warning of a large earthquake is a serious matter, something that seismologists are reluctant to do unless they are very certain. They don't like to cause panic by issuing a warning of an event that turns out to be non-existent. Scientists who issue such a mistaken warning will be attacked by many and, what is worse, any future warnings by them will be disregarded. What is needed is a rule-based warning service clearly stating what a scientific observer must do in such situations—an observer's guide. With such a warning service, scientists would be more liekly to issue warnings because they followed a prescribed schedule. Such a warning schedule should of course be agreed between scientists and the ICPA on the basis of scientific evidence.

It is the duty of Earth observation agencies to provide warnings if there are signs of a large impending earthquake. But there is always the doubt that it might not

occur before the end of the advised warning period. To solve this problem it is important

- to carefully define levels of warnings and which actions should be taken in light of these levels;
- that any sign of an impending large earthquake should lead to issuing a warning to a Civil Protection agency detailing the level of the warning and discussing adequate actions to be taken.

It is easy for outsiders to say with the benefit of hindsight that a micro-earthquake swarm observed an hour before an earthquake should have led immediately to issuance of a low-order warning to the ICPA. What they overlook is that earthquake swarms are frequent in Iceland and in this case there simply was not the time to analyze the significance of it as an earthquake forerunner.

An active and continuously operating Earth-watch system along the lines briefly mentioned here could have automatically carried out in real time a significant part of the fast analysis needed for issuing some kind of short-term warning. What is more, some of the observational research that is currently carried out after the event could have been done before the earthquake (e.g., the hindsight studies of Ragnar Slunga). Slunga discovered, albeit in hindsight, a high level of instability in micro-earthquakes at a depth of 7 km, just below the hypocenter of the Ölfus earthquake, between 2005 and 2008 (see Section 4.10.3 for more about his method). Had this been known at the time foreshocks started on May 29, 2008 at Ölfus, it would have added significantly to the information base needed for a short-term warning before the 2008 earthquake.

4.12 SUMMARY OF OBSERVATIONS OF VALUE IN EARTHQUAKE PREDICTION

In this section my intention is to summarize observations about crustal processes leading up to the large earthquakes in 2000. I mainly concentrate on premonitory activity related to nucleation of the June 17, 2000 earthquake (the initial earthquake). The situation before the June 21, 2000 earthquake was largely set by the first earthquake and the ensuing swarm of aftershocks which helped to predict the second earthquake, but at the same time hid the variability of small activity necessary to predict an earthquake. Experience of the 2008 earthquake is used in this summary but is limited because studies of the event are still ongoing. The experience gained from studying these earthquakes in the SISZ can be used with caution to help predict earthquakes.

We start with real-time predictions, followed by hindsight observations.

Real-time predictions

- It was possible to provide a useful prediction of the sites of the two magnitude-6.6 (M_s) earthquakes in 2000 a decade before they occurred.

This was done on the basis on historical earthquake information and understanding of the tectonics of the region, supported by seismicity information. Not only were the sites of the two earthquakes predicted, but also the sites of the next large earthquakes in the zone. By "large earthquakes" is meant those with magnitude between 6 and 7.

- Short-term predictions were made of the time, site, and size of the second of the two 2000 earthquakes, on the basis of (1) earlier prediction of its site and size, (2) microearthquake distribution along the predicted fault after the first earthquake, and (3) an assumption that slow fault slip started down in the ductile part of the crust, before it broke through the elastic/brittle crust as an earthquake.
- There was a long-term (5-year) prediction of the magnitude-6.3 earthquake in 2008, based mainly on the regular pattern of earthquakes released on SISZ faults since 1700.

Observations to find the site and magnitude of an impending earthquake

- The long-term spatial pattern of faults and destruction wreaked by historical earthquakes is significant for finding the site and size of future earthquakes.
- The long-term temporal pattern of seismicity leading up to the 2000 earthquakes reveals a physically understandable pattern of relaxation in that part of the SISZ between 1912 and 1940, followed by two to three decades in which there were a few magnitude-4 and magnitude-5 earthquakes near the faults of the 2000 earthquakes (Holt and Hestfjall in Figure 4.8), and then there followed a relative absence of earthquakes larger than magnitude 2 for two decades before the large earthquakes occurred in 2000.
- In the 9 years leading up to the 2000 earthquakes, micro-earthquake activity was observed at two impending faults revealing a physically understandable pattern. This pattern was explained by the presence of a hard core (i.e., an asperity) inside a weak fault zone (i.e., the SISZ). The asperity was being deformed by continuous plate motion. This hard core was located at the fault of the initial large earthquake. This was a significant result and helped in finding the site and size of the impending large earthquake.
- Detailed mapping of the *b*-values of micro-earthquakes was performed. As a result, the hard core (asperity) of the initial 2000 earthquake was discovered albeit in hindsight, along with other significant pre-earthquake features of SISZ tectonics.
- Estimations of absolute local stress (from data of the 8-year period leading up to the earthquakes) based on individual micro-earthquake mechanisms could be used to detect the buildup of stress along the fault of the initial earthquake and its closeness to instability at the site of the second earthquake.
- A so-called "SRAM" method was developed. This method quantifies seismicity in the zone by assuming given fault directions and in this way indicated the sites of both impending faults and earthquake epicenters (albeit in hindsight).

Observations used to find the time of the impending earthquake

- From the beginning of 1997 to 2000 there was a gentle increase in micro-seismic activity at the site of the initial 2000 earthquake, indicating gradual buildup of stress.
- The depths of the majority of micro-earthquakes below the initial earthquake source were between 8 km and 10 km. There were many exceptions (i.e., shallowing of activity from a few days up to a month). The number of such shallowing swarms increased in the leadup to the initial earthquake.
- The distribution of microseismicity, which for 9 years before the initial 2000 earthquake tended to be volumetric (concentrated northwest–southeast), changed to planar along the developing fault plane in the 2 weeks leading up to the initial earthquake.
- The mechanisms behind micro-earthquakes also rotated slightly in the 2 weeks leading up to the first earthquake. This rotation indicated, together with the change in distribution of microseismicity, that slow slip across the developing fault plane had started at and below the brittle–ductile boundary 2 weeks before the initial earthquake.
- A simple algorithm was developed to show how micro-earthquake sources started to be distributed along the impending fault plane 2 weeks before the initial earthquake, but were concentrated at a hard core (an asperity) 24 hours before it.
- An interesting observation was made that increasing the sensitivity of seismic observations at developing faults would have garnered much more accurate information about the slow slip expressed in micro-earthquakes that manifested themselves 2 weeks before the initial large earthquake.
- Micro-earthquakes manifesting themselves an hour before the 2008 earthquake had a remarkable planar distribution on the plane below the hard core, indicating right-lateral slip of the earthquake fault had started at depth before the earthquake.
- Estimation of stress from individual fault plane solutions indicated the change from a high stress level well before to unstable (high CFS) shortly before both the first 2000 earthquake and the initial 2008 earthquake.
- Monitoring shear wave splitting in micro-earthquake data indicated an increase in stress in the SISZ in the few months leading up to the first 2000 earthquake and stress relaxation in the few weeks before it, which coincided with other indications of the start of instability in the fault at this time.

Processes in the uppermost couple of kilometers of the crust

- A strainmeter in a borehole a few kilometers from the epicenter of the initial 2000 earthquake recorded a 400-nanostrain contraction signal starting 19 days before the earthquake. It relaxed two days later. This signal had a shallow origin but was not fully understood. What tied it to the earthquake was its closeness in space and time and the fact that such a signal had not been recorded at this station for 20 years. It was further tied to the earthquake by

the minor extension indicated by the strainmeter after the contraction pulses until the earthquake occurred.

- A geothermal borehole, 10 km to the north of the north end of the initial earthquake fault, registered a 6-meter lowering in water level 24 hours before the earthquake (this was probably a very short-lived phenomenon, lasting less than a minute).
- Months before the 2000 earthquakes, radon anomalies were recorded throughout the SISZ. Such a long-lasting period of radon fluctuations may reflect strain change over a large area and a common source of not only the two large earthquakes but also the Hekla eruption that took place 3–4 months earlier.
- Manifestation of a strong and unusual swarm of very shallow earthquakes 6 months before that were close to the epicenter of the 2008 earthquake.

It is difficult to link such shallow processes physically to the release of the impending earthquake. They probably reflect slow deformation and stress changes down in the seismogenic part of the crust and may be, in conjunction with physically better constrained processes, significant tools for short-term prediction.

Triggering by or coupling with other events

- There is some support for speculation that the 2000 earthquake sequence was triggered by volcanic eruptions to the east and west of the SISZ shortly before, or by a large event common to and causing all this activity. It is even suggested that the major eruption of Gjálp in the Vatnajökull ice cap in 1996 may have influenced long-term nucleation of the 2000 earthquakes.
- Less than a minute after the initial 2000 earthquake it dynamically triggered smaller but still potentially dangerous earthquakes 60 km to 85 km distant.
- Models have shown that stress change caused by the initial earthquake could have triggered the second earthquake 3.4 days later.

Other observed processes

Among other processes (detailed in Chapter 4) that were significant in understanding crustal processes leading up to the 2000 earthquakes the following warrant a mention:

- stress estimations based on historical seismicity;
- stress estimations based on composite inversion of micro-earthquake fault plane solutions and their spatiotemporal variation;
- measurements of deformation by borehole strainmeters, GPS, and InSAR.

Of course, other crustal processes might have been observed before the 2000 earthquakes had more observing tools been available. However, at the time of monitoring these earthquakes we had little choice but to be satisfied with the tools then available to us (i.e., as mentioned in this section and described in Chapter 4).

5

A new dynamic model involving upward migration of fluids from below the brittle crust

Stefánsson and Halldórsson (1988) proposed that there was interplay between local intrusions of fluids from below the brittle crust in the South Iceland Seismic Zone (SISZ) and strain buildup by plate motion and release in earthquakes. This was called the "dual-mechanism model" (described briefly in Chapter 3). This made a lot of sense for Iceland with its volcanism. However, in volcanic rift zones earthquakes are frequent, but small, rarely larger than around magnitude 5. Dyke intrusions there result in land deformation, volcanic eruptions, and areas of fumarolic high-temperature activity, which quickly and effectively release strains at seismogenic depths in the crust and do not lead to large earthquakes. This was in stark contrast with the non-volcanic transverse zones of Iceland where day-to-day seismicity is low but large earthquakes occur at long intervals. The dual-mechanism model could explain many observed seismic patterns in the transverse zones but it was not well constrained physically. It was revived at a meeting of the PRENLAB group in 1999 (Stefánsson, 1999) as it was considered to be a more robust physical model.

The questions faced by the PRENLAB group were:

(1) Is it possible, under the conditions that prevail in the SISZ, for fluids migrating upward to play a significant role in conjunction with crustal plate motion in the creation of conditions for the release of large earthquakes there?
(2) Is it possible to create a physically well-constrained and Earth-realistic model to explain multidisciplinary geophysical and geological observations?

Maurizio Bonafede (see Appendix 2.B) and his group at the University of Bologna in Italy took up the challenge to undertake such a task. The following boxed material summarizes the outcome of this modeling work.

R. Stefánsson, *Advances in Earthquake Prediction: Seismic Research and Risk Mitigation*, Springer Praxis Books, DOI 10.1007/978-3-540-47571-2_5, © Springer-Verlag Berlin Heidelberg 2011

- Under favorable conditions, high values of pore/fluid pressure can in response to plate motion strain effectively migrate from the brittle–ductile boundary at a depth of around 10 km up towards the meteoric aquifer boundary at a depth of 3 km to 4 km.
- At seismogenic depths in the crust, fluids retain near-lithostatic pressure values long enough for fracturing conditions to change significantly.

Favorable conditions involve a crust with low intrinsic permeability, as is the case in the basaltic crust of the SISZ, and low temperature so as to provide a brittle rheology.

By high values of pore/fluid pressure is meant pressures close to the lithostatic pressure (rock pressure) in contrast to the hydrostatic pressure prevailing in fluids at shallower depths than 3 km to 4 km. Water, which is compressible at the temperature and pressure prevailing at depth in the crust, is the fluid used for modeling.

The model created is called the Fluid–Strain Model (the F-S model). It explains the multidisciplinary geophysical and geological observations carried out in the zone (Zencher *et al.*, 2006; Bonafede *et al.*, 2007; Stefánsson *et al.*, 2010). The evolution of the model and how it matches observations will be detailed in the following sections.

5.1 HOW FLUIDS FROM A GREAT DEPTH MODIFY FRACTURING CONDITIONS IN THE CRUST: EVOLUTION OF THE F-S MODEL

In this section I describe the evolution of a model for fluid migrating up from the brittle–ductile boundary in response to strain and how it can be expected to modify fracturing conditions in the seismogenic crust on both a long and a short timescale.

In an effort to explain some features of strain buildup and strain release in earthquakes in the SISZ, Stefánsson and Halldórsson (1988) tentatively suggested the dual-mechanism model. This model involved interplay between the buildup of plate motion strain in the zone and probable injections of fluids from below. They argued that the close arrangement of faults side by side, which had not been repeated at the same place since at least 1700, indicated the dominant role of deep fluids in not only selecting where in the zone each new earthquake would occur but also triggering it. Based on magnetotelluric measurements, a low-resistivity layer had been found at a depth of around 15 km (Beblo and Björnsson, 1980; Gebrande *et al.*, 1980; Hersir *et al.*, 1984), which could be the supply source for the fluids. The dual-mechanism model is further described in Stefánsson (1999). However, this model did not hold up well under physical constraints. If these injections of fluids were magmatic dyke injections like those in rift zones, why did we not see signs of recent volcanism in the SISZ as we see in rift zones, and why were the earthquakes much larger in the SISZ than in rift zones? Another question that needed to be answered was: If fluids are made of volatiles released by deeper magma, how can they migrate up to a

shallow depth and transport the high pore pressure necessary for failure conditions to arise in the elastic/brittle part of the crust? Yet another question was: Is it really possible for hot fluids from below, during a protracted period of time, to raise stresses in the seismogenic part of the zone without pressure being released by reacting or melting into the surrounding rock? These were the principal questions asked.

It was also suggested that some observations of crustal processes before the 2000 earthquakes (as described in Chapter 4) could be better explained by such a model. Also, as confirmed by observations of micro-earthquakes after the 2000 earthquakes, after a fault breaks in a major earthquake, micro-earthquakes on and near the fault persist for at least a century, as expressed by the microseismicity and high *b*-values found in the fault regions of the 1896 earthquakes (Figure 5.1, see also Figures 4.9 and 4.11).

Such was the basis for the modeling work which will be described in the following sections (Stefánsson *et al*., 2010).

5.2 A NEW MODEL FOR UPWARD MIGRATION OF MAGMATIC FLUIDS

Fluids (mainly water and CO_2) are continuously released from ascending magma in volcanic regions, due to melting because of pressure decrease (e.g., Hirth and Kohlstedt, 1996). Rheological changes accompanying the extraction of water from the mantle during partial melting are important in explaining the bathymetry, the crustal thickness, and the Bouguer anomaly along the Mid-Atlantic Ridge near Iceland in terms of plume head broadening and decoupling from the overlying lithosphere. The interaction of mantle plumes with mid-ocean ridges has been modeled by Ito *et al*. (1999, 2003) and Marquart and Schmeling (2004), among others. In particular, these models predict the velocities of plume upflow ~50 times greater than the spreading ridge velocity. The upward migration of water extracted in this way from the shallowest part of the mantle (the asthenosphere) is expected to take place at lithostatic pressure until it reaches the bottom of the brittle crust, where deviatoric stress induced by plate motion becomes significant with respect to gravity load. The steady (or maybe episodic) migration of this high-pressure water from below the brittle–ductile (B-D) transition up to meteoric aquifers has significant effects on rock strength according to the Coulomb failure stress criterion.

Zencher *et al*. (2006) modeled the migration of water from a deep reservoir, at lithostatic pressure, toward a shallow reservoir where hydrostatic fluid pressure prevailed, across a layer of brittle rock (transition layer), where deviatoric stresses were superposed on lithostatic stress $P_L = \rho_r gz$ (Figure 5.2). Such modeling is important for understanding the interaction between pore pressure p_p and rock permeability K. The modeling was based on the assumption of a specific crack model of pressure-dependent permeability, in which water flows across a regular network of tensile hydrofractures which open up when pore pressure exceeds

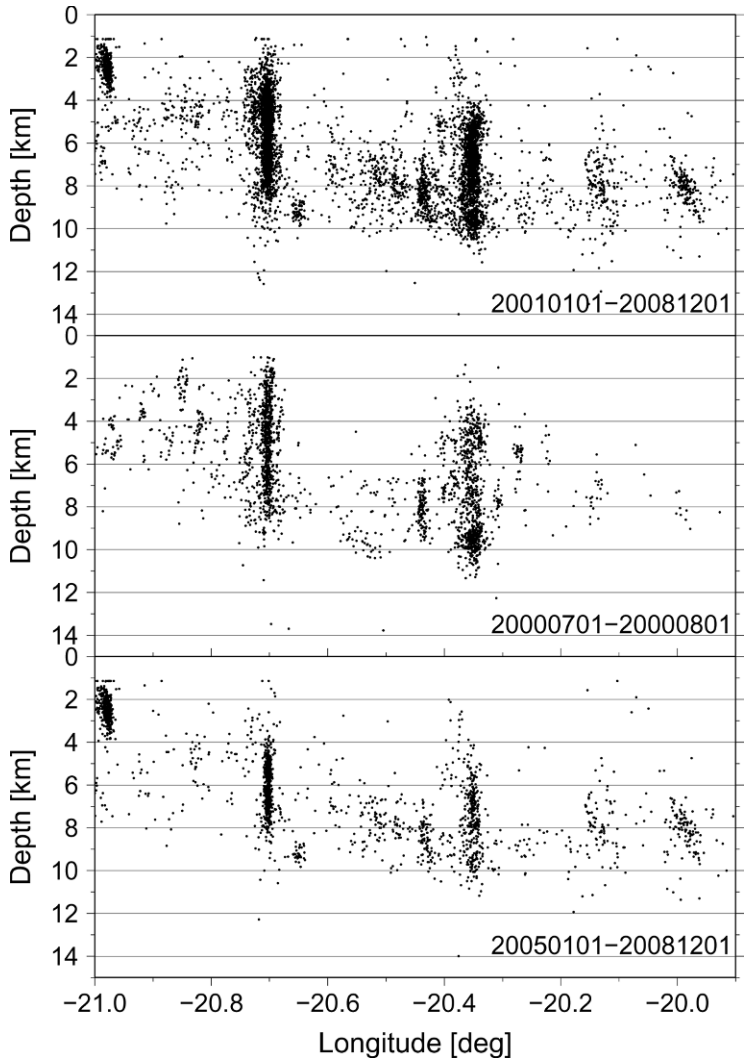

Figure 5.1. Depth of micro-earthquakes since 2001 from west to east, along a large part of the SISZ. The clusters at longitude −20.37° and −20.71° are aftershocks of the large earthquakes of 2000. The two distinct clusters farther east are at the faults of the largest of the 1896 earthquakes and at the 1912 earthquake (compare Figure 4.9 for a geographic view of the earthquake positions). Deepening of the brittle–ductile boundary from west to east is clear (see Chapter 3). The top image shows activity half a year after the earthquakes until the present. The middle image shows activity half a month after the earthquake and lasting one year. The bottom image shows activity since 2005. Comparing the middle and the bottom images we see that micro-earthquake activity at the faults of the 2000 earthquakes reached significantly shallower depths immediately after the earthquakes than during the last 4 years. The activity at the faults of the earthquakes 100 years ago is mainly between depths of 7 km and 10 km (i.e., only a couple of kilometers above the brittle–ductile boundary).

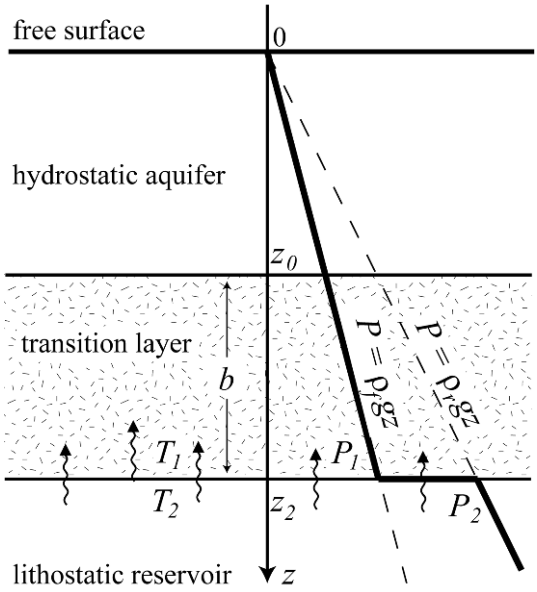

Figure 5.2. Schematic diagram of the model. The layer $z_0 < z < z_2$ is a fluid-saturated porous medium (a transition layer); ρ_f and ρ_r are, respectively, the density of fluid and rock; and g is gravity. P and T are values of pressure and temperature. At $z = z_0$ a meteoric aquifer is present at $T = T_1$ and at hydrostatic pressure $P = \rho_f g z_0$. In $z = z_2$ the transition layer is in contact with a hot fluid reservoir at lithostatic pressure $P_2 = \rho_r g z_2$ and at temperature T_2 (Zencher *et al.*, 2006).

minimum horizontal confining pressure. Despite this permeability model being assumed, they showed that high pore pressure values can, in response to strain, efficiently migrate up from the brittle–ductile transition at a depth of *ca.* 10 km, toward (but below) the meteoric aquifer at a depth of 3 km to 4 km, in rock with low intrinsic permeability, as is the case in the SISZ. The flow negligibly affects the thermal gradient if permeability is low (e.g., 10^{-18} m^2) so that the geotherm would remain close to the conductive regime (i.e., upwelling fluids would have temperatures close to the rock surrounding them, so the transition region would remain brittle/elastic).

The permeability of the basaltic crust of Iceland is assumed to be below 10^{-18} m^2 and may even be down at 10^{-20} m^2 (see Appendix 5.A). From the time-dependent modeling of Zencher *et al.* (2006), it seems that several thousands of years would be necessary to attain the steady state conditions for upward migration, if intrinsic permeability is as low as 10^{-19} m^2 throughout the transition layer. Pore/fluid upflow in the uppermost mantle is much faster as steady state permeability there is much higher than in the brittle/elastic crust. This creates conditions at the bottom of the crust for fluid pressure buildup and release in conjuntion with deviatoric stresses in the brittle crust. The presence of joints and fractures which likely occur in fault regions may easily create patches of higher permeability. In hydrothermal

systems, permeability values as high as $10^{-12}\,m^2$ to $10^{-15}\,m^2$ are typical. If such high-permeability regions become connected to a near-lithostatic pressure domain, a pore pressure pulse diffuses across them with timescales <1 month according to Zencher *et al.* (2006).

A limitation of the model described by Zencher *et al.* (2006) is that the geometry of crack distribution was assigned *a priori* and the flow rate was not prescribed. However, it adjusts to changing permeability since pore pressure is assigned at both ends of the transition region. In the following it is demonstrated that the increase in pore pressure up to near-lithostatic values is a necessary corollary of magma dehydration in the asthenosphere if intact rock permeability is low (Stefánsson *et al.*, 2010). It is further demonstrated that results very similar to those of Zencher *et al.* (2006) can be obtained in the steady state regime without assuming a specific pressure-dependent permeability model.

The model created was called the Fluid–Strain Model (the F-S model). It was a continuation of the modeling described above, which was encapsulated in it. The F-S model is described in detail in Appendix 5.A. Appendix 5.A contains a description of the asperity model, which is based on the F-S model and on micro-earthquake observations in the SISZ. Appendix 5.A also discusses the consequences of the F-S model's explanation of dynamics at a plate boundary.

5.3 HOW DOES THE F-S MODEL MATCH THE OBSERVATIONS DESCRIBED EARLIER IN THIS BOOK

The F-S (fluid–strain) model explains several observations of spatial and temporal distribution of inter-earthquake seismicity in the SISZ (see Appendix 5.A which discusses the consequences for the seismogenic plate boundary in light of the model).

5.3.1 The distribution of microseismicity and *b*-values can be explained by the model

The concentration of areally and temporally spread micro-earthquake activity near the brittle–ductile boundary (Figures 3.6, 4.13, 4.14, and 4.15), as well as generally large *b*-values at a depth between 8 km and 10 km in the SISZ (Figure 4.11), may be explained by high pore fluid pressures, predicted by the model at these depths if $Q_0 \geq Q_{eq}$ (see point 1 in Appendix 5.A.1). A complementary way to interpret high *b*-values is to relate them to the fractal dimension D (i.e., to a high density of fractures that would also lead to high b). According to the model for upward fluid migration in the SISZ, highly fractured rock would increase permeability, and if permeability is confined by some barrier below the hydrostatic boundary it would lead to high pore fluid pressures. So, in these cases high b means high pore fluid pressures (see also Wyss, 1973; Wyss *et al.*, 1997). Another link that connects high pore pressures to small earthquakes comes from laboratory

tests under wet conditions (Lockner and Byerlee, 1994). When faults start slipping under such conditions the presence of fluids soon brings fault slip to an end, so mostly small earthquakes are released (i.e., high pore pressure, which helps to trigger small earthquakes, drops immediately when fracturing occurs and inhibits faults from growing larger). This is in agreement with Segall and Rice (1995) who point out that under such conditions dilatancy strengthens faults thus preventing the release of large earthquakes. A major earthquake occurs when an impervious asperity, or an asperity with low pore pressure, is present (point 5 in Appendix 5.A.1). Such an asperity is capable of building up uniform and sufficiently large deviatoric stress before breaking and thus triggering slips along a large part of the fault.

5.3.2 Role played by asperities

The southeast–northwest striking configuration of the micro-earthquakes between 1991 and 2000 preceding and following the first earthquake (Figure 4.9) cannot be explained by a slow fault slip across a vertical fault with such a strike (as might be suggested). There is practically no shear stress acting in this direction and normal stress acting on such a fault plane is large in the area and locks the fault. However, it can be explained by the F-S model (as described in Appendix 5.A.2 and Figure 5.4).

5.3.3 Shallowing episodes

The episodic shallowing of micro-earthquakes, which occurred in swarms within a timespan of a few tens of days at the site of the initial 2000 earthquake (as seen in Figure 4.16) can be explained by the model (see points 2–5 in Appendix 5.A.1) as a slip/overpressure process of fluid migration toward the hydrostatic layer. These episodes do not necessarily involve migration of fluids on every occasion from the brittle–ductile boundary. However, according to the model high pore fluid pressures can be trapped in the crust below the hydrostatic level and stay there for a long time, only to be released in response to plate motion strain. All episodes have a swarm-like character which can be linked to the transient migration of fluids.

5.3.4 Time-dependent heterogeneities

Time-dependent heterogeneities in the crust involve the crust responding differently at different times to the buildup of steady plate motion strain, such as was the case before and after the 2000 earthquakes (as described in Section 4.10.2 and by Bellou, 2006). After the large earthquakes the zone returned to higher levels of frictional strength than it had before them. The F-S model can explain this: because fluid pressures were high in the SISZ before the earthquakes, they were released by the large earthquakes and triggered aftershocks all along the zone, which thus became stronger.

As described in Section 4.3 on stress transfer, micro-earthquakes and medium-size earthquakes were triggered to the west and to the north of the first earthquake on June 17, 2000. This was not repeated after the second large earthquake although

it occurred closer to these areas. A probable reason is that high pore fluid pressures, which were built up locally, had already been released by the first earthquake and associated triggered aftershocks.

Another example of time-dependent heterogeneities is provided by the seismicity that followed the Hekla eruptions of 1991 and 2000 (Figure 4.33). These eruptions triggered very different patterns of coupled seismic activity, although they had similar influence on strain in the zone (as was observed by strainmeters). Earthquakes and volcanic eruptions can trigger earthquakes almost immediately in a large area either dynamically or by static strain change. In many cases they trigger local processes that then trigger earthquakes in the next few hours or days if conditions in the crust are right.

In the SISZ the most likely local processes causing time-dependent heterogeneities are those involved in fluid mobility. Micro-earthquakes are triggered locally in response to plate motion because of local heterogeneities. Local heterogeneities that are variable in time and space may be caused by fluids available in the medium, fluids that can be triggered to move around. The F-S model predicts that high pore fluid pressures can locally migrate upward in response to strain changes and thus cause short-term buildup or release of fracturing conditions locally (points 4 and 5 in Appendix 5.A.1). Solid heterogeneities (i.e., harder or softer parts compared with the surrounding rock) can also be expected, of course. However, these would certainly remain fixed and react similarly to strain loading of the crust.

As described in Section 4.10.2, a dyke injection was likely below a depth of 7 km to 8 km at the site of the June 17 earthquake 4 years before it occurred (i.e., in 1996). At these depths a significant number of earthquakes were of the type described as normal faulting (i.e., extensional), indicating intrusion of incompressible mass. Shallower earthquakes during this episode were of the strike slip type as is most common for the SISZ. This is in accordance with crack modeling (e.g., Bonafede and Danesi, 1997): tensional stress induced by dyke opening decreases sharply above the dyke tip leading to strike slip earthquakes being triggered there. However, the long-term seismic rate increased after this episode compared with what it had been before (Figure 4.10). This can be explained by the F-S model: upward migration of compressive fluid (water), in response to plate motion strain, increased because its source became more productive. The dyke injection increased the surface area of the magma releasing the compressive fluid that migrated upward in the seismogenic crust (the dyke injection caused increased Q_0, see point 2 in Appendix 5.A.1).

Estimations of stress at each of the two earthquakes (see Section 4.10.3 and Figure 4.29) revealed it to be strongly heterogeneous. Even though the rheological conditions and plate motion strain at both sites were similar, high shear stress characterized the first earthquake fault and a high CFS the second, when considering the 9-year period before the 2000 earthquakes. This feature was repeated in the different rate of seismic release at the two sites (as detailed earlier; Figure 4.10). The F-S model explains the difference as being the different time histories of the buildup process. The earthquake that was released on June 21 had a strong input of fluids from below before stress across the fault was sufficiently high to trigger a large earthquake there. Additional strain from plate motion was frequently released in

small fluid-driven earthquakes on and around the fault, instead of building up sufficient stress along the fault to release a large earthquake there. When the highly stressed asperity of the June 17 earthquake ruptured 17 km away it provided additional shear stress on the pre-existing north–south fault of the June 21 earthquake to trigger slow motion on it at depth, which in 3 days built up fracturing conditions to nucleate plate slip around the shallower part of that fault.

Detailed studies of *b*-values in the zone point toward a crustal fabric of only 2 km in the SISZ (as pointed out in Section 4.6.3). Geological mapping of faults on the surface seem to point to the same result (i.e., a distance between north–south earthquake faults of only 2 km). So, the sequence of earthquakes before 1700 might have been, at least to some extent, in between faults in the sequence since 1700 (see Figure 4.7). The triggering effect of upward fluid migration (according to the F-S model) would explain this as fluid supply cells below the brittle–ductile boundary being very narrow, maybe 2 km in diameter, so one earthquake would only empty a 2 km diameter supply. In other words, the release in earthquakes of fluid supply cells before 1700 acelerated fluid inflow into supply cells of nearby old faults which gradually created the conditions for releasing earthquakes there after 1700.

The arrangement of large earthquakes since 1700 cannot be predicted by the historically calculated stress levels in the zone with the exception of short time intervals (as discussed in Section 4.10.1; see also Roth, 2004; Richwalski and Roth, 2008). In some places, earthquakes often occur long before they are expected on the basis of historically estimated stress. This may be caused by triggering local heterogeneity. It is likely that the selection of earthquake faults from among a dense fabric of faults is governed by local heterogeneity, which is variable in time according to the F-S model. In light of the general conditions in and below the SISZ it is most likely that heterogeneities are brought about by fluids upwelling over a protracted period from depth in response to gradually changing local straining within the brittle crust of the fault zone (as described by the model). This fluid upwelling is local and has the effect of modifying conditions in the seismogenic crust to a different degree at different places and selecting the site of the earthquake when it, together with plate motion strain, reaches the fracturing level there (point 4 in Appendix 5.A.1).

A consequence of the F-S model (points 4 and 5 of Appendix 5.A.1) and asperity modeling (Appendix 5.A.2) is that upward fluid migration would tend to lock nearby lanes of fluid migration horizontally. This would tend to leave some parts unpenetrated, a probable reason for the creation of asperities like the one before the June 17 earthquake. This would also be in agreement with the regular pattern (i.e., 6 km distances between active parallel faults since 1700) in the dense fault fabric of the SISZ. An expanding fault would close a contiguous old fault at each site every time (Figure 4.7).

5.3.5 Triggered seismicity

Several other observations (described in Sections 4.1–4.11) can be explained by the F-S model. The availability of fluids at depths of the order of 15 km, as constrained by magnetotelluric measurements, is the basis for the model. High pore fluid

pressures indicated by the seismic velocity structure at seismogenic depths in the crust inside the SISZ are a sign of strain-modified upward migration of high-pressure fluids, renewing pore pressures released in large earthquakes. According to strain observations and modeling, the volcanic eruptions of Mt. Hekla decrease the horizontal confining pressure in most of the SISZ and thus decrease friction on all faults. The swarm of earthquakes in the zone following repeated eruptions are thus a sign of the high pore fluid pressures that had already built up in the dense fault system, which were subsequently released by the additional expansion caused by upward migration of lava before the eruption. The triggering of earthquakes at long distances (60–85 km away) a few tens of seconds after the first magnitude-6.6 earthquake at the western continuation of the SISZ was (as discussed earlier) interpreted as dynamic triggering, because of just how close these sites were to failure, either because of high shearing stresses or high pore fluid pressures.

5.3.6 Aftershock distribution

According to the F-S model, the linear dense concentration of micro-earthquakes at faults, after the occurrence of the 2000 earthquakes, would indicate remaining patches of fluids in the faults, which would have the effect of opposing normal stress from the fault wall. Gradually, the faults will close as the surrounding fault wall dries out while the supply of new magmatic fluids is not available. The fault will weld together starting from the top and then gradually proceed to deeper and hotter parts closer to magmatic fluid sources. This evolution shows up in the distribution of aftershocks, in depth and time, on the faults of the two large earthquakes (as seen in Figure 5.1).

However, Figure 5.1, which relates to much of the SISZ, shows that currently there are micro-earthquakes on faults of earthquakes that occurred in 1896 and 1912. The F-S model explains why faults from these 100-year-old earthquakes still appear as micro-earthquakes but, in agreement with the evolution described above, are concentrated at greater depths than the seismic remnants of the 2000 earthquakes (as seen in Figure 5.1).

It is most likely that fluids from deep in the faults migrated upward during the earthquake, released their pressure to the surface, but kept near-lithostatic pressure below the solidified part of the fault, all of which resulted in micro-earthquakes. This would be consistent with studies of post-earthquake ground movements by Jónsson *et al.* (2003), who conclude that they "cannot rule out a longer pore-pressure transient at the depth of the aftershocks" (as discussed in Section 4.11.4).

5.3.7 Pre-earthquake patterns

Prior to the 2000 earthquakes there were faults and slow fault slips deep in the crust; the micro-earthquakes that occur around and above them because of steady ongoing strain loading reveal this. The directions of seismic sources and horizontal compressions, shown by micro-earthquakes around the origin of the first 2000 earthquake during the fortnight before it occurred (Sections 4.7.2 and 4.7.3), can be explained by

slow slip motion across the earthquake fault, below seismogenic depth, before the earthquake (as explained in Figure 4.20). Planar declustering of micro-earthquakes starting at depth during the same period of time (shown in Figures 4.21–4.23) is evidence of the same. According to the F-S model this would be established by a fault below the B-D boundary that was kept open by high pore fluid pressure and was not subject to shear stresses to release micro-earthquakes. This ductile part of the fault is expected to slip continuously for hundreds and hundreds of years, the slip velocity of the top modified by stick–slip contact with the brittle crust, releasing pore pressure in episodic upward fluid migrations. Studies of anisotropy in the Husavík–Flatey fault in the TFZ (Figure 3.2), which has not experienced a large earthquake since 1872, reveal high pore fluid pressure at seismogenic depths in the fault (as described in Section 4.9.4). The most likely explanation of this would be fluids bringing high pore fluid pressures upward from below the brittle–ductile boundary.

It might be opposed that near-lithostatic pore fluid pressures below the hydrostatic boundary in the zone are necessarily caused by upward fluid migration. These high pore fluid pressures would have been there all the time, but, over a protracted period, high pore fluid pressure in seismic zones would be released in frequent large earthquakes, so the renewal of high-pressure underground fluids is needed to keep the pressure high. This is certainly in accordance with the F-S model, which predicts high pressures building up from upwelling fluids lasting a hundred years or so, time enough to modify conditions for large earthquakes in the SISZ

5.4 THE F-S MODEL AND OTHER MODELS FOR SISZ EARTHQUAKES

Let us now take a brief look at other models describing observed patterns of strain release in the SISZ area. The ''bookshelf model'' (see Section 3.3) was first proposed by Einarsson *et al.* (1981), Einarsson and Eiríksson (1982), and Einarsson (1991). It explains the characteristic arrangement of faults in the SISZ: in spite of left-lateral transform motion along the east–west striking zone, the faults of individual historical earthquakes in the zone are perpendicular to it and display right-lateral slip motion, analogous to a bookshelf when all the books fall to the side.

The ''dual-mechanism model'', proposed by Stefánsson and Halldorsson (1988), explains the dense arrangement of faults in the SISZ as an interplay between fluid intrusions and strain buildup and release.

Angelier *et al.* (2004a, 2008) describe the fault pattern in the SISZ as a ''Riedel (1929) type distribution, for immature fault zone'' (i.e., not containing left-lateral earthquake displacements along the zone, but north–south as well as northeast–southwest striking faults are claimed to have been observed in some cases).

The dual-mechanism model is in good agreement with our fluid–strain model. However, the F-S model is better based physically and can explain more observations. The bookshelf model as well as the Riedel-type model are kinematic models describing observed fault patterns in the zone. They agree with the dynamic models described here. However, dynamic models go farther and explain historical and

geophysical observations as well; they also explain how kinematic fault patterns are created.

A criticism leveled at the bookshelf model is that we do not see geological traces of the anti-clockwise rotation expected in the SISZ. The following is suggested on the basis of observations and the F-S model to explain the lack of rotation of faults. There continue to be north–south faults in the east–west shear zone. Each earthquake fault is probably created during a long process of hydrofracturing necessary to bring about fluid pressure–plate motion conditions. This means each earthquake fault would be created from components in the dense fabric of old faults in the neighborhood. Any rotation would be complemented by activating new right-lateral north–south fault segments that fit the general stress conditions best. Micro-faults that release micro-earthquake swarms all around the zone tend to have a nearly north–south strike, showing the preference of such crack directions in the zone. This was also reflected in the aftershocks of the two large earthquakes. The faults are not flat planes, they are composed of a few strike slip segments that have slightly different directions (but close to north–south) and short connecting segments (see Section 4.2 and Figures 4.3 and 4.4).

The three features of the F-S model that make it the best available model to describe SISZ seismicity are (1) the availability of fluids at lithostatic pressure below the brittle–ductile boundary, (2) Earth-realistic modeling revealing the possibility of upward migration of lithostatic fluids in response to strain, and (3) good agreement with geophysical observations (as described here).

5.A APPENDIX: A NEW MODEL FOR UPWARD MIGRATION OF MAGMATIC FLUIDS

In Section 5.2 the steady (or maybe episodic) migration of high-pressure water from below the brittle–ductile transition up to meteoric aquifers was shown to have significant effects on rock strength S, according to the Coulomb failure stress criterion. It is described by the following formula:

$$S = S_0 + f(\sigma_n - \alpha p_p)$$

where S is shear stress at failure; S_0 is intrinsic strength; σ_n is normal stress; f is a friction coefficient; p_p is pore pressure; and $\alpha = 1 - B/B_s$ (B being the drained bulk modulus and B_s the bulk modulus of the solid matrix, see Nur and Byerlee, 1971). I will refer to S as the Coulomb failure threshold. According to this criterion, failure may take place, with low stress drop and low slip, if pore pressure is close to σ_n and $\alpha \sim 1$ (high fracture density), while high stress drop and high slip require high shear stress and low pressure or low α (low fracture density).

In the following it is demonstrated that the increase in pore pressure up to near-lithostatic values is a necessary corollary of magma dehydration in the asthenosphere if intact rock permeability is low (M. Bonafede, pers. commun.; Stefánnson *et al.*, 2010). The main features of the pore pressure field may be understood according to the following arguments: water released from the asthenosphere at lithostatic

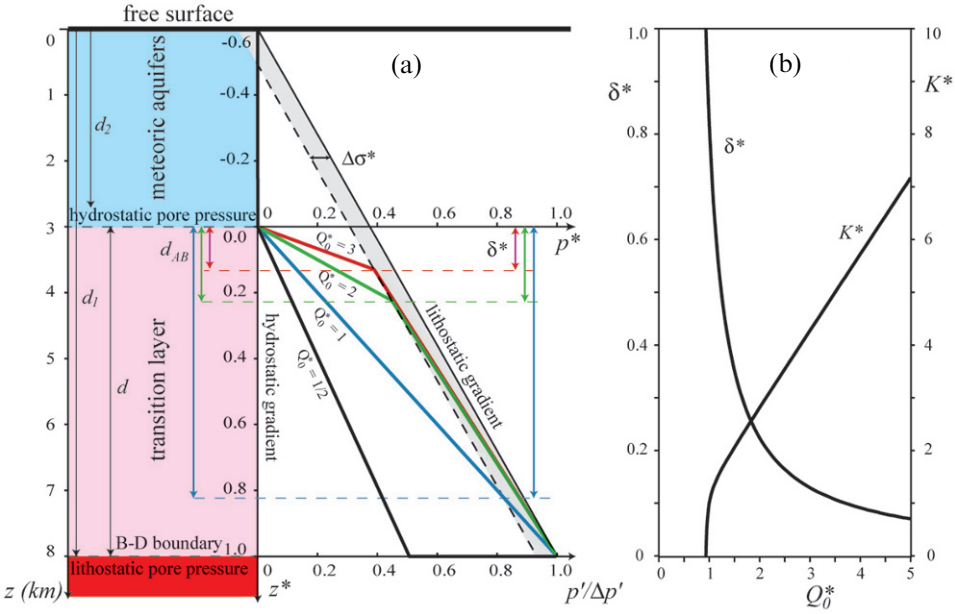

Figure 5.3. (a) Sketch of the transition region $d_2 < z < d_1$ and pore pressure $p^* = p'/\Delta p'$ in non-dimensional units across it, for a few values of the non-dimensional flow rate $Q_0^* = Q_0/Q_{eq} = \frac{1}{2}, 1, 2, 3$ (p' is pore pressure in excess of hydrostatic pressure; $\Delta p'$ is the difference between lithostatic and hydrostatic pressure at depth d_1). The near-lithostatic region is shaded. Parameter values employed: $d_1 = 8$ km, $d_2 = 3$ km, $\rho_r = 2{,}900\,\mathrm{kg/m^3}$, $\rho_w = 1{,}000\,\mathrm{kg/m^3}$, $g = 9.80\,\mathrm{m/s^2}$, $\Delta\sigma = 10$ MPa. (b) Depth $\delta^* = d_{AB}/d$ of transition between domains A and B and permeability ratio $K^* = K_B/K_A$ *vs.* non-dimensional flow rate Q^*.

pressure is continuously supplied at an assigned flow rate Q_0 to the base of the brittle crust, at depth d_1, which may be schematically identified as the brittle–ductile boundary, where pore pressure is lithostatic (Figure 5.3). Water migrates upward toward meteoric aquifers at depth d_2, where pressure is hydrostatic, through a transition layer with thickness $d = d_1 - d_2$ and rock permeability K_A. According to Darcy's law, the volumic flow rate Q of a fluid with viscosity η across a medium with permeability K is

$$Q = -\frac{K}{\eta}\nabla p'$$

where $\nabla p'$ is the pressure gradient in excess of the hydrostatic value $\rho_w g \delta_{i_3}$. The equilibrium flow rate in the steady state regime across the transition layer is then

$$Q_{eq} = \frac{K_A}{\eta}(\rho_r - \rho_w) g \frac{d_1}{d}$$

where ρ_r and ρ_w are, respectively, the density of rock and water. If the actual flow rate Q_0 released from the asthenosphere is higher than Q_{eq}, increasing amounts of water should accumulate at the bottom of the transition layer, until hydrofractures

or pore pressure–assisted shear fractures occur, which increase the effective permeability from K_A to K_B. In other words, effective permeability must adjust itself in order to fulfill redundant boundary conditions (both pressure and flow rate are imposed at the bottom of the transition region).

If K_A and K_B were assigned we might determine the vertical extent of the fractured region B. Alternatively, if K_A is known the pore pressure at the transition B–A may be assigned and K_B may be computed. The pore pressure at the transition depth d_{AB} is expected to be close to the minimum horizontal confining pressure $P_c = \rho_r gz - \Delta\sigma$ (where $\Delta\sigma$ is the deviatoric stress of tectonic origin) in order for hydrofractures to open.

Then, the redundant boundary value problem may be easily solved for the pressure field in both domains A and B and for K_B and d_{AB}. Some results are shown in Figure 5.3. No significant increase in permeability K_B is needed to transmit a low flow rate (close to the equilibrium flow rate Q_{eq}), while K_B must increase significantly above K_A, over most of the transition layer, in order to accomplish higher flow rates. Employing the numerical values given in Figure 5.3—and $K_A = 10^{-19}\,\mathrm{m}^2$, $\eta = 10^{-3}\,\mathrm{Pa\,s}$—the equilibrium flow rate is $Q_{eq} = 3 \times 10^{-12}\,\mathrm{m/s}$. If magma ascends at a speed of 50 cm/yr, and the water released by dehydration is between 100 ppm and 200 ppm by weight (as suggested by Ito *et al.*, 1999), Q_0 may be evaluated as $\sim 4.5 - 9 \times 10^{-12}\,\mathrm{m/s}$, which corresponds to $Q^* = Q_0/Q_{eq} = 1.5 - 3$. If K_A is higher (e.g., $K_A = 10^{-18}\,\mathrm{m}^2$), Q_{eq} increases proportionally and hydrofractures cannot open.

The pore pressure fields shown in Figure 5.3 are qualitatively similar to the steady state solutions obtained by Zencher *et al.* (2006) when $t \to +\infty$; the main difference is that no specific permeability model is employed here (the only assumption made is that two distinct permeability values pertain to the two domains A and B) and that the flow rate Q_0 from asthenospheric depths is assigned (in addition to the pressure values at the top and bottom of the transition layer). The pore pressure profiles in Figure 5.3 resemble measurements taken in deep wells in southern California (Yerkes *et al.*, 1990), showing a transition region below a depth of 2 km to 3 km, where pore pressure gradients change from hydrostatic to near-lithostatic and where high stress drop events are located. These modeling results may be summarized as:

- If $K_A \approx \dfrac{\eta Q_0}{\nabla p'}$, near-lithostatic pore pressure is found only close to the brittle–ductile boundary, where the Coulomb failure threshold (CFT) is low; microseismicity is then expected to be present close to the brittle–ductile transition in regions endowed with intermediate permeability.
- If $K_A < \dfrac{\eta Q_0}{\nabla p'}$, fluid flow takes place through the transition layer but only a fraction of Q_0 can be transmitted; increasing volumes of fluids accumulate below the brittle–ductile transition until hydrofractures or pore pressure–assisted shear fractures take place, increasing the effective permeability from K_A to K_B in the lower domain B of the transition layer. The increase in

permeability brings near-lithostatic pore pressure from the brittle–ductile boundary up to depth d_{AB}; "near-lithostatic" means pressure values lower than lithostatic by less than the deviatoric stress $\Delta\sigma$ built up by tectonic motions (from $\Delta\sigma$ we must subtract the intrinsic strength S_0 which must be overcome in order to produce fractures).

The time needed to approach the steady state regime cannot be evaluated from present day steady state analysis. From the time-dependent modeling of Zencher *et al.* (2006), it seems that several thousands of years would be necessary to attain steady state conditions if the intrinsic permeability K_A were as low as 10^{-19} m^2 throughout the transition layer; however, when high-pressure fluids meet a region of higher permeability, the migration of pore pressure considerably quickens, since the diffusivity of pore pressure is proportional to permeability (Rice and Cleary, 1976). The presence of joints and fractures which likely occur in fault regions may easily create patches of higher permeability; values as high as 10^{-12} m^2 to 10^{-15} m^2 are typically inferred within hydrothermal systems. If such high-permeability regions become connected to a near-lithostatic pressure domain, a pore pressure pulse diffuses across them with timescales <1 month (Zencher *et al.*, 2006, fig. 10-f).

The assumption of low intrinsic permeability of the compact Icelandic basaltic crust (i.e., of the order of 10^{-19} m^2) is in agreement with available laboratory tests of basaltic samples subject to a confining pressure (as is the case at a depth of 2 km) indicating very low permeability (i.e., 10^{-19} m^2 and 7×10^{-19} m^2; Christensen and Ramananantoandro, 1988). Other measurements of basalt permeability are given by Yoshida *et al.* (1998) in which the intrinsic permeability of Icelandic basalts is even lower (i.e., 10^{-20} m^2).

5.A.1 Consequences for the seismogenic plate boundary according to the model

The fluid–strain (F-S) model has the following consequences for the seismogenic plate boundary in Iceland:

1. High pore fluid pressures gradually build up at the bottom of the brittle crust over long periods of time. Pore pressure–assisted fractures generate frequent and uniformly distributed microseismicity close to the brittle–ductile boundary for a wide range of flow rates $Q_0 \geq Q_{eq}$, where Q_0 is the ascending flow rate of volatiles released from magma below the B-D boundary and Q_{eq} is the equilibrium flow rate in the unfractured medium above.
2. On the other hand, if Q_0 is higher than Q_{eq} (i.e., permeability is low) fluids with near-lithostatic pressure gradually migrate upward toward meteoric aquifers in a hydraulically assisted process that triggers swarms of micro-earthquakes of shallow seismicity when they meet patches with higher permeability.
3. Increasing tectonic stress $\Delta\sigma$ helps to drive fluids upward, by changing fracture conditions at the transition depth d_{AB} (Figure 5.3).
4. The upwelling fluid selects paths where the pressure is least in the heterogeneous stress field leaving less pervious regions laterally (asperities), endowed with high

stress and high CFT. The strain released by micro-earthquakes and plastic processes in shallow regions where the pressure is less concentrates the high and uniform stress within the asperity, where high CFT is also attained because of low fracture density (low α) and maybe also because of low pore pressure.

5. An earthquake ripping through an asperity cuts the whole crust, releasing the high pore fluid pressures at the bottom of the crust and at the same time releasing plate motion strain. The previously impervious asperity becomes a high-permeability region, and the high-pressure fluids migrating toward the released fault maintain micro-earthquake activity close to the fault for a considerable time after the earthquake.

5.A.2 Modeling the effects of an asperity in a weak zone in light of the F-S model

The southeast–northwest striking configuration of the micro-earthquakes between 1991 and 2000 preceding the first earthquake (described in Section 4.6.1 and Figure 4.9) cannot be explained by a slow fault slip across a vertical fault directed southeast–northwest (as might be suggested). There is practically no shear stress acting in this direction and normal stress acting on such a fault plane is large and compressive in the area (see Section 4.9.2).

However, it can be explained by the F-S model. This southeast–northwest configuration has been modeled (Bonafede *et al.*, 2007) in light of upward migration of lithostatic fluids in response to plate motion strain that modifies conditions in the zone that trigger microseismicity (points 2–4 of Section 5.A.1). In the model a highly rigid asperity is assumed in between the two centers of swarm activity, around the hypocenter of the June 17 earthquake (Figure 5.4). The highly rigid asperity is imbedded within a region of the SISZ where there is generally lower effective rigidity.

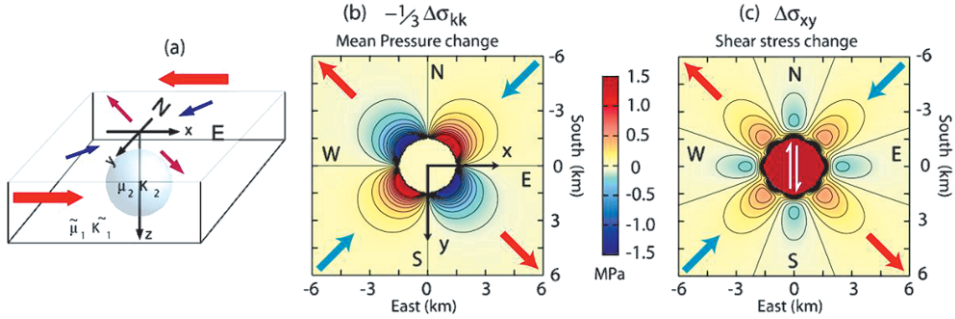

Figure 5.4. A schematic image describing the modeling. (a) Stress induced by viscoelastic relaxation on the mid-plane of the asperity. (b) The change in confining pressure (mean pressure) induced by the asperity enhances the opening of hydrofractures where it is negative, and inhibits the opening where it is positive. Low pressures are to the northwest and southeast of the asperity, where near-lithostatic fluid pressures can flow in from below and help to create the swarms of micro-earthquakes described. (c) Within the asperity, shear stresses grow to be large, uniform, and coherent with the tectonic field (Bonafede *et al.*, 2007).

In response to east–west shearing across the SISZ, areas of low pressure are created to the southeast and northwest of the asperity. In response to the slow buildup of pore pressures at depth and shearing plate motion strain, fluids are released into these low-pressure shadows in accordance with the fluid model to trigger microseismicity there (as observed). It is justified to assume the SISZ zone has relatively low viscosity, which over time has been penetrated by numerous earthquakes close by in the past. It is also in agreement with the findings of Tryggvason *et al.* (2002) who report a low V_P/V_S ratio (as briefly described in Section 3.2). Resolution of the seismic velocity data in the area of the first 2000 earthquake is not good enough to confirm the existence of a highly rigid core 3 km in diameter. The existence of such a core at the center of the fault of the first 2000 earthquake has been demonstrated on the basis of other observations (as described in Chapter 4). In the modeling described above (Bonafede *et al.*, 2007) only a marginal viscosity contrast is needed to be seen in a long-term deformation for pressure shadows to be caused behind the hard and unfractured asperity.

Appendix 5.A was the result of a series of personal communications between Maurizio Bonafede and me in 2008.

6

Emerging new understanding on the release of earthquakes and the earthquake cycle

Efforts to predict earthquakes started long before seismology and seismometers. Earthquakes were like monsters hiding deep below the surface, waking up, and breaking out of their grottos when we least expected them. Often they were preceded by tremors which were felt by people or animals (which are more sensitive to tremors) or some other phenomena related to the waking up of the giant. For thousands of years stories were told over and over again about such phenomena. When people sensed phenomena like those described in the stories they feared an earthquake was approaching and sometimes reacted to save themselves from its effects. These predictions were not based on physical understanding of the causes of the earthquakes, but on observing similar phenomena as had been observed before in relation to earthquakes.

With the advent of good seismic recorders about 100 years ago, a new and more sensitive tool became available, one that was able to record some of the earth tremors. However, it did not lead immediately to a new understanding of the dynamics preceding large earthquakes. In some cases earthquake recordings were little more than an add-on to the old stories. New phenomena that preceded earthquakes were observed in some cases. High-standard methods of statistics and pattern search were developed to discover the common denominators for the phenomena that precede earthquakes, often called ''precursors''. However, problems remained, in particular because of the length of time, maybe hundreds of years, between earthquakes at the same place. It soon became obvious that it was difficult to make comparisons between forerunners of earthquakes that occurred in different environments and at different places.

Geological sciences developed fast during the last century resulting in new possibilities for geophysics to explore hidden parts of the Earth. Models were developed to create the same patterns as were observed, implying that these models were correct as far as we could judge from our observations. These models were simple and had freedom parameters that made them fit the observations of

R. Stefánsson, *Advances in Earthquake Prediction: Seismic Research and Risk Mitigation*, Springer Praxis Books, DOI 10.1007/978-3-540-47571-2_6, © Springer-Verlag Berlin Heidelberg 2011

large earthquakes that were available. The models were plates imitating the thickness of the brittle crust or half-space models sometimes layered with known variations in seismic velocity. Sometimes these models had micropores of fluids in the rock as part of their intrinsic and homogeneous rheology. For pre-earthquake processes these models were far too simplistic. The buildup of stress and fracturing conditions for large earthquakes takes hundreds of years, while the release of the same stress in earthquakes takes a few seconds. In the same way the size of observed signals preceding large earthquakes is infinitesimal compared with signals observed during large earthquake release. The observations of large earthquakes did not have the necessary resolution to detect, and thus to model, such infinitesimal initiation features. It was necessary to increase sensitivity to be able to observe the weak pre-earthquake process.

As geophysics developed, new possibilities to study the fine structure of crustal and sub-crustal processes were created. However, progress in making use of them in earthquake prediction research was slow, to say the least. Quite correctly, many criticized earthquake prediction research for assuming models that were too simple for the statistical evaluation and bore little resemblance to nature as we observe it. In short, the models were not Earth-realistic.

There were four principal reasons for the slow progress of earthquake prediction:

(1) Lack of political and economic impetus because of the fear of change. This has always been the case for scientific progress throughout the world when there is a major change in the fundamental basis of our knowledge.
(2) Conservatism, reflected by scientists who stick to the 1,000 years of phenomenological studies of earthquake precursors, who only add statistics to the studies of phenomena, and who in many cases assume wrongly that the precursors to earthquakes tend to be the same worldwide.
(3) Monitors that are simply not sensitive enough. To be able to observe the small changes that occur before earthquakes you need monitors that are infinitely more sensitive to crustal processes than those used in the study of large earthquakes and their aftershocks which, unfortunately, has long been the main objective of seismology.
(4) The belief that it will never be possible to predict earthquakes. Why spend effort and money on what many leading scientists and engineers consider impossible. If that is the case, then let us find the money to build houses strong enough to withstand earthquakes. Mistaken warnings ahead of earthquakes have the undesirable effect of adding to the anxiety and suffering caused by them.

6.1 MULTINATIONAL AND MULTIDISCIPLINARY EARTHQUAKE PREDICTION RESEARCH IN ICELAND: GOALS AND RESULTS

This was the situation when multinational earthquake prediction research started in Iceland shortly before 1990. We took on board criticisms that the models used

previously were too simple and we decided to change things. Our aim was to come up with more sensitive monitors to detect and interpret the weak preparatory processes of large earthquakes.

The multinational earthquake prediction research project—which selected Iceland as the test area—involved a new approach to research: a physical approach. This involved studying and understanding the physical processes leading to large earthquakes. The best way to do this was to gather signals and information from a large number of very small earthquakes—micro-earthquakes—which are abundant in seismic zones. The goal was to develop a new technology, a seismic network that in practice could detect all earthquakes in the SISZ down to magnitude 0, and make good use of the information transmitted to us, by developing and adopting new technology to interpret the signals—technology whose aim was to reveal crustal conditions at depth and their changes with time on both a long-term and short-term basis.

By adding information from micro-earthquakes of size down to and sometimes below magnitude 0 significantly increased the necessary resolution of some applications. Heterogeneities the size of tens of meters could be directly observed. Pore fluid pressures close to lithostatic values could be sensed at the bottom of the brittle crust and at seismogenic depths in the brittle crust (i.e., the depths where large earthquakes originate). Upward movements of high-pressure fluids from the brittle–ductile boundary in response to strain could be detected, as could the durability of high fluid pressures at seismogenic depths, leading to ongoing expansion and corrosion of fault contacts.

Micro-faults of the order of one hundred meters long could be mapped by the new technology as could motion across these faults and their failure conditions. The use of micro-earthquakes made it possible to study the strongly heterogeneous stress field within the fault area of impending large earthquakes, heterogeneity with size of the order of a kilometer, and also to estimate just how close faults were to instability. A few days before a large earthquake a small slip motion, less than a millimeter, could be detected on the fault below the elastic/brittle crust.

The buildup of micro-earthquake technology led the way to multidisciplinary approaches, seismic and geological history, and deformation monitoring. Based on information from micro-earthquake technology and other multidisciplinary results, theoretical work was carried out, which resulted in the emergence of a dynamic model that could explain the pre-earthquake process and at the same time comply with new observations. This was the Fluid–Strain Model—often abbreviated as the F-S model.

The emerging new understanding is manifold. It is a new understanding of how earthquake processes gradually build toward their release in the South Iceland Seismic Zone. It involves new models for earthquake preparatory processes which may be applicable at other places in the world. It signifies the importance of micro-earthquakes in studying preparatory processes, and indicates that we should *a priori* assume that preparatory processes are different for all earthquakes, contrary to what is often assumed in the statistical approach.

6.2 EARTHQUAKE BUILDUP AND RELEASE IN THE SISZ: A SUMMARY

At a depth of around 100 km below Iceland, basaltic fluids are released from the upwelling mantle plume. These fluids, proposed to be mainly water fluids from the mantle, migrate in a slow or stable way through the ductile and highly permeable material below the elastic/brittle part of the crust. The permeability of the brittle/elastic crust in Iceland is much lower, around or below 10^{-19} m^2, so fluids cannot effectively migrate through it in the same way. So, they accumulate at the brittle–ductile boundary and create fluid pockets or pores, which are kept open by their high (i.e., lithostatic) fluid pressure. Under the combined effect of high fluid pressure and shearing crustal strain, upward fluid migration can continue episodically, in a pressure/slip mode, and along distinct lanes that open up. Upward migration is strain conditioned: it is fast during periods of fast strain changes as during earthquakes, and slow or no upflow during interseismic periods (see Chapter 4). The conditions exist for such a strain-conditioned upward fluid migration in many seismic zones, because of the fast strain changes there.

The boundary between hydrostatic and lithostatic pressure conditions (the H-L boundary) is expected at a depth of around 3 km to 4 km. It is probably more correct to say that under SISZ conditions lithostatic pore pressures cannot build up at depths shallower than 3 km to 4 km. If fluids of magmatic origin could penetrate higher they would move at high speed continuously out into the surrounding system of open fractures, release the near-lithostatic pore fluid pressures, and instead create high-temperature areas close to the surface, as is characteristic of rift zones. They would not build up high fluid pressure at seismogenic depths.

Episodic fluid migration from the B-D boundary at a depth of 10 km up into the brittle crust of the SISZ has the effect of lowering internal friction in individual faults. Finding their way up through the crust they lose heat and thus do not react effectively with the surroundings. And, as they are trapped below the hydrostatic/lithostatic boundary, they can build up high and enduring fluid pressure in pores or other closed fractures. Locally, they have near-lithostatic pressure values and thus decrease the threshold to instability there, may trigger seismic swarms, and in time weaken contacts between the walls of large faults.

Such episodic upward migration of high-pressure fluids in response to strain was observed to last many decades before release of a large earthquake in the SISZ. They could be observed because they triggered small earthquakes on their way. Most significantly and primarily, fluids migrate upward inside an old fault to "corrode it" (i.e., cause unstable patches of high fluid pressures in it intermittently with hard dry cores). A fault that is slowly slipping at great depth (i.e., under ductile conditions) and gradually activated at a shallower depth (i.e., in the brittle crust) causes deformation and stress heterogeneity in its environment during this process. Fluids from below migrate episodically into pressure lows behind hard obstacles in this deformed volume. In this way they gradually even out, on a local scale, stress heterogeneities that are created around the deforming fault. This leads to volumes of homogeneous stress conditions close to the fault, but gradually also to larger

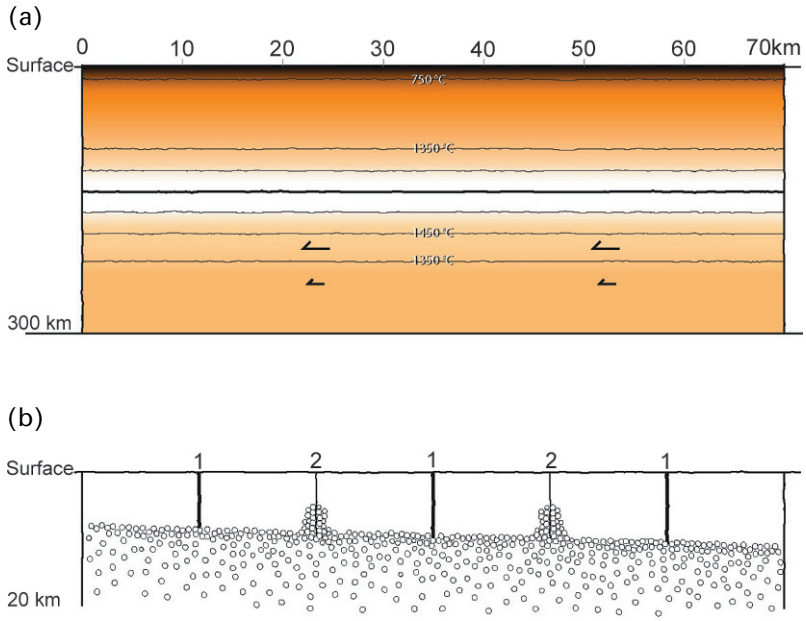

Figure 6.1. The sketch shows fluid flow from the mantle below the SISZ up into the elastic/brittle crust in vertical cross-section along the SISZ. (a) Temperature gradients below and above the 120 km depth where basaltic fluids are released from the mantle, indicated in white (Ito *et al.*, 1999, 2003). (b) Small circles indicate high pore fluid pressures at the base of the low-permeability brittle crust. At two places they rise above the B-D boundary in response to plate motion strain. Vertical lines labeled 1 are faults of earthquakes that were released long ago (say 100 years). Lines labeled 2 are faults of earthquakes yet to come (i.e., faults that released earthquakes several hundred years ago, gradually being reborn with the help of high-pressure fluids penetrating up from below).

patches of high fluid pressure and instability inside the fault itself. Earthquakes that occur on one of the hard patches somewhere in the fault itself can grow to become large earthquakes if stress conditions are homogeneous along other parts of it. Thus if stress is high enough for an earthquake somewhere along the fault it may trigger a whole fault rupture if surrounding stress conditions (say, pressure normal to the fault) have evened out along the whole fault.

Earthquakes are built up and released at seismogenic depths in the SISZ in the interplay between local buildup of high pore fluid pressures (mainly because of compressible fluids from below) and general strain buildup by plate motion along the SISZ plate boundary. This complex process is better explained in the figures.

Figure 6.1 shows fluid flow from the mantle up into the brittle crust. Mantle flow from the deep center of the Iceland Hot Spot releases hot basaltic fluids from depths of 100 km to 120 km to migrate upward in the crust. Below the B-D boundary, the crust temperature gradient reflects ductility and high permeability. On reaching the boundary of the elastic/brittle crust, where intrinsic permeability is low, fluids

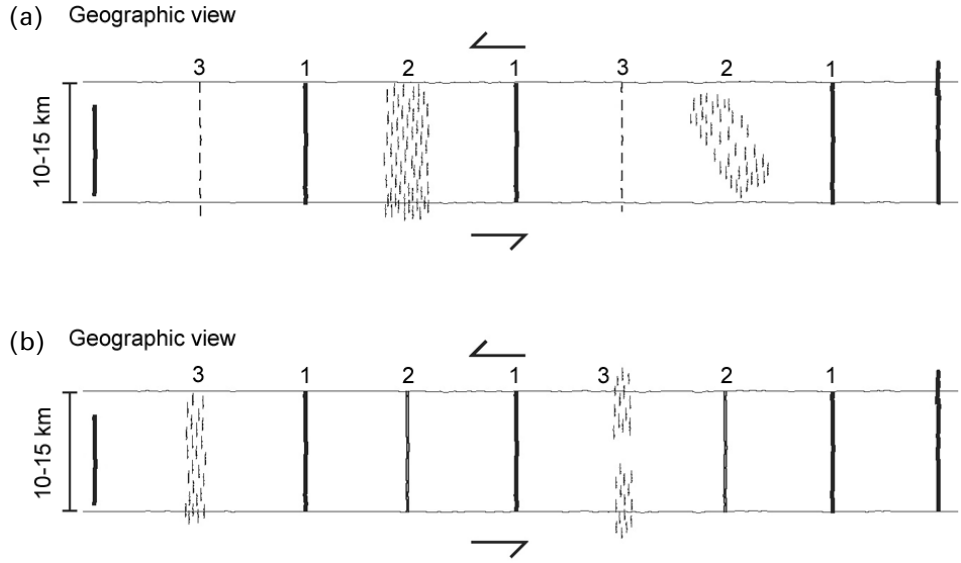

Figure 6.2. (a) The distribution of micro-earthquakes before large earthquakes at places labeled 2, resembling the real seismicity in the SISZ from 1991 to 2000 before the large 2000 earthquakes (Chapter 4). (b) The situation in the future long after the earthquakes. The high pore fluid pressures (at 2) around the epicenters have been released, but areas of renewed microearthquake activity (3) have been created, reflecting renewed buildup of high pore fluid pressures at new places in response to steadily ongoing plate motion.

concentrate and create volumes of high pore pressures, which in response to plate motion strain penetrate up into the brittle crust where they modify stress conditions locally.

Figure 6.2 visualizes the distribution of micro-earthquakes (reflecting local high pore fluid pressures), in horizontal view, at seismogenic depths along the SISZ, before and after a large earthquake.

Figure 6.3 shows how failure conditions around an individual principal earthquake like the one on June 17, 2000 is gradually created over tens to hundreds of years by fluid "corrosion" of the crust in response to plate motion strain. The buildup/release cycle of each large-earthquake fault takes more than 300 years in the SISZ.

The results described in this section indicate that the prediction in time and space of an impending earthquake is dependent on keeping a weather eye on rheological conditions and extrapolating from local information of changing crustal conditions into the near future and nearby places.

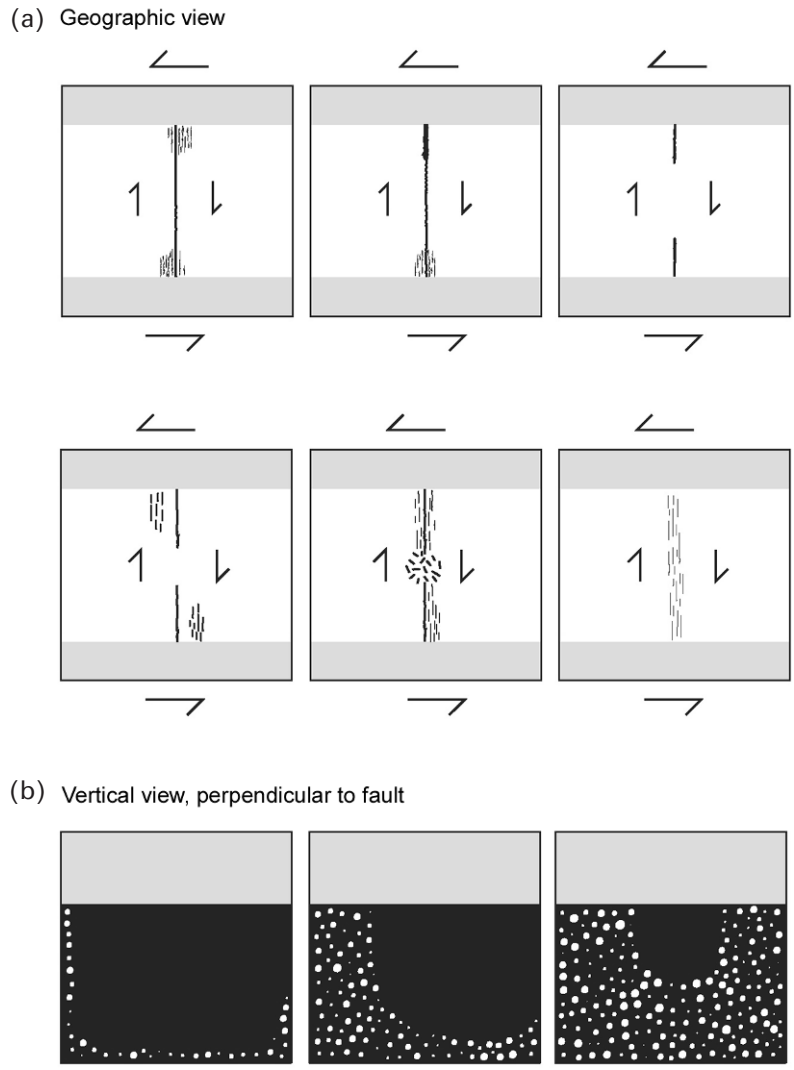

Figure 6.3. Gradual corrosion of the crust around an old north–south fault since the last failure, which was more than 300 years ago. (a) A horizontal view in which white indicates relatively low viscosity in the 10 km to 15 km wide SISZ compared with its surrounding (gray) in the viscoelastic crust around the impending earthquake. (*From left to right and down with time*) A horizontal view of how fluids migrating upward in response to plate motion cause earthquakes as a result of micro-fissuring (short line segments) at the boundary between lower and higher viscosity. Gradually a hard core (an asperity) forms and significantly modifies the stress conditions around the fault as a result of its strength. At last it starts to crack in a random way and breaks, thereby allowing slip motion along the fault as a whole. (b) From the side of the fault we can see how the strength of the asperity is gradually lowered. High-pressure fluids eat into the hard core (the shrinking asperity) from viscosity contrasts at the brittle–ductile boundary at depth and from both ends of the old fault.

6.3 THE EARTHQUAKE CYCLE IN THE SISZ

6.3.1 A hypothesis for the earthquake cycle in the SISZ based on the F-S model and observations

The SISZ is a fractured shear zone that varies in width from 10 km to 20 km at the plate boundary. It is dynamically heterogeneous and its heterogeneities are time-dependent. They depend on local inflow of high-pressure fluids from below into the brittle part of the crust. This upward fluid migration, probably mostly compressible water, occurs in the interaction with strain buildup caused by large-scale plate motion. The F-S migration model together with the closely related asperity model (discussed and compared with observations in Chapters 4 and 5) is our basis for the following description of the buildup and release process of earthquakes in the SISZ.

Step 1. The buildup of a fluid well occurs at lithostatic pressure below an old fault near the bottom of the seismogenic crust (i.e., near the brittle–ductile boundary) in the SISZ. We do not know how long this buildup process takes (i.e., the time since the last fluid release in a large earthquake at each site), before it will contribute to the buildup of conditions for a new release process. In a large part of the zone, earthquakes have not repeated on the same fault for at least 300 years indicating that this buildup time at each earthquake site is slow compared with the buildup time of plate motion strain in the zone as a whole, which is ~140 years before the break-up of it as a whole. The upper part of the old fault released pore/fluid pressure and healed well after the last large earthquake. The deepest part of the fault did not completely heal after the last earthquake, and pore fluids were trapped keeping it open, as can be seen in long-term remnants of seismicity of individual earthquake faults (see, for example, Figure 5.1). After some delay fluids from beneath the brittle–ductile boundary start to feed the deepest part of the fault and gradually high pressures are built up. The buildup process for a large earthquake on the fault in the brittle crust originates from the interaction between stable slip on the deepest part of the fault down in the ductile layer and the buildup of strain and stress in the upper part where no overall strain releasing slip occurs for the time being.

Step 2. Fluids (mostly water) at the bottom of the elastic/brittle crust infiltrate upward into the brittle crust in response to plate motion strain, especially along low-pressure heterogeneities. Such low-pressure heterogeneities are at this early stage likely at the ends of the approximately 10 km long fault (i.e., where weak fault zone viscosity meets higher viscosities outside the zone). These fluids do not normally cross the H-L boundary (some 3–4 km deep), but create volumes of near-lithostatic pore fluid pressures below this depth. Gradually, upward migration weakens and corrodes some parts of the fault, leaving some parts—possibly a central part—unfractured. Fault motion at depth coupled with a strong unfractured part of the fault (i.e., an asperity) gradually modifies strain patterns around the fault creating low-pressure channels where fluids continuously infiltrate, until the fault slips as a whole. The dilatant region created in this way around the fault only produces small

earthquakes because of the heterogeneous stress field and the stabilizing role of fluids against larger earthquakes (i.e., stress hardening, see Chapter 5). Slow slip, especially along the deeper part of the fault, and upward fluid migration inside it build up patches of weakness intermittent with hard dry cores which do not fracture or yield until stress is sufficiently high to break them. If stress drop is high enough and the other parts of the fault are weak enough, an earthquake occurs which rips through a large part of the corroded fault and ultimately goes through the whole crust, releasing both plate motion strain and pore fluid pressures. Intermediate-size earthquakes may of course occur on parts of the fault during the long time of its development before a large earthquake. However, intermediate-size earthquakes neither rip through the whole crust nor release a significant part of the pore/fluid pressure. It is also worthy of note that (as was the case in the second earthquake in 2000) the first earthquake can serve to unlock a second earthquake on another fault and trigger a nucleation process there, especially if this fault has already reached a high degree of instability.

Step 3. During and after a large earthquake, high pore pressures and plate motion strain are released at seismogenic depths, but fluids continue to flow toward the fault and lubricate it. This had long been reflected in micro-earthquakes that concentrate densely along the fault, especially at the ends of the fault and at other spots where the slip along the fault was incomplete in the earthquake. However, this inflow ceases with time and the fault locks or heals effectively, especially the shallower parts, where high-pressure fluids have dried out, and are cooler than below. The fault is expected to heal from above because of precipitation of minerals during cooling of upward migrating fluids. This healing from above can be seen in the distribution of seismicity with depth on earthquake faults where some 100 years have passed since the last earthquake (Figure 5.1). A scar is left in the deepest part of the fault which in due time will start again as Step 1 at this very place. We do not know how long it will take for this fault to produce a large earthquake again. In 300 years of observations of historical seismicity we have not seen a repetition on the same fault, probably the only exception was the fault in the westernmost part of the zone (i.e., close to the WVZ, Figure 4.7). However, we must be mindful, based on studies of *b*-values and surface fissures, of earthquake faults that may be denser than those observed during the last 300 years. Some earthquakes pre-dating 1700 seem to have occurred at significantly different places from the later earthquakes (Clifton and Einarsson, 2005; Angelier *et al.*, 2008).

6.4 FROM EARTHQUAKE PREDICTION RESEARCH TO USEFUL WARNINGS AHEAD OF LARGE EARTHQUAKES

The crustal processes described here and the earthquake cycle indicate that any approach to practical warnings has to be gradual (i.e., from identifying places demonstrating preparatory activity long before the earthquake occurs to studying

and modeling the dynamic process by adequate multidisciplinary observations. The objective of watching procedures should be to discover constitutive laws that describe the future of the process in each case.

6.5 EXPECTED AND OBSERVABLE PRE-EARTHQUAKE PROCESSES

No two earthquake preparatory processes are the same. However, the following common features should be continuously studied both by observations and near–real time Earth-realistic modeling. The goal of modeling is to create constitutive laws to extrapolate ongoing fault processes into the future:

- Pore fluid pressures that are near-lithostatic migrate episodically upward into the crust of the SISZ in response to strain and modify fracturing conditions there on both a long and a short timescale.
- In the long term, corrosion of an old and partly solidified fault starts at depth, just above its deepest and unsolidified part. Corrosion is driven by strain caused by general plate motion and by the local source of high-pressure fluids which are created at rheological contrasts at the B-D boundary of the crust, at a depth of around 10 km. Corrosion also grows at the north and south ends (which are under strain) of the faults where the fractured rock of the SISZ meets the slightly stronger (higher effective rigidity) rock to the north and south of the zone.
- The stress field is strongly heterogeneous near reactivated faults within the SISZ, both in time and space. On the fault itself we have, in time, growing patches where fluid pressure is high and the fault is unstable (i.e., it slips easily). We have, in time, diminishing patches of hard and dry cores, which are obstacles to overall slip on the fault. Around the fault we also expect an irregular stress field, both in time and space, created by deformation in the close environment of the active fault and strain-conditioned fluid flow from below.
- Crustal processes can be expected before large earthquakes occur in the SISZ, which are probably observable decades to minutes before them. Observations of these may in time reveal significant information regarding the site, fault size and stresses, or—more generally—fracturing conditions before an impending earthquake. A large earthquake occurs after a long period of reactivation of an old fault, when the shearing stress in a hard core (or cores) on or near the fault has reached the breaking strength of the dry unfractured rock and when uniform instability is reached along a major part of the fault itself. This may be expressed in the directivity of locations of seismic sources and fault plane solutions of micro-earthquakes, and especially in Coulomb failure stress values, which are close to zero. This may in general be expressed in various observable effects that reflect slow slip along these parts of the fault.

Based on experience in the SISZ test area, all of the processes mentioned in the last paragraphs and highlighted by bullets are observable with existing micro-earthquake technology (as briefly described earlier, see Chapter 3). The most significant

information about processes expected before earthquakes (i.e., those in the seismogenic parts of the crust) will be carried by pore pressure–triggered micro-earthquakes, some well below magnitude 0 and revealing high *b*-values. The objective of observation schemes for earthquake prediction purposes should be to maximize the sensitivity of seismic monitoring around likely impending earthquake faults and to enhance existing technology to interpret observations in real time.

Although micro-earthquakes bring us detailed information regarding crustal pre-earthquake processes, GPS monitoring is significant in providing constraints on the state of the active volume and for its long-term observation. Borehole strainmeters with their enormous short-term sensitivity will help to detect possible intrusions of incompressible fluids and near-surface effects that reflect deformation and slips at depths. The same can be the said for radon and other geochemical monitoring. Monitoring of water in boreholes at a high sampling rate and at the right place may sense strain changes at depth, related to the slow pre-earthquake slip on a large fault, better than direct deformation measurements.

6.6 MICRO-EARTHQUAKE TECHNOLOGY IS A POWERFUL TOOL FOR OBSERVING PRE-EARTHQUAKE PROCESSES

The most significant available tool to monitor processes ahead of large earthquakes is micro-earthquake technology, which involves both basic monitoring and detection technology as well as the interpretation methods needed to observe continuous crustal processes.

Based on the experience of various approaches in Iceland, detecting the site of an earthquake fault at a preparatory stage and monitoring its development to becoming a large earthquake can be done most effectively by

(1) Evaluating the distribution of micro-earthquakes in time and space. This includes the value of information carried by them for source studies, fault planes, inversions of fault plane solutions to find stress directions, and calculation of absolute stress and instability, all of which should be complemented by historical and geological studies.
(2) Studying the path effects of waves from micro-earthquakes, such as shear wave splitting, revealing changes in shearing stress and fracturing conditions, and P/S velocity changes (possibly reflecting changes of effective rigidity and volumes of high pore pressure).

Monitoring and evaluation methods were briefly described in Chapter 2 (especially Appendix 2.A), Sections 3.4–3.8, and Chapter 4.

6.6.1 Scaling of measurements

In all such observations we must be mindful of the scaling of measurements. Under conditions that can be explained by the F-S model, our success is based on measuring

very small movements in the preparatory stage of a large earthquake. We cannot assume that pre-earthquake stress will gradually build up to a level that results in a large earthquake, when the breaking strength of the crust is reached. Heterogeneities, especially fluids flowing around in the crust in a random way, will defeat any method of calculating this. Instead, we should make use of heterogeneities and try to catch the signal they transmit ahead of the earthquake, analogous to weather forecasting when meteorologists try to detect a deep low-pressure system that may in time become a significant weather hazard, when it hits a coast or a mountain range. But, if we are to catch a signal lasting a few hours or a few days, which is in practice the maximum length of a signal for short-term warnings ahead of earthquakes, our observation density has to be much greater during that period and, to get rid of all sorts of noise on the surface of the crust, we need a sampling rate that is several times greater than the disturbing frequencies in the noise.

Strain buildup over the whole earthquake cycle lasting decades to hundreds of years is comparable with the strain released in the few seconds of the earthquake's life. Significant strain changes taking hours to days in interseismic periods are hardly measurable by any of the direct methods used for deformation estimation, not only because of noise but also powerful yet poorly understood filtering effects in the crust that combine to make resolution in the signal impossible. However, high-frequency seismic waves from frequently occurring micro-earthquakes contain the necessary information for the wave path to be corrected and the necessary resolution to see seismic slips, just a fraction of a millimeter in size down in the seismogenic crust, a signal demonstrating the nucleating micro-fracturing that is a forerunner of an earthquake. Observations of short-term processes before the initial 2000 earthquake can be used to verify this.

As discussed in Chapter 4, micro-earthquakes displayed some 2–3 weeks before the first 2000 earthquake a pattern that is interpreted as caused by slow pre-earthquake right-lateral slip in deep parts of the north–south striking fault. As described in Section 4.7.4, even very sensitive borehole strainmeters placed 2 km to 20 km from the fault did not sense it—at least, not well above the noise level. We do not know the velocity of slow slip motion along the fault at depth during this period. However, the absence of a contemporary strain signal tells us that it was very slow, but we can estimate the maximum rate from the absence of the signal. Over a fortnight a strainmeter can be expected to sense continuous buildup or release of 10 nanostrains (i.e., 10^{-8} strain). Fault motion of 0.1 mm at a depth of around 5 km would give such a signal. So, the lack of a pre-earthquake strain signal indicates that slip across the earthquake fault plane, which seems to have started 2–3 weeks before the June 17 earthquake, was less than 0.1 mm at a depth of 5 km. Strain monitoring also indicates that the fault was effectively locked at shallower depths near and above the hydrostatic pressure boundary. Slow slip at shallow depths would probably have caused disturbances in the rock–fluid equilibrium. Slow quakes or short-term rock–fluid pulses, measurable by the nearest strainmeter, would have occurred at these shallow depths. Individually, micro-earthquakes that were observed at a depth of 5 km or deeper had slips of only 0.01 mm to 0.1 mm. During this period of time, micro-earthquake sources covered only very limited parts of the fault plane in the

brittle crust, so the total slip during the fortnight of pre-earthquake time was less than this. Nevertheless, as observed, slip motion could be sensed from information carried by the micro-earthquakes.

The detection of earthquakes in the SISZ is almost complete down to magnitude 0. When studying the pre-earthquake process at depth, using available micro-earthquakes below that magnitude, better information was gained. The high *b*-values of seismicity near the bottom of the elastic/brittle crust also indicate that below this depth—where seismic resolution is good—there may still be more micro-earthquakes that could give significant information, in accordance with the hypothesis that high *b*-values are found in environments subject to high pore fluid pressures (see Figure 4.11).

The fact that seismic signals smaller than magnitude 0 (i.e., down at the limit of seeing such a signal with the present seismic system) carry information that is significant indicates that a denser network should be applied around the fault of an impending earthquake to increase sensitivity so that such a small pre-earthquake slip can be detected as expected. It also implies that tools designed to monitor even weaker signals, possibly not resolvable as individual micro-earthquakes but as endogenous noise, could be chosen to observe such small slips, connected fluid movements, and phase shifts.

6.7 SIGNIFICANCE OF DEFORMATION MONITORING

It is very significant to study the strain field and how it changes over time by direct observation of deformation by borehole strainmeters, GPS measurements, and InSAR imaging. This is significant for understanding and modeling both long-term and short-term preparatory processes ahead of earthquakes.

Although strainmeters in the area (the middle part of the SISZ) did not directly show the slow slip motion at depth before the first earthquake in 2000, the absence of a signal is significant for understanding the faulting and nucleation process. The same can be said about the use of GPS or other comparable observations of deformation, such as InSAR images. Short-term changes that occur prior to earthquakes (as we have already observed) seem to be too small to be measured by the technology available to us at the present. Measurements are currently made on the surface, where there is much atmospheric noise. Moreover, signals stemming from the seismogenic crust deeper down are strongly attenuated and affected in a complicated way. However, because of the long-term stability of GPS and in some cases InSAR measurements, they are significant for long-term monitoring and modeling of pre-earthquake processes. They are also very significant for fast modeling of the effects of a primary earthquake and of its deformation in a large area, which can be significant for warnings ahead of triggered or coupled earthquakes, besides their general importance for understanding earthquake release processes.

While what we have just discussed refers to the middle part of the SISZ, near the volcanic zones at its extremities the intrusion of incompressible fluids may be greater and make deformation measurable by borehole strainmeters or GPS. In 1987

borehole strainmeters sensed, from distances between 20 km and 40 km, pre-earthquake activity before a magnitude-5.8 earthquake, which occurred at the junction of the SISZ and the EVZ. This was suggested as being caused by magmatic intrusion in this recently volcanic area (Ágústsson *et al.*, 1999).

6.8 OTHER SIGNIFICANT OBSERVATIONS REFLECTING SHALLOW PROCESSES THAT CAN BE MADE PRIOR TO EARTHQUAKES

Observable shallow processes in the crust (i.e., processes that take place in the fractured and water-saturated uppermost part of the crust above the seismogenic part) are the most frequently reported phenomena preceding earthquakes. Such observations may be significant for alerting and short-term warnings, even if we cannot relate them physically to the earthquake process for the time being. Many such observations can be explained as secondary reflections of processes, such as strain changes down in the seismogenic crust. Strain changes may not be directly observable by deformation measurements on the surface, but can be amplified in the fractured part of the crust, near the surface. Variable local conditions near the surface may influence how these stresses appear and where. It is therefore difficult to use them to describe the crustal process we are trying to monitor.

As the physics of preparatory earthquake processes becomes more sophisticated it will gradually be possible to better understand shallow, possibly earthquake-related processes. History provides us with many tales about animal behavior, phenomena in the sky, sounds, changes in water height, etc. We should take such stories into account in our preparations, add them to our state of readiness, use them to draw our attention to what may be going on and try to explain them in our pre-earthquake modeling. Reluctance to listen to descriptions by Joe Public about unusual phenomena he has observed is not only arrogant but a negative aspect that all sciences display during their development.

The following observations are examples of significant pre-earthquake phenomena even if they cannot definitively be related to our model of earthquake preparation.

As described in Section 4.7.4, 19 days before the June 17 earthquake the strainmeter at Station SAU, close to the fault, showed a 400-nanostrain contraction signal and a rise + relaxation time of 24 hours. Such a signal has not been seen at this station since 1982, when several similar signals were observed over a period of one year. These signals have been confirmed to be of shallow origin, certainly no lower than 2 km. A tentative interpretation is that there had been a small rock slip that released a flow of water at a shallow depth near the station, but it might reflect a deep pre-earthquake slip, amplified in the fractured rock near the surface. Even if we could physically see such phenomena ahead of earthquakes, it is not easy to use them in isolation for warnings, as we have so far no physical link to the pre-earthquake process, although we can claim afterwards that they were most likely caused by such a process. The same could be the case for GPS measurement at a single station. It might reflect a motion that is caused locally in the shallow fractured part of the crust

by some pre-earthquake process, but not confirmed to be a pre-earthquake signal until after the earthquake.

Measurements of water heights in boreholes where the water supply reaches seismogenic depths can be, in effect, like a huge strainmeter sensor down at these depths. We saw a good example of this before the June 17 earthquake, which coincided with fault movements one day before the earthquake (Section 4.7.1). In the SISZ there are many boreholes at which such monitoring could be carried out. What is more, selecting some of them for continuous monitoring is a relatively inexpensive way of monitoring crustal changes. However, our knowledge is not yet at the stage where sites can be pinpointed for drilling holes for monitoring purposes. Moreover, there would be the question of where to put limited funds (i.e., would they be better placed to monitor signals that physically can be related to the pre-earthquake process in question?). But, observations of many phenomena by people (or instruments that are already in use) may be an inexpensive way to obtain significant information, especially if it only involves the additional cost of bringing observations to the monitoring center.

Radon anomalies that were observed before the June 2000 earthquakes (Section 4.8) were directly caused by processes in a shallow and fractured part of the crust, though they might also be explained by processes taking place deeper down (over a large area) that preceded the earthquakes. Such observations can be enhanced by monitoring other chemicals released from rock in the shallow fractured crust and of chemicals with a more direct mantle origin, like helium and carbon dioxide. A problem with such monitoring is that (for the time being at least) it is difficult to relate it to the preparatory processes of an individual earthquake until it is too late. However, by further physical modeling we can expect to better understand the causes of shallow processes, so it may be better to treat them as complementary to pre-earthquake processes that are better understood physically.

Swarms of very shallow micro-earthquakes no lower than 3 km deep in the fractured uppermost part of the crust may be induced by interaction between deformation at depth and high fluid pressures from above. Such an intensive swarm was observed 6 months before the 2008 earthquake in the SISZ, only 4 km to the east (Section 4.11). A plausible explanation given later was that it was demonstrating deformation at greater depths. The scientists at IMO who noticed this swarm actually thought this might be a precursor to a large earthquake release. However, no physically established link between such a swarm and an impending earthquake was found and there were no other measurements at that time to constrain such a connection.

No two earthquakes are the same, hence no two preparatory processes can be assumed to be the same. Previous earthquakes can and do teach us about shallow phenomena that precede them. This can be used to alert us to the probability of an impending event. But if we are to predict an earthquake—its site, size, and time—we must take the deterministic route of detecting and analyzing the long-term preparatory processes of the earthquake itself and ascertain where this process is bound to go. This is based on our understanding of the causality between physical events that are close in space and time in order to discover the constitutive laws that describe the

future of the process. Many of the observations that we now call phenomenological because of the lack of such an understanding may become more useful in the future when we better understand physical causality in the crust.

6.9 THE FLUID–STRAIN MODEL AND ITS CONSEQUENCES FOR MONITORING PRE-EARTHQUAKE PROCESSES

New achievements made by the research community and improved methods of observations are combined in the new dynamic models for pre-earthquake processes (as described in detail in Chapter 5). All earthquake prediction efforts and the work carried out by warning services depend for their success on careful Earth-realistic modeling, which should be carried out continuously to interpret the steady flow of observations and to detect details of the seismogenic process.

The F-S model is not the first model to explain foreshocks or other premonitory changes preceding earthquakes. Models describing rate/state-dependent friction explain the release of foreshocks before earthquakes and the aftershocks that follow them (Dietrich, 1992; Roy and Marone, 1996). Rate/state models describe movements that start on a small scale across an old fault. The assumption is usually a fault plane with various degrees of roughness between the fault walls (a function describing the state of the fault), with static stress across it, and with the inertia of mass movement, which is especially significant during the pre-earthquake period. It is possible to take changes in normal pressure on fault planes into modeling assumptions, which in many cases is equivalent to applying fluid pressure from inside the fault. Modeling is based on laboratory experiments which apply stresses to rock samples. The basic assumption in the rate/state-dependent model for pre-earthquake processes is that they start to work when pre-earthquake slips commence on the assumed fault. Many applications of the rate/state-dependent model will certainly be useful in modeling pre-earthquake processes in the SISZ.

The F-S model is volumetric and explains time-dependent stress heterogeneity in space. The main cause of time-dependent heterogeneity in the crust is fluid mobility. When fluid pressures at the bottom of the brittle crust and local plate motion strain reach breaking point, fluids can rise in the crust and modify the fracturing conditions there in both the short and long term, if the crust does not quickly release its fluid pore pressures to the surface as happens in volcanic areas and in high-temperature fields.

Although an old fault is assumed to be the locus for earthquake slip that is developing, a large volume of pre-earthquake processes take place around the fault. Stresses vary with time through the whole of this volume. The only way to get an idea of the complicated stress field (i.e., to have enough resolution) is to observe the loci of micro-earthquakes and the stresses released individually by them. There are two significant approaches to this. First, estimate the stress around individual micro-earthquake sources when they occur, based on earthquake mechanisms and by assuming near-lithostatic pore fluid pressures (see Section 4.9.3). The other approach is to analyze and map the location of fracture criticalities reached in time and space

(Coulomb stress limit), without necessarily knowing *a priori* the contribution of each, the fluid pressure, or strain. This means that we are watching how fracturing proceeds in reality and can extrapolate from that (see Sections 4.7.2 and 4.7.3). Because of the many unknown parameters in all such studies, both approaches should be used. Stress, relative stress, or closeness to fracturing criticality can also be studied by shear wave–splitting recorded in the crust above swarm activity (Section 4.9.4). It integrates the stress values over the volume containing the wave path from the source to the seismic sensor, but has less resolution than methods directly based on stress release in the sources of micro-earthquakes.

6.10 CONTINUOUS WATCHING IS NECESSARY

Both because pre-earthquake processes can be observed and because we cannot assume that they are the same for all earthquakes, every earthquake fault showing signs of pre-earthquake processes must be continuously watched. This may sound an impossible task. But with the help of computer technology it can be done. To a degree, such a watching system already exists in the automatically and manually run SIL system in Iceland, which extracts significant information from micro-earthquakes. We have to incorporate other significant monitoring into the same automatic system. We have to develop a watching system that merges all data and adapts models to include them. We have to hire a few extra scientists to help in real-time research. We have to organize a geo-warning system to effectively make use of all the geophysical information and set up rule-based schemes to provide warnings. I am not estimating the cost of such a project, but compared with the disasters it can help to prevent, the cost is low.

The pattern that characterized the last 9 years before the earthquakes in 2000 in the SISZ was a part of a process period that probably lasted for many decades on or around the activated fault. It was observable during that period, but could have been much better observed if the technology available today had existed at that time. The long-term process expected according to the F-S model is complex and self-organizing to a certain degree, and we don't know yet how to set up a model of internal causality which would predict long-term development. It is much easier to predict at a given moment the short-term evolution of an active fault which little by little will help us to set up constitutional relationships to extrapolate our observations gradually to the impending earthquake. To extrapolate the process into the future our observations must have the resolution to describe a semi-continuous process in time and space. In much the same way as a row of digits can describe the future of a continuous signal, if we can assume that we know the form of it. As in signal theory, the time between observations must be significantly shorter than the period of the signal that we are trying to describe in our extrapolation.

This book demonstrates the importance of extending the time of observation of each site of every earthquake back in time, as far back as information is available. The aim is of course to have as much information related to this site and this fault as can be made available.

6.11 LARGE CRUSTAL EVENTS TRIGGERING EARTHQUAKES

We described in Section 3.4.3 the successful and useful warning made before the second of the large June 2000 earthquakes in Iceland. This earthquake can be considered a continuation of the first earthquake. Micro-earthquakes occurred on that fault soon after the first earthquake and their distribution indicated linearity along the expected fault plane. Observers at IMO correctly predicted it and warned communities and civil defence committees even though they felt it only probable. As for time prediction they simply provided the following wording: ''Be prepared for an impending earthquake at this fault anytime soon.''

Those receiving this warning prepared for an immediate earthquake, but the warning did not go public following the advice of IMO observers.

The warning could have been much more definite and possibly useful as a public warning had more information been available about the triggering power of the first earthquake at the site of the second and about the crustal conditions prevailing there. Rapid hypocenter location of the micro-earthquakes that occurred between the first and second earthquake was all that was applied for the prediction—not more detailed source information. Rapid estimation of the CFS (Coulomb failure stress) exerted by the first earthquake on a probable fault nearby, based on direct deformation measurements by GPS (Section 4.11), would certainly have helped in constraining better what was imminent.

Another example of one earthquake triggering another was the second earthquake with a magnitude around 6.2 in the western part of the SISZ on May 29, 2008, which was immediately triggered (as described in Section 4.12).

The main shock of June 17, 2000 which triggered shocks with magnitudes larger than 5 some 100 km away is another example of immediate triggering (Section 4.11.1). The few seconds between the initial earthquake and the triggered event gave no time to react. However, it would be significant for rescue purposes to know as soon as possible the site of triggered events. Such a prediction should be part of predicting the initial earthquake, but it calls for profound knowledge about constantly changing fracturing conditions in the area of the triggered earthquake even before the initial large earthquake struck. A dynamic map indicating closeness to fracturing criticality at any site in the SISZ would have been needed to predict secondary earthquakes in the zone following the large earthquake.

We saw in Section 4.11.2 an example of triggering, caused by the eruption of the volcano Hekla, of a crustal process which led to seismic activity in a large area, some 30 km long. There are indications that magmatic intrusions before the large Vatnajökull eruption of 1996 led to micro-earthquake swarms and stress changes more than 150 km away (Sections 4.9.4 and 4.10.5). In many cases we have neither the knowledge nor physical model to constrain or reject the possibility for triggering at long distances. More intensive micro-earthquake and deformation monitoring will gradually help long-distance triggering to be understood.

In general, understanding how observed crustal events come to be coupled is very significant for prediction. More multidisciplinary modeling is needed. Geophysicists often claim that an earthquake cannot trigger another at long

distances. This is based on the fact that an earthquake causes much less strain change at the second site than ocean tides or frequent changes in atmospheric pressure. As has already been pointed out, such a statement is based on models that are far too simplistic to describe the real crust where, as has been demonstrated, the conditions for releasing earthquakes vary rapidly with time and from site to site.

6.12 WHAT DOES THE FUTURE HOLD?

Pre-earthquake processes are faint and hard to detect; even with modern instruments it is difficult to observe them. These long-term processes are a result of shearing in a large area (measurable by deformation instruments) and the distribution of seismicity, which is also expected to show changes shortly before large earthquakes (as described in Chapter 4).

Very significant information comes from micro-earthquakes that are smaller than magnitude 0. Magnitude 0 was set at an early stage as a goal for the seismic observing system in the SISZ (Chapters 2 and 3). There is a need in the SISZ to apply methods able to measure hydrofracturing at the bottom of the brittle/elastic crust more satisfactorily. This can partly be achieved by increasing the number of micro-earthquake sensors around a fault that is in a preparatory phase. There is also a need to discover whether the process of increased hydrofracturing related to beginning fault slip at depth could be better observed by acoustic methods. Such a hydro-fracturing process coupled with fluid flow may give rise to high-frequency harmonic tremors or apparent tremors caused by a continuous sequence of micro-earthquakes that are so small and so dense that they cannot be resolved as individual events. Monitoring low-frequency earthquakes that are related to fluid intrusions should also be studied with the aim of getting a better idea of the preparatory process.

7

Earthquake warnings to government bodies and the public

Warnings of impending earthquakes are made on various timescales and for various purposes. In some cases a warning may lead to better observation of a particular area. In other cases a warning may lead to rescuing people from houses that may be vulnerable to the expected hazard. In countries where destructive earthquakes are the norm, there needs to be continuous interactive communication between geoscientists and government bodies regarding observation, prediction, and selection of the most appropriate steps to be taken to mitigate risks. Warnings may involve assessing the effects of a destructive earthquake in a particular area. Earthquake warning may involve assessing which fault will most probably rupture next inside a seismic zone. Warnings may be time-dependent (i.e., indicating on a short-term or long-term basis the imminence of an earthquake).

Significant warning systems have been established to warn for the effects of large earthquakes in many countries. The goal is to help rescue work and to mitigate the destructive effects of earthquakes on people and societal infrastructure, even if it was not possible to give a warning ahead of them. Worldwide, there are now systems that warn for so-called "coupled events" (such as tsunamis caused by earthquakes).

Warnings from the scientific community include providing clear advice to government bodies about risk-mitigating actions that need to be taken. These actions can be anything from increased monitoring and enhanced scientific evaluation to rescue in the case of a destructive imminent earthquake on a short-term basis. In Iceland warnings to the public and government bodies go through the National Civil Protection Agency (NCPA) which, based on information and advice from the scientists, takes the necessary steps (such as advising people about precautions to be taken). Predictions of an earthquake are never issued without advice on what to do and how to be best prepared for it.

In light of frequent volcanic and seismic hazards in Iceland, procedures have gradually been developed for interactive communication between Earth scientists and government bodies. Communication is via telephone and email and if there is

R. Stefánsson, *Advances in Earthquake Prediction: Seismic Research and Risk Mitigation*, Springer Praxis Books, DOI 10.1007/978-3-540-47571-2_7, © Springer-Verlag Berlin Heidelberg 2011

time by meetings. On the initiative of scientists or the NCPA an advisory board is called to evaluate and discuss data concerning the likelihood of an earthquake and about actions to be taken. These meetings involve scientists from several institutions and representatives from the government (mostly NCPA staff).

When scientists consider an event to be imminent they report this to the NCPA or directly to local Civil Protection groups, which are linked to the NCPA and usually also linked to local councils. This report contains a description of the likely impending event and advice on how to prepare for it. Civil Protection then take the relevant preparatory action and inform the public when they consider the threat to be real together and give advice on how to prepare for the possibly impending event.

7.1 WARNING SCENARIOS FOR EARTHQUAKES AND OTHER GEOHAZARDS

Earthquake warnings must be based on continuous and well-organized observation of what is going on down in the crust. The same is true for warnings of volcanic eruptions and coupled events such as tsunamis, landslides, and avalanches. Continuous monitoring of many kinds of geophysical observations is necessary. Significant information may come from many other kinds of observations as well, such as observations and reports from the public. Evaluation and comparison of the various observations must be as fast as technically possible. Effective geohazard watching also involves research into what the observations mean. On the one hand, this is based on earlier research results, and, on the other hand, ongoing research as a result of intensive observation—"real-time research" as it is sometimes called. The results of this research activity must be available for scientists monitoring the activity to be able to apply them in time for the expected hazard.

Effective watching needs to be backed up by an automatic and manual system for data to be merged quickly, for modeling and for comparison with earlier observations. The aim of such a system is to detect automatically and to merge together various patterns (or signals) that have earlier been found before large earthquakes. Equally significant is the work of scientists interpreting these changes and looking for unusual patterns in the data, patterns not seen before, which may be significant for understanding ongoing crustal processes. A major part of watching is getting new research results into a database, where they can be easily accessible to the multidisciplinary group of scientists involved.

Let us now discuss a watching system that is under development and whose main objective is to provide warnings of impending earthquakes. Watching systems for other geohazards are in many ways similar.

The first task for an earthquake-watch procedure is to discover where a large earthquake is probable, to estimate how soon it may occur, and what effects (intensities, accelerations) can generally be expected. Such estimations change with time, as our understanding of the focal region and the earthquake in question develops. This is based on the assumption (described in Chapter 4) that we learn most about

impending earthquakes and their preparatory processes by monitoring and interpreting significant observations from the region where earthquake preparatory processes have started. We assume that shortly before an earthquake occurs we can predict the place and the expected effects much better that we can do long before it. After the earthquake occurs, another watching task is to forecast earthquake effects (i.e., to predict the consequences and the destruction area better than we could do before it) and then supply all the emerging information to Civil Protection and rescue teams in the best possible way. It is also the goal of watching to try to predict the likely sites and effects of earthquakes and other geohazards that might be triggered by a first event (i.e., coupled events). In Chapter 4 (especially Section 4.4), I described examples of warnings of large earthquakes in Iceland. New methods have been found to help us discover significant changes predictive of large earthquakes. It would be wrong to claim that we can predict all earthquakes. However, with our present knowledge and observational techniques it is realistic to discover at an early stage an ongoing process that might develop into an earthquake. We will probably be able to issue some kind of warning before all earthquakes.

Taking our present understanding and watching capabilities into account, earthquake warnings are feasible under the following scenarios.

(1) A warning issued years to months in advance about the site, destructive power, and the overall affected area of an impending earthquake

Such a warning would allow scientists and the local Civil Protection group to take long-term steps to mitigate the risk. They would have time to compile background observations and increase the number of general observations. Data analysis and Earth hazard modeling, efforts to strengthen infrastructure, and local Civil Protection group preparedness in the area could be carried out without undue pressure.

(2) A warning issued weeks to days in advance

Local Civil Protection and rescue groups get themselves ready. Efforts are made to raise the preparedness of people. Increased sensor-based observations and increased scientific real-time watching.

(3) A warning issued days, hours, or minutes in advance of an impending earthquake

Local Civil Protection group preparations for an event are instantly triggered. Scientists and the local Civil Protection group communicate continuously to provide the best possible advice on the actions to be taken when the earthquake strikes and possible coupled hazards. They also participate in declaring an end to the warning period if the probability of an impending hazard is no longer considered a threat. Such a warning in much the same way as the initial warning would only be given to the public by Civil Protection organizations.

(4) The earthquake occurs

Actions are taken to mitigate the impact on people and societal infrastructure by real-time damage assessment and general advice is given on the best possible way

of reducing such an impact. Warnings for possible coupled events and estimation of their impact.

(5) Post-quake information
Explaining the science of the event to the public and governmental bodies. Assessing and warning for possible coupled events.

Observations and warnings preceding eruptions and glacial water floods are in many ways comparable with earthquake-warning scenarios. In many cases the same kinds of sensors are used, as is the case for the communication and evaluation systems.

7.2 FOUR MORE EXAMPLES OF OBSERVATIONS LEADING TO WARNINGS

Warnings and predictions of volcanic eruptions are in many ways similar to those that apply to earthquakes. The same monitoring and alerting tools are used, and in both cases we are trying to analyze the crustal process and anticipate what it is going to do. When developing geo-watching systems we should include earthquakes, volcanoes, and other geohazards. Three of the warning examples mentioned in the following sections are volcano warnings. Much of what we learn from them is of great value for earthquake warnings.

Section 4.4 described how it was possible to issue long-term warnings before the two magnitude-6.6 earthquakes struck in 2000 in the SISZ as well as a significant short-term warning before the second one. This success was brought about by long-time scientific research, real-time monitoring, and automatic (to a certain degree) evaluation of observations. Section 4.11 described a low-order, long-term prediction before a magnitude-6.3 earthquake in the SISZ in 2008 and a missed opportunity to give a short-term warning.

Chapter 4 (summarized in Section 4.12) also contains many examples of pre-earthquake patterns that, in hindsight, could have been used to improve warnings and bring about a more effective multidisciplinary geohazard-watching system.

In the following I will give a brief description of four more examples of warnings given before the geohazard in question occurred.

7.2.1 Stress forecast before the magnitude-5 earthquake struck in Ölfus, November 13, 1998

Analysis of shear wave splitting (see Section 4.9.4) allowed the successful stress forecast in real time of a magnitude-5 earthquake in southwest Iceland in 1998 three days before it occurred (Crampin *et al*., 1999).

Prior to 2000 there had never been real warnings or predictions of earthquakes in Iceland except for the so-called "stress forecast" by Stuart Crampin of a magnitude-5 earthquake on November 10, 1998 in the Ölfus area of southwest Iceland. The epicenter was near the western end of the SISZ at its junction with

the Western Volcanic Zone (WVZ, see Figure 4.1). The circumstances surrounding the forecast are described in Crampin *et al.* (1999).

Since 1994 volcano-tectonic activity had been ongoing in a large area around the Hengill volcanic complex (Figure 3.3). Seismic activity culminated early in 1998 with an earthquake of magnitude just above 5 on June 4 in the northern part of the area. This activity was closely watched by the Icelandic Meteorological Office (IMO) who, based on their experience of seismic activity between 1953 and 1955, feared a magnitude-5.5 earthquake in the southern part of the area, breaking crustal "barriers" south of Hengill.

On October 27 and again on October 29, 1998 Stuart Crampin of the University of Edinburgh sent an email containing a stress forecast to IMO, warning of an impending earthquake. This gave rise to discussion between Stuart Crampin at Edinburgh and me, Ragnar Stefánsson, at IMO (as described in Crampin *et al.*, 1999).

Based on a request from IMO, a meeting was held among scientific advisors of the Icelandic Civil Protection Agency where stress forecast data and other data from an area surrounding Hengill were discussed. The conclusion reached at the meeting was that no further action was required by the ICPA and IMO intensified seismic monitoring.

On November 10, 1998 Stuart Crampin sent another email containing a further stress forecast to IMO declaring, on the basis of recent estimates of shear wave splitting in the area: "This means that an event could occur anytime between now ($M \geq 5$) and end of February ($M \geq 6$)" (the exact wording is in quotes).

The stress forecast was based on stress changes estimated from shear wave splitting (SWS) time delays. Figure 7.1 shows almost three years of SWS delays at the station BJA, which was only a few kilometers from the epicenter of the earthquake that would occur on November 13, 1998. The latest data used in the forecast were from November 7, 1998 six days before the earthquake occurred. Crampin's institute in Edinburgh did not have the resources to monitor all data immediately, so there was a delay of a few days in receiving the data.

The models used in such forecasting assume that stress is evenly distributed over a large area, which tells us that the site of the impending earthquake cannot be forecast by SWS variations alone, although it provides information that helps in estimating the time and magnitude of an impending earthquake. In the forecast described here an earthquake was expected at a magnitude and a location comparable with what actually happened in the November 13 earthquake. This was based on general tectonic considerations during real-time observations of the area (Crampin *et al.*, 1999). The assumption of evenly distributed stress over a large area cannot be considered Earth-realistic. Studies of the absolute stresses released in micro-earthquakes indicate that stresses can vary significantly within small areas both in time and space (see Section 4.10.3). Near active faults, strong stress heterogeneity should be expected in space and time. Swarms of small earthquakes used for estimating stress by means of shear wave splitting are released at places where there are crustal heterogeneities, and as these stress estimations can only be used for crustal volumes immediately above the earthquake sources, the tendency will be

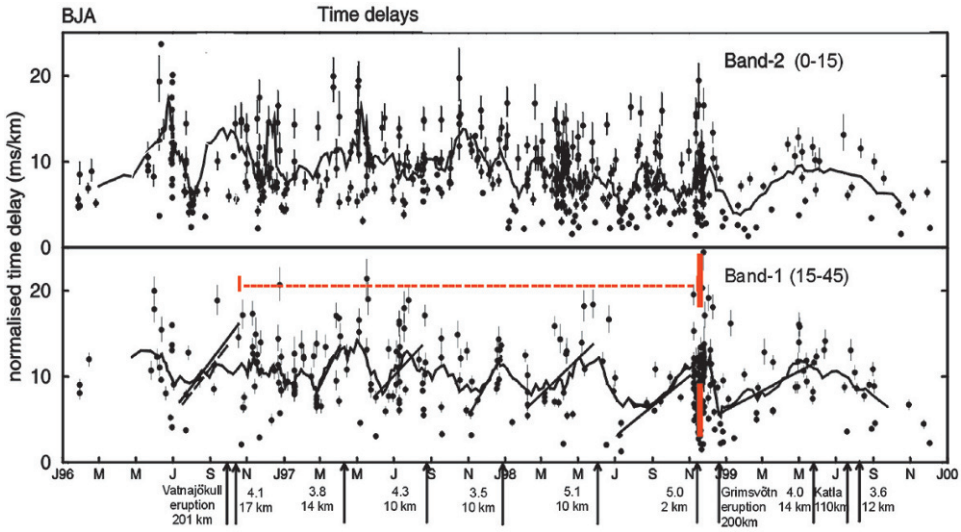

Figure 7.1. Time delays between split shear waves at Station BJA, caused by small earthquakes occurring close to the station (below a depth of 5 km) between January 1996 and December 1999. The time of the November 13 earthquake is shown by a red vertical line. The times of prior earthquakes occurring closeby are shown. The trace shows 5-day moving averages of the time delays between the two S waves. The original forecast message sent before the earthquake was based on data available on November 7, 1998 (based on Volti and Crampin, 2003).

that stress changes indicated by shear wave splitting are expressing changes in anomalous stress. Were we able to interpret such anomalous stress correctly it would be no less significant.

The stress forecast described above is typical of what to expect when trying to predict earthquakes. We should not expect a single algorithm to give us the significant information necessary for issuing a warning; our understanding of the crust, crustal processes, and all its heterogeneities is too limited for that. But any method that helps to reveal the physics of crustal processes at a fault of an impending earthquake is a significant contribution to the multidisciplinary information and modeling necessary for providing successful warnings.

7.2.2 Significant very short–term warnings before the 2000 eruption of Hekla

Chapter 4 described the eruption of Hekla (Figure 4.1), a volcano near the eastern end of the SISZ on February 26, 2000. Figure 7.2 shows (in red) the record from a Sacks–Evertson volumetric strainmeter at station BUR, 15 km distant from the volcano, and the magnitudes of small earthquakes occurring below it. This information was used to give a short-term warning of the eruption. No other direct observations indicated nucleation of the eruption.

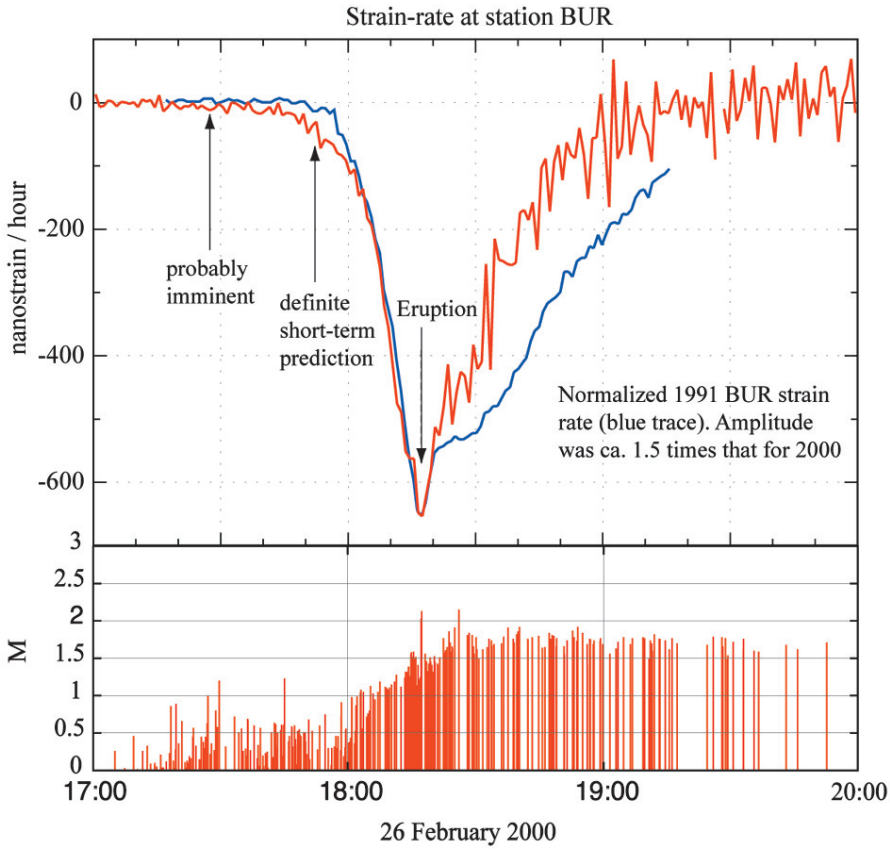

Figure 7.2. The record of the strain rate, the red trace, measured by a borehole strainmeter (at Station BUR) at a distance of 15 km from the volcano Hekla, during the initiation and the first stage of the eruption on February 26, 2000. The eruption started at 18:17 UTC, as indicated by the abrupt change in strain rate, which coincided with visual observations. Based on micro-earthquakes (red magnitude pillars) a warning was issued to the National Civil Protection Agency (NCPA) shortly before 17:30 that an eruption was probably imminent. At 17:53, also based on strain rate, a definite short-term prediction was issued to the NCPA, specifying the probable start of the eruption in around 20 minutes. Around 24 minutes after the warning the eruption started. The prediction was based on scientific evaluation given to the NCPA. The agency forwarded the warning to Iceland's national radio and the warning was relayed all over the country in the 6 o'clock radio news (i.e., at 18:00 UTC). Application of the strain rate to confirm the first warning and to estimate the onset time was made by comparison with strain monitoring before Hekla erupted in 1991 (shown by the blue trace).

From 1970 there were unusually frequent eruptions of Hekla: 1970, 1980, and 1991. The eruption of 1991 was particularly well recorded by strainmeters and modeled (Linde *et al.*, 1993). This formed the basis for the accurate prediction regarding both time and estimated intensity of the eruption in 2000. Warnings were issued that it would be similar in intensity to the 1991 eruption.

The formalities of such warnings can become very personal in Iceland. The story surrounding the Hekla eruption in 2000 goes as follows. It was a Saturday. At around 17:00 Páll Einarsson, a professor at the University of Iceland in Reykjavík, went to his office in the university to change the paper on some of the recorders, one of which was remotely recording direct signals from a seismometer on Hekla. He noticed a series of very small earthquakes (between magnitude 0 and 1) on the record. Earthquakes, even micro-earthquakes, are very rare below Hekla except during or just after eruptions. I was sitting in a coffee house when he phoned me to let me know what he had seen. He interpreted it as a probable precursor to an eruption. He then phoned the NCPA to provide the warning that an eruption was probably imminent. I went to IMO to look at recordings from the countrywide automatic SIL seismic network and from the borehole strainmeters in the SISZ. As I came through the door, the automatic alert signal sounded, warning that earthquake activity above predefined levels had started in Hekla. I succeeded to get online to the strainmeter closest to the volcano, and compared the record with the strain signal that preceded the eruption in 1991, nine years earlier. The match was good and was the basis for the precise time prediction given by IMO, which was immediately reported to the NCPA, who then passed it to Iceland's national radio to broadcast a warning. Consequently, many people in Iceland were looking toward the summit of Hekla in beautiful weather to witness the start of the eruption. Moreover, even before the eruption started, meteorologists with colleagues abroad started to predict the ash trajectories of the expected 10 km high ash plume of the impending eruption as a result of the warning. This was particularly significant for national and international air traffic over Iceland, and led to immediate changes in flight paths of aircraft (Ágústsson *et al.*, 2000, see also Stefánsson, 2000).

7.2.3 Subglacial eruption: significant warnings before the eruption of Grímsvötn volcano in Iceland in 2004

A description of the warnings issued and how successful they were was published in the journal *EOS* (Vogfjörd *et al.*, 2005). The Grímsvötn volcano is situated below the Vatnajökull ice cap, the largest ice cap in Iceland, and far away from where people are living (see Figure 3.2). Nevertheless, ash emission from large eruptions there may be a threat to people and domestic animals. A further danger is the height of the eruption plume (up to 12 km in this eruption), which is a hazard for air traffic. Moreover, heavy flooding is expected from eruptions below the ice cap (*jökulhlaup*), which can be a hazard for road traffic.

Figure 7.3a shows a significant increase in the activity of small earthquakes even as early as September 2003. This and other geophysical observations led to special attention being given to the area. Seismicity increased significantly on October 18, 2004 (Figure 7.3b) coinciding with westward movement of the GPS station SKRO which is situated 50 km to the west of the volcano, This may be interpreted as resulting from strain changes as a result of magma upwelling below the Grímsvötn volcano. On October 24, 2004 IMO staff released a warning to the

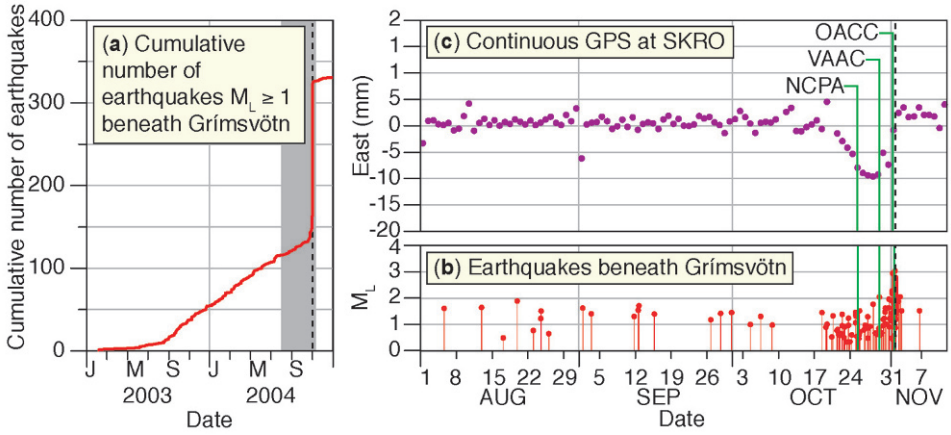

Figure 7.3. Precursory signals. (a) Cumulative number of earthquakes located beneath Grímsvötn volcano since 2002, showing the increase in activity in July 2003. (b) Local magnitude (M_L) of Grímsvötn earthquakes in the months preceding the eruption, showing the sudden increase in seismicity on October 18, 2004. (c) The eastern component of continuous GPS measurements from station SKRO, 50 km to the west of Grímsvötn, showing the westward movement of stations coinciding with increased seismic activity. Times of the first issued NCPA *jökulhlaup* (glacial floods) warning and the first London VAAC and Icelandic OACC eruption warnings are indicated (see text for explanations). Dashed vertical line indicates onset of the eruption (Vogfjörd *et al.*, 2005).

National Civil Protection Agency (NCPA) in Iceland saying that a volcanic hazard was probably imminent. On October 29, 2004 the Volcanic Ash Advisory Center (VAAC) in London was warned of a possible eruption during the next days. On November 1, IMO informed the Icelandic Aviation Oceanic Area Control Center (OACC) that a volcanic eruption seemed inevitable.

Figure 7.4 describes in more detail the start of the eruption. At 20:10 on the evening of November 1, 2004 IMO sent a warning to the NCPA and the OACC that a subglacial eruption at or near Grímsvötn was either about to begin or was already in progress. This warning led to all air traffic being immediately diverted away from the area, to avoid the predicted trajectory of the expected ash plume from Grímsvötn. At 21:50 earthquake activity subsided, coinciding with an increase in harmonic tremor, indicating the start of the eruption. The eruption was probably ongoing below the ice for an hour or so. It was not until 22:50 that the ash plume of the eruption was high enough to be detected by weather radar 260 km away (i.e., at a height of 8 km above the volcano). Because of severe weather at the ice cap the eruption was not visible until much later.

These warnings were very significant and their preparation demonstrates procedures that are in many ways similar to what we use in earthquake warnings. The information that was the basis for the warnings is not detailed here, nor is the information and warnings provided to the public. They can be seen in Vogfjörd *et al.* (2005).

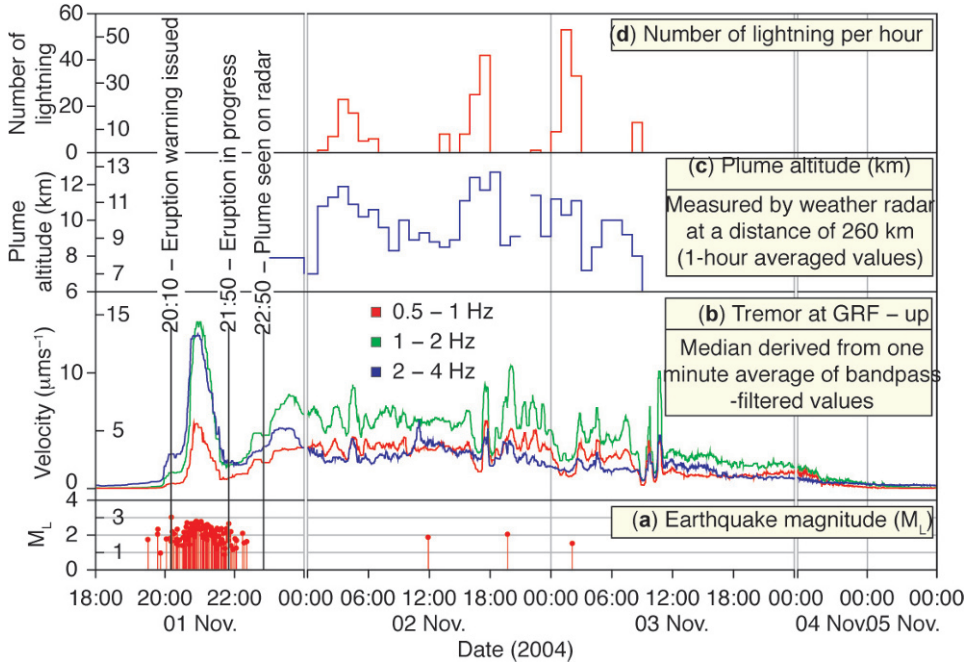

Figure 7.4. Signals shortly before the eruption and following it. Time is Universal Time Coordinated. Micro-earthquakes originating from the volcano and tremors at the closest seismic station (GRF) are shown in the two bottom rows. Height of ash plume and number of eruption-related lightning flashes are shown in the two upper rows (Vogfjörd *et al.*, 2005).

7.2.4 The Eyjafjallajökull eruption, which started March 20, 2010

The eruption in Eyjafjallajökull became known all over the world, mainly because of its ash clouds which disrupted air traffic across large areas. What is less known is that it caused major problems for farmers in South Iceland, close to the volcano. Floods destroyed some roads and farmland. Some feared that the eruption would harm the growing Icelandic tourist industry, because of the disturbance to air traffic and the danger inherent in being close to an erupting volcano. Surprisingly, nobody was killed by the ongoing eruption and nobody seriously injured. Farmers in the area in cooperation with their local Civil Protection group and local and state authorities have fought hard to secure their way of life and the productivity of the fertile farmland of South Iceland. At the time this book was being written the eruption had stopped, at least for the time being. But the fight to secure their way of life in this region is still going on.

The splendid work carried out by scientists and Civil Protection is the reason it has still been possible to avoid serious accidents and to significantly mitigate destruction. Local evacuation has been undertaken a few times at certain locations. Regular information about the status of the eruption was issued by scientists every day, which frequently contained warnings for various dangers stemming from the

eruption. Long-term work preparing for eventual eruptions and floods in this area together with long-term research work into understanding crustal processes have justified their activities and proven their significance. In spite of the difficulties, people living in the area are optimistic about living with volcanoes in the southernmost part of Iceland, just 10 km away.

The experience gained in tackling this eruption process has highlighted some shortfalls, so we need to intensify our work not only in Iceland but also worldwide in predicting and tackling eruptions with a view to doing better in the future. Experience also shows the value of international cooperation in avoiding risks for air traffic during volcanic eruptions anywhere. The experience garnered from this eruption will be of major value not only for scientists but also for those involved in risk mitigation worldwide as a result of eruptions.

Eruptions have long been expected in this part of the country. This is the reason such a good micro-earthquake monitoring system has been operated here for almost two decades and recently other geophysical monitoring has been gradually intensified. This now forms a very good basis for research work, so much so that worldwide efforts to understand volcanoes and to mitigate their risks should benefit enormously.

Let us now turn briefly to some of the main phases of the eruption and the steps taken to tackle it. It is often said that it is much easier to predict volcanic eruptions than earthquakes. Those who say this seem to interpret "prediction" as simply foreseeing the time of the start of the eruption and possibly some indication of its size before it starts. However, the fact is that predictions of the various dangers stemming from volcanic eruptions are needed as they proceed. Moreover, work to assess all possible hazards and to prepare effective warnings should start as early as possible before the onset of a volcanic eruption. Predictions of eruptions concern the multiplicity of dangers that stem from them. This is a long-lasting process, with new dangers presenting themselves daily.

Most earthquakes release their energy in next to no time, sometimes triggering other hazards. Earthquakes undergo a preparatory process, which starts decades before they cut through the crust. As already indicated, earthquakes may be triggered over the long term by high-pressure fluids from great depths, in much the same way as eruptions. In this way they are closely related to eruptions. There is much to be learned from volcanoes about how to predict earthquakes.

The procedures followed for predicting volcanic eruptions and earthquakes have much in common. Both hazards are based on long-term monitoring. Real-time evaluation and modeling enable us to understand ongoing crustal processes at each site. Both are based on building a database of many kinds of measurements and scientific results which is easily accessible when preparing for real-time research work and when we have to work against the clock to provide timely warnings of various aspects of the hazards. Multidisciplinary cooperation among geoscientists in both the long and the short term is necessary to merge the mass of information and new developments in our understanding of processes which we are collecting. Long-term and short-term cooperation with Civil Protection agencies and other authorities is necessary for each of the two hazards.

7.2.4.1 Warnings of the eruption

For a much more detailed description of warnings visit the IMO webpage at *http://en.vedur.is/earthquakes-and-volcanism/articles/*, which contains links to other webpages and to articles that have gradually been published about this eruption.

The Eyjafjallajökull volcano is in the southernmost part of Iceland (Figures 7.5 and 3.3). It is to the west of the Katla volcano below the Mýrdalsjökull ice cap. Both volcanoes are covered by thick ice. The ice-free pass, Fimmvörðuháls, separates the two mountains.

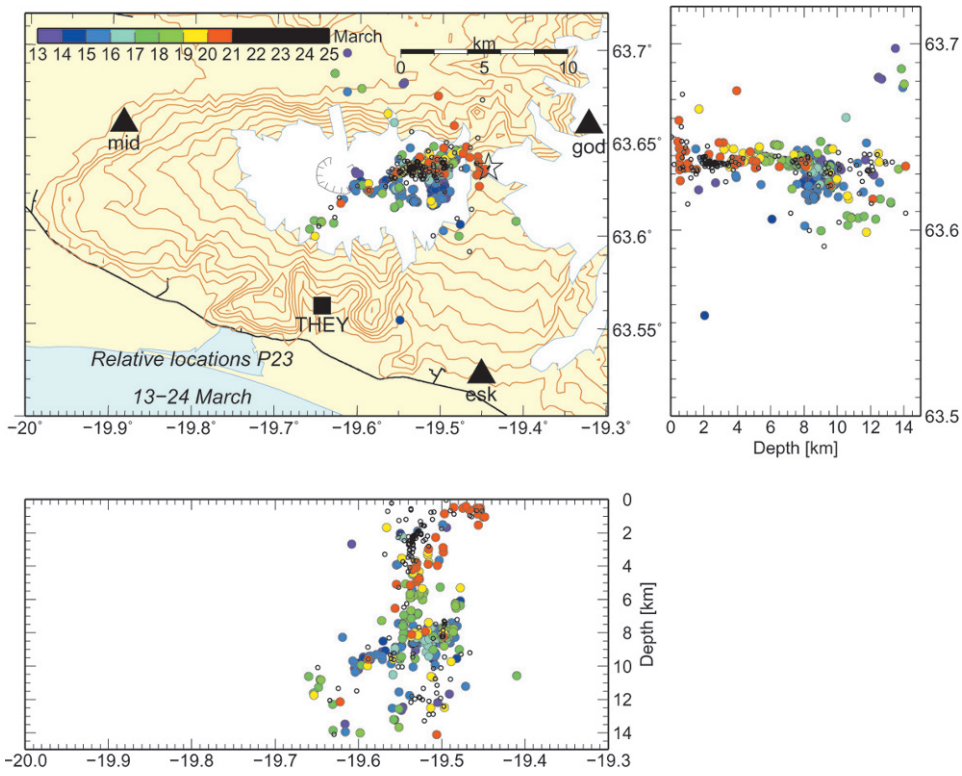

Figure 7.5. The figure shows Eyjafjallajökull in white and to its east a small part of Mýrdalsjökull ice cap, site of the Katla volcano. Figures 3.2 and 3.3 show the area's relationship to other parts of Iceland. Continuously operating micro-earthquake seismic stations of the SIL type are shown by triangles and a GPS station by a square. Circles of various colors represent the small earthquakes that occurred between March 13 and 24, 2010, the color bar showing their time of occurrence. The earthquake sources in this figure were later located by a method used to find the absolute and relative locations of similar events (as described in Appendix 2.A). They show how magma upwelled in the Eyjafjallajökull volcano through a central conduit called the "volcanic pipe", which is however deflected east at the top. A star indicates where the eruption started on March 20 (i.e., in the Fimmvörðuháls pass). The main eruption started 5 km farther west, directly above the central conduit, on April 14, 2010 (Hjaltadóttir *et al.*, 2010).

The eruption started as a flank eruption in the Fimmvörðuháls pass about 8 km east of the top of Eyjafjallajökull on March 20, 2010, at around 23:30 UTC. An eruption had been anticipated at Eyjafjallajökull for some years. There had been a high intensity of small earthquakes appearing in swarms at various depths below the mountain, the most significant of which were in 1994 and 1999. Source depth was frequently some 20 km down. There had also been relatively high activity from the beginning of 2010. Among other signs indicative of an impending eruption was surface elevation all across the mountain, which could be observed by continuous GPS measurements, starting in January 2010. At the end of February, after contacting the National Civil Protection Agency (NCPA) and their scientific advisory committee, the IMO staff put seismologists on call.

Three weeks before the eruption there was relatively intensive seismic activity below the mountain with magnitudes reaching 2.5. Origin depths were mostly between 7 km and 11 km and epicenters were near the center of the volcano. On March 16, three days before the eruption, a new seismic phase started, probably indicative of a new injection from more than 15 km down. On March 17 deeper earthquakes became frequent, some 15 km down. The subsequent earthquakes were shallower (e.g., at a depth of 2 km) during March 20, before the start of the eruption. The epicenters also moved eastward toward the Fimmvörðuháls pass, where the first phase of the eruption started late on March 20 (Figure 7.6).

For several weeks before the eruption, IMO observers were frequently in contact with the National Civil Protection Agency (NCPA), and this became daily during the last week before the eruption, to report the situation below the volcano, especially the apparent shallowing of earthquakes during the last days. There was some uncertainty about determining source depths, because of the complicated and little-known seismic structure below the volcano. Experience showed that swarms of very shallow small earthquakes were highly likely to occur close to the surface, caused by strain changes at depth, without being followed by eruptions. IMO observers contacted the NCPA at 12:00 UTC on Saturday, March 20, 2010 to report the shallowing and eastward movement of the epicenters. Although this could indicate the exact place and the imminence of an eruption they said that they would not be able to declare an eruption until the continuous seismic tremor expected to appear at the start of or shortly before an eruption was evident. The seismologist on call would sound the alarm if the automatic alert system showed such an increase in tremor intensity.

A continuous tremor showed up at 22:00 UTC on seismometers, however it was much weaker than that expected at the beginning of an open eruption. It was assumed that this tremor could be caused by the increasingly bad weather at that time. Therefore, no time warning of the start of the eruption was issued on that occasion. Around 23:30 UTC local observers reported that an eruption had started.

It was anticipated that eruptions in Eyjafjallajökull would cause a number of different hazards. Dangerous flood waters were expected as a result of the overlying ice cap melting rapidly. Ash would be carried to great heights in the atmosphere, becoming a danger to air traffic. In addition, ash fall nearby would pose a danger for people, crops and farm animals, let alone the fauna and flora of the area.

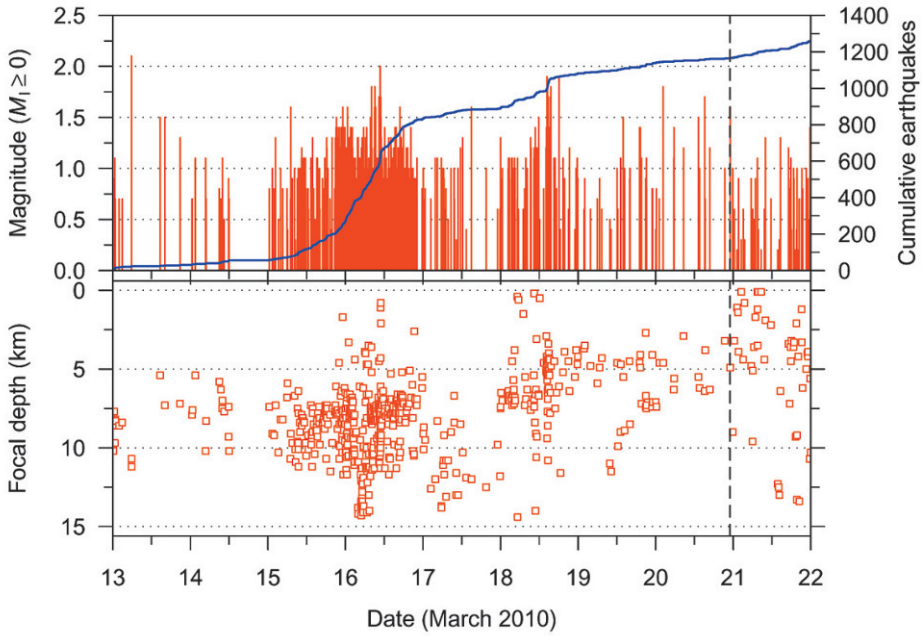

Figure 7.6. The topmost image shows the time pattern, magnitudes and cumulative number of earthquakes during the nucleation of the eruption. The bottom image shows changes of depth with time for locations of small earthquakes between March 13 and March 22, 2010. The eruption started (the vertical broken line) in the Fimmvörðuháls pass, 8 km east of the top of Eyjafjallajökull (see Figure 7.5) late in the evening of March 20, 2010.

The long-term and short-term information about nucleation of the eruption was very useful for preparations preceding it, even though the exact site and time of its start was not predicted in the short term. The site of the eruption, the Fimmvörðuháls pass, was not covered by ice, so dangerous water floods were less likely at the beginning of the eruption there. However, because of uncertainty about the precise location the NCPA played safe and ordered public evacuation at several flood-prone places close to rivers.

The eruption started with little mass ejection in the first hours. The lack of a strong eruption tremor probably indicates that gases were most significant in this first phase of the eruption. The outpouring lava was basaltic and relatively thin flowing. This phase of the eruption was not explosive and produced little ash. Evacuation from some places near the volcano was ordered at about 04:00 UTC on March 21. In hindsight, it could be claimed that it was not needed so soon. The reason for the evacuation was that we could not rule out the possibility that the start of the eruption was below the icecap, which would have been much more dangerous, leading to floods and much more ash fall.

Rivers began to break their banks about 10 hours after the start of the eruption, but flooding was short-lived and caused only minor disturbances. Some Icelanders

started to talk about the eruption as a possible tourist eruption, describing it as a ''beautiful red glowing fountain and a lava stream at a comfortable distance, little disturbed by ash.'' On April 12, 2010 the seismic tremor reduced in intensity and some other measurements indicated that the eruption might be slowing down. This was certainly the case at the Fimmvörðuháls pass.

7.2.4.2 A new eruptive explosive phase

On April 14, 2010 a large eruption started around 5 km farther west, below Eyjafjallajökull's ice cap, directly up from the central conduit (as indicated by the earthquakes in Figure 7.5). However, this was not so beautiful, would create many more problems, and would involve many more risks than the first phase in Fimmvörðuháls. The eruption here was much more acid in chemical composition, with a rock type similar to andesite. While the magma in the Fimvörðuháls eruption came directly from depths between 10 km and 15 km, the new eruption brought with it more acidic material from shallower depths—material that was considerably more explosive. The ash that poured out was much more fine-grained than in the first phase and was transported by wind much longer distances. What is more, the melting of the ice cap contributed considerably to the explosive character of the eruption, resulted in higher levels of ash production, and increased the risk of flooding.

Since the start of the eruption (i.e., March 20, 2010) information about the volcano's eruptive status, including warnings of various aspects of the eruption, were frequent. These were primarily issued by IMO but also by the Institute of Earth Sciences at the University of Iceland and by the NCPA. Weather forecasts gradually became more and more important for ash prediction, both locally and for air traffic. Calculating the amount of ash spewed out formed the basis for international efforts to predict clouds of ash in the atmosphere that are dangerous for air traffic. Predictions of flooding led to the evacuation of people at some localities near the volcano, especially at the beginning of the explosive phase.

The eruption involved many types of risks. Had we known before the eruption what we know now, the warnings given and rescue work undertaken would have been much better based. In some cases there could have been fewer evacuations, in others we could have been better prepared for some risks that had not been planned for in the warning program until after the eruption started.

In addition to daily information and warnings regarding the ongoing eruption, it was necessary to predict other possible hazards in the neighborhood that may be coupled to or triggered by the ongoing eruption. Katla volcano was in the neighborhood and would be capable of causing major flooding in the lowlands around it. To the north–northeast was the site of the huge Eldgja eruption in 930. Offshore to the southwest were Surtsey which erupted between 1963 and 1966 and Heimaey (Vestman Islands) which erupted in 1973.

7.3 GEOWATCHING SYSTEMS IN USE AND UNDER DEVELOPMENT

Useful predictions and warnings of earthquake and volcanic hazards are based on

- long-term monitoring, scientific evaluation, and modeling to find and understand the causal crustal process at each site;
- creating constitutive rules to extrapolate the process to some future event;
- visualizing the multiplicity of possible risks that can stem from the impending hazard.

For this purpose an effective Earth-watch system is needed, based on real-time monitoring and scientific evaluation, in which modern computer and information technology complements and supports scientific input.

In the remainder of this section, I describe observing systems that are either under development or in use at IMO (at least to a certain degree) for watching earthquakes, volcanic eruptions, and coupled events like avalanches and floods:

(1) the automatic alert system (ALERT), in use since 1992;
(2) near–real time shake maps;
(3) the early information and warning system (EWIS), in use for scientists evaluating information carried by seismic signals;
(4) the fast visualizing tool (FVT) for daily visualization and comparison of many types of geophysical signals is under preparation (it will have the ability to pattern-search in a complicated data stream and amend algorithms to take account of a multiplicity of observations).

7.3.1 The ALERT system

This system, which has been in operation since 1992, receives signals from automatic geophysical measuring and processing equipment. Currently, it is only based on the SIL seismic system operated by IMO. When various parameters describing the strength of seismic activity override predefined limits, the automatic system provides alerts within a couple of minutes containing information about epicenters, origin times, and magnitudes of small earthquakes. Examples of such alerting parameters include increase in number of micro-earthquakes over time in predefined locations or relatively large magnitudes of earthquakes at these locations. The staff at IMO, especially those who are on 24-hour weather watch, receive these alerts through computers or GSM phones. Based on their own judgment and on predefined rules they contact scientists for further study of anomalous patterns causing the alerts and decide on how to react to them.

These alerts are based on fast automatic evaluation of earthquake location, magnitude, and a few other source parameters. The alerts are released within a few tens of seconds, the time depending on the size of the seismic network used in each case for evaluation.

This system is meant to bring information to the attention of scientists on ongoing changes in the crust which might be a forerunner to an eruption or an earthquake (Stefánsson, 2003).

Other than the alerts described above (which are automatically issued after the alerting earthquake has been localized), the staff at IMO receive station alerts directly from individual seismic stations with immediate (of the order of a second) information about large seismic signals before their sources have been localized.

7.3.2 Near–real time shake maps

Early information about the severity of a large earthquake at various sites is extremely significant in the aftermath of a large earthquake, not only for rescue work but also for warnings of coupled events. Such information is often presented in the form of maps called "shake maps".

To provide data for near–real time generation of shake maps for earthquakes, an algorithm has been installed in SIL seismic stations. It reports values for peak ground velocity (PGV) and peak ground acceleration (PGA), when these significantly exceed the background level in any of four separate frequency bands. As soon as the first such report arrives at the SIL center, alert maps can be generated displaying the ground motion values at each station as well as time information.

Once the location and magnitude have been determined for the earthquake, a shake map can be generated for the area where earthquake intensities are largest. In order to estimate local surface effects on observed intensity, available information on near-surface lithology is collected.

Of course, shake maps can also be made on the basis of knowledge of the earthquake source, of the crust, and of surface effects, hence their significance in earthquake prediction. If we can predict the position and direction of a fault and its slip we can produce a useful shake map before the earthquake hits. An operational prediction service would do this in real time, as soon as a new prediction about the source became available.

7.3.3 The early information and warning system (EWIS)

EWIS is designed to collect all observations of use in predicting earthquakes and volcanic eruptions (Figure 7.7). It is a software system (accessible through the Internet) designed to analyze conditions and processes in the Earth's crust. The tool looks at direct continuous readings and automatically processed results from monitoring and evaluation systems like the SIL system. It also takes account of the latest scientific processes and research that little by little are included in the database. In addition to dynamic information to understand the ongoing process, the database contains static information, of vital importance in providing an effective warning service. In the future it is expected that the system will be able to provide fast access to relevant written articles and reports.

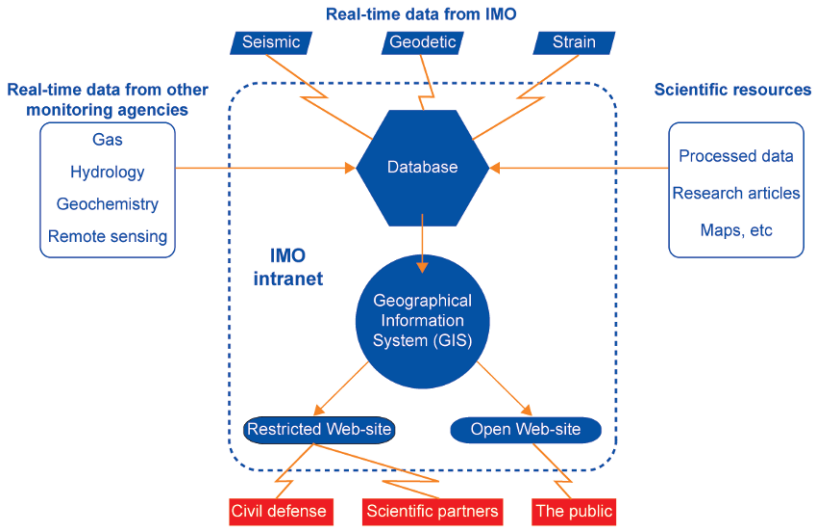

Figure 7.7. The main functions of the EWIS system.

Another feature of the system is that scientists and Civil Protection staff participate in estimating the situation and its likely consequences with what might be called "real-time research". It includes, for example, algorithms to speed up data processing, like pattern analysis in the multiplicity of incoming data, and in estimating new hazards according to the latest information. The system also offers the possibility to communicate with the general public regarding information that works both ways. The general public sends in information from hazard areas and the scientists present relevant new information to the public. The EWIS system is designed to present information visually and to be easily understandable for the powers that be and the general public. So far the system is only partly in use.

7.3.4 Fast visualization tool (FVT)

Daily observation of possible pre-earthquake and pre-eruption patterns is done by means of a mixture of manual and automatic inspection and evaluation. The stream of observations relevant for warnings is immense and increasing. As we have seen, significant pre-hazard processes may be very short, lasting only hours to days. To catch such processes and to understand them we need to be able to evaluate all incoming signals in real time. The daily inspection team making manual observations must be equipped with a software tool that quickly merges multidisciplinary information from sensors to be able to compare them. It must also contain algorithms that can come up with a quick preliminary evaluation of the situation in the crust at various locations on the basis of these observations.

A member of this team should be able to discover unusual patterns in the observations by quickly scanning through the possible hazard areas of the

country, and should have the necessary tools to investigate quickly what these patterns may be telling us (e.g., by comparing them with older observed patterns in the same area). By "observations" I mean not only direct observations but also the results of automatic real-time evaluation of, say, the focal mechanisms of earthquakes, and strain or stress changes based on various technologies.

This system is comparable with or complementary to EWIS. The main difference is that the FVT is intended to work automatically (day and night) at preliminary evaluation of a few predefined patterns and to make them quickly observable to the daily inspection team member on a map of Iceland. Although some quick further evaluations can be made by the FVT, EWIS is applied to study any anomalous processes more thoroughly and to study more patterns. The FVT can be considered as an extension to the currently operational ALERT system. It will gradually be extended to take into account more real-time information than it does now.

A simple example of the FVT is demonstrated in Figure 7.8. The daily inspection team member has clicked his pointer at Bárðarbunga, a volcano below the

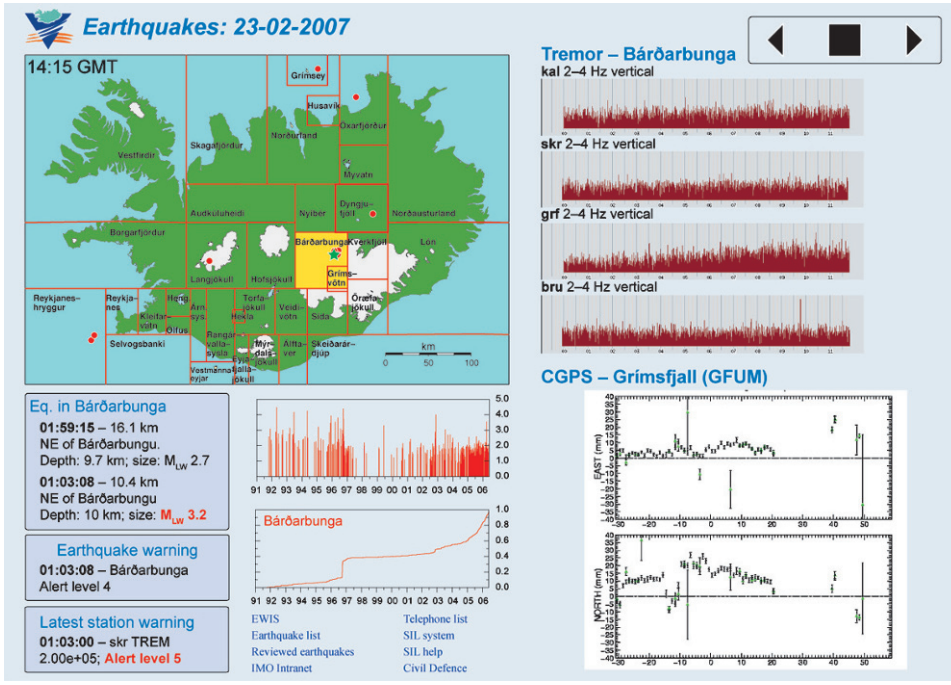

Figure 7.8. How a fast visualizing tool (FVT) could be applied in daily observing. Iceland is here divided into alert regions with boundaries at the red lines. The information in the diagrams refers to the yellow region of the map. It shows a few of the many observed seismic and deformation patterns relevant for volcanoes in the Bárðarbunga area. The time pattern of seismicity is shown from 1991 indicating magnitudes and numbers. In the upper right corner we see a real-time plot of continuous tremor records at three nearby station. In the lower right corner we see changes in time of continuous GPS measurements. Useful links to other systems are given at the bottom and in the middle of the figure.

Vatnajökull ice cap. Some time patterns of observations at or relevant to this subglacial volcanic region are immediately seen.

Unfortunately, the FVT is still not operational, it is under development though.

7.4 A LONG-TERM POLICY FOR EARTH HAZARD WATCHING

As discussed previously, straining of the crust at individual places, on the one hand, depends on large-scale straining of the crust by crustal plate motion, possibly interacting with large-scale effects of the Iceland Mantle Plume, and, on the other hand, on local heterogeneities that are strongly variable both in time and space. Changes in local heterogeneities depend significantly on upward fluid migration: slow upwelling is expected in the seismic zone and faster upwelling in volcanic zones. The interaction between fluid pressure and rock slip leads not only to short episodic processes at the local scale but also at the large scale, which influence fracture criticality over wide areas. Large crustal events may trigger processes at short and long distances. It is said that no two earthquakes are the same and this is equally true of their preparatory processes. The same can be said about eruptions. Observable preparatory processes in both cases may last for decades. Therefore, the path science should take toward giving warnings at a specified site is one of deterministic prediction of the development of ongoing crustal processes in nearby volumes over short time periods. This is based on the emerging understanding (described in Chapter 6) that most of what is learned about nucleation of an impending earthquake is the consequence of detailed observation of ongoing preparatory processes and of constitutive physical relationships established for these processes. However, they must steadily be modified in accordance with ongoing observations.

This sets the rules for a well-organized watching methodology that involves

(1) large-scale monitoring of the dynamics of Iceland's crust, including the large-scale dynamics of the Icelandic Mantle Plume and its interaction with plate motion;
(2) careful search for singular sites in time and space where large stresses (or general closeness to fracture criticality) are observed (i.e., so-called "red spots");
(3) decisions taken on the best way of concentrating watching efforts at red spots;
(4) physical modeling of ongoing processes at the local scale and of possible large-scale coupling between more distant events (i.e., coupled events);
(5) rule-based procedures for long-term and short-term warnings about sites, expected hazards, and closeness in time, including who should receive these warnings, how they should be rated, and advice on how to react;
(6) well-organized procedures and data collection to prepare for the multiplicity of coupled and long-lasting events following the initial event for which warnings have to be given.

For watching to be as effective as possible all available knowledge of the crustal structure of Iceland and state-of-the-art earthquake prediction research should be

applied. All possibly relevant geophysical observations should be merged and analyzed to study ongoing processes.

This watching methodology, although mainly focused on earthquake warnings, is also relevant for watching and warning of volcanic eruptions.

There will of course be those who protest that this system will cost a lot of money to build and to operate. This was also said when we were planning the automatic SIL seismic system more than 20 years ago. But now, just as was the case then, modern computer technology with its fast-increasing CPU speed will help us to keep operational costs down. However, it should be kept in mind that development of such a system is of vital importance for Earth hazard mitigation throughout the world, and should be a common undertaking of scientists and civil protection groups in many countries, in much the same way as the SIL system was and continues to be.

8

Application of earthquake prediction to other earthquake-prone regions

Since 1988 the South Iceland Seismic Zone (SISZ) has been a test area for multinational and multidisciplinary earthquake prediction research. The basic objective of various research projects has been to study the physical processes leading to large earthquakes. Chapter 2 contains a short overview of the projects. The hope is that the experience gained in the SISZ will be applied at the many places of the world prone to dangerous earthquakes.

The SIL project was the first large-scale earthquake prediction research project in the Icelandic test area. The following guidelines were established at its initiation in 1988:

(1) The fundamental requisite to predict earthquakes is understanding the physical processes leading up to them.
(2) The best way to study these processes is to retrieve information from very small earthquakes (down to magnitude 0). Small earthquakes occur all the time in seismic zones, near the plate boundaries, and can provide, in time and space, detailed information about the conditions below. If we can develop methods to retrieve information from the signals of small earthquakes, we might be able to assess prevailing stresses near their sources. We could also gather information about the nature of fractures at their origins and about variations in the velocities of their signals on their way to the surface, which reflect stresses along their paths.
(3) This task, which could involve monitoring thousands of micro-earthquakes per day, would require the development of new methods for automatic acquisition of seismic signals, and for automatic, real-time evaluation of the enormous amounts of information carried—almost continuously—up to us from deep in the crust. Automatic, real-time evaluation would also make it

R. Stefánsson, *Advances in Earthquake Prediction: Seismic Research and Risk Mitigation*,
Springer Praxis Books, DOI 10.1007/978-3-540-47571-2_8, © Springer-Verlag Berlin Heidelberg 2011

possible to provide short-term warnings if likely short-term pre-earthquake activity could be recognized from the data.

I hope that what I have been describing in previous chapters convinces you that we selected the right path from the outset. These three objectives are not being put up as being unique to Iceland. In fact, we learned from the experience of scientists in Sweden how significant information on crustal processes can be extracted from micro-earthquakes. Many of us were not convinced from the beginning that earthquakes with magnitudes between 0 and 2 would give us the necessary information to understand crustal processes preceding large earthquakes in the zone.

The Icelandic experience of working according to the above guidelines should encourage others to use them in other earthquake areas of the world.

Based on our 20 years of experience, the following guidelines can be added for Iceland, but they are equally relevant to any earthquake-prone part of the world:

(4) Multidisciplinary studies of the physical processes that are likely to lead to large earthquakes are fundamental to earthquake prediction research. Careful analysis of the information carried by micro-earthquakes about conditions down in the crust is key to understanding these processes.
(5) Earthquake preparatory processes may be observable long before failure, in Iceland this means decades. We use a gradual approach to predict the site, intensity, and time by extrapolating observed ongoing processes of each earthquake fault, from the time activity begins (i.e., from the time we receive information about it).
(6) It should be possible to issue warnings in some way of all earthquakes. The (required) conditions are, besides understanding of the crustal process, to watch the process in real time, to apply all relevant measurements and tools to describe and explain as soon as possible what is going on, and to predict the future of the process. The observational scope should cover everything from deciding how to enhance the monitoring system and evaluation procedures to determining preparatory actions on both a short-term and long-term basis. Any system created to do this will consist of automatic evaluation algorithms, rule-based manual observation, and maintaining steady contact with ongoing scientific research to carry out the necessary real-time research.

Although every earthquake-prone country has to develop its own watching system, based on its own needs and infrastructure, it can learn much from other nations. Chapters 4 and 5 described observations and modeling of pre-earthquake processes carried out by people from many countries in the SISZ of Iceland. Chapter 6 summarized how new state-of-the-art understanding can be merged. Chapter 7 described further experiences of carrying out real-time watching in Iceland, with the aim of providing warnings and of building up a watching system that takes a gradual approach to warning provision.

8.1 THE ICELANDIC EXPERIENCE CAN BE APPLIED ANYWHERE ON EARTH

No two earthquakes are the same, and this is also true of pre-earthquake processes. But the physics behind the processes may be the same. This claim has been made several times in this book. Assuming it to be true we should concentrate our earthquake prediction research studies in every case on faults where we expect destructive earthquakes in the near future. I think experience gained in multinational earthquake prediction research studies in the SISZ will be a helpful contribution to such work anywhere. We start by identifying the site, enhance multidisciplinary monitoring of it, and try to catch the process and predict where it is heading.

A multiplicity of observable pre-earthquake processes and conditions have been discovered in the 20 years of earthquake prediction research in the SISZ. These processes were also tested in real-time efforts to predict earthquakes and volcanic eruptions.

In 2000 the SISZ "test earthquakes" demonstrated pre-earthquake activity which we may find everywhere large earthquakes occur. These features could be monitored and studied in detail because of the special natural conditions that prevail in the SISZ and because of the available technology. In the following sections I sum up some pre-earthquake processes from the SISZ that are comparable to processes found worldwide. A detailed description can be found in Chapters 4 and 5, where observations and modeling are described.

8.1.1 Identifying the site of the next large earthquake

Despite the well-documented history of earthquakes in the SISZ spanning 300 years, pre-earthquake gaps were discovered in the earthquake release process. These could be filled together with other observations to successfully predict the sites and orders of magnitude of two large earthquakes in 2000 in the SISZ. The earthquakes were predicted to be the next large earthquakes in the SISZ. This was stated in journal papers 7–12 years before the earthquakes occurred. In the pre-earthquake period we observed crustal processes which through Earth-realistic modeling could be linked to impending earthquakes. In the 10-year period before the earthquakes, seismic processes were observed by the highly sensitive SIL seismic system, providing high-resolution data on the ongoing process. Although these data were not fully understood before the earthquake, they were a significant contribution to long-term prediction. The quality of these data and modeling based on them opened our eyes to the 30-to-40-year process at the same locations—a process that could partly in fact have been observed from the records of old-type seismometers.

Probably all large earthquakes on Earth occur at sites where there is an existing weakness or local stress heterogeneities and on old faults. In areas where strain buildup as a result of plate motion is ongoing these heterogeneities are expressed in crustal processes which we aim to make observable. Our goal is to be able to observe them as early as possible on each fault, based on all available data from the historical to micro-earthquakes.

After the 2000 earthquakes new methods were developed to interpret these processes. The methods and technology developed in the SISZ test area to observe them may, if applied, help to discover the sites of impending earthquakes and to monitor any long-term pre-earthquake process anywhere on Earth.

8.1.2 Discovering high-stress asperities, instability, and stable slip

Among the main concerns of those looking for pre-earthquake processes is how to estimate fault instability and how to discover the site and size of probable hard cores (i.e., the so-called "asperities") on faults. In the SISZ experiment we could see an asperity of the impending initial 2000 earthquake in data that preceded it. It showed up in the characteristic distribution of micro-earthquakes and in the stress field which varied in time and space, close to the fault, well before the earthquake. Also, based on information from micro-earthquakes, fault instability could be observed, especially approaching the time of earthquake release. The second 2000 earthquake did not have such a clear asperity or high pre-earthquake stress. During 10 years of good micro-earthquake observations, it showed signs of instability rather than buildup of stress. We could see how breaking of the small asperity immediately triggered the release of the first earthquake along its whole fault. We watched in real time how the first earthquake triggered the second large earthquake, three and a half days later. This led to the short-term warning that preceded it (as better described in Chapter 4).

Stable slip below the elastic/brittle crust preceded the initial 2000 earthquake. This was reflected in micro-earthquake observations in the fortnight before the large earthquake was released. Such stable slip at great depth below the brittle crust has often been suggested to explain nucleation of both strike slip and thrust-faulting earthquakes at various places on Earth. In modeling work at some sites on Earth it was necessary to assume this so that constitutive laws regarding postulated pre-earthquake slips along faults could be fulfilled. However, available technology and natural conditions in the SISZ made it possible to observe the slow and deep slip process almost directly, by studying micro-earthquake distribution and their mechanisms in the brittle crust above.

8.1.3 Triggering of earthquakes by other earthquakes or eruptions

Coupled events (i.e., when major earthquakes directly cause other geohazards) are considered a significant tool in trying to predict a "second event" anywhere, although the nature of these relationships is not fully understood. It is much more complicated than some models of coupled events assume.

As part of the SISZ projects, we have observed and modeled dynamic triggering at distances up to 100 km at the time it takes *S*-waves to travel there. Triggering was supposed to have occurred because the crust at triggered sites was close to fracturing criticality. But was it just a coincidence that fracturing criticality was reached at both places at the same time: the triggering site and the triggered site? Another explanation could be that the short-term pre-earthquake process applied to a far greater area

than just the close environment of the initial 2000 earthquake. This is possible and needs to be further studied.

With the benefit of hindsight the fault of the second large SISZ earthquake in 2000 was subject to static stress change caused by the first earthquake, which could have triggered it. This was based on Coulomb stress modeling (as described in Chapter 4). However, real-time observations showed that the first large earthquake almost immediately caused a micro-earthquake sequence at the fault of the second earthquake. This was a nucleation process which three and a half days later triggered the second large earthquake. Tentative real-time modeling of what the micro-earthquake indicated led to the successful short-term prediction of the second earthquake 26 hours before it occurred.

In the SISZ, sequences of small earthquakes have been observed which were apparently triggered by slow intrusive activity below two volcanoes, one a few tens of kilometers distant, the other 150 km distant (as described in Chapter 4). The impact on the SISZ was much too large to be explained by static changes caused by the primary event only. The suggested coupling is that intrusive upward migration from a great depth below the volcanoes lowered rock pressures in the SISZ. Such an effect was directly observed by volumetric strainmeters positioned 20 km and 50 km from one of the volcanoes (Hekla). This lowering of pressure triggered the upwelling of fluids that spawned micro-earthquakes at sites in the SISZ that were already close to fracturing criticality, because of ongoing plate boundary strain and long-term buildup of high pore fluid pressures in the seismogenic part of the crust. Analogous to this and supported by some observations, there is an indication that the strong and long-lasting micro-earthquake swarms that started in the SISZ in early 1996 were triggered by the upwelling of volcanic material from great depth at a distance of 150 km, a precursor to the huge Gjálp eruption, which began below the Vatnajökull ice cap in October 1996.

There are several examples worldwide where triggering over long distances has been suggested. Often these suggestions are made by ordinary people after listening to the news or by journalists. A typical off-the-cuff answer by scientists is that the supposed triggered event is much too far away from the initial event to have been triggered by it. Another is that triggering has to be immediate. Yet another is that tidal changes and atmospheric pressure changes would cause more impact at the triggered site than the original but distant earthquake. Such conclusions are based on a simple homogeneous Earth model. SISZ experience suggests that this is far too simple a model. It also suggests that we should be looking for a currently unknown means of transmission of strain energy at long distances so that such connections can be judged. We should also consider the possibility of a local process being triggered at the triggered site which in time might trigger earthquakes (as described above).

8.1.4 The earthquake cycle

The cycle for large earthquakes in the SISZ is proposed in Chapter 6. It is based on geophysical observations and modeling described in Chapters 4 and 5 and on tectonics in Chapter 3. The nucleation process on the faults of the 2000 earthquakes

could have been monitored for decades. Based on geological observations and Earth-realistic modeling it would seem that at least 300 years should elapse before the next large earthquake (i.e., those with magnitudes between 6 and 7) on the same fault in the area.

Earlier earthquakes left a scar in the crust on an impending fault, reaching down to a great depth, probably well below the brittle crust. Slip is continuous at such depths. However, the shallower parts of the old fault were locked, healed by the loss of pore pressures in the previous earthquake and solidified because of precipitation of minerals in the cold shallow environment. Deeper parts, where temperatures are higher, were kept open by continuous strain changes and fluids trapped there by the locked upper part of the fault.

A corrosion process started below the fault at an early state, possibly hundreds of years ago. Plate motion strain and a fluid-driven corrosion process gradually created conditions in the fault consisting of patches of instability intermittent with unfractured hard cores (i.e., asperities). A major earthquake is released when stress exerted on an asperity reaches the shear strength of the dry and unfractured rock, and instability prevails—whereas stress is evenly distributed—on other parts of the fault.

This model of the earthquake cycle is based on earthquake history in the SISZ and on the fluid–strain model (the F-S model) described in Chapter 5. The model assumes that compressible fluids from below the crust can penetrate up into the crust in response to plate motion strain in the SISZ. The fluids retain a near-lithostatic pressure there and can modify fracturing conditions in the seismogenic part of the crust. This leads to an observable fluid–strain process there, then earthquakes of all sizes, and finally a whole fault release. The model of the earthquake cycle is described in more detail in Chapter 6.

8.1.5 Icelandic results can be applied to all earthquake-prone areas

It is sometimes claimed that the results obtained in Iceland to discover a pre-earthquake failure process are unique to Icelandic conditions and thus to the earthquake cycle described there. Such comments often relate to the possibility of partial melt below Iceland's seismic zones, which can produce high-pressure fluids that can modify conditions in the seismogenic part of the crust. As described in Chapters 4–6, the modeling of fluid upwelling into the crust to build up conditions for the release of large earthquakes at the SISZ plate boundary is mainly based on the following two conditions:

(1) the availability of lithostatic fluids below the brittle crust;
(2) the low value of intrinsic permeability in the crust.

Both conditions are probably available elsewhere than just in the seismic zones of Iceland. We know that at depths of 50 km to 100 km in the subduction zones the hydrated lithosphere, brought there by subduction, melts and creates pockets of magmatic melts which seek their way up to the surface, at some places as eruptions,

at other places the thermal heat in these melts causes high pore fluid pressures above the melts, in much the same way as observed above the Iceland Mantle Plume, although the direct origin is different. The only way to discover whether comparable conditions to Iceland exist at other places is through making observations. It would be unscientific to claim that such conditions exist in all earthquake zones. It would be just as unscientific to claim the opposite without studying it. The main difference might be that very few places in the world have a seismic monitoring system that is as sensitive to micro-earthquake sources as the SIL system in Iceland. Also the elastic/brittle crust in Iceland is relatively thin. In other seismic zones it is often deeper down (where high-pressure fluids may be trapped) than it is in the SISZ, and thus more difficult to observe.

High pore fluid pressures at depth are often discovered (by magnetotelluric measurements) as volumes of low electrical resistivity. In Iceland a layer of low resistivity was discovered in this way between 1980 and 1985 (Beblo and Björnsson, 1980; Hersir *et al*., 1984; Eysteinsson and Hermance, 1985), at a depth of 10 km to 20 km (see also Björnsson, 2008). In the SISZ this depth coincides by and large with the depth of the limit for earthquake release (i.e., the so-called brittle–ductile boundary). To reiterate what has already been said several times, we can reach the following conclusions:

- fluids migrating upward create conditions for the local release of earthquakes where the strain is large;
- small earthquakes triggered by these fluids carry information almost continuously to the surface which makes it possible to study preparatory processes at depth, from the time they become observable until they release a large earthquake.

Studies along these lines (i.e., by making use of small and deep crustal earthquakes and by magnetotelluric measurement) should be carried out at more sites to ascertain whether high fluid pressures are available below the brittle crust.

In thrust regions of the Himalayas, where we expect large earthquakes, low resistivity has been found at depths of around 20 km to 30 km (Arora, 2002). Small earthquakes are also found above this depth in these regions. This suggests fluids that are close to lithostatic pressure at such depths at the plate boundary in the Himalayan crust. This is a good candidate for study by a micro-earthquake system that is sensitive down to magnitude 0, along the lines of that used in the SISZ.

The Apennine seismic belt in Italy is another tectonically active place where fluids of deep origin are present in a low-permeability crust. Correlation has been found there between seismic activity and CO_2 degassing from the mantle (Chiodini *et al*., 2004; Miller *et al*., 2004). The models and methods described here to monitor crustal processes may be applicable there also.

We should not exclude the possibility that conditions comparable with those in the SISZ for releasing earthquakes may be found at more sites of the world. Although conditions may not be so different, it is easier to see the symptoms in Iceland. The consequence of finding long-term and short-term premonitory

processes in Iceland, mainly based on information carried by micro-earthquakes from a great depth in the crust, suggests that a similar approach should be applied in earthquake prediction research in all earthquake-prone areas of the world. The monitoring technology is already available as are tried-and-tested methods to extract information on crustal processes from micro-earthquakes.

8.2 APPLYING RESULTS FROM THE SISZ TO THE TJÖRNES FRACTURE ZONE

The results of earthquake prediction research in the SISZ test area are starting to be applied to the Tjörnes Fracture Zone (TFZ, see Figure 3.2) off the north coast of Iceland.

8.2.1 Mapping the faults of small earthquakes in the Tjörnes Fracture Zone

Figure 8.1 shows the results of fault mapping based on micro-earthquake information off the north coast of Iceland. This figure shows the power of micro-earthquake technology. Micro-earthquakes which here originate far from land are used to map faults and sense their slips in this oceanic area. Micro-earthquakes that provide this information have a fault radius of one hundred to a few hundred meters and slips of a fraction of a millimeter. The figure also provides an insight into a different tectonic environment that can be studied by methods used in the earthquake prediction research project in the SISZ.

8.2.2 Mapping the fault planes and slip directions of historical earthquakes

We have started to apply results from earthquake prediction research in the SISZ in the complex zone of large earthquakes off the north coast of Iceland.

Results obtained in the SISZ indicate that earthquake faults can be determined in micro-earthquakes up to 100 years after a large earthquake. This has been applied to the Tjörnes Fracture Zone (Figure 8.2) to study the position and strike of faults of historical earthquakes since 1755.

A magnitude-7 earthquake occurred in the westernmost part of the Tjörnes Fracture Zone in 1963 (Figure 8.2) and was well recorded. It had a fault plane solution based on observations from seismological stations all over the world (Stefánsson, 1966). Such solutions give two nodal planes perpendicular to each other, one of which is the real fault plane (for explanations see Appendix 2.A). In most cases the distribution of aftershocks expected on fault planes is used to find which of the nodal planes is the fault plane. Observed aftershocks following the 1963 earthquake were too few and too badly located to be useful to distinguish which of the two planes was the fault plane. On the basis of structural features of the ocean bottom the author (Stefánsson, 1966) suggested that the nodal plane closest to the north–south direction would be the direction of the fault plane. Later, with the

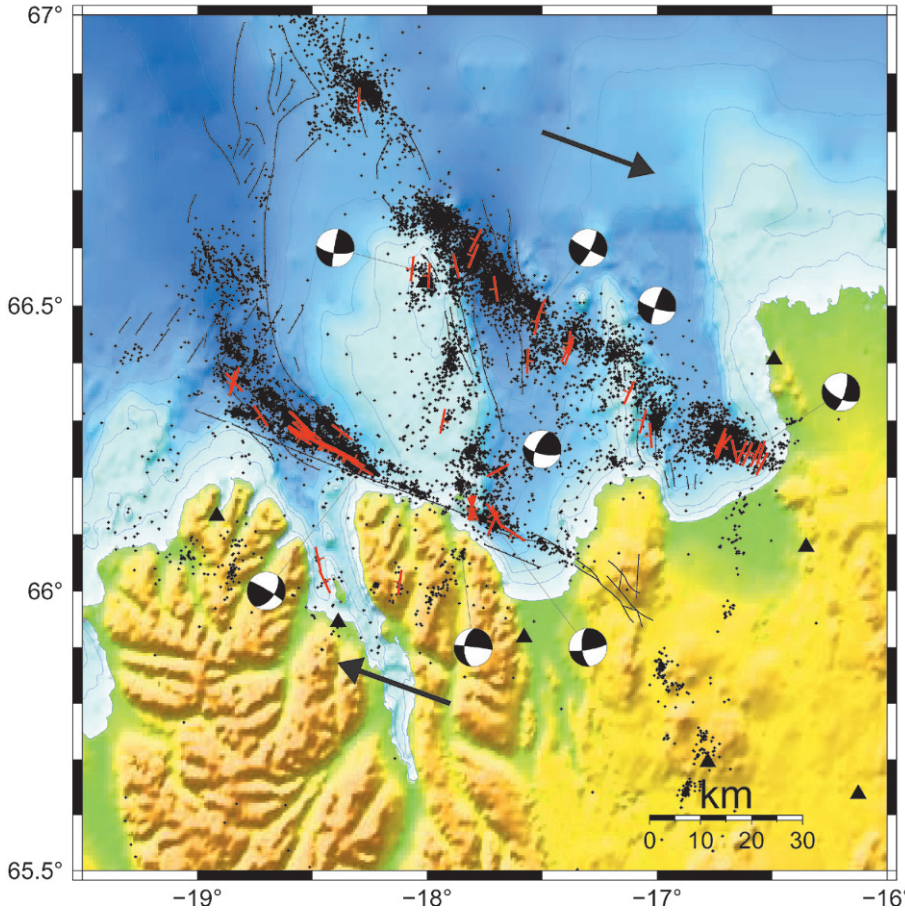

Figure 8.1. Mapped faults within the Tjörnes Fracture Zone. The red lines are the 62 active fault segments mapped using accurate relative locations of micro-earthquakes and their mechanism. The fault plane solutions of selected earthquakes are shown on an equal area projection of the lower hemisphere. Black lines indicate faults mapped by conventional reflection seismic methods or on land by direct geological observations. Triangles denote seismic stations and open circles (dots) epicenters of small earthquakes (often hidden by red lines). The long straight WNW–ESE line denotes the Húsavík–Flatey transform fault. The arrows denote the direction of relative plate motion across the zone (DeMets *et al.*, 1990). The depth contour interval is 100 m. The slip on near north–south striking faults is left-lateral, but on east–west striking faults, like the Húsavík–Flatey fault, the slip is right-lateral (based on Rögnvaldsson *et al.*, 1998).

advent of plate tectonics, it was suggested by some that the wrong plane had been selected as the fault plane: the east–west striking nodal plane should have been selected instead as the fault plane (i.e., the direction of the real transform fault in the TFZ). Some 40 years passed before an efficient micro-earthquake system (a SIL-type system) was installed in northern Iceland. It was soon realized that

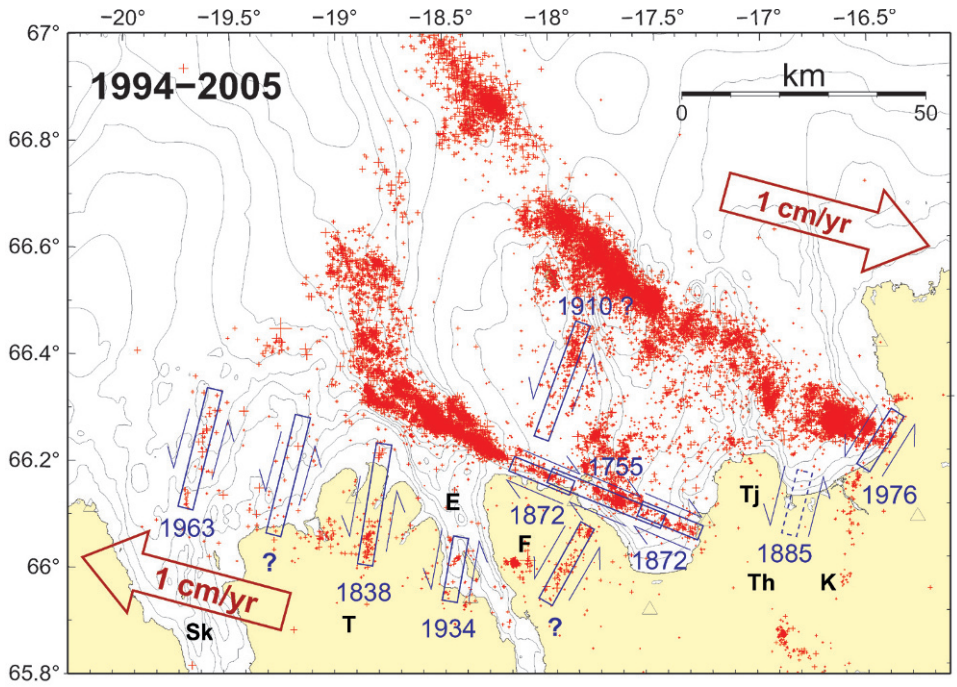

Figure 8.2. Micro-earthquakes recorded between 1994 and 2005 shown by red dots, at the north coast of Iceland, delimit the Tjörnes Fracture Zone. Blue boxes and arrows show the results of efforts to find fault planes and infer slip directions of historically and instrumentally evaluated magnitude-6 and magnitude-7 earthquakes in the area. Year numbers are used to identify large earthquakes, and capital letters are initials of geographic names. Depth contour interval is 100 m (based on Stefánsson *et al.*, 2008).

earthquakes were still found on the suggested north–south striking fault there (Figure 8.2). They indicated a 30 km long fault whose direction within a couple of degrees matched one of the two possible fault planes of the 1963 earthquake: the northward-striking plane of the nodal plane solutions. The good fit of this micro-earthquake line with one of the well-constrained nodal planes of international observations, coupled with results from the SISZ indicating that faults can be determined in micro-earthquakes 100 years after their occurrence, encouraged us to map old faults at other places in the Tjörnes Fracture Zone on the basis of such micro-earthquake lines (see Figure 8.2).

As demonstrated in Figure 8.2, historical information, old seismological studies, new earthquake research, and new technology have made it possible to map faults of historical earthquakes in the area going back 250 years, despite large parts of the area being below the ocean (Stefánsson *et al.*, 2008). These and many other studies suggest that we should pursue this further and initiate earthquake prediction research along the north coast of Iceland comparable with that carried out in South Iceland.

8.3 DOUBTS ABOUT ISSUING EARTHQUAKE PREDICTIONS

The success of earthquake prediction research in the SISZ is based on the physical approach to understand processes leading to large earthquakes and on real-time monitoring and real-time research. It is a deterministic approach. No pre-earthquake activity can be assumed *a priori* to be the same. This makes using statistics problematic when issuing predictions. Of course, statistics are used to prepare warnings, but these are statistics of signals within the ongoing long-term pre-earthquake process on the same fault. If we see a suspicious and possibly pre-earthquake signal in this long process, we would investigate it to find out whether we have seen such a signal before, and in such a case use statistics to estimate the significance of a possible earthquake warning.

Central to the criticism of earthquake prediction research was the claim that the models were too simple (see Chapter 1). A part of the reason for this was that very few data were used, or available, on which to base the modeling. Many scientists, trying to establish prediction algorithms, based their work only on the time patterns of relatively large earthquakes reported in classical catalogs of the 20th century. Often these catalogs only listed earthquakes of magnitudes 3 or 4, or larger. Such earthquakes are so rare in time and space that they have little value in explaining the continuous process by which they are caused. Such a process could possibly have been discovered had the density of seismic observations been higher (i.e., the earthquakes smaller and thus more numerous).

In studies of earthquake patterns confined to earthquakes of magnitudes 3 or 4, seismologists frequently detected a silence ahead of large earthquakes. Silence is not good enough for prediction because we get no information during the most significant period of time: the time when symptoms of a possible pre-earthquake process can be detected, which is fundamental for short-term prediction.

Direct measurements of deformation have gradually been added to be fulfilled by the models. However, even if GPS measurements are becoming more accurate, they have not been able to detect pre-earthquake processes on such a scale in time and space to be useful for short-term predictions. Even the volumetric strainmeters in Iceland, which are much more sensitive in the short term than GPS measurements and situated inside the faulting area of the June 17, 2000 earthquake, received no signals that could safely be identified as part of a pre-earthquake process at seismogenic depths. The possibility of making short-term predictions depends on detecting and monitoring accelerated pre-earthquake processes along weaknesses in the fault. Micro-earthquake technology is the most powerful tool to do this, because micro-earthquakes relay back information that can be used to find processes on and near faults at seismogenic depths. These changes in many cases do not involve strain changes, which are large enough to be directly measured by available deformation technology. They are difficult to identify with a possibly impending fault slip. However, deformation measurements as well as observable processes in the shallowest part of the crust can be expected to be a valuable addition to understanding of deep processes for short-term warnings.

The usual simplifying assumption in modeling crustal processes is that rheological conditions in a seismic zone are permanent, although in rate/state-dependent friction models conditions are variable around the fault after its slip has started. Another simplification in many models for pre-earthquake processes is that they only consider processes on the main fault, which in most cases are assumed locked until the influence of the transitional (slow-slipping) parts of the fault breaks the lock. Even if it is generally accepted that water on the Earth's surface comes from inside the Earth, I have seen very little serious modeling that takes into account how such an up-flow of compressible fluids participates in self-organizing processes in zones of large earthquakes. Episodic upward flows of compressible fluids cause local changes in strains and stresses, which can only be revealed by micro-earthquakes. Strain change associated with this upward migration of compressible fluids is hardly measurable directly until the larger earthquakes it helped to release have occurred. The only way, known so far, to see such processes is through micro-earthquake information. However, the sensitivity of such observations is usually insufficient to provide modelers with the necessary data for more Earth-realistic models.

Many models of pre-earthquake processes are far too simple to be Earth-realistic. Well-constrained and sophisticated methods of statistics have been applied in the false world of simplifications in attempts to predict the underlying process, but in so doing missed the central issue. This resembles the development of astronomy at a time when we still believed that the Earth was at the center. Sophisticated models were created by placing the Earth at the center and adding new epicycles on the older circular tracks to explain the new astronomical observations that were piling up. This was an established scientific truth on how to explain the strange behavior of the stars until Galileo, walking out of the inquisition court, where he confessed that he was wrong in supporting the Copernican heliocentric system, mumbled it (the Earth) still rotates. Earthquake prediction science, like many other sciences, suffers from the misuse of statistics in atempts to compare signals or processes that are physically not comparable.

The buildup processes of an earthquake in and around a fault probably take a long time—in the SISZ this is possibly hundreds of years. Observable buildup time is defined as the time available for close and detailed study of a pre-earthquake process, for studying its tectonic environment, and for gradually being able to predict future aspects of the process. This long-term process involves self-organized redistribution of strains around the developing fault. On a short-term basis the changes are so small that they cannot be resolved as observable strain changes by our technology for direct deformation monitoring. We have to rely on indirect information (e.g., from micro-earthquakes) to detect possible pre-earthquake processes and local stress changes. The Icelandic experience is evidence that micro-earthquakes carry information that can be used to see and monitor such self-organized redistribution in real time.

In all earthquake-prone areas there should be a focus on micro-earthquake studies so that the physics of the area can be understood and monitored. Such an understanding will help in the understanding of other measurable signals, thus

adding greatly to the study of general crustal processes. Our approach to understanding the pre-earthquake process is basically deterministic. However, we will use statistics to prepare warnings. Statistics can also be used to compare the frequency of processes or signals within the long-term process leading up to the earthquake. We saw such processes in Chapter 4 (see Figures 4.22 and 4.23). But how many times have such processes occurred on the fault without an earthquake happening? Such information from many processes can be used to prepare warnings, and statistics can now be used to constrain warnings and to prepare relevant actions to be taken.

8.4 EARTHQUAKES ARE BOTH DIFFERENT AND SIMILAR

The physical approach to earthquake prediction (as described in this book) should be applied to all earthquake-prone areas. In that way the experience gained in the South Iceland Seismic Zone can be applied anywhere. At the beginning of this chapter I listed six main results of our experience that can be applied to other earthquake-prone areas. They all concern methodology. The methodology applied in Iceland can certainly be applied anywhere.

Whether or not the Fluid-Strain model (developed under Icelandic conditions) is relevant for other earthquake-prone areas can only be answered by multidisciplinary studies at each site. This can be done by applying a micro-earthquake methodology in line with what has been developed in the Iceland test area.

The methods described in this book to monitor stresses or fracturing criticality in time and space and to map active faults by using information from micro-earthquakes can and should be applied in all earthquake-prone areas of the world.

So, the answer to the question often posed "Can the experiences from the SISZ test area be applied to other earthquake zones?" can be given in a single word: Yes.

8.5 PRE-EARTHQUAKE ELECTRIC AND ELECTROMAGNETIC SIGNALS

This book has described the results of multinational earthquake prediction research, such as has been proceeding for 20 years in Iceland, especially in the South Iceland Seismic Zone (SISZ). Our approach is a physical one (i.e., meaning that multidisciplinary studies to understand and to monitor crustal processes leading to large earthquakes are employed). Significant results have been achieved. Many are ready for application in warning systems and will be useful for mitigating risks.

However, the book does not describe methods of applying electric and electromagnetic observations to monitor pre-earthquake processes. The reason is simply that in the test area under consideration no such methods were used. However, the book does describe how magnetotelluric surveys in Iceland led to the discovery of a layer of very low electric resistivity at a depth of 15 km below most of Iceland, caused by high pore fluid pressures there. This was significant not

only to understand crustal processes leading to earthquakes but also for the creation of the F-S model described in Chapter 5.

There have been many descriptions over the centuries of earthquake lights that preceded large earthquakes. Recently there has been much discussion about electrical methods like the Greek VAN method (see, e.g., Uyeda, 1998). Intensive research work is ongoing to understand and to model such signals, which often involve stress-induced currents. As an introduction to such work I recommend Freund (2006, 2009), Freund *et al*. (2006), and Balk *et al*. (2009).

8.6 DEDICATED OBSERVATION AND REAL-TIME EVALUATION ARE NOT ONLY KEY TO PROVIDING USEFUL WARNINGS BUT ALSO BASIC FOR THE SCIENCE OF SEISMOLOGY

It is through research that we know how to find oil and other sources of energy within the crust of the Earth. The driving force behind such research was not the established knowledge of what science and technology believed was possible to achieve, it was the need to find such energy sources and the money involved that drove us towards scientific goals and the necessary understanding. It is also through research that we are discovering more and more exploitable sources in the shallowest part of the crust.

What is the driving force behind earthquake prediction research? It is certainly not to make money; when lives need to be saved, money is not a consideration. The driving force is certainly not seeking to become famous for scientific achievements; such research is not currently of major interest to leading scientific bodies.

Some may consider politicians who care or are responsible for the welfare and lives of their people to be a driving force. There are examples of politicians who lost their positions of authority because people felt they should have done more to cushion them from the dangers of earthquakes.

When the president of India visited Iceland in 2005, one of his wishes was to ascertain how Icelanders had been so successful in earthquake prediction research. This was his way of taking responsibility for looking after his people. As a scientist and in keeping with fellow scientists, he believed in looking for the truth that is often hidden beyond what is generally accepted to be the truth. In a special one-hour lecture we described our work procedures. We also explained to him that the reason for our success depended in no short measure on work carried out by scientists from many countries—many lessons had been learned from Indian scientists. Ultimately though, we told him, that our progress and success was based on the special conditions in our country and a strong wish to be able to predict earthquakes for the benefit of the Icelandic people.

We told the president that we always kept in mind a simple thought: if warnings could be issued before eruptions, then why should this not also be the case for earthquakes? Of course, some may say they are very different. Yes, they are very different, but they also have much in common. Earthquakes in India occur under tectonic conditions that are very different from Icelandic conditions, but there is still

much in common. Before proclaiming what is possible in Iceland is not necessarily possible in India, we have to study it. Let the lives and welfare of people benefit from the doubt. I believe the Indian president was thinking along these lines, but he also felt the search for truth had value in itself.

Earthquake prediction research in Iceland has the aim not only of saving people's lives but also protecting their way of life. However, the technology and knowledge gained from this research can be used to find thermal energy sources at depth in the crust. So, at the end of the day research will probably pay for itself even if it does not create money in the short term.

But, prediction research on its own is not enough to mitigate risk. This is in the hands of observers who daily have to apply the latest scientific results, just like a hospital doctor making use of the most up-to-date scientific knowledge in his daily tasks and decision making.

The real driving force behind earthquake prediction research is the people living in earthquake-prone areas and those who act on their behalf. This is the reason this book is written in such a way that its main message can reach everybody. In short, the main message is that it is possible in Iceland and probable in many other earthquake-prone areas of the world to provide useful warnings of earthquakes before they occur if the following is provided:

- Relevant and continuous geophysical observations to discover possible pre-earthquake processes on both a regional and a local scale, thereby immediately providing scientists with the necessary data for evaluation.
- Physically well-constrained models that are based on observations and on the understanding that is slowly but surely increasing about the nucleation processes of earthquakes in the area.
- Hazard assessment that is based on historical knowledge and on new emerging knowledge about probable release processes for earthquakes in the area.
- Immediate application of new understanding of crustal processes in a well-organized early information and warning system.
- A geowatching system with a rule-based warning schedule must be operating to link scientific evaluation to adequate action by people and society.

8.7 BUILDING AN INFRASTRUCTURE FOR EARTHQUAKE PREDICTION RESEARCH

Maybe the most significant help that Icelanders connected with earthquake warnings can provide is advice on how to build an infrastructure that combines careful observation and earthquake prediction research, with the goal of providing useful warnings. This infrastructure should consist of people working closely together from all walks of life from scientists, through technicians and local Civil Protection

groups, to ordinary people living in areas subject to risk. Scientific and local Civil Protection groups should have experience from other areas. Building up a nucleus of risk-mitigating groups, having the confidence to build and coordinate scientific projects, is more fruitful than simply seeking solutions from high-profile scientists around the world who claim that they have universal methods to predict earthquakes. Equally it is also more fruitful than seeking solutions from those who claim that it is not possible and never will be to warn of earthquakes.

Success in providing useful pre-earthquake warnings depends on all manner of things: from studying the physics of processes leading to earthquakes and careful daily observation of the Earth to the ways in which local Civil Protection groups respond. In all earthquake-prone areas we have to build a human infrastructure to bring this about. We also have to recruit international specialists in Earth sciences and learn from their experiences. Such a local multidisciplinary human infrastructure must be robust, be confident enough to lead and carry out this work, and of course be motivated.

References

Aki, K. and P. Richards (1980). *Quantitative Seismology, Theory and Methods*. W. H. Freeman & Co., New York.

Allen, R.M. (2002). Imaging the mantle beneath Iceland using integrated seismological techniques. *J. Geophys. Res.*, **107**(B12), 2325, doi: 10.1029/2001JB000595.

Almannavarnaráð (1978). A report in Icelandic: *Landskjálfti á Suðurlandi :Skýrsla vinnuhóps Almannavarnaráðs um jarðskjálfta á Suðurlandi og varnir gegn þeim*. Almannavarnir ríkisins, Reykjavík, 54 pp. [in Icelandic].

Angelier, J., F. Bergerat, M. Bellou, and C. Homberg (2004a). Co-seismic strike-slip displacement determined from push-up structures: The Selsund Fault case, South Iceland. *Journal of Structural Geology*, **26**, 709–724.

Angelier, J., R. Slunga, F. Bergerat, R. Stefansson, and C. Homberg (2004b). Perturbation of stress and oceanic rift extension across transform faults shown by earthquake focal mechanisms in Iceland. *Earth Planetary Science Letters*, **219**, 271–284.

Angelier, J., F. Bergerat, R. Stefánsson, and M. Bellou (2008). Seismotectonics of a newly formed transform zone near a hotspot: Earthquake mechanisms and regional stress in the South Iceland Seismic Zone. *Tectonophysics*, **447**(104), 95–116.

Antonioli, A., M.E. Belardinelli, A. Bizzarri, and K.S. Vogfjord (2006). Evidence of dynamic triggering during the seismic sequence of year 2000 in South Iceland. *J. Geophys. Res.*, **111**, B03302.

Ágústsson, K., A. Linde, R. Stefánsson, and S. Sacks (1999). Strain changes for the 1987 Vatnafjöll earthquake in south Iceland and possible magmatic triggering. *J. Geophys. Res.*, **104**(B1), 1151–1161.

Ágústsson, K., R. Stefánsson, A.T. Linde, P. Einarsson, I.S. Sacks, G.B. Gudmundsson, and B. Thorbjarnardóttir (2000). Successful prediction and warning of the 2000 eruption of Hekla based on seismicity and strain changes. *EOS, Trans. Am. Geophys. Union*, **81**(48), Fall Meeting Suppl., Abstract V11B-30.

Árnadóttir, T., S. Hreinsdóttir, G.B. Gudmundsson, P. Einarsson, M. Heinert, and C. Völksen (2001). Crustal deformation measured by GPS in the South Iceland Seismic Zone due to two large earthquakes in June 2000. *Geophys. Res. Lett.*, **28**(21), 4031–4033, doi: 10.1029/2001GL013207.

Árnadóttir, Th., S. Jónsson, R. Pedersen, and G. Gudmundsson (2003). Coulomb stress changes in the South Iceland Seismic Zone due to two large earthquakes in June 2000. *Geophys. Res. Lett.*, **30**(5), doi:10.1029/2002GL016495.

Árnadóttir, Th., W. Jiang, K.L. Feigl, H. Geirsson, and E. Sturkell (2006). Kinematic models of plate boundary deformation in southwest Iceland derived from GPS observations. *J. Geophys. Res.*, **111**, B07402, doi:10.1029/2005JB003907.

Árnadóttir Th., Geirsson, H., and Jiang, W. (2008). Crustal deformation in Iceland: Plate spreading and earthquake deformation. *Jókull*, **58**, 59–74.

Árnadóttir, Th., B. Lund, W. Jiang, H. Geirsson, H. Björnsson, P. Einarsson, and T. Sigurdsson (2009). Glacial rebound and plate spreading: Results from the first country-wide GPS observations in Iceland. *Geophys. J. Int.*, **177**(2), 691–716, doi: 10.1111/j.1365-246X.2008.04059.x.

Arora, B.R. (2002). Seismotectonics of the frontal Himalaya through electrical conductivity imaging. In: Y. Fujinawa and A. Yoshida (Eds.), *Seismotectonics on Convergent Plate Boundaries*. Terra Scientific Publishing (TERRAPUB), Tokyo, pp. 261–271.

Båth, M. (1960). Crustal structure of Iceland. *J. Geophys. Res.*, **65**, 1793–1807.

Bakun, W.H. and A.G. Lindh (1985). The Parkfield, California, earthquake prediction experiment. *Science*, **229**, 619–624.

Bakun, W.H. and T.V. McEvilly (1984). Recurrence models and Parkfield, California, earthquakes. *Journal of Geophysical Research*, **89**(B5), 3051–3058.

Balk, M., M. Bose, G. Ertem, D.A. Rogoff, L.J. Rothschild, and F.T. Freund (2009). Oxidation of water to hydrogen peroxide at the rockwater interface due to stress-activated electric currents in rocks. *Earth and Planetary Science Letters*, **283**, 87–92.

Beblo, M. and A. Björnsson (1980). A model of electrical resistivity beneath NE-Iceland, correlation with temperature. *Journal of Geophysics*, **47**, 184–190.

Bellou, M. (2006). Analyse sismotectonique de la zone sismique Sud-Islandaise. Thèse de doctorat de L'Université Paris VI. Soutenne publiquement le 11 December 2006, 314 pp.

Benioff, H. (1951). Earthquakes and rock creep: Part 1. *Bulletin of the Seismological Society of America*, **41**, 31–62.

Bjarnason, I. (2008). An Iceland hotspot saga. *Jökull*, **58**, 3-16.

Bjarnason, I. and H. Schmeling (2009). The lithosphere and the asthenosphere of the Iceland hotspot from surface waves. *Geophys. J. Int.*, **178**, 394–418.

Bjarnason, I., W. Menke, Ó. Flóvenz, and D. Caress (1993). Tomographic image of the mid-atlantic plate boundary in Southwestern Iceland. *J. Geophys. Res.*, **98**, 6607–6622.

Björnsson, A. (2008) Temperature of the Icelandic crust: Inferred from electrical conductivity, temperature surface gradient, and maximum depth of earthquakes. *Tectonophysics*, **447**, 136–141.

Björnsson, A., G. Johnsen, G. Sigurdsson, S. Thorbergsson, and E. Tryggvason (1979). Rifting of the plate boundary in North Iceland 1975–1978. *J. Geophys. Res.*, **84**, 3029–3038.

Björnsson, A., H. Eysteinsson, and M. Beblo (2005). Crustal formation and magma genesis beneath Iceland: Magnetotelluric constraints. In: G.R. Foulger, J.H. Natland, D.C. Presnall, and D.L. Anderson (Eds.), *Plates, Plumes and Paradigms* (GSA Spec. Pap. 388, pp. 665–686). Geological Society of America, Boulder, CO.

Björnsson, G., Ó.G. Flóvenz, K. Sæmundsson, and P. Einarsson (2001). Pressure changes in Icelandic geothermal reservoirs associated with two large earthquakes in June 2000. *Proceedings of the 26th Workshop on Geothermal Reservoir Engineering, Stanford University, Stanford, California, January 29–31.*

Björnsson, S. and P. Einarsson (1981). *Jardskjálftar—in; Náttúra Íslands*, Almenna Bókafélagid, Reykjavík, pp 121–155 [in Icelandic].

Bödvarsson, R. and B. Lund (2003). The SIL seismological data acquisition system—as operated in Iceland and in Sweden. In: T. Takanami and G. Kitagawa (Eds.), *Methods and Applications of Signal Processing in Seismic Network Operations* (Lecture Notes in Earth Sciences 98, pp. 131–148). Springer-Verlag, Berlin.

Bödvarsson, R., S.Th. Rögnvaldsson, S.S. Jakobsdóttir, R. Slunga, and R. Stefánsson (1996). The SIL data acquisition and monitoring system. *Seism. Res. Lett.*, **67**(5), 35–46.

Bödvarsson, R., S.Th. Rögnvaldsson, R. Slunga, and E. Kjartansson (1999). The SIL data acquisition system: At present and beyond year 2000. *Phys. Earth. Plan. Int.*, **113**, 89–101.

Bödvarsson, R., B. Lund, and A. Tryggvason (2005). Seismicity ratio with applied mechanism (Abstract). *EGU General Assembly, Vienna, Austria, April 24–29*.

Bolt, Br. (1978). *Earthquakes*. W.H. Freeman & Co., New York.

Bonafede, M. and S. Danesi (1997). Near-field modifications of stress induced by dyke injection at shallow depth, *Geophys. J. Int.*, **130**, 435–448.

Bonafede, M., C. Ferrari, F. Maccaferri, and R. Stefánsson (2007). On the preparatory process of the M6.6 earthquake of June 17th, 2000, in Iceland. *Geophysical Res. Lett.*, **34**, L24305, doi: 10.10029/2007GL031391.

Brandsdóttir, B. and W.H. Menke (2008). The seismic structure of Iceland. *Jökull*, **58**.

Burton, P.W. (1979). Seismic risk in southern Europe through to India examined using Gumbel's third distribution of extreme values. *Geophys. J. R. Astr. Soc.*, **59**, 249–280.

Burton, P.W. and K.C. Makropoulos (1985). Seismic risk of circum-Pacific earthquakes, II: Extreme values using Gumbel's third distribution and the relationship with strain energy release. *Pageoph*, **123**, 850–869.

Celin Wang, Qi-Fu Chen, Shihong Sun, and Andong Wang (2006). Predicting the 1975 Haicheng earthquake. *Bulletin of the Seismological Society of America*, **96**, June, doi: 10.1785/0120050191.

Chen Yong, Kam-ling Tsoi, Chen Feibi, Gao Zhenhuan, Zou Qijia, and Chen Zhangli (1988). *The Great Tangshan Earthquake of 1976*. Pergamon Press, Oxford, U.K., 153 pp.

Chieh, M., J-P. Avounac, V. Hjartardóttir, T.-R. Alex Song, Chen, Ji, Sieh, K. (2007). Coseismic slip. *Bulletin of the Seismological Society of America*, **97**, January.

Chiodini, G., C. Cardellini, A. Amato, E. Boschi, S. Caliro, F. Frondini, and G. Ventura (2004). Carbon dioxide Earth degassing and seismogenesis in central and southern Italy. *Geophys. Res. Lett.*, **31**, L07615, doi: 10.1029/2004GL019480.

Christensen, N.I. and R. Ramananantoandro (1988). Permeability of the oceanic crust based on experimental studies of basalt permeability at elevated pressures. *Tectonophysics*, **149**, 181–186.

Claesson, L., A. Skelton, C. Graham, C. Dieti, M. Mörth, P. Tossander, and I. Kockum (2004). Hydrochemical changes before and after a major earthquake. *Geology*, **32**(8), 641–644, doi: 10.1130/G20542.1

Clifton, A. and P. Einarsson (2005). Styles of surface rupture accompanying the June 17 and June 21 earthquakes in the South Iceland Seismic Zone. *Tectonophysics*, **396**, 141–159.

Crampin, S. (1994). The fracture criticality of crustal rocks. *Geophys. J. Int.*, **118**, 428–438.

Crampin, S. and S. Chastin (2003). A review of shear-wave splitting in the crack-critical crust. *Geophys. J. Int.*, **155**, 221–240.

Crampin, S. and J.H. Lovell (1991). A decade of shear-wave splitting in the Earth's crust: What does it mean? What use can we make of it? And what should we do next? *Geophys. J. Int.*, **107**, 387–407.

Crampin, S., T. Volti, and R. Stefánsson (1999). A successfully stress-forecast earthquake, *Geophys. J. Int.*, **138**, F1–F5.

Crampin, S., T. Volti, S. Chastin, A. Gudmundsson, and R. Stefánsson (2002). Indications of high pore-fluid pressures in a seismically active fault zone. *Geophys. J. Int.*, **151**, F1–F5.

Dapeng Zhao, H. Kanamori, H. Negishi, and D. Wiens (1996). Tomography of the source area of the 1995 Kobe earthquake: Evidence for fluids at the hypocenter? *Science*, **274**(5294), 1891–1894, doi: 10.1126/science.274.5294.1891.

Darbyshire, F.A., I.Th. Bjarnason, R.S. White, and Ó.G. Flóvenz (1998). Crustal structure above the Iceland mantle plume imaged by the ICEMELT refraction profile. *Geophys. J. Int.*, **135**, 1131–1149.

DeMets, C., R.G. Gordon, D.F. Argus, and S. Stein (1990). Current plate motions. *Geophys. J. Int.*, **101**, 425–478.

DeMets, C., R.G. Gordon, D.F. Argus, and S. Stein (1994). Effect of recent revisions to the geomagnetic reversal time scale on estimates of current plate motions. *Geophys. Res. Lett.*, **21**, 2191–2194.

Dietrich, J.H. (1992). Earthquake nucleation on faults with rate- and state-dependent strength. *Tectonophysics*, **211**, 115–134.

Einarsson, P. (1985). Jarðskjálftaspár. *Náttúrufræðingurinn*, **55**(1), 9–29 [in Icelandic].

Einarsson, P. (1991). Earthquakes and present-day tectonism in Iceland. *Tectonophysics*, **189**, 261–279.

Einarsson, P. (2008). Plate boundaries, rifts and transforms in Iceland. *Jökull*, **58**, 35–58.

Einarsson, P. and J. Eiríksson (1982). Earthquake fractures in the districts Land and Rangárvellir in the south Iceland seismic zone. *Jökull*, **32**, 113–120.

Einarsson, P. and K. Sæmundsson (1987). Earthquake epicenters 1982–1985 and volcanic systems in Iceland, map. In: T. Sigfússon (Ed.), *Í hlutarins edli: Festschrift for Thorbjörn Sigurgeirsson*. Menningarsjóður, Reykjavík.

Einarsson, P., S. Björnsson, G. Foulger, R. Stefánsson, and Th. Skaftadóttir (1981). Seismicity pattern in the South Iceland seismic zone. In: D. Simpson and P. Richards (Eds.), *Earthquake Prediction: An International Review* (AGU Maurice Ewing Series 4, pp. 141–151). American Geophysical Union, Washington, D.C.

Einarsson, P., B. Brandsdóttir, and M.T. Gudmundsson (1997). Center of the Iceland Hotspot experiences volcanic unrest. *EOS, Trans. Am. Geophys. Union*, **78**(35), September.

Einarsson, P., P. Theodórsson, Á. R. Hjartardóttir, and G.I. Gudjónsson (2008). Radon changes associated with the earthquake sequence in June 2000 in the South Iceland Seismic Zone. *Pure and Appl. Geophys.*, doi: 10.1007/s00024-007-0292-6.

Ellsworth, W.L. (1990). Earthquake history, 1769–1989. In: R.E. Wallace (Ed.), *The San Andreas Fault System, California* (USGS Prof. Pap. 1515, pp. 153–187). U.S. Geological Survey, Reston, VA.

Ellsworth, W.L. (1993). Getting beyond numerology. *Nature*, **363**, 206–207.

Eysteinsson, H. and J.F. Hermance (1985). Magnetotelluric measurements across the eastern volcanic zone in South Iceland. *J. Geophys. Res.*, **87**, 10093–10103.

Filson, J.R. (1988). The role of the federal government in the Parkfield Earthquake Prediction Experiment. *Earthquakes & Volcanoes*, **20**(2), 56–59.

Flóvenz, Ó.G. and K. Gunnarsson (1991). Seismic crustal structure in Iceland and surrounding area. *Tectonophysics*, **189**, 1–17.

Foulger, G.R., M.J. Pritchard, B.R. Julian, J.R. Evans, R.M. Allen, G. Nolet, W.J. Morgan, B. Bergsson, P. Erlendsson, S. Jakobsdottir *et al.* (2001). Seismic tomography shows that upwelling beneath Iceland is confined to the upper mantle. *Geophys. J. Int.*,**146**, 504–530.

Freund, F.T. (2006). When the Earth speaks: Understanding pre-earthquake signals. Paper presented at *13th ECEE & 30th General Assembly of the ESC, Geneva, Switzerland, September 3–8*.

Freund, F. (2009). Stress-activated positive hole charge carriers in rocks and the generation of pre-earthquake signals. In: M. Hayakawa (Ed.), *Electromagnetic Phenomena Associated with Earthquakes*. Signpost, New Delhi, pp 41–96.

Freund, F.T., A. Takeuchi, and B.W.S. Lau (2006). Electric currents streaming out of stressed igneous rocks: A step towards understanding pre-earthquake low frequency EM emissions. *Physics and Chemistry of the Earth*, **31**, 389–396.

Gao, Y. and S. Crampin (2004). Observations of stress relaxation before earthquakes. *Geophys. J. Int.*, **157**, 578–582.

Gebrande, H., H. Miller, and P. Einarsson (1980). Seismic structure of Iceland along RRISP-Profile I. *Journal of Geophysics*, **47**, 239–249.

Geirsson, H., Th. Árnadóttir, C. Völksen, W. Jiang, E. Sturkell, T. Villemin, P. Einarsson, F. Sigmundsson, and R. Stefánsson (2006). Current plate movements across the Mid-Atlantic Ridge determined from 5 years of continuous GPS measurements in Iceland. *J. Geophys. Res.*, **111**(B9), B09407, doi: 10.1029/2005JB004092.

Gephart, J.W. and D.W. Forsyth (1984). An improved method for determining the regional stress tensor using earthquake focal mechanism data: Application to the San Fernando earthquake sequence. *J. Geophys. Res.*, **89**, 9305–9320.

Gudmundsson, A. and S.L. Brenner (2003). Loading of a seismic zone to failure deforms nearby volcanoes: A new earthquake precursor. *Terra Nova*, **15**, 187–193.

Gudmundsson, A. and S.L. Brenner (2005). How local stress fields prevent volcanic eruptions. *Journal of Volcanology and Geothermal Research* (submitted).

Gudmundsson, G. and K. Sæmundsson (1980). Statistical analysis of damaging earthquakes and volcanic eruptions in Iceland from 1550–1978. *J. Geophysics*, **47**, 99–109.

Halldörsson, P. (1992). Seismic hazard assessment based on historical data and seismic measurements. In: *International Conference on Preparedness and Mitigation for Natural Disasters '92, 28–29 May 1992, Reykjavík, Iceland* (pp. 53–63). Available at *http://www.vedur.is/media/vedurstofan/utgafa/greinargerdir/1995/HalldorssonP.pdf*

Halldórsson, P. (2005). *Jardskjálftavirkni á Nordurlandi* (Report 05021—VÍ-ES-10). Icelandic Meteorological Office, Reykjavík. Also available at *http://www.vedur.is/utgafa/greinargerdir/2005/*

Hauksson, E. and J.G. Goddard (1981). Radon earthquake precursor studies in Iceland. J.Geophys. Res. 86, 7037-7054.

Heki, K., G.R. Foulger, B.R. Julian, and C.H. Jahn (1993). Plate dynamics near divergent boundaries: Geophysical implications of postrifting crustal deformation in NE Iceland. *J. Geophys. Res.*, **98**(B8), 14279–14297.

Hersir, G.P., A. Björnsson, and L.B. Pedersen (1984). Magnetotelluric survey across the active spreading zone in Southwest Iceland. *J. Volcanol. Geotherm. Res.*, **20**, 253–265.

Hirth, G. and D.L. Kohlstedt (1996). Water in the oceanic upper mantle: Implications for rheology, melt extraction, and the evolution of the lithosphere. *Earth Planet. Sci. Lett.*, **144**, 93–108.

Hjaltadóttir, S. and K. Vogfjörd (2005). *Subsurface Fault Mapping in Southwest Iceland by Relative Location of Aftershocks of the June 2000 Earthquakes* (report). Iceland Meteorological Office, Reykjavík.

Hjaltadóttir, S., K. Vogfjörd, Þ. Árnadóttir, P. Einarsson, and P. Suhadolc (2005). *A Model of the Release of the Two June 2000 Earthquakes Based on All Available Observations*

(Report 05020). Vedurstofa Íslands, Reykjavík. Available at *http://www.vedur.is/utgafa/greinargerdir/2005/*

Hjaltadóttir, S., K.S. Vogfjörd, and R. Slunga (2010). Seismicity revealing evolution of magmatic intrusions in the Eyjafjallajökull volcano, XL-380. *EGU Spring Meeting, Vienna, May 2–7*.

Hofton, M.A. and G.R. Foulger (1996). Post-rifting anelastic deformation around the spreading plate boundary, north Iceland, 1: Modeling of the 1987–1992 deformation field using a viscoelastic Earth structure. *J. Geophys. Res.*, **101**, 25403–25421.

Hreinsdóttir, S., P. Einarsson, and F. Sigmundsson (2001). Crustal deformation at the oblique spreading Reykjanes peninsula, SW Iceland: GPS measurements from 1993 to 1998. *J. Geophys. Res.*, **106**, 13803–13816.

Hreinsdóttir, S., T. Árnadóttir, J. Decriem, H. Geirsson, A. Tryggvason, R.A. Bennett, and P. LaFemina (2009). A complex earthquake sequence captured by the continuous GPS network in SW Iceland. *Geophys. Res. Lett.*, **36**, L12309, doi: 10.1029/2009GL038391.

Ishimoto, M. and K. Iida (1939). Observations of earthquakes registered with the microseismograph constructed recently. *Bulletin Earthquake Res. Inst. Tokyo Univ.*, **17**, 443–478.

Ito, G., Y. Shen, G. Hirth, and C. Wolfe (1999). Mantle flow, melting, and dehydration of the Iceland mantle plume. *Earth and Planetary Science Letters*, **165**, 81–96.

Ito, G., J. Lin, and D. Graham (2003). Observational and theoretical studies of the dynamics of mantle plume–mid ocean ridge interaction. *Rev. Geophys.*, **41**(4), doi: 10.1029/2002RG000117.

Jakobsdóttir, S.S. (2008). Seismicity in Iceland 1994–2007. *Jökull*, **58**, 75–100.

Jakobsdóttir, S.S., G.B. Gudmundsson, and R. Stefánsson (2002). Seismicity in Iceland 1991–2000 monitored by the SIL seismic system. *Jökull*, **51**, 87–94.

Jónsson, S. and P. Einarsson (1996). Radon anomalies and earthquakes in the South Iceland Seismic Zone 1977–1993. In: B. ßorkelsson (Ed.), *Seismology in Europe* (papers presented at the XXV ESC General Assembly, Reykjavík, Iceland, September 9–14, 1996, pp. 247–252). Icelandic Meteorological Office, Reykjavík.

Jónsson, S., P. Segall, R. Pedersen, and G. Björnsson (2003). Post-earthquake ground movements correlated to pore-pressure transients. *Nature*, **424**, 179–183.

Kagan, Y.Y. and D.D. Jackson (1995). New seismic gap hypothesis: Five years after. *J. Geophys. Res.*, **100**, 3943–3959.

LaFemina, P.C., T.H. Dixon, R. Malservisi, T. Árnadóttir, E. Sturkell, F. Sigmundsson, and P. Einarsson (2005). Geodetic GPS measurements in south Iceland: Strain accumulation and partitioning in a propagating ridge system. *J. Geophys. Res.*, **110**, B11405, doi: 10.1029/2005JB003675.

Larsen, G., M.T. Gudmundsson, and H. Björnsson (1998). Eight centuries of periodic volcanism at the center of the Iceland hotspot revealed by glacier tephrostratigraphy. *Geology*, **26**, 943–946.

Lay, T., H. Kanamori, C. Ammon, M. Nettles, S. Ward, R. Aster, S. Beck, S. Bilek, M. Brudzinski, R. Butler *et al.* (2005). The Great Sumatra-Andaman Earthquake of December 26, 2004. *Science*, **308**, 1127–1133, doi: 10.1126/science.1112250.

Linde, A.T., K. Ágústsson, I.S. Sacks, and R. Stefánsson (1993). Mechanism of the 1991 eruption of Hekla from continuous borehole strain monitoring. *Nature*, **365**, 737–740.

Lockner, D. and J. Byerlee (1994). Dilatancy in hydraulically isolated faults and the suppression of instability. *Geophys. Res. Lett.*, **21**(22), 2353–2356.

Lomnitz, C. (1994). *Fundamentals of Earthquake Prediction*. John Wiley & Sons, New York, 326 pp.

Lund, B., M. Lindman, M. Arvidsson, R. Slunga, and R. Bödvarsson (2005). Stress variations before and during the two $M = 6.5$ earthquakes of June 2000 in the South Iceland Seismic Zone, *EOS, Trans. Am. Geophys. Union*, **86**(52), Fall Meeting Suppl. T21B-0468. Electronic version available at *www.agu.org*

Marquart, G. and H. Schmeling (2004). A dynamic model for the Iceland plume and the North Atlantic based on tomography and gravity data. *Geophys. J. Int.*, **159**, 40–52.

Ma Zongjin, Fu Zhengxiang, Zhang Yingzheb, Wang Chengmin, Zhang Guomin, and Liu Defu (1990). *Earthquake Prediction: Nine Major Earthquakes in China*. Seismological Press, Beijing/Springer-Verlag, Berlin, 332 pp.

Menke, W. and V. Levin (1994). Cold crust in a hot spot. *Geophys. Res. Lett.*, **21**, 1967-1970.

Miller, S., C. Collettini, L. Chiaraluce, M. Cocco, M. Barci, and B.J.P. Kaus (2004). Aftershocks driven by a high-pressure CO_2 source at depth. *Nature*, **427**, 724–727.

Morgan, W.J. (1972). Deep mantle convection plumes and plate motion. *Am. Assoc. Pet. Geol. Bull.*, **56**, 203–213.

Nur, A. and J.D. Byerlee (1971). An exact effective stress law for elastic deformation of rock with fluids. *J. Geophys. Res.*, **76**, 6414–6419.

Pálmason, G. (1971). *Crustal Structure of Iceland from Explosion Seismology*. Vísindafélag Íslands, Greinar, 187 pp.

Pedersen, R., S. Jónsson, Th. Árnadóttir, F. Sigmundsson, and K.L. Feigl (2003). Fault slip distribution of two $M_w = 6.5$ earthquakes in South Iceland estimated from joint inversion of InSAR and GPS measurements. *Earth and Planetary Science Letters*, **213**, 487–502.

Philip, H., E. Rogozhin, A. Cisternas, J.C. Bousquet, B. Borisov, and A. Karakhanian (1992). The Armenian earthquake of 1988 December 7: Faulting and folding, neotectonics and palaeoseismicity. *Geophys. J. Int.*, **110**(1), 141–158, doi: 10.1111/j.1365-246X.1992.tb00718.x.

Purcaru, G. and H. Berkheimer (1978). A magnitude scale for very large earthquakes. *Tectonophysics*, **49**, 189–198.

Reid, H.F. (1910). *The Californian Earthquake of April 18, 1906, 2: The Mechanics of the Earthquake*. Carnegie Institution of Washington, Washington, D.C., 192 pp.

Rhoades, D.A. and F.F. Evison (1993). Long-range earthquake forecasting based on a single predictor with clustering. *Geophys. J. Int.*, **113**, 371–381.

Rice, J.R. and M.P. Cleary (1976). Some basic stress-diffusion solutions for fluid-saturated elastic porous media with compressible constituents. *Reviews of Geophysics and Space Physics*, **14**, 227–241.

Richwalski, S.M. and F. Roth (2008). Inelastic and visco-elastic stress triggering in the South Iceland seismic zone due to large earthquakes since 1706. *Tectonophysics*, **447**, 127–135.

Riedel, W. (1929). *Zur Mechanik geologischer Brucherscheinungen*. Zentralblatt für Mineralogie, Geologie und Paläontologie, pp. 354–368.

Rikitake, T. (1976). *Earthquake Prediction*. Elsevier Scientific Publishing, Amsterdam, 357 pp.

Roberts, M.J. (2004). Early warning and information system for geologic hazards in Iceland. In: C. Corbin (Ed.), *Portfolio of Case Studies, GINIE: Geographic Information Network in Europe* (Report D3.6.7, pp. 354–368). Geologie und Paläontologie.

Rögnvaldsson, S.Th. and R. Slunga (1993). Routine fault plane solutions for local networks: A test with synthetic data. *Bulletin of the Seismological Society of America*, **83**(4), 1232–1247.

Rögnvaldsson, S.Th. and R. Slunga (1994). Single and joint fault plane solutions for microearthquakes in South Iceland. *Tectonophysics*, **237**, 73–80.

Rögnvaldsson, S.Th., A. Gudmundsson, and R. Slunga (1998). Seismotectonic analysis of the Tjörnes Fracture Zone, an active transform fault in north Iceland. *J. Geophys. Res.*, **103**, 30117–30129.

Roth, F. (2004). Stress changes modeled for the sequence of strong earthquakes in the South Iceland seismic zone since 1706. *Pageoph*, **161**(7), 1305–1327, doi: 10.1007/s00024-004-2506-5.

Roy, M. and C. Marone (1996). Earthquake nucleation on model faults with rate- and state-dependent friction: Effects of inertia. *J. Geophys. Res.*, **101**(B6), 13919–13932.

Sacks, I.S., S. Suyehiro, D.W. Evertson, and Y. Yamagishi (1971). Sacks–Evertson strainmeter: Its installation in Japan and some preliminary results concerning strainsteps. *Papers in Meteorology and Geophysics*, **22**, 195–208.

Sacks, I.S., A.T. Linde, and R. Stefánsson (1980). *Installation of a Borehole Strainmeter Array in Iceland* (DTM Yearbook 79, pp. 495–498). Carnegie Institute of Washington, Washington, D.C.

Segall, P. and Yijun Du (1993). How similar were the 1934 and the 1966 Parkfield Earthquakes? *J. Geophys. Res.*, **98**(B3), 4527–4542.

Segall, P. and J.R. Rice (1995). Dilatancy, compaction, and slip instability of a fluid-infiltrated fault. *J. Geophys. Res.*, **100**(B11), 22155–22171.

Shomali, Z.H. and R. Slunga (2000). Body wave moment tensor inversion of local earthquakes: An application to the South Iceland Seismic Zone. *Geophys. J. Int.*, **140**, 63–70.

Sigmundsson, F. (2006). *Iceland Geodynamics*. Springer/Praxis, Heidelberg, Germany/Chichester, U.K.

Sigmundsson, F., P. Einarsson, R. Bilham, and E. Sturkell (1995). Rifttransform kinematics in south Iceland: Deformation from Global Positioning System measurements, 1986 to 1992. *J. Geophys. Res.*, **100**, 6235–6248.

Slunga, R. (1981). Earthquake source mechanism determination by use of body wave magnitudes: An application to Swedish earthquakes. *Bulletin of the Seismological Society of America*, **71**, 25–35.

Slunga, R. (1991). The Baltic Shield earthquakes. *Tectonophysics*, **189**, 323–331.

Slunga, R. (2001). *Foreshock Activity, Fault Radius and Silence: Earthquake Warnings Based on Microearthquakes* (Report 01003). Vedurstofa Íslands, Reykjavík. Available at *http://www.vedur.is/utgafa/greinargerdir/2001/01003*

Slunga, R. (2003). Microearthquake analysis at local seismic networks in Iceland and Sweden and earthquake precursors. In: T. Takanami and G. Kitagawa (Eds.), *Methods and Applications of Signal Processing in Seismic Network Operations* (Lecture Notes in Earth Sciences 98, pp. 149–172). Springer-Verlag, Berlin.

Slunga, R. (2007). Use of stress tensor field for earthquake warnings. *Geophys. Res. Abstracts*, **9**, 07147, doi: 1607-7962/gra/EGU2007-A-07147.

Slunga, R. (2010). Development and implementation of seismic early warning processes in South West Iceland, Safer-2. Available at *http://www.vedur.is/um-vi/utgafa/skyrslur/*

Slunga, R., S.Th. Rögnvaldsson, and R. Bödvarsson (1995). Absolute and relative locations of similar events with application to microearthquakes in southern Iceland. *Geophys. J. Int.*, **123**, 409–419.

Stefánsson, R. (1966). Methods of focal mechanism studies with application to two Atlantic earthquakes. *Tectonophysics*, **3**, 209–243.

Stefánsson, R. (1967). Some problems of seismological studies on the mid-Atlantic ridge. *Iceland and the Mid-Ocean Ridges* (Vol. 38, pp. 80–90). Societas Scientiarum Islandica, Reykjavik, Iceland.

Stefánsson, R. (1999). A tentative model for stress buildup and stress release in and around the SISZ. Available at *http://hraun.vedur.is/ja/prepared/reports/*

Stefansson, R. (2000). A report. Available at *http://hraun.vedur.is/ja/englishweb/heklanews.html*

Stefánsson, R. (2003). Information and warnings to authorities and to the public about seismic and volcanic hazards in Iceland. In: J. Zschau and A.N. Küppers (Eds.), *Early Warning Systems for Natural Disaster Reduction* (papers presented at the International IDNDR-Conference on Early Warning Systems for the Reduction of Natural Disasters, Potsdam, Germany, September 7–11, 1998). Springer Verlag, Berlin, pp. 521–526.

Stefánsson, R. (2006). *PREPARED Final Report* (Report 06009). Vedurstofa Islands, Reykjavík. Available at *http://www.vedur.is/skjalftar-og-eldgos/skyrslur_og_rit/*

Stefánsson, R. and G.B. Gudmundsson (2005). *About the State-of-the-art in Providing Earthquake Warnings in Iceland* (Report 05003). Vedurstofa Islands, Reykjavík. Available at *http://www.vedur.is/utgafa/greinargerdir/2003/05003*

Stefánsson, R. and P. Halldórsson (1988). Strain release and strain build-up in the South Iceland seismic zone. *Tectonophysics*, **159**, 267–276.

Stefánsson, R., R. Bödvarsson, R. Slunga, P. Einarsson, S. Jakobsdóttir, H. Bungum, S. Gregerson, J. Hjelme, and H. Kerhonen (1993). Earthquake prediction research in the South Iceland Seismic Zone and the SIL Project. *Bulletin of the Seismological Society of America*, **83**, 696–716.

Stefánsson, R., R. Bödvarsson, and G.B. Gudmundsson (1996). Iceland plume tectonics, some speculations and facts. In: B. Þorkelsson (Ed.), *Seismology in Europe* (papers presented at the XXV ESC General Assembly, Reykjavík, Iceland, September 9–14, pp. 505–511). Icelandic Meteorological Office, Reykjavík. Available at *http://hraun.vedur.is/ja/Grein_Ragnar_1996.pdf*

Stefánsson, R., Th. Árnadóttir, G. Björnsson, G.B. Gudmundsson, and P. Halldórsson (2000). The two large earthquakes in the South Iceland seismic zone in June 2000: A basis for earthquake prediction research (abstract). *AGU Fall Meeting, San Francisco, California, December 15–19*.

Stefánsson, R., G.B. Gudmundsson, and P. Halldórsson (2003). *The South Iceland Earthquakes 2000: A Challenge for Earthquake Prediction Research* (Report 03017). Vedurstofa Islands, Reykjavík. Available at *http://www.vedur.is/utgafa/greinargerdir/2003/03017*

Stefánsson, R., G.B. Gudmundsson, and M.J. Roberts (2006a). *Long-term and Short-term Earthquake Warnings Based on Seismic Information in the SISZ* (Report 06006). Vedurstofa Islands, Reykjavík.

Stefánsson, R., M. Bonafede, F. Roth. P. Einarsson, Þ. Árnadóttir, and G. B. Gudmundsson (2006b). *Modeling and Parameterizing the Southwest Iceland Earthquake Release and Deformation Process* (Report 06005). Vedurstofa Islands, Reykjavík.

Stefánsson, R., G.B. Gudmundsson, and P. Halldórsson (2008). Tjörnes fracture zone: New and old seismic evidence for the link between the North Iceland rift zone and the Mid-Atlantic Ridge. *Tectonophysics*, **447**, 117–126.

Stefánsson, R., M. Bonafede, and G.B. Gudmundsson (2010). Earthquake prediction research and the year 2000 earthquakes in the South Iceland Seismic Zone. *Bulletin of the Seismological Society of America* (submitted).

Stein, R.S., S. Toda, T. Parson, and E. Grunewald (2006). A new probabalistic seismic hazards assessment for greater Tokyo. *Phil. Trans. R. Soc. A*, **364**, doi: 10.1008/rsta.1006.1808

Sykes, L.R. (1971). Aftershock zones of great earthquakes, seismicity gaps, and earthquake prediction for Alaska and the Aleutians. *J. Geophys. Res.*, **76**(32), 8021–8041.

Theodórsson, P. and G.I. Gudjónsson (2003). Increased radon detection sensitivity: Extraction from 200 ml of water and liquid scintillation counting. *Health Phys*., **85**(5), 610–612.

Thoroddsen, Th. (1899). *Jardskjálftar á Sudurlandi*. Hid Íslenska Bókmenntafjelag, Kaupmannahöfn, 199 pp. [in Icelandic].

Thoroddsen, Th. (1905). *Landskjálftar á Íslandi*. Hid Íslenska Bókmenntafjelag, Kaupmannahöfn, 269 pp. [in Icelandic].

Tryggvason, A., S.Th. Rögnvaldsson, and Ó.G. Flóvenz (2002). Three-dimensional imaging of the P- and S-wave velocity structure and earthquake locations beneath Southwest Iceland. *Geophys. J. Int*., **151**, 848–866.

Tryggvason, K., E. Husebye, and R. Stefánsson (1983). Seismic image of the hypothesized Icelandic hot spot. *Tectonophysics*, **100**, 97–118.

Tse, S.T and J.R. Rice (1986). Crustal earthquake instability in relation to the depth variation of frictional slip properties. *J. Geophys. Res*., **91**(B9), 9452–9472.

Vogfjörd, K.S., S.S. Jakobsdóttir, G.B. Gudmundsson, M.J. Roberts, K. Ágústsson, T. Arason, H. Geirsson, S. Karlsdóttir, S. Hjaltadóttir, U. Ólafsdóttir *et al*. (2005). Forecasting and monitoring a subglacial eruption in Iceland. *EOS, Trans. Am. Geophys. Union*, **86**(26), June.

Volti, T. and S. Crampin (2003). A four-year study of shear-wave splitting in Iceland, 2: Temporal changes before earthquakes and volcanic eruptions. In: D.A. Nieuwland (Ed.), *New Insights into Structural Interpretation and Modeling* (Special Publiction 212). Geological Society of London, pp. 135–149.

Waldhauser, F. and W.L. Ellsworth (2000). A double-difference earthquake location algorithm: Method and application to the Northern Hayward Fault, California. *Bulletin of the Seismological Society of America*, **90**(6), 1353–1368.

Wang, Z., Y. Fukao, S. Kodaira, and R. Huang (2008). Role of fluids in the initiation of the 2008 Iwate earthquake (M7.2) in northeast Japan. *Geophys. Res. Lett*., **35**, L24303, doi: 10.1029/2008GL035869.

Ward, P.L. (1971). New interpretation of the geology of Iceland. *Geol. Soc. Am. Bull*., **82**, 2991–3012.

Wilson, J.T. (1963). A possible origin of the Hawaian Islands. *Can. J. Phys*., **41**, 863.

Wolfe, C., I.Th. Bjarnason, J.C VanDecar, and S.C. Solomon (1996). Seismic structure of the Iceland mantle plume. *Nature*, **385**, 245–247.

Wu, J., Y. Gao, S. Crampin, T. Volti, and Y.-T. Chen (2005). Smaller source earthquakes and improved measuring techniques allow the largest earthquakes in Iceland to be stress-forecast (with hindsight). *Geophys. J. Int*. (submitted).

Wyss, M. (1973). Towards a physical understanding of earthquake frequency distribution. *Geophys. J. R. Astron. Soc*., **31**, 341–359.

Wyss, M. and R. Stefánsson (2006). Nucleation points of recent main shocks in southern Iceland mapped by *b*-values. *Bulletin of the Seismological Society of America*, **96**, 599–608, doi: 10.1785/0120040056.

Wyss, M., K. Shimazaki, and S. Wiemer (1997). Mapping active magma chambers by *b* values beneath the off-Ito volcano, Japan. *J. Geophys. Res*., **102**, 20413–20422.

Yerkes, R.F., P. Levine, and C.M. Wentworth (1990). *Abnormally High Fluid Pressures in the Region of the Coalinga Earthquake Sequence and Their Significance* (USGS Prof. Pap. 1487, pp. 237–257). U.S. Geological Survey, Reston, VA.

Yoshida, S., O.C. Clint, and P.R. Sammonds (1998). Electric potential changes prior to shear fracture in dry and saturated rocks. *Geophys. Res. Lett*., **25**(10), 1577–1580.

Zatsepin, S.V. and S. Crampin (1997). Modelling the compliance of crustal rock, I: Response of shear wave splitting to differential stress. *Geophys. J. Int.*, **129**, 477–494.

Zencher, F., M. Bonafede, and R. Stefánsson (2006). Near-lithostatic pore pressure at seismogenic depths: A thermo-poro-elastic model. *Geophys. J. Int.*, **166**, 1318–1334, doi: 10.1111/j.1365-246X.2006.03069.x.

Index